DEVELOPMENT AN
BOMBARDME
BON

DEVELOPMENT AND OPTIMIZATION OF MATRICES FOR FAST ATOM BOMBARDMENT AND THERMALLY ASSISTED FAST ATOM BOMBARDMENT MASS SPECTROMETRY

By

Curt Einar Heine

A DISSERTATION

Submitted to
Michigan State University
in partial fulfillment of the requirements
for the degree of

DOCTOR OF PHILOSOPHY

Department of Chemistry

1990

DEVELOPMENT

BOMBARD

B

Fast atom

desorption ionizatio

kiloelectronvolt neu

thermally labile and

participation of a li

Unfortunately, the

can significantly im

goals of sample p

minimize the interfe

Optimization

contribute to the rea

the analyte from mi

conveniently depos

analyte ion abunda

shown to alleviate s

proposed to accoun

ABSTRACT

DEVELOPMENT AND OPTIMIZATION OF MATRICES FOR FAST ATOM BOMBARDMENT AND THERMALLY ASSISTED FAST ATOM BOMBARDMENT MASS SPECTROMETRY

By

Curt Einar Heine

Fast atom bombardment (FAB) has become the most widely used desorption ionization technique in mass spectrometry. This experiment utilizes a kiloelectronvolt neutral beam to produce sustained secondary ion signals from thermally labile and nonvolatile analytes. A critical aspect of this process is the participation of a liquid support compound, which is known as the FAB matrix. Unfortunately, the matrix (e.g., glycerol) also provides a mass spectrum which can significantly impede spectral interpretation of the analyte. Hence, important goals of sample preparation in FAB are to maximize analyte ion signals and minimize the interfering matrix signals.

Optimization of the matrix to analyte ratio is shown in systematic studies to contribute to the realization of both these goals. This strategy involves sampling the analyte from minute portions of matrix (e.g., 0.10 mg of glycerol), which are conveniently deposited from dilute aqueous solutions. Besides increasing analyte ion abundances and decreasing matrix ion abundances, this approach is shown to alleviate suppression effects among mixtures of peptides. A model is proposed to account for the spectral enhancement.

Another aspe
optimization of a re
assisted fast atom
simulates differentia
tertiary samples wh
water. A benefit of t
valid background su
unique behavior. Ev
(i.e., greater than 90
abundances of high
Mixtures of glycerol
FAB matrices, and
abundances in comp
The final chapter of
of matrices) to FAB
for four different co
stachyose.

Another aspect of this project involved the further development and optimization of a related desorption ionization technique known as thermally assisted fast atom bombardment (TA-FAB) mass spectrometry. TA-FAB stimulates differential desorption ionization of analyte versus matrix by heating tertiary samples which contain the analyte, a saccharide (e.g., fructose), and water. A benefit of the differential desorption ionization is the potential to perform valid background subtractions. A mechanism is proposed to account for this unique behavior. Evaluation of TA-FAB for the analysis of high mass compounds (i.e., greater than 900 u) revealed the tendency of the technique to produce lower abundances of high mass analyte ions than the conventional FAB experiment. Mixtures of glycerol, fructose, and water were subsequently developed as TA-FAB matrices, and shown to provide increased high mass analyte ion abundances in comparison to those measured from the aqueous fructose matrix. The final chapter of this dissertation compares TA-FAB results (using both types of matrices) to FAB results (involving manipulation of the matrix to analyte ratio) for four different compounds including bradykinin, HC-I toxin, digitonin, and stachyose.

to my brother, Eric

I will beg
for the love an
undertaken in m
for guidance wh
for some magnif
due to Jack Holl
would also like to
final stages of hi
research with B
school.

I owe a g
MSU Mass Spec
Vicki McPharlin,
invaluable assis
Musselman and
computer specia
designing the T
necessary parts.

Several
include Dr. J. A
heptasaccharide
(HC-I toxin). Sp
Fernando Osorio

ACKNOWLEDGMENTS

I will begin by thanking my family (Dad, Mom, Eric, Carl, Mark, and Bobbi) for the love and support they have provided during every endeavor I have undertaken in my life. I would then like to mention my preceptor, J. T. Watson, for guidance which allowed me the independence to mature as a scientist, and for some magnificent fishing expeditions on Lake Michigan. Special thanks are due to Jack Holland, who was a constant source of creativity and enthusiasm. I would also like to thank my FAB brother, Brad Ackermann, for involving me in the final stages of his project. The camaraderie inherent to sharing that initial year of research with Brad stands out as one of my fondest memories of graduate school.

I owe a great deal to the competence, cooperation, and patience of the MSU Mass Spectrometry Facility staff. These helpful people include secretaries Vicki McPharlin, Jo Dutson, and Melinda Berning (special thanks to Melinda for invaluable assistance in formatting this dissertation); facility managers Brian Musselman and Doug Gage; electronics specialist Mike Davenport; and computer specialist Mel Micke. I want to thank John Stults for assistance in designing the TA-FAB probe for the JEOL, and Russ Guyer for machining the necessary parts.

Several people contributed important materials for my work. These include Dr. J. A. Smith (oligonucleotides), Dr. C. C. Sweeley (mannosidosis heptasaccharides), Dr. William Reusch ($CH_3C(CH_2OH)_3$), and Dr. J. D. Walton (HC-I toxin). Special thanks go to Dr. James Steffe and his graduate student Fernando Osorio, for their assistance in conducting viscosity measurements.

No list of a
Watson group mer
to refine the ideas
other cohorts in the
assisted in making
A ready sou
wood, and ice rink
1936 national char
1990 Big 10 char
together for the d
wolverines. No m
MSU number one i
dominant athletic c
And, finally,
in East Lansing w
something far mor
To my wife Mary, I
you contributed
tremendous lift the

No list of acknowledgments would be complete without mentioning the Watson group members, past and present, whose criticisms and insights helped to refine the ideas presented in the following pages. I would also like to thank my other cohorts in the chemistry department at MSU (you know who you are), who assisted in making graduate school a more enjoyable experience.

A ready source of inspiration was the effort spent on the gridiron, hard wood, and ice rink by Spartan athletic teams. Special mention is reserved for the 1986 national champion hockey team, the 1988 Rose Bowl champions, and the 1990 Big 10 champion basketball team. I appreciate Sparty holding himself together for the duration of my stay, in spite of repeated assaults from lowly wolverines. No matter where the future takes us, Mary and I will always keep MSU number one in our hearts. We will also forever recognize the Big 10 as the dominant athletic conference in the country.

And, finally, I come to the most important acknowledgment of all. I arrived in East Lansing with the intention of earning a degree, but I leave MSU with something far more valuable: a partner with whom I will share the rest of my life. To my wife Mary, I can only say that the patience, understanding, and love which you contributed during these years will always be remembered for the tremendous lift they gave me in my journey through graduate school.

LIST OF TABLE
LIST OF FIGURE
Chapter 1. Litera
I. Introduction
II. Survey of Des
a. Field De
b. Electroh
c. Desorpt
d. Plasma
e. Second
f. Laser D
g. Thermo
h. Ion Eva
i. Rapid H
III. Fast Atom Bo
a. Ion Typ
b. Matrix
c. Instrum
d. Continu
e. Quantita
f. Accurat
g. FAB-MS

TABLE OF CONTENTS

	Page
LIST OF TABLES	xii
LIST OF FIGURES	xiii
Chapter 1. Literature Review	
I. Introduction	1
II. Survey of Desorption Ionization Techniques	3
a. Field Desorption	3
b. Electrohydrodynamic Ionization	4
c. Desorption Chemical Ionization	5
d. Plasma Desorption	5
e. Secondary Ion Mass Spectrometry	6
f. Laser Desorption	7
g. Thermospray	8
h. Ion Evaporation Techniques	9
i. Rapid Heating Techniques	10
III. Fast Atom Bombardment	10
a. Ion Types	12
b. Matrix	14
c. Instrumentation	19
d. Continuous-Flow FAB	29
e. Quantitation	33
f. Accurate Mass Measurements	35
g. FAB-MS/MS	37

h. LC/FAB
IV. Mechanistic C
a. Unified
b. Energy
c. Role of
d. Surface
e. Fragme
f. Preform
g. Gas Ph
h. Produc
i. Reactio
V. Applications
a. Peptide
b. Saccha
c. Nucleo
d. Miscel
VI. References
Chapter 2. Influ
Resp
I. Introduction
II. Experimenta
a. Mass
b. Materi
c. Sampl
III. Results and
a. 4 nmo
Glycer

Page

h. LC/FAB-MS 38

IV. Mechanistic Considerations 39

a. Unified Models 40

b. Energy Deposition 44

c. Role of the Matrix 48

d. Surface Effects 51

e. Fragmentation 57

f. Preformed Ions 58

g. Gas Phase Ionization 60

h. Products of FAB 63

i. Reactions Involving Matrix 65

V. Applications 68

a. Peptides 68

b. Saccharides 72

c. Nucleotides 74

d. Miscellaneous 74

VI. References 76

Chapter 2. Influence of the Ratio of Glycerol to Analyte on the FAB-MS Response of Peptides

I. Introduction 96

II. Experimental 97

a. Mass Spectrometry 97

b. Materials 97

c. Sample Preparation and Analysis 98

III. Results and Discussion 99

a. 4 nmol of Bradykinin Sampled from 1 ul of 56% Aqueous Glycerol vs. 1 ul of 5% Aqueous Glycerol 99

b. Respo
Functi
c. Ionizat
Aqueo
d. Role o
e. Eviden
Enhan
f. Propos
g. Effect
h. Effect
i. Effect
Compo
j. Influen
k. Implica
l. Alterna
IV. Conclusion
V. References
Chapter 3. Con
Assi
I. Introduction
II. TA-FAB Fun
III. Experimenta
a. Materi
b. TA-FA
c. TA-FA
d. Sampl
e. Viscos
IV. Results and
a. Mecha

Page

b. Response Profiles for Bradykinin and Glycerol Ions as a Function of Glycerol/Water Composition 101

c. Ionization Efficiency for Bradykinin Sampled from 1 ul of 56% Aqueous Glycerol vs. 1 ul of 5% Aqueous Glycerol 103

d. Role of Water in Spectral Enhancement 105

e. Evidence of Surface Enrichment Contributing to Spectral Enhancement 110

f. Proposed Model to Explain Mass Spectral Enhancement 116

g. Effect of Peptide Hydrophobicity Upon Spectral Enhancement 117

h. Effect of Constant Ratio of Glycerol to Bradykinin 124

i. Effect of Acidic Modifiers on Optimal and Nonoptimal Sample Compositions 128

j. Influence of Ratio of Glycerol to Analyte on Peptide Mixtures 129

k. Implications for CF-FAB Mechanism 139

l. Alternative Mechanistic Explanations 140

IV. Conclusion 146

V. References 148

Chapter 3. Continued Development and Optimization of Thermally Assisted Fast Atom Bombardment Mass Spectrometry

I. Introduction 150

II. TA-FAB Fundamentals 151

III. Experimental 157

a. Materials 157

b. TA-FAB on Varian MAT CH5 158

c. TA-FAB on JEOL HX-110 158

d. Sample Preparation 159

e. Viscosity Measurements 159

IV. Results and Discussion 159

a. Mechanistic Investigations 159

b. Impl
c. Opti
d. Opti
e. Evid
f. Anal
g. Nega
h. TA-F
i. TA-F
j. Optir
k. Heat
l. Effec
m. Alter
n. Prop
V. Conclusion
VI. Reference
Chapter 4. Dir
I. Introductio
II. Experimen
a. Mass
b. Mate
c. Samp
III. Results an
a. Brady
b. HC-I
c. Digito
d. Stach

Page

b. Implementation of TA-FAB on the JEOL 177

c. Optimization of Fructose Composition 184

d. Optimization of Heating Parameters 186

e. Evidence of Fructose Polymerization 188

f. Analysis of Higher Mass Compounds 188

g. Negative Ion TA-FAB 197

h. TA-FAB Using Glycerol Matrix 202

i. TA-FAB Using Hybrid Matrix 209

j. Optimization of Glycerol/Fructose/Water Matrix Composition 213

k. Heating Parameter Optimization for Hybrid Matrix 215

l. Effect of Stainless Steel vs. Copper Probe Tip 216

m. Alternative Tertiary TA-FAB Matrices 217

n. Proposed Model for TA-FAB Using Hybrid Matrix 218

V. Conclusion 219

VI. References 220

Chapter 4. Direct Comparison of FAB and TA-FAB

I. Introduction 222

II. Experimental 223

a. Mass Spectrometry 223

b. Materials 224

c. Sample Preparation and Analysis 224

III. Results and Discussion 224

a. Bradykinin 224

b. HC-I Toxin 228

c. Digitonin 236

d. Stachyose 245

IV. Conclusion

V. Future Work

VI. References

Page

IV. Conclusion 253

V. Future Work 255

VI. References 257

Table

1.1 Several co

2.1 Sample co

2.2 Peptides u
2.11.

2.3 Sample co

2.4 Peptides u

LIST OF TABLES

Table		Page
1.1	Several commonly used FAB matrices.	20
2.1	Sample compositions represented in Figures 2.2-2.5.	106
2.2	Peptides used for experiments represented in Figures 2.10 and 2.11.	119
2.3	Sample compositions represented in Figures 2.13 and 2.14.	125
2.4	Peptides used for mixture analyses.	130

Figure

1.1 Relations
decompo
behavior
by Beuhl
permissi

1.2 Depictio
referenc

1.3 FAB mas
with per

1.4 Depictio
occur in
99 (p. 2

1.5 Depictio
nozzle c
84 with

1.6 Diagram
referenc

1.7 Diagram
referenc

1.8 Schema
propose
171 wit

1.9 Artist's
Adapte
Publish

1.10 Nonline
upper
(GABA
analysi
glycero
John W

1.11 Repres
Roepst
permis

LIST OF FIGURES

Figure		Page
1.1	Relationship between the rate constants for vaporization and decomposition as a function of reciprocal temperature. This behavior was shown to be typical of thermally labile compounds by Beuhler and coworkers (50). Reprinted from reference 52 with permission of the American Chemical Society.	11
1.2	Depiction of the operating principles in FAB-MS. Adapted from reference 99 (p. 208) with permission of Raven Press.	13
1.3	FAB mass spectrum of neat glycerol. Adapted from reference 182 with permission of the American Chemical Society.	16
1.4	Depiction of ion formation and neutralization as it is believed to occur in the saddle-field fast atom gun. Reprinted from reference 99 (p. 210) with permisson of Raven Press.	22
1.5	Depiction of ion neutralization by charge transfer occurring at the nozzle of the capillaritron fast atom gun. Reprinted from reference 84 with permission of John Wiley and Sons Ltd.	24
1.6	Diagram of the continuous-flow FAB probe. Reprinted from reference 115 with permission of Elsevier Science Publishers.	30
1.7	Diagram of the coaxial continuous-flow probe. Reprinted from reference 124 with permission of Heydon and Son Ltd.	34
1.8	Schematic diagram of the unified model for desorption ionization proposed by Cooks and Busch in 1983. Reprinted from reference 171 with permission of Elsevier Science Publishers.	43
1.9	Artist's conception of energy transfer through a collision cascade. Adapted from reference 178 with permission of Elsevier Science Publishers.	45
1.10	Nonlinear calibration curves obtained from FAB experiments. The upper plot corresponds to the analysis of 4-aminobutyric acid (GABA) in acidified glycerol, and the lower plot corresponds to the analysis of acetyl glyceryl ether phosphocholine (AGEPC) in glycerol. Adapted from references 131 and 134 with permission of John Wiley and Sons Ltd.	53
1.11	Representation of the nomenclature for peptide ions proposed by Roepstorff and Fohlman. Adapted from reference 289 with permission of John Wiley and Sons Ltd.	71

Figure

2.1 (a) FAB n
nmol/ul) a
glycerol n
1.0 ul of
glycerol.

2.2 Plots of p
m/z 527
glycerol.
total samp

2.3 Plots of p
93 (midd
Each sam
volume in

2.4 Peak inte
(middle),
(describe
amount c
than the
contains
the same

2.5 Peak inte
(middle),
(describe
amount c
than the
contains
the same

2.6 Response
(middle),
indicated

2.7 Response
(middle),
indicated

2.8 Response
(middle),
indicated

2.9 Response
(middle),
indicated

2.10 Plots of
absolute
nmol of an

Figure		Page
2.1	(a) FAB mass spectrum of 1.0 ul of aqueous bradykinin solution (4 nmol/ul) added to 1 ul of glycerol. Major peaks derived from the glycerol matrix are labeled with a "G". (b) FAB mass spectrum of 1.0 ul of bradykinin solution added to 1.0 ul of 10% aqueous glycerol.	100
2.2	Plots of peak intensity for selected bradykinin ions (m/z 70 (top), m/z 527 (middle), and m/z 1060) versus weight percentage glycerol. Each sample contained 4 nmol of bradykinin and the total sample volume in each case was 2 ul.	102
2.3	Plots of peak intensity for selected glycerol ions (m/z 75 (top), m/z 93 (middle), and m/z 277) versus weight percentage glycerol. Each sample contained 4 nmol of bradykinin and the total sample volume in each case was 2 ul.	104
2.4	Peak intensity for selected bradykinin ions (m/z 70 (top), m/z 527 (middle), and m/z 1060) plotted against sample composition (described in Table 2.1). Samples A, B, and C contain the same amount of glycerol, but significantly different amounts of water than the optimum composition (sample 3, Table 2.1). Sample D contains more than the optimum amount of glycerol and water, but the same weight percentage of glycerol in water as sample A.	108
2.5	Peak intensity for selected glycerol ions (m/z 75 (top), m/z 93 (middle), and m/z 277) plotted against sample composition (described in Table 2.1). Samples A, B, and C contain the same amount of glycerol, but significantly different amounts of water than the optimum composition (sample 3, Table 2.1). Sample D contains more than the optimum amount of glycerol and water, but the same weight percentage of glycerol in water as sample A.	109
2.6	Response for selected bradykinin ions (m/z 120 (top), m/z 572 (middle), and m/z 1060) produced from samples composed of the indicated amount of bradykinin in 1.3 mg of glycerol.	111
2.7	Response for selected glycerol ions (m/z 75 (top), m/z 185 (middle), and m/z 369) produced from samples composed of the indicated amount of bradykinin in 1.3 mg of glycerol.	113
2.8	Response for selected bradykinin ions (m/z 120 (top), m/z 572 (middle), and m/z 1060) produced from samples composed of the indicated amount of bradykinin in 0.10 mg of glycerol.	114
2.9	Response for selected glycerol ions (m/z 75 (top), m/z 185 (middle), and m/z 369) produced from samples composed of the indicated amount of bradykinin in 0.10 mg of glycerol.	115
2.10	Plots of $[M+H]^+$ peak intensity for three peptides versus the absolute amount of glycerol in sample. All samples contain 4 nmol of analyte.	120

Figure

2.11 Plots of [gly
amount of g
indicated pe

2.12 Plot of [glyc
amount of g

2.13 Plots of abu
491 (middle
All samples
to bradykini
vary.

2.14 Plots of abu
(middle), ar
samples po
bradykinin
vary.

2.15 Plot of fra
concentratio
chlorides in
Elsevier Sc

2.16 FTI plots
containing
portion of g

2.17 FTI plots
containing
portion of g

2.18 FTI plots
containing
portion of g

2.19 Schematic
stable surfa
Adapted fr
Ltd.

3.1 Averaged
fructose so
reference 1

3.2 Mass therm
alanyl-leucy
aqueous fr

3.3 (a) Conver
glycine in 0
monomer.

Figure Page

2.11 Plots of $[glycerol+H]^+$ peak intensity (at m/z 93) versus absolute amount of glycerol present in samples containing 4 nmol of the indicated peptide. 122

2.12 Plot of $[glycerol+H]^+$ peak intensity (at m/z 93) versus absolute amount of glycerol present in samples containing no peptide. 123

2.13 Plots of abundance of selected bradykinin ions (m/z 70 (top), m/z 491 (middle), and m/z 1060) versus nmol of bradykinin in sample. All samples possess a constant ratio (300:1) of glycerol molecules to bradykinin molecules, although the absolute quantities of each vary. 126

2.14 Plots of abundance of selected glycerol ions (m/z 75 (top), m/z 93 (middle), and m/z 185) versus umol of glycerol in sample. All samples possess a constant ratio (300:1) of glycerol molecules to bradykinin molecules although the absolute quantities of each vary. 127

2.15 Plot of fractional total ion current (FTI) versus total bulk concentration for equimolar solutions of four acylcarnitine chlorides in glycerol. Adapted from reference 8 with permission of Elsevier Science Publishers. 133

2.16 FTI plots (comparing $[M+H]^+$ ion abundances) for mixtures containing 4 nmol of each peptide dispersed in the indicated portion of glycerol. 134

2.17 FTI plots (comparing $[M+H]^+$ ion abundances) for mixtures containing 0.5 nmol of each peptide dispersed in the indicated portion of glycerol. 136

2.18 FTI plots (comparing $[M+H]^+$ ion abundances) for mixtures containing 2 nmol of each peptide dispersed in the indicated portion of glycerol. 138

2.19 Schematic diagram showing the difference in appearance of a stable surface and an unstable surface on the CF-FAB probe tip. Adapted from reference 20 with permission of Heydon and Son Ltd. 141

3.1 Averaged mass spectrum produced from 0.5 ul of an aqueous fructose solution under the conditions of TA-FAB. Adapted from reference 1 with permission of the American Chemical Society. 152

3.2 Mass thermograms obtained from a TA-FAB analysis of 2 ug of alanyl-leucyl-glycine (upper thermograms) sampled from an aqueous fructose matrix (lower thermograms). 154

3.3 (a) Conventional FAB mass spectrum of 1 ug of alanyl-leucyl-glycine in 0.5 ul of glycerol. The letter "G" represents the glycerol monomer. (b) TA-FAB mass spectrum of 1 ug of alanyl-leucyl-

Figure

glycine
region.
Adapted
Chemica

3.4 Typical
the abu
a matrix

3.5 Mass th
atypical
maintair
through
which w
distilled

3.6 Current
uncertai

3.7 Mass t
obtained
analyze
bottom

3.8 X-ray di
differen
(lyophil
permiss

3.9 Repres
direct in
arrow i
inserted

3.10 TA-FAB
aqueou
obtaine
the JEO

3.11 TA-FAB
aqueou
from th

3.12 Backgr
sample
obtaine
are lab

3.13 BMT s
glycine
spectru

glycine in aqueous fructose solution averaged over the BMT region. (c) TA-FAB spectrum after background subtraction. Adapted from reference 1 with permission of the American Chemical Society. 156

3.4 Typical behavior of a sample subjected to TA-FAB represented in the abundance profiles of an analyte ion (upper thermogram) and a matrix ion (lower thermogram). 161

3.5 Mass thermogram of $[M+H]^+$ ion of alanyl-leucyl-glycine for an atypical TA-FAB experiment: scans 19-51 were obtained while maintaining a constant current (representative of the BMT) through the emitter. This was followed by a typical TA-FAB run which was recorded after rejuvenation of the sample with 1.0 ul of distilled water. 164

3.6 Current/temperature relationship obtained for the ECP. The uncertainty of this curve is estimated to be $\pm 10^{0}C$. 166

3.7 Mass thermograms for two fructose ions (upper two panels) obtained when 0.5 ul of an aqueous fructose solution was analyzed by TA-FAB. A total ion current trace is shown in the bottom panel. 170

3.8 X-ray diffractograms obtained for aqueous solutions of fructose at different concentrations (weight %), as well as solid fructose (lyophilized and vitreous). Adapted from reference 9 with permission of Elsevier Science Publishers. 173

3.9 Representation of the JEOL HX-110 ion source (upper) and the direct insertion probe as it was modified for TA-FAB (lower). The arrow indicates the opening through which the probe tip is inserted. 178

3.10 TA-FAB data from 2 ug of alanyl-leucyl-glycine mixed with aqueous fructose. The upper fructose thermograms were obtained from the CH5, and the lower fructose thermograms from the JEOL. 180

3.11 TA-FAB data from 2 ug of alanyl-leucyl-glycine mixed with aqueous fructose. The upper ALG thermograms were obtained from the CH5, and the lower ALG thermograms from the JEOL. 182

3.12 Background subtracted spectrum of alanyl-leucyl-glycine (from a sample composed of 2 ug of ALG mixed with aqueous fructose) obtained from a TA-FAB experiment on the JEOL. Analyte signals are labeled with an "A". 183

3.13 BMT spectra in the TA-FAB analyses of 2 ug of alanyl-leucyl-glycine mixed with aqueous solutions containing 0.62 mg (upper spectrum) and 0.10 mg (lower spectrum) of fructose. Analyte

Figure

signals a
with a "B

3.14 Mass the
0.31 mg

3.15 Part of s
3.14.

3.16 Bradykin
containin

3.17 Spectrun
FAB ana

3.18 (lower) S
run repre
region of

3.19 TA-FAB
mode. T
containir
fructose.

3.20 Mass th
aqueous
peptide
correspo
correspo

3.21 TA-FAB
mixed w
correspo
correspo

3.22 Mass ch
arsenobe
correspo
correspo
16 with p

3.23 Comparis
optimizin
points) v
glycerol
of bradyk
sample c
for three
(middle),

3.24 Comparis
optimizing

Figure		Page
	signals are marked with an "A" and fructose signals are marked with a "B".	185
3.14	Mass thermograms obtained from an aqueous sample containing 0.31 mg of fructose.	189
3.15	Part of scan 179 from the TA-FAB analysis represented in Figure 3.14.	190
3.16	Bradykinin thermograms obtained from an aqueous sample containing 4 nmol of the nonapeptide and 0.16 mg of fructose.	192
3.17	Spectrum containing the maximum $[M+H]^+$ signal from the TA-FAB analysis represented in Figure 3.16.	194
3.18	(lower) Spectrum obtained during the final stages of the TA-FAB run represented in Figure 3.16. An expansion of the low mass region of this spectrum is shown in the upper portion of the figure.	195
3.19	TA-FAB background spectrum measured in the negative ion mode. This was the first scan obtained from an aqueous sample containing 4 ug of the delta sleep inducing peptide and 0.62 mg of fructose.	198
3.20	Mass thermograms from a negative ion TA-FAB analysis of an aqueous sample containing 4 ug of the delta sleep inducing peptide and 0.62 mg of fructose. The lower 4 thermograms correspond to matrix ions and the upper 3 thermograms correspond to analyte ions.	200
3.21	TA-FAB analysis of a sample containing 4 nmol of bradykinin mixed with 1 ul of glycerol. The lower three thermograms correspond to glycerol ions, and the upper five thermograms correspond to analyte ions.	203
3.22	Mass chronograms representing a conventional FAB analysis of arsenobetaine dispersed in glycerol. The signal at m/z 185 corresponds to a prominent glycerol ion and that at m/z 179 corresponds to $[M+H]^+$ for the analyte. Reprinted from reference 16 with permission of Elsevier Science Publishers.	205
3.23	Comparison of the mass spectral enhancement obtained by optimizing the matrix to analyte ratio in conventional FAB (first two points) versus that obtained in a TA-FAB analysis using the glycerol matrix (final two points). Each sample contained 4 nmol of bradykinin. The nonoptimal FAB sample and the initial TA-FAB sample contained 14 umol of glycerol. The comparison is made for three bradykinin ions including m/z 120 (upper), m/z 572 (middle), and m/z 1060 (lower).	207
3.24	Comparison of the mass spectral enhancement obtained by optimizing the matrix to analyte ratio in conventional FAB (first two	

Figure

points) v
glycerol
of bradyk
sample c
for three
and m/z

3.25 TA-FAB
bradykin
glycerol
correspo
thermog

3.26 Two mas
hybrid m

3.27 Hybrid m
sample c

4.1 Compari
70 (top),
from the
4 nmol o

4.2 Structure

4.3 Compari
44 (top),
from the
1.4 ug of

4.4 Compari
(top), m/
the FAB
toxin.

4.5 (upper) F
14 umol
backgrou
1.4 ug of

4.6 (upper) T
from hybr
spectrum
matrix.

4.7 Structure
fragmenta

4.8 (upper) FA
umol of gl
dispersed

Figure Page

points) versus that obtained in a TA-FAB analysis using the glycerol matrix (final two points). Each sample contained 4 nmol of bradykinin. The nonoptimal FAB sample and the initial TA-FAB sample contained 14 umol of glycerol. The comparison is made for three glycerol ions including m/z 75 (upper), m/z 277 (middle), and m/z 461 (lower). 208

3.25 TA-FAB analysis of a sample containing 1.0 ul of an aqueous bradykinin solution (4 nmol/ul) added to 1.0 ul of 50% glycerol/20% fructose/30% water. The lower four thermograms correspond to ions derived from the matrix, and the upper five thermograms correspond to analyte ions. 210

3.26 Two mass spectra selected from the TA-FAB analysis (using the hybrid matrix) represented in Figure 3.25. 212

3.27 Hybrid matrix solutions evaluated for TA-FAB. The understood sample component is weight % water. 214

4.1 Comparison of peak intensities for selected bradykinin ions (m/z 70 (top), m/z 572 (middle), and m/z 1060) which were obtained from the FAB and TA-FAB experiments. Each sample contained 4 nmol of bradykinin. 226

4.2 Structure of HC-I toxin. 229

4.3 Comparison of peak intensities for selected HC-I toxin ions (m/z 44 (top), m/z 240 (middle), and m/z 437) which were obtained from the FAB and TA-FAB experiments. Each sample contained 1.4 ug of the peptide. 231

4.4 Comparison of peak intensities for selected glycerol ions (m/z 75 (top), m/z 185 (middle), and m/z 369) which were obtained from the FAB experiments. Each sample contained 1.4 ug of HC-I toxin. 233

4.5 (upper) FAB mass spectrum of 1.4 ug of HC-I toxin dispersed in 14 umol of glycerol. Major peaks associated with the matrix background are labeled with a "B". (lower) FAB mass spectrum of 1.4 ug of HC-I toxin dispersed in 1.1 umol of glycerol. 234

4.6 (upper) TA-FAB mass spectrum of 1.4 ug of HC-I toxin sampled from hybrid matrix. (lower) Background subtracted TA-FAB mass spectrum of 1.4 ug of HC-I toxin sampled from aqueous fructose matrix. 235

4.7 Structure of digitonin with a diagram of some important fragmentation pathways. 237

4.8 (upper) FAB mass spectrum of 2 ug of digitonin dispersed in 14 umol of glycerol. (lower) FAB mass spectrum of 2 ug of digitonin dispersed in 1.1 umol of glycerol. 238

Figure

4.9 Comparison
(top), m/z 4
the FAB an
are sugges
digitonin.

4.10 Comparison
(top), m/z 1
the FAB ex

4.11 (upper) Lo
containing
mass portio
digitonin a
analyte ion

4.12 (upper) Lo
digitonin ar
backgrounc
analyzed fr

4.13 Structure
fragmenta

4.14 (upper) FA
NaCl disp
spectrum c
umol of gly

4.15 Mass ther
(m/z 73 an
and 689).
mg of fruct

4.16 Scan 53 fr

4.17 Compariso
365 (top),
from the
suggested
stachyose

4.18 Comparisc
93 (top), r
from the
stachyose

4.19 Comparisc
(top), m/z
the FAB e
and 1 ug c

Figure		Page
4.9	Comparison of peak intensities for selected digitonin ions (m/z 295 (top), m/z 449 (middle), and m/z 611) which were obtained from the FAB and TA-FAB experiments. Structures of these fragments are suggested in Figure 4.7. Each sample contained 2 ug of digitonin.	240
4.10	Comparison of peak intensities for selected glycerol ions (m/z 75 (top), m/z 185 (middle), and m/z 369) which were obtained from the FAB experiments. Each sample contained 2 ug of digitonin.	242
4.11	(upper) Low mass portion of FAB spectrum from a sample containing 2 ug of digitonin and 14 umol of glycerol. (lower) Low mass portion of FAB spectrum from a sample containing 2 ug of digitonin and 1.1 umol of glycerol. Peaks corresponding to analyte ions are labeled with an "A".	243
4.12	(upper) Low mass portion of TA-FAB spectrum from 2 ug of digitonin analyzed from hybrid matrix. (lower) Low mass portion of background subtracted TA-FAB spectrum from 2 ug of digitonin analyzed from aqueous fructose matrix.	244
4.13	Structure of stachyose with a diagram of some important fragmentation pathways.	246
4.14	(upper) FAB mass spectrum of 19 ug of stachyose and 1 ug of NaCl dispersed in 14 umol of glycerol. (lower) FAB mass spectrum of 19 ug of stachyose and 1 ug of NaCl dispersed in 1.1 umol of glycerol.	247
4.15	Mass thermograms for two common fructose background ions (m/z 73 and 85) and higher mass background ions (m/z 365, 527, and 689). The sample was an aqueous solution containing 0.22 mg of fructose and 1 ug of NaCl.	248
4.16	Scan 53 from TA-FAB experiment represented in Figure 4.15.	250
4.17	Comparison of peak intensities for selected stachyose ions (m/z 365 (top), m/z 527 (middle), and m/z 689) which were obtained from the FAB experiments. Structures of these ions are suggested in Figure 4.13. Each sample contained 19 ug of stachyose and 1 ug of NaCl.	251
4.18	Comparison of peak intensities for protonated glycerol ions (m/z 93 (top); m/z 185 (middle), and m/z 277) which were obtained from the FAB experiments. Each sample contained 19 ug of stachyose and 1 ug of NaCl.	252
4.19	Comparison of peak intensities for natriated glycerol ions (m/z 115 (top), m/z 207 (middle), and m/z 299) which were obtained from the FAB experiments. Each sample contained 19 ug of stachyose and 1 ug of NaCl.	254

Chapter 1. L

I. Introductio

For ma
compounds c
as electron im
the last two d
emerged to b
problems whi
group of ioniz
ionization", to
directly from a
by a variety
nonvolatile,
Consequently
pursuits wher
extensive deri
major scientific
mass spectro
important mole
ionization mas
future.

This dis
desorption ioni
MS). The no

Chapter 1. Literature Review

I. Introduction

For many years, mass spectrometry was limited to the analysis of volatile compounds due to the exclusive practice of gas phase ionization methods such as electron impact ionization (EI) and, subsequently, chemical ionization (CI). In the last two decades, however, an entire family of new ionization techniques has emerged to broaden the potential of mass spectrometry in solving a range of problems which few would have imagined applicable twenty years ago. This new group of ionization techniques has been classified under the heading "desorption ionization", to emphasize the capacity of these methods to sample the analyte directly from a condensed phase. This common feature (which is accomplished by a variety of different approaches) permits the analysis of many polar, nonvolatile, and thermally labile compounds by mass spectrometry. Consequently, mass spectrometry now enjoys a very natural application in pursuits where its past use has been much more problematic (e.g., requiring extensive derivatization of analytes to increase their volatility). One arena of major scientific interest which will benefit from a greatly increased participation by mass spectrometry is that which depends upon the analysis of biologically important molecules. Of course, this is only one of many areas where desorption ionization mass spectrometry will be utilized with increased frequency in the future.

This dissertation focuses on the most commonly used technique in the desorption ionization family: fast atom bombardment mass spectrometry (FAB-MS). The novel research presented here addresses two aspects of the

experiment which
its powerful poten
and understandin
first area has ad
work devoted to
preparation will r
presented in the f
solution to the s
preparation will a
whether it is c
fragmentation, dir
with a prior sepa
exacting, but can
community. T
considerations im
Our modest contr
(i.e., optimizing
desorption ioniza
technique. Howev
conclusions from
conclusions from l

This manus
method known as
spectrometry. T
understand this t
Before discussing
provided to place

experiment which require continued attention in order for FAB-MS to fully realize its powerful potential. These issues include optimization of sample preparation, and understanding the mechanism for desorption ionization in FAB. Work in the first area has advanced, although probably not with the same enthusiasm as work devoted to the second of these issues. Progress in optimizing sample preparation will require the rigorous and systematic types of studies that are presented in the following chapters of this dissertation. There is not one correct solution to the sample preparation problem. Different strategies in sample preparation will accomplish different goals for a FAB analysis, depending on whether it is desired to maximize analyte ion abundances, maximize fragmentation, direct the type of fragmentation, optimize the coupling of FAB-MS with a prior separation step, etc. This sort of research can be repetitious and exacting, but can yield extremely pragmatic and satisfying benefits for the user community. The work presented here also addresses mechanistic considerations important to understanding the process of desorption ionization. Our modest contribution in this area resulted directly from our efforts in the first (i.e., optimizing sample preparation). Refining the understanding of the desorption ionization process is critical to fully exploiting the potential of the technique. However, care should be exercised in drawing limited, but defensible conclusions from an abundance of experimental data, rather than multiple conclusions from limited, and sometimes ambiguous data.

This manuscript also describes work with a separate desorption ionization method known as thermally assisted fast atom bombardment (TA-FAB) mass spectrometry. These efforts were designed to further develop, optimize, and understand this technique, which was pioneered at Michigan State University. Before discussing the results of these studies, however, the background must be provided to place both FAB and TA-FAB in context. A literature review will begin

in the next sectio

used in mass spe

II. Survey of Desc

The followi

description of de

Instead, it will focu

have proven sign

those techniques c

of fast atom bomb

be mentioned in

description of the c

a. Field Des

The use of

thermally labile org

published the field

subjected to analy

form microneedles

V/cm) applied to

heating the emitte

An extensive rev

theoretical approa

which involved th

The theoretical u

in the next section, with a survey of the major desorption ionization techniques used in mass spectrometry today.

II. Survey of Desorption Ionization Techniques

The following discussion is not meant to provide a complete listing or description of desorption ionization methods used in mass spectrometry. Instead, it will focus on the introduction of key and innovative techniques which have proven significant to the maturation of desorption ionization. Especially those techniques developed prior to (and which set the stage for) the introduction of fast atom bombardment mass spectrometry will be noted. The techniques will be mentioned in the approximate order in which they emerged, and a brief description of the operating principles for each will be included.

a. Field Desorption

The use of desorption ionization mass spectrometry for the analysis of thermally labile organic molecules essentially began in 1969 when H. D. Beckey published the field desorption (FD) mass spectrum of glucose (1). Samples subjected to analysis by FD are deposited upon an emitter, which is activated to form microneedles for the purpose of enhancing the high electric fields (10^7-10^8 V/cm) applied to the sample. Elevated temperature (obtained by resistively heating the emitter) is necessary to observe desorption ionization of the analyte. An extensive review of the technique is provided by Schulten (2). An early theoretical approach to FD resulted from the work of Gomer and Swanson (3,4), which involved the analysis of metals and carbon monoxide from the emitter. The theoretical understanding of the technique was embellished by a debate

regarding the rela

the production of

of field desorptio

relatively little fra

training necessary

b. Electroh

Electrohydr

Evans and Hendr

technique, but it e

transported into

Desorption ioniza

tube. Initial work

thereafter used to

application, the an

with an electrolyte

fluid determines

correlated to the s

to obtain useful

discussion of

electrohydrodynan

normally provide s

regarding the relative importance of thermal versus field-related phenomena in the production of ions by FD (5-10). Disadvantages associated with the practice of field desorption mass spectrometry include transient analyte ion signals, relatively little fragmentation for most analytes, and the somewhat extensive training necessary before an operator can consistently obtain FD spectra.

b. Electrohydrodynamic Ionization

Electrohydrodynamic (EHD) mass spectrometry was introduced in 1972 by Evans and Hendricks (11). An intense electrostatic field also is used in this technique, but it extracts ions from a liquid (rather than solid) sample which is transported into the mass spectometer source by means of a capillary. Desorption ionization occurs at the liquid meniscus in the end of the capillary tube. Initial work involved the analysis of liquid metals, but EHD was shortly thereafter used to obtain spectra of nonvolatile organic compounds. In the latter application, the analyte is dissolved in a host fluid (e.g., glycerol) which is doped with an electrolyte (e.g., NaI). The concentration of the electrolyte in the host fluid determines the conductivity of the solution, which can ultimately be correlated to the size of the charged droplets produced, and hence, the capacity to obtain useful mass spectra of the analyte. Chan and Cook provide a discussion of the various factors which affect sensitivity in the electrohydrodynamic experiment (12). EHD mass spectrometry does not normally provide structurally significant fragmentation.

c. Desorpt

In 1973, M
of mass spectra f
chemical ionizatio
is most commo
spectrometry. Th
sample inside the
presence of a re
analyte. The DC
manufacturers to
have been studie
involves the shor
ionization in the g
scanning, and the
somewhat limited
due to the require

d. Plasma

Plasma
bombardment as
fragile species.
coworkers (17).
analyte solution
sample preparat
thin layer (18).

c. Desorption Chemical Ionization

In 1973, McLafferty and Baldwin introduced a technique for the generation of mass spectra from relatively nonvolatile compounds, which they called direct chemical ionization (DCI) mass spectrometry (13). Today, the same experiment is most commonly referred to as desorption chemical ionization mass spectrometry. The technique requires volatilization of the analyte by heating the sample inside the source of the mass spectrometer. This process occurs in the presence of a reagent plasma and results in the chemical ionization of the analyte. The DCI approach has become common enough for several instrument manufacturers to produce DCI probes (14). Various aspects of the experiment have been studied and optimized (15, 16). A disadvantage of the technique involves the short time interval in which many analytes are actually available for ionization in the gas phase. This transient sampling time necessitates very rapid scanning, and therefore, a sacrifice in sensitivity. The practice of DCI has been somewhat limited to the analysis of relatively low molecular weight compounds, due to the requirement of at least marginal volatility.

d. Plasma Desorption

Plasma desorption mass spectrometry (PDMS) utilizes particle bombardment as the means of energy deposition for the analysis of thermally fragile species. This experiment was introduced in 1974 by Macfarlane and coworkers (17). Sample preparation typically involves electrospraying the analyte solution on a very thin aluminum or aluminized mylar foil. This method of sample preparation is necessary to insure that the analyte is deposited in a very thin layer (18). Megaelectronvolt energy fission fragments (which are produced

by the spontar

particles. The

support in orde

surface such a

improved the

desorption has

molecular weig

primary particl

substantially in

flight mass ana

range associat

technique inher

analysis (23).

protection from

e. Seco

A kiloele

molecules for th

(24). This tech

ions characteri

spectrometry (S

primary ion curr

metal surface, th

particles/cm^2 (2

second primary

previous primary

by the spontaneous decay of the ^{252}Cf nucleus) are used as the bombarding particles. The fission fragment must penetrate both the sample and sample support in order for analyte ions to be detected (19). Various additives to the surface such as glutathione (20) or the ion exchanging polymer Nafion (21) have improved the mass spectrometric response for particular samples. Plasma desorption has set the standard for high mass analysis by measuring several molecular weights well in excess of 10,000 u (22). PDMS suffers from a low primary particle flux, which necessitates summation of sequential spectra and substantially increases analysis time. It is most often implemented with a time-of-flight mass analyzer to benefit from the high ion transmission and large mass range associated with this type of mass spectrometer. Unfortunately, the technique inherits the problems in mass resolution associated with time-of-flight analysis (23). The plasma desorption experiment also requires thorough protection from the radioactive processes occurring inside the instrument.

e. Secondary Ion Mass Spectrometry

A kiloelectronvolt energy ion beam was applied to the analysis of organic molecules for the first time in 1976 by Benninghoven, Jaspers, and Sichtermann (24). This technique uses the primary ion beam to produce gaseous secondary ions characteristic of the analyte and is known as secondary ion mass spectrometry (SIMS). An important parameter of the SIMS experiment is the primary ion current density. For the analysis of organic molecules deposited on a metal surface, the primary current density should not exceed a total dose of 10^{13} particles/cm^2 (25). In this "static" SIMS mode, there is little probability of a second primary ion impacting a portion of the surface already sampled by a previous primary particle. Therefore, radiation damage of the analyte does not

contribute to
relatively long
concurrent re
SIMS experin
molecules, thi
detection of ra

Sample

obtained by
surface, the
overcome to d
the surface
fragmentation
deposited on
sample charg
experiment. T
for the applic
sample prepa
ammonium ch
fragmentation)
light of the fort

f. Lase

Although
of a mass sp
common use o
analysis of non

contribute to subsequent spectra. Although mass spectra may be acquired for relatively long time periods by reducing the primary ion current density (26), a concurrent reduction in secondary ion abundance also results. The "dynamic" SIMS experiment incorporates higher primary current densities. For organic molecules, this mode involves the loss of molecular weight information and the detection of radiation-damaged species, as well as products of vertical sampling.

Sample preparation is a critical factor in determining the quality of results obtained by SIMS. Since the analyte is deposited directly upon the metal surface, the binding energy between the analyte and the surface must be overcome to desorb analyte species into the gas phase. Therefore, the nature of the surface affects the sensitivity of the analysis and also the extent of fragmentation observed (27, 28). Controlling the thickness of the analyte layer deposited on the metal surface appears to be a significant factor in preventing sample charging by the ion beam (29), and, therefore, is critical in optimizing the experiment. This consideration sometimes leads to the use of elaborate methods for the application of thin layers of analyte solution (30). Another aspect of sample preparation in molecular SIMS regards the use of solid matrices (e.g., ammonium chloride) to provide softer desorption ionization (i.e., decreased fragmentation) for the analyte (31). This observation is especially interesting in light of the forthcoming discussion regarding the use of liquid matrices in FAB.

f. Laser Desorption

Although investigations into the use of lasers for forming ions in the source of a mass spectrometer have been conducted since the early 1960s, the common use of laser desorption (LD) mass spectrometry as a technique for the analysis of nonvolatile organic molecules began with the work of Posthumus and

coworkers in 1978
thin layer on a m
process results in
analyzed. An adv
to the use of lase
incident radiation
both the molecula
believed to play a
A disadvantage
preparation requi
LD also suffers fr

g. Thermo

While dev
(LCMS) in 1980
ionization techni
The thermospra
spectrometer so
process results
extracted. Ion
concentrations
mass spectrom
involves extens
proposed by V
sensitivity has
either with an

coworkers in 1978 (32). The experiment requires application of the sample in a thin layer on a metal support, followed by irradiation with a laser beam. This process results in the formation of ions from the sample, which are then mass analyzed. An advantage of laser desorption involves the great fexibility inherent to the use of lasers as an energy source. The pulse duration and power of the incident radiation can be adjusted to optimize the production of ions indicative of both the molecular weight and structure of the analyte. Thermal processes are believed to play a dominant role in the production of gaseous ions by LD (33, 34). A disadvantage of the technique involves the relatively specialized sample preparation required to produce thin layers of analyte on the supporting surface. LD also suffers from poor reproducibility of mass spectral signals (35).

g. Thermospray

While developing a liquid chromatographic interface to mass spectrometry (LCMS) in 1980, Blakley, Carmody, and Vestal discovered a new desorption ionization technique (36) which is now commonly known as thermospray (TSP). The thermospray experiment requires the rapid vaporization in the mass spectrometer source of a solution containing the nonvolatile analyte. This process results in the formation of a supersonic vapor jet, from which ions can be extracted. Ionic additives (e.g., ammonium acetate) present in particular concentrations in the sample solution are an important factor in maximizing the mass spectrometric response for neutral analytes (19). A mechanism which involves extensive desolvation of large cluster ions in the gas phase has been proposed by Vestal to be operative (37). In some applications, increased sensitivity has been obtained for this experiment by incorporating CI conditions, either with an external filament (filament-on TSP) or an electric discharge (38).

Thermospray has

interface and ion

This alrea

complemented b

and Tyler (39). T

section, but befo

ionization metho

h. Ion Eva

The first d

from charged dr

contained a theo

evaporation" (40

polar and therma

expanding in us

particularly intere

multiply charged

these compound

recent study ai

corresponding to

can be implemen

Thermospray has received considerable attention for its obvious potential as an interface and ionization mode for LCMS.

This already diverse community of desorption ionization techniques was complemented by the introduction of FAB in 1981 by Barber, Bordoli, Sedgwick, and Tyler (39). The FAB experiment will be thoroughly discussed in the following section, but before completing this survey, two additional categories of desorption ionization methods will be mentioned.

h. Ion Evaporation Techniques

The first category involves the use of high electric fields to extract ions from charged droplets in a source held at atmospheric pressure. Early work contained a theoretical discussion of this process, which was referred to as "ion evaporation" (40, 41). The method was subsequently applied to the analysis of polar and thermally labile molecules (42). Closely related techniques which are expanding in usage include electrospray (43, 44) and ionspray (45). A particularly interesting aspect of these experiments regards their capacity to form multiply charged ions from very large molecules, thereby enabling the analysis of these compounds with instruments of relatively limited mass range (46-48). A recent study aids in the interpretation of mass spectra containing peaks corresponding to multiply charged ions, and describes helpful algorithms which can be implemented on a personal computer (49).

i. R

Fina
species int
approach w
carried out
formation
decomposit
tendency fo
constant fo
generalized
obviously
decomposit
preformed
phase (52,

III. Fast At

Initia
Manchester
publications
desorb/ioni
double-focu
beam const
existing keV
Such an ap
charging of

i. Rapid Heating Techniques

Finally, those techniques which employ rapid heating to desorb nonvolatile species into the gas phase will be mentioned. The theoretical basis for this approach was developed by Beuhler and coworkers in 1974 (50). This group carried out kinetic studies which clarified the influence of temperature on the formation of intact molecular species in the gas phase versus molecular decomposition products for thermally labile compounds. They determined the tendency for decomposition to dominate at lower temperatures, while the rate constant for vaporization is favored at higher temperatures. These findings are generalized in the Arrhenius plot shown in Figure 1.1. Rapid heating rates are obviously necessary to achieve the higher temperatures before significant decomposition occurs. This knowledge has been exploited to volatilize both preformed ions (51) and neutrals, which can be subsequently ionized in the gas phase (52, 53).

III. Fast Atom Bombardment

Initial reports of the FAB experiment emerged from the University of Manchester Institute of Science and Technology in 1981. These early publications discussed the use of a neutral primary beam (2-10 keV) to desorb/ionize nonvolatile molecules for mass analysis in both a quadrupole and a double-focusing magnetic sector instrument. The neutral character of the particle beam constituted one of the two innovations inherent to FAB with respect to the existing keV particle impact technique used for organic analysis, static SIMS. Such an approach alleviated the focusing problems associated with sample charging of solids impacted by an ion beam, in addition to simplifying

Figure 1.1.

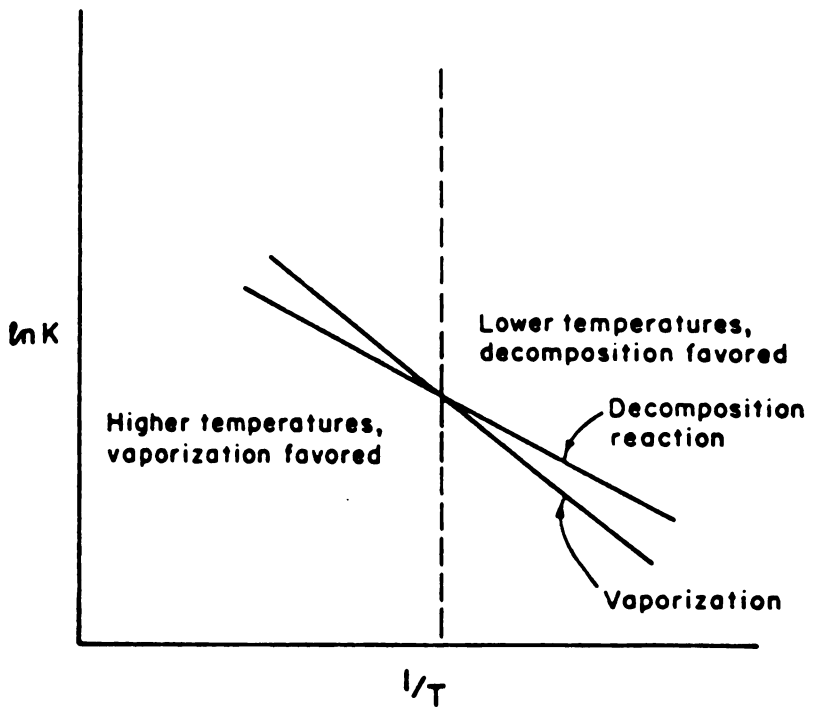

Figure 1.1. Relationship between the rate constants for vaporization and decomposition as a function of reciprocal temperature. This behavior was shown to be typical of thermally labile compounds by Beuhler and coworkers (50). Reprinted from reference 52 with permission of the American Chemical Society.

implementa
be noted th
utilized a ne
including th
the direct an
tripeptides (
the analysis
importance
including "th
deposited o
allowed for
initial refere
innovation a

The c
in Figure 1.2
the sample.
support con
terminology
process, and

a. Ion

The s
electron varie
opposed to
Abundant oc
circumstance

implementation on high voltage magnetic sector mass spectrometers. It should be noted that this innovation was not entirely original; Devienne and coworkers utilized a neutral beam as early as 1966 for the analysis of nonvolatile analytes including those from biological samples (54). Two early FAB papers described the direct analysis of solid samples (individual amino acids (29), and two isomeric tripeptides (55)) by sputtering with the neutral beam. Those reports of success in the analysis of higher molecular weight compounds, however, mentioned the importance of a "support system" for the analyte (39). In particular, properties including "the viscosity and volatility of the medium from which the sample is deposited on the stage" were viewed as critical, and if chosen appropriately, allowed for sensitive analyses "over periods of hours" (56). These rather vague initial references implied the existence of the second (and more important) innovation associated with the FAB experiment: use of the liquid matrix.

The operating principles of the FAB technique are illustrated schematically in Figure 1.2. A keV beam of neutrals (usually xenon or argon) is directed upon the sample. The sample contains both the nonvolatile analyte and the liquid support compound known as the FAB matrix. Secondary ions (the SIMS terminology was retained) are formed from both analyte and matrix in this process, and are subsequently mass analyzed.

a. Ion Types

The secondary ions formed by FAB are predominantly of the even-electron variety which are commonly observed in chemical ionization spectra, as opposed to the odd-electron ions associated with electron impact ionization. Abundant odd-electron ions have been noticed in FAB under certain circumstances (which will be described in a later section), but they generally

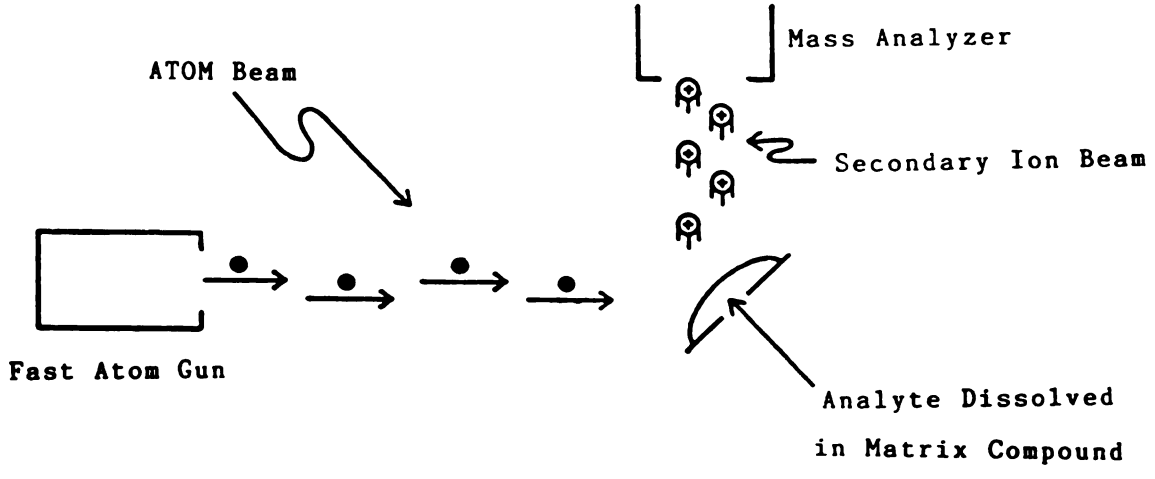

Figure 1.2. Depiction of the operating principles in FAB-MS. Adapted from reference 99 (p. 208) with permission of Raven Press.

represent t
commonly
raising que
phase from
could exist
atom beam
the section
molecular v
lithium, soc
information
molecules.
or by spiki
preparation
molecular v
structurally
has addres
volatile com
these speci
spectral inte
the analyte
formation o
presently in

b. Ma

The c
the widespre

represent the exception to the bulk of the reported experimental data. The commonly formed even-electron ions are typically stable in solution, thereby raising questions as to their point of origin. Ionization could occur in the gas phase from an ion/molecule reaction involving the desorbed neutral, or the ions could exist in solution and only require desorption into the gas phase by the fast atom beam to facilitate detection. This hotly debated topic will be addressed in the section regarding mechanistic considerations. In the positive ion mode, molecular weight information is provided by the protonated or cationized (by lithium, sodium, potassium, etc.) molecule. Analogously, molecular weight information in the negative ion mode is provided by deprotonated or anionized molecules. These ion types can be promoted by adjusting the pH of the sample, or by spiking the sample with ionic additives. Such strategies in sample preparation have been evaluated and are widely applied (57, 58). Besides molecular weight information, many analytes provide signals corresponding to structurally significant fragmentation under fast atom bombardment. McLafferty has addressed the decomposition of some even-electron ions derived from volatile compounds, and noticed an increased tendency for rearrangement of these species in comparison to decomposition of odd-electron ions (59). Finally, spectral interpretation can be complicated by the creation of adduct ions between the analyte and matrix, as well as reaction products involving the rupture and formation of covalent bonds. These sorts of interactions will be discussed presently in greater detail.

b. Matrix

The critical aspect of the FAB experiment which is largely responsible for the widespread popularity of the technique, involves the participation of the

matrix compo
that the "geni
projectile but
in a mobile m
liquid matrix i
comparison to
ion currents f
in sample p
thicknesses
requires a mi
matrix allows
in dynamic S
products. Th
signal. No o
especially at t
existing mass

Althoug
of nonvolatile
widely used
spectrum glyc
The protonate
corresponding
especially ann
which occupy
cluster peaks
some contribu
the mass rang

matrix compound in the desorption ionization process. In 1982, Macfarlane wrote that the "genius of FAB may not reside so much in the neutral charge state of the projectile but rather in the isolating, self-healing, powers of the solvated monomer in a mobile medium" (60). Benefits directly attributable to the presence of the liquid matrix include a decrease in fragmentation of the molecular adduct ion in comparison to desorption from a solid surface (31), and sustained, reproducible ion currents for long periods of time (56). Sample longevity combined with ease in sample preparation (no need to activate emitters or apply monolayer thicknesses of analyte) make FAB an extremely forgiving technique which requires a minimum of operator expertise. The "self-healing" characteristic of the matrix allows the use of very high primary particle fluxes (equivalent to that used in dynamic SIMS) without the pronounced accumulation of radiation-damaged products. The higher incident flux results directly in an increased secondary ion signal. No other desorption ionization technique enjoys all these advantages, especially at the relatively modest cost required for implementation of FAB on an existing mass spectrometer.

Although the FAB matrix provides great benefits for desorption ionization of nonvolatile species, it also introduces significant disadvantages. The most widely used matrix compound is glycerol, and Figure 1.3 shows the mass spectrum glycerol itself provides under conditions of fast atom bombardment. The protonated glycerol molecule gives a signal at m/z 93. At lower mass, peaks corresponding to fragment ions are evident. At higher mass, one notices the especially annoying tendency of glycerol molecules to form protonated clusters which occupy a very wide mass window. Not only are the individual protonated cluster peaks evident, but in the magnified regions of the spectrum one notices some contribution from the FAB matrix at essentially every m/z value throughout the mass range. The mass spectrum of the analyte will be superimposed in

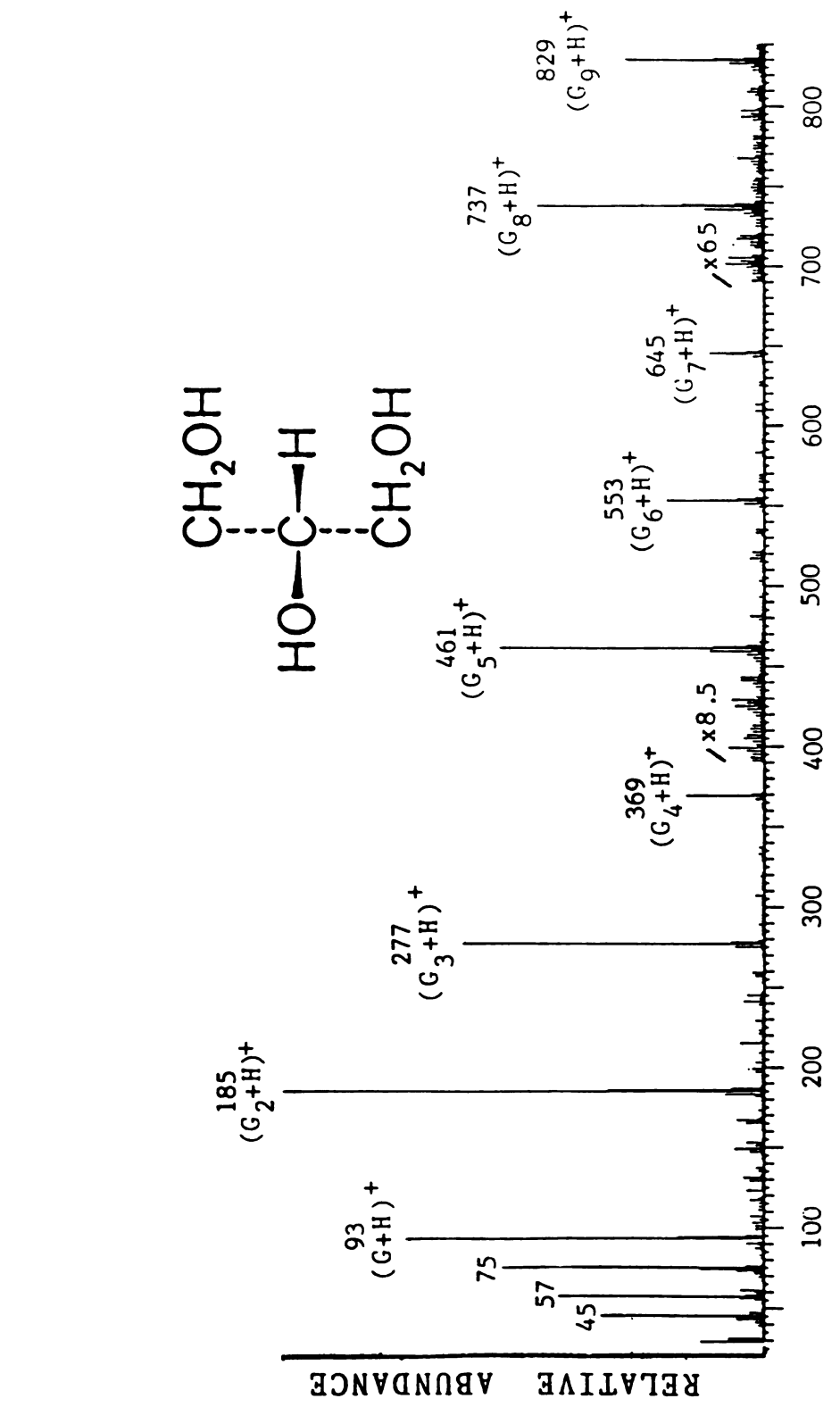

Figure 1.3. FAB mass spectrum of neat glycerol. Adapted from reference 182 with permission of the American Chemical Society.

some fa
spectrom
signals w
the sever
similar cl
extensive
On
backgroun
samples c
approach
of the mat
spectra ob
prevents
undersubtra
is evident if
etc.). Thes
resulting in
background
background
interference
interference
formulated b
Mater
certain prope
volatile liquid
reduced time
appears to be

some fashion over this interfering matrix spectrum, and so the mass spectrometrist is constantly striving to increase the magnitude of the analyte ion signals with respect to the interfering matrix ion signals. Glycerol is not unique in the severity of its spectral interference; the vast majority of FAB matrices exhibit similar clustering behavior, and the overall spectral interference is more extensive than that of glycerol in many cases.

One method for dealing with the matrix interference would involve background subtraction of the neat glycerol spectrum from spectra obtained with samples containing both the matrix and the analyte. This computer-assisted approach is associated with distinct shortcomings. For example, the intensities of the matrix peaks are different in spectra obtained from neat samples than in spectra obtained from mixtures containing the analyte. This complication prevents a valid background subtraction due to oversubtraction or undersubtraction of the matrix interference. Another difficulty with this approach is evident if the analyte contains any cationic impurities (e.g., sodium, potassium, etc.). These cations readily form adducts with glycerol and glycerol clusters, resulting in the appearance of additional peaks derived from the matrix background which were not apparent in the neat glycerol spectrum. Hence, such background subtraction is not a preferred method for eliminating the matrix interference. A very thorough treatment of the problems associated with matrix interference and various attempts to contend with these problems has been formulated by Ackermann (61).

Materials which have been used with success as FAB matrices share certain properties. They tend to be viscous liquids of limited volatility. More volatile liquids have been used, but they support desorption ionization for reduced time intervals. Some solubility of the analyte in the matrix compound appears to be essential, but superior results have been clearly demonstrated for

analytes which
more detailed
labile hydrogen
and basic matri
best choice w
attributes of a F
and a minimal
in the highly en

A survey
(62). As previo
matrix. Other
butanetriol. Th
for several ana
acid, thio-2,2'-b
dithioerythritol
melted in this
matrices in t
triethanolamine
molecules incl
excessive mat
nitrobenzyl alc
tetragol, and t
analysis of org
analysed by FA
reported the us
of individual m
application. S

analytes which preferentially concentrate in the surface layers of the matrix. A more detailed discussion of solubility considerations will follow. Matrices with labile hydrogens can promote protonation of analytes for positive ion detection, and basic matrices can likewise foster deprotonation to form negative ions. The best choice will clearly depend upon the properties of the analyte. Ideal attributes of a FAB matrix would also include minimal mass spectral background, and a minimal tendency to react adversely with other sample components, even in the highly energized environment of fast atom bombardment.

A survey of matrix compounds used in FAB was contributed by Gower (62). As previously mentioned, glycerol has been the most widely reported FAB matrix. Other highly hydroxylated matrices include aminoglycerol and 1,2,4-butanetriol. Thiols have been associated with increased sensitivity at high mass for several analytes (63-65). These matrices include thioglycerol, thioglycolic acid, thio-2,2'-bis(ethanol), and a 5:1 mixture of the solids dithiothreitol (DTT) and dithioerythritol (DTE), respectively, which form a liquid at room temperature when melted in this ratio (66). Basic compounds which are commonly used as matrices in the negative ion mode include diethanolamine (DEA) and triethanolamine (TEA). Less polar matrices which aid in the analysis of less polar molecules include polyethylene glycols (PEGs) (which often suffer from excessive matrix interference (67)), o-nitrophenyl octyl ether (NPOE), m-nitrobenzyl alcohol (NBA) (68), sulpholane (69), tetramethylenesulfone (70), tetragol, and teracol (71). Crown ethers have been used successfully in the analysis of organometallic compounds (72). Tetraphenyl porphyrins have been analysed by FAB in liquified pyrophosphoric acid (73). Caldwell and Gross have reported the use of dodecanol in the analysis of fatty acid mixtures (74). Mixtures of individual matrices are often used to enhance performance for a particular application. Sometimes cosolvents are added to increase the solubility of an

analyte in a

purpose (75

of several m

not meant to

and shows t

c. In

This

accomodate

and ion guns

matrices. A

technology (v

the electroch

equipment, w

As pre

experiments

samples (29,

practical due

and other ins

primary beam,

secondary ions

charge build-up

secondary ion

provided by Ag

experiment by

Such stringen

analyte in a particular matrix; dimethylsulphoxide (DMSO) has been used for this purpose (75). Unfortunately, DMSO also contributes to the background spectrum of several matrices (76). This list of FAB matrices and reported applications is not meant to be complete. Table 1.1 summarizes some commonly used matrices and shows their structures.

c. Instrumentation

This section will focus on the novel instrumentation developed to accomodate the FAB technique. It will begin with a description of both keV atom and ion guns which have been used to sputter secondary particles from liquid matrices. A brief discussion regarding the evolution of high field magnet technology (which has been spurred by the practice of FAB) will follow. Finally, the electrochemical FAB experiment, which requires somewhat specialized equipment, will be described.

As previously mentioned, some of the early fast atom bombardment experiments carried out in Manchester involved the direct sputtering of solid samples (29, 55). The use of a primary ion beam for such experiments was not practical due to problems associated with charge build-up in powders, polymers, and other insulating materials. Sample charging reduces the energy of the primary beam, and tends to deflect it away from the sample. The energies of the secondary ions sputtered from the surface also change as a function of time (or charge build-up), and this phenomenon results in substantial defocusing of the secondary ion beam. An excellent characterization of sample charging effects is provided by Appelhans (77). This problem is usually avoided in the static SIMS experiment by preparing the analyte in a very thin layer over a metal surface. Such stringent requirements in sample preparation, however, reduce the

Table

glyc

thio

dith

trie

m-n

o-n

Table 1.1. Several commonly used FAB matrices.

glycerol	$HOCH_2CH(OH)CH_2OH$
thioglycerol	$HSCH_2CH(OH)CH_2OH$
dithiothreitol/ dithioerythritol	$HSCH_2CH(OH)CH(OH)CH_2SH$
triethanolamine	$N(CH_2CH_2OH)_3$
m-nitrobenzyl alcohol	$HOCH_2C_6H_4NO_2$
o-nitrophenyl octyl ether	$C_8H_{17}OC_6H_4NO_2$

convenienc
alleviated t
advantage
magnetic s
acceleratio

As t
knowledge
influence c
neutral ato
developed

At l
relatively l
which is p
principles
of this gu
introduced
a round di
voltage ch
Sufficient
formation
The electr
the periph
the center
greatest k
energetic
of this el
cathode.

convenience with which SIMS can be practiced (30). A neutral primary beam alleviated the deleterious effects of sample charging (29, 77, 78). The other advantage of the neutral beam was to simplify implementation in high voltage magnetic sector instruments, where an ion gun must float at a potential above the acceleration potential (78).

As the use of liquid matrices became widespread in FAB, so did the knowledge that the charge state of the impacting particle did not significantly influence desorption ionization from the liquid (73, 79, 80). Therefore, both neutral atom guns and ion guns operating in the keV energy domain have been developed and applied to desorption ionization from liquids.

At least two types of fast atom guns have been sold commercially at relatively low cost. The first of these to be discussed is the saddle-field gun, which is produced by Ion Tech, Ltd. Figure 1.4 is helpful in understanding the principles of ionization and neutralization which are operative in the performance of this gun (81). A neutral bombardment gas (usually argon or xenon) is introduced into the high voltage region of the atom gun. The anode is shaped in a round disk (with a hole in its center) and is situated near the middle of the high voltage chamber. The periphery of this chamber is lined by the cathode. Sufficient voltage is applied to stimulate a discharge in the gas, resulting in the formation of a plasma containing positively charged ions, electrons, and neutrals. The electrons follow a well-defined path in this saddle field, due to repulsion by the peripheral cathode combined with attraction to the point of lowest potential in the center of the anode. During this repetitive cycle, the electrons possess their greatest kinetic energy while being accelerated toward the anode and are least energetic in the vicinity of the cathode where they change direction. In the midst of this electron cloud, positively charged ions are accelerated toward the cathode. Near the cathode they may interact with and capture a low energy

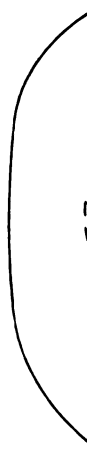

Figure 1.4.

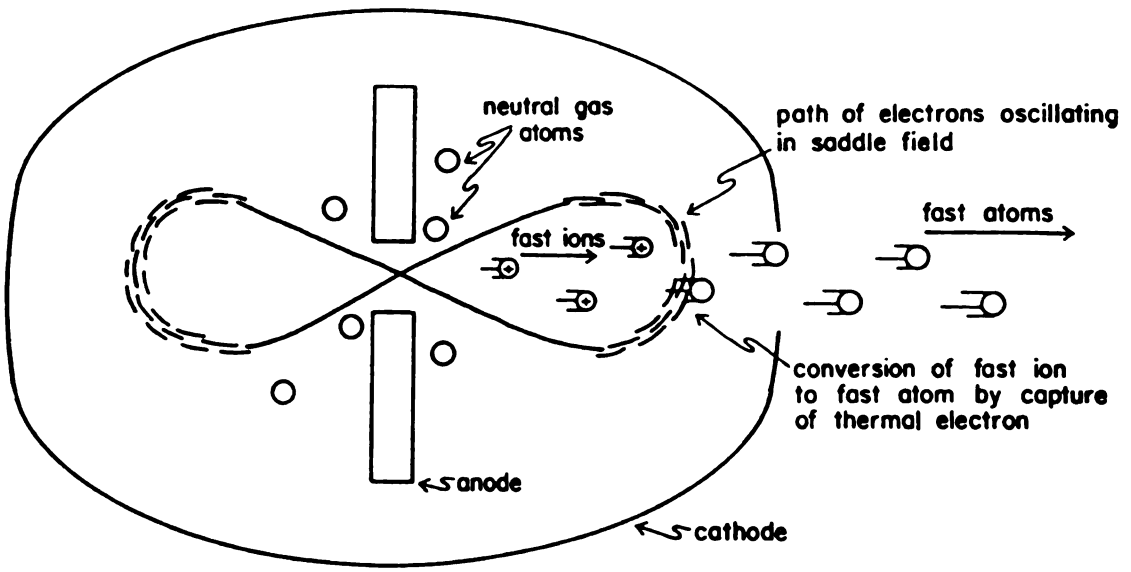

Figure 1.4. Depiction of ion formation and neutralization as it is believed to occur in the saddle-field fast atom gun. Reprinted from reference 99 (p. 210) with permisson of Raven Press.

electron

voltage

electron

produce

of the s

T

Reports

(81).

produc

numero

gun ma

the ca

capilla

design

Positiv

neutra

charge

the ion

ions fr

tip of

entry

this c

asser

vacu

availa

electron, resulting in neutralization. These fast atoms may then escape the high voltage region through an opening and impinge upon the sample. Captured electrons may be replaced by continued discharge or by secondary electrons produced when energetic particles strike the chamber wall. The characteristics of the saddle-field charged particle oscillator have been carefully studied (82).

The ionic contribution to the saddle-field primary beam has been debated. Reports from the manufacturer describe a very low ionic content (less than 1 %) (81). A study by Ligon, however, indicates that the xenon primary beam produced by an Ion Tech gun contains significant ionic character, including numerous multiply charged ions (83).

The second type of commercially produced FAB gun is the capillaritron gun manufactured by Phrasor Scientific, Inc. (84). Initial ionization of the gas in the capillaritron design occurs as the neutral gas flows toward the end of a capillary in the presence of a kilovolt potential gradient. As in the saddle-field design, a discharge occurs in the gas, resulting in the formation of a plasma. Positive ions are immediately accelerated by the electric field and some are neutralized by charge transfer with neutral gas atoms. A percentage of these charge-transfer interactions occur in "near-miss collisions" with negligible loss of the ion's initial momentum. Deflection plates are necessary to cleanse surviving ions from the emerging beam. Figure 1.5 depicts the processes occurring at the tip of the capillaritron nozzle. A novel design which does not require an extra entry port to the source of the mass spectrometer has been produced (85). In this configuration, the sample target and FAB gun are housed in the same probe assembly. Such an arrangement eliminates the need for modification of the vacuum flange or ion source in those cases where a convenient entry port is not available.

Figure 1

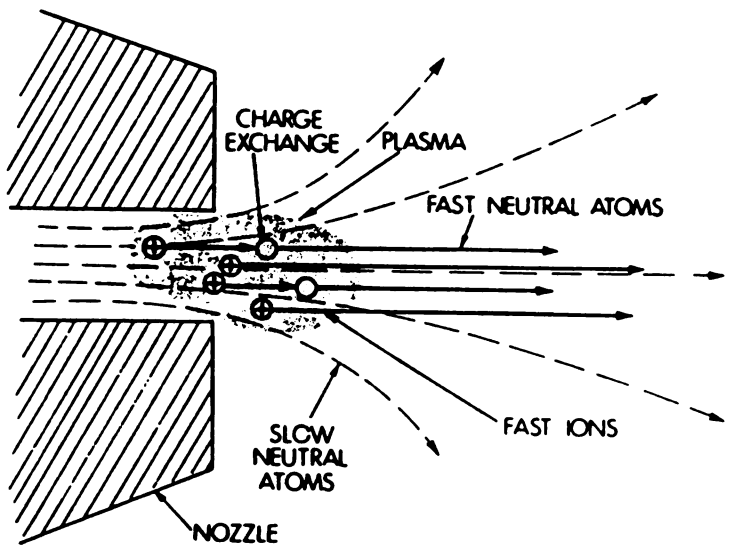

Figure 1.5. Depiction of ion neutralization by charge transfer occurring at the nozzle of the capillaritron fast atom gun. Reprinted from reference 84 with permission of John Wiley and Sons Ltd.

incide

throug

to the

(86).

mecha

well-s

captur

There

electr

and a

time f

Rema

summ

where

a bear

second

from

quanti

The l

achiev

lifetime

attentio

The FAB guns described above produce a very broad, unfocused flux of incident particles due to the difficulties involved in maintaining a focused beam through the process of ion neutralization. Some interesting recent work has led to the development of a focused, rasterable beam of sulfur hexafluoride neutrals (86). Formation of such a beam is realized through a novel neutralization mechanism known as autoneutralization. The sulfur hexafluoride molecule is well-suited for autoneutralization because its properties include a high electron capture cross section combined with a relatively low electron affinity (c.a., 1 eV). Therefore, sulfur hexafluoride neutrals placed in an environment conducive to electron capture will tend to form negative ions. These ions can then be focused and accelerated down a flight tube of reasonable length (c.a., 18 cm) to provide time for ions in certain autoneutralizing excited states to expel an electron. Remaining ions are deflected from the neutral beam. The entire process is summarized by the following reactions:

$$SF_6 + e^- \rightarrow SF_6^{-*} \xrightarrow{k} SF_6 + e^-$$

where 1/k (the mean lifetime of SF_6^{-*}) is 10-20 us. The future application of such a beam in desorption ionization should be interesting.

Work in different laboratories has documented an increase in the secondary ion yields obtained by pulsing the FAB beam in comparison to results from continuous bombardment (87, 88). Tecklenburg, Castro, and Russell quantify this effect with comparative experiments utilizing a saddle-field gun (89). The latter study discusses the importance of the higher beam densities achievable in the pulsed mode, and reports a dramatic increase in sample lifetime evident from the pulsed experiments. This phenomenon warrants further attention.

In

sensitivi

(90). I

activate

interacti

process

section

FAB gu

Aberth.

In

positive

(80). Th

cesium

°C). Th

pedesta

seconda

guns wh

ion yield

of a supp

effect wi

term "liq

matrices

laborator

secondar

Ac

those of

advantag

In a discussion of the various parameters which affect high mass sensitivity, Aberth points out the problems due to pressure effects in the source (90). Ions accelerated to a high energy can decompose through collisionally activated dissociation (CAD) or be neutralized by charge exchange, due to interaction with a low energy neutral gas. An increase in the efficiency of these processes is suggested for higher mass ions, partially due to an enhanced cross section for interaction. The gas load attendant to the conventional operation of FAB guns is typically sufficient to produce the deleterious effects documented by Aberth.

In 1982, a keV particle gun was developed which produced a beam of positive cesium ions, while not contributing significantly to the source pressure (80). The cesium beam was formed by the evaporation of cesium ions from a cesium alumina silicate surface (requiring temperatures of approximately 1000 ^{o}C). The cesium ions could then be focused and accelerated toward the sample pedestal. Operation of the cesium gun was observed to provide increased secondary ion yields from liquid samples in comparison to conventional FAB guns which utilized argon or xenon primary beams. The increase in secondary ion yield is more pronounced for higher mass ions, and is related to the absence of a supporting gas and the larger mass of the incident particle (73, 90); the latter effect will be discussed in more detail in the section regarding mechanisms. The term "liquid SIMS" originated from this initial work involving sputtering from liquid matrices by a cesium ion beam (80). A subsequent study from the same laboratory investigated the influence of the orientation between the primary and secondary ion beams upon desorption ionization from liquid matrices (91).

Advantages of focusing the primary beam to dimensions smaller than those of the sample were reported by Stoll, Harvan, and Hass (92). These advantages include a significant increase in the analyte signal with respect to the

chemical background, and a concurrent increase in the sample lifetime. A xenon primary beam was used for this work. Various types of ion guns with different capacities for focusing have been developed and applied to sputtering from liquid matrices (93-96). Pulsed ion guns allow the coupling of liquid SIMS with time-of-flight mass analysis (97, 98).

The maturation of FAB both stimulated and required the simultaneous maturation of high mass instrumentation. This impetus was especially felt in the manufacture of high field magnetic sector mass spectrometers. The abundant and prolonged secondary ion yields produced by FAB were ideal for exploitation of the high resolution capabilities of multisector magnetic instruments. However, in the early 1980s, the mass range of such instruments was clearly not sufficient to accomodate the potential of FAB. The mass-to-charge ratio (m/z) for an ion which impinges upon a detector after having traversed a magnetic field in a vacuum is (99)

$$m/z = r^2B^2/2V$$

In this expression, r is known as the radius of the magnet and corresponds to the radius characterizing the circular orbit followed by selected ions in the magnetic field. B represents the magnetic field strength and V denotes the acceleration potential. Early successes in detecting high mass ions produced by FAB were often achieved by reducing the acceleration potential of the instrument, and thereby substantially sacrificing sensitivity (100). Efforts to improve the mass range by enlarging the radius of the magnet, as well as by increasing the magnetic field strength quickly developed. Instrument companies which made (and continue to make) substantial contributions in this area include Kratos, VG Analytical, and JEOL. Progress has been rapid and impressive. In the mid-

1970s, t
full sens
mass ra
lies bey
reviews
attentio
organic
the less
nitroger
an exte
observe
represe
average
charact
electroc
originat
volatility
apparat
potentia
range.
high die
have de
some no
with this

1970s, the upper mass limit for commercially available instruments operating at full sensitivity was 1500 u; today, instruments are available with ten times that mass range at full acceleration potential (101). A detailed treatment of this topic lies beyond the scope of this dissertation, but is the subject of at least two reviews (102, 103).

The desire to achieve well-resolved spectra at high mass has focused attention on one issue which received little previous discussion. Very large organic ions (especially those larger than 5,000 u) contain significant numbers of the less abundant isotopes of the individual atoms (e.g., carbon, oxygen, and nitrogen). Measurable populations of these ions actually exist as represented by an extensive multiplet of isotope peaks. In many cases, the most intense peak observed in the multiplet can be several mass units removed from the peak representing the monoisotopic ions. In these situations, determination of the average mass of the ion envelope has been suggested as a means of characterizing the mass associated with the collective signal (104, 105).

A FAB experiment which requires very unique instrumentation is the electrochemically assisted FAB technique (E-FAB) (106-108). This experiment originated in an attempt to address the relatively nonpolar molecules of limited volatility which often prove troublesome for conventional FAB analysis. The apparatus consists of a ring-disk electrode (109) on the FAB probe tip. The potential difference between the ring and disk electrodes is variable over a ±15 V range. Glycerol is a reasonable solvent for electrochemistry, due to its relatively high dielectric constant of 42. Using this arrangement, Bartmess and Phillips have demonstrated the ability to substantially enhance the ion abundances for some nonpolar compounds by increasing an applied potential. A major difficulty with this approach for accomplishing the stated objective appears to be the

procureme

analyte, w

d. C

The

important

Caprioli an

novel appr

shown sch

beam via

stainless st

length of t

arrangemer

in solution.

Tran

problematic

introduced

solution cou

analyte solu

introduction

both evapo

compound f

for analyses

quickly bec

solutions.

procurement of nonvolatile matrix compounds which will solubilize the nonpolar analyte, while simultaneously conducting adequate electrical current.

d. Continuous-Flow FAB

The origin of the continuous-flow sample probe represents an extremely important event in the optimization and application of FAB-MS (110). Richard Caprioli and coworkers at the University of Texas Medical School developed this novel approach for continuous sample introduction. The apparatus involved is shown schematically in Figure 1.6. Analyte and matrix are presented to the FAB beam via transport through a fused silica capillary which is encased by a stainless steel shaft. The capillary tube extends from the probe tip, through the length of the flow probe, and finally to the exterior of the instrument. This arrangement allows for convenient and continuous sampling of analytes present in solution.

Transport of the glycerol matrix through the narrow bore capillary can be problematic due to the viscous nature of glycerol; therefore, the glycerol was introduced as a dilute aqueous solution (c.a., 10-20%). The glycerol support solution could then be pumped into the flow probe (where it was mixed with the analyte solution) at a constant rate (typically, 5-10 ul/min). This rate of glycerol introduction combined with the rate of glycerol depletion at the probe tip (through both evaporation and sputtering), permitted the analysis of the nonvolatile compound from significantly smaller portions of matrix than were commonly used for analyses with the conventional direct probe. Important analytical advantages quickly became associated with the use of these dilute aqueous glycerol solutions.

Figure

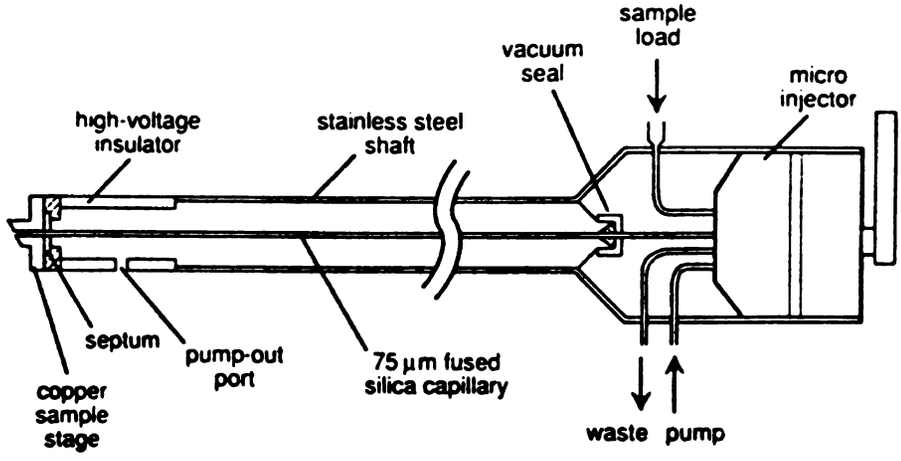

Figure 1.6. Diagram of the continuous-flow FAB probe. Reprinted from reference 115 with permission of Elsevier Science Publishers.

increas
was fou
with an
detectio
comple
sugges
analysis
desirab
be dev
spectra
may re
differen
more hy
obtained
compara
when su
of pepti
suppres
Data ob
continuo
mixtures
mapping
(115).
analyte s

Initially, the most apparent of these advantages was a pronounced increase in the ratio of analyte signal to chemical background. This observation was found to result from a dramatic decrease in glycerol ion abundances coupled with an increase in analyte ion abundances (111). A substantial decrease in the detection limit for various analytes was demonstrated as the net effect of these complementary factors. An explanation to account for these observations was suggested and will be discussed in a subsequent section.

Another advantage of the continuous-flow approach was discovered in the analysis of peptide mixtures (112). Brief mention has already been made of the desirability of concentrating the analyte in the surface layers of the matrix. As will be developed more fully, this requirement is important because FAB mass spectra tend to reflect the surface composition of the sample. This consideration may result in uneven sampling efficiencies for different analytes which have different surface activities in the matrix. For example, signals obtained from a more hydrophobic peptide mixed in glycerol tend to be more intense than signals obtained from an equivalent amount of a less hydrophobic peptide mixed in a comparable portion of glycerol (63). These inequities tend to be exacerbated when such compounds are sampled together as a mixture in the matrix. Studies of peptide mixtures have demonstrated that more surface-active components suppress desorption ionization of less surface-active components (113, 114). Data obtained from aqueous glycerol solutions used in conjunction with the continuous-flow probe indicate substantially minimized suppression effects for mixtures of peptides. This feature provides a great advantage for the FAB mapping of proteins and peptides (113).

Continuous-flow FAB has been practiced in two distinct operating modes (115). The "constant-flow" mode involves the continuous introduction of the analyte solution to the probe tip. In the "flow-injection" mode, sample introduction

is acco

automa

liquid t

optima

spuriou

probe

appare

of Cap

involve

119).

mixture

CF-FA

continu

has rec

for cap

FAB-M

(126, 1

Caprio

use of

with a

growing

has be

electrop

the co

is accomplished at discrete time intervals. Operation of both modes can be automated.

Careful control of experimental parameters such as the flow rate of the liquid to the probe tip and the temperature of the probe tip is critical for the optimal and reproducible operation of CF-FAB. Failure in this regard results in spurious and unstable ion currents. During stable operation, the surface of the probe tip appears to be wetted with a viscous liquid, but no defined droplet is apparent (110).

The potential applications of CF-FAB are far-reaching and exciting. Much of Caprioli's work immediately prior to development of the continuous-flow probe involved determining kinetic constants for biological reactions by FAB-MS (116-119). Such work was often done by analyzing individual aliquots of the reaction mixture with the direct probe at discrete intervals after the reaction had begun. CF-FAB provides a convenient means for monitoring reactions (115). The use of continuous-flow interfaces for the coupling of liquid chromatography with FAB-MS has received considerable recent attention (120-123). Continuous-flow interfaces for capillary electrophoresis/FAB-MS have also been reported (124, 125). CF-FAB-MS/MS results have been obtained with triple quadrupole mass analyzers (126, 127). Quantitation has been performed by continuous-flow FAB (122, 126). Caprioli suggests the ability to quantitate (by determining peak areas) without the use of internal standards (115). Accurate mass measurements have been made with a continuous-flow system (128). Two reviews concerning CF-FAB and its growing application are referenced (115, 129).

Recently, a continuous-flow probe incorporating coaxial capillary columns has been developed for both liquid chromatography/FAB-MS and capillary electrophoresis/FAB-MS (123, 124). This design allows independent delivery of the column effluent and the FAB matrix to the probe tip. Benefits of this

configura

eliminati

the end

undesira

step. A

e.

W

by certa

associat

achievin

deviation

curves.

measurin

matrix si

(131) (a

calculati

because

suppress

mixtures

quantitat

No

been obs

for this e

be largely

133, 134)

configuration include the ability to differentially optimize both flow rates, and the elimination of a transfer line (for mixing the matrix and analyte solutions) between the end of the column and the probe tip. Such transfer lines are generally undesirable because they inevitably lead to band broadening after the separation step. A diagram of the coaxial interface is shown in Figure 1.7.

e. Quantitation

Widespread and routine quantitation using FAB-MS has been hampered by certain aspects of the experiment (130). The extensive background signal associated with FAB detracts from the detectability of the analyte, and in achieving good accuracy and precision in quantitative analyses. Positive deviations from linearity are commonly observed near the origin of calibration curves. This effect has been associated with the difficulty in accurately measuring analyte signals of approximately the same intensity as interfering matrix signals which exist at essentially every m/z value in the mass spectrum (131) (a helpful device in this situation may be the unique signal to background calculation suggested by Ackermann and coworkers (132)). Furthermore, because FAB mass spectra tend to reflect the surface composition of the sample, suppression effects due to surface-active impurities or other components of mixtures can substantially reduce analyte signals and otherwise complicate quantitation.

Nonlinearities in ion signal for relatively large amounts of analyte have been observed by several investigators (63, 70, 131, 133, 134). An explanation for this effect has been advanced and will be discussed later. This problem can be largely overcome by the use of isotopically labeled internal standards (131, 133, 134). According to Beckner and Caprioli, one can expect linear and reliable

Figu

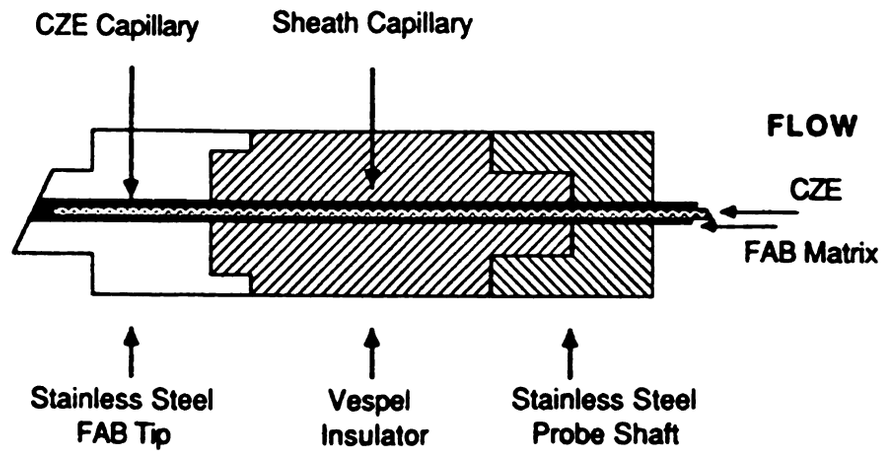

Figure 1.7. Diagram of the coaxial continuous-flow probe. Reprinted from reference 124 with permission of Heydon and Son Ltd.

resu

stan

conv

the

from

pea

one

elen

refe

this

pre

unk

Kno

acc

pea

(99

ioni

pea

extr

mas

in j

det

results for analyte concentrations from one tenth to ten times that of the internal standard (134). Several examples of successful quantitative analyses by conventional FAB-MS using internal standards are provided (131, 133-137).

f. Accurate Mass Measurements

FAB is well-suited for accurate mass measurements, particularly due to the sustained and reproducible secondary ion currents obtained by sputtering from liquid matrices. The most commonly used method to accomplish this goal is peak matching. To perform an accurate mass measurement by peak matching, one must have available a reference signal (corresponding to an ion of known elemental composition) within 10 % of the unknown mass to be determined. The reference signal may be provided by an internal or an external standard. Once this requirement is met, the magnetic field strength may be held constant while precise manipulation of the acceleration potential serves to superimpose the unknown and reference signals on alternate sweeps of an oscilloscope. Knowledge of the exact mass of the reference ion combined with the ratio of the acceleration potentials necessary to superimpose the reference and unknown peaks is sufficient to provide an accurate mass determination (within 10 ppm) (99).

Although high resolution is desirable when peak matching with any ionization technique, it is especially important with FAB in order to resolve the peak of interest from the widespread background signals. Contribution of any extraneous signals to the peak-matched signal will degrade the accuracy of the mass determination. Because high resolution conditions necessitate a decrease in ion transmission through the mass spectrometer, specialized and sensitive detection schemes have been investigated for use with peak matching (138).

The c
matching by
standards, b
high mass) r
Suppression
confound at
mass range.
sample targ
which desorp
unknown sar
compete for
reported in c
compromise
in mass det
developmen
could be ob
measureme
determined
Accu
careful sca
standards c
ability to de
run.

The choice of mass standards represents a particular concern when peak matching by FAB-MS. Matrix peaks often can be used conveniently as internal standards, but many times the scarcity of intense matrix signals (especially at high mass) requires spiking the sample with an additional reference compound. Suppression effects caused by analyte, matrix, or reference compound may confound attempts to produce two relatively intense signals within a desired mass range. The use of external standards has been explored with special split sample targets. Such probe tips contain at least two distinct platforms from which desorption ionization can occur. The idea is to irradiate both reference and unknown samples simultaneously, without allowing them to mix on the probe and compete for the same liquid surface. Unfortunately, difficulties have been reported in optimizing the focus for both samples at the same time. Attempts to compromise the focus between the two samples resulted in unacceptable errors in mass determination. A resourceful approach to this problem involved the development of a rotatable probe from which identical optimal focus conditions could be obtained for both reference and unknown samples (139). Exact mass measurements made with this probe were nearly as accurate as those determined with internal standards.

Accurate mass determinations have also been accomplished through very careful scanning of the instrument (140, 141). Both internal and external standards can be used with this approach. A benefit inherent to this mode is the ability to determine accurate mass values for several different signals in the same run.

g

F

spectror

when co

advanta

protonat

measuri

(althoug

Comple

between

applicati

readily c

This app

compour

C

molecula

daughte

apparen

reduced

target ga

charge-t

is compe

been em

improved

high volta

experime

g. FAB-MS/MS

FAB has been employed as a source of ions for mass spectrometry/mass spectrometry (MS/MS) experiments. This instrumental configuration, especially when combined with collisionally activated dissociation (CAD), provides several advantages for sputtering from liquid matrices. For example, selecting the protonated molecule of an analyte with the first mass analyzer and subsequently measuring the daughter ion spectrum after CAD, is an extremely effective (although expensive) means of eliminating the interfering matrix spectrum (142). Complex and unusual interactions between analyte and matrix (143), as well as between the analyte and itself (144), have been understood by the powerful application of MS/MS. Mass spectra characteristic of a single compound can be readily obtained from complex mixtures with tandem mass spectrometry (145). This approach also has been used to advantage for the differentiation of isomeric compounds by FAB (146).

CAD constitutes a powerful tool for inducing fragmentation. As the molecular weight of the parent ion increases, however, a decrease in the daughter ion yield is generally observed. This has been explained by the apparent decrease in parent ion intensity with increasing mass, coupled with a reduced efficiency for CAD (147). The latter observation may result partially from target gas excitation by the energetic, high mass ion through processes including charge-transfer reactions. It has been suggested that such target gas excitation is competitive with collisional activation (148, 149). Different approaches have been employed for collisional activation of large ions. Several laboratories show improved results from high energy (keV collisions) CAD experiments involving high voltage sector instruments, in comparison to low energy (eV collisions) CAD experiments involving quadrupole or hybrid instruments (150, 151). Accordingly,

very hi

constru

publica

longer

flight i

accele

consis

accom

The e

quadru

associ

recent

biologi

glycos

mass s

major

Early w

the chr

beam t

been c

Disadva

source

sputteri

very high performance (and expensive) multiple sector instruments have been constructed which can provide high resolution MS/MS data (152). A recent publication has demonstrated an increased tendency for large ions to fragment at longer ion residence times. This kinetic study was accomplished with a time-of-flight instrument on which ion residence times were increased by reducing the acceleration voltage and delaying ion extraction (153). Such an observation is consistent with the belief that a decrease in the rate constant for decomposition accompanies an increase in the number of internal degrees of freedom (154). The enhanced fragmentation at longer residence times has been exploited on quadrupole instruments, where the analysis time is significantly longer than that associated with high energy sector instruments (155). Tomer has provided a recent review of FAB-MS/MS (156), and also a very thorough compendium of biological applications for peptides, nucleosides, nucleotides, saccharides, glycosides, bile salts, steroid conjugates, and phospholipids (157).

h. LC/FAB-MS

A field of great interest involves the coupling of liquid chromatography with mass spectrometry. This discussion will confine itself to a brief mention of the major happenings which have contributed to the development of LC/FAB-MS. Early work in this area incorporated a moving belt to transport the effluent from the chromatographic column into the source of the mass spectrometer. The FAB beam then sputtered the sample directly off the surface of the belt. Results have been obtained both with and without addition of a liquid matrix (158, 159). Disadvantages inherent in the use of this interface include the need for significant source modification as well as a lack of sensitivity due to difficulties in efficiently sputtering material from the belt. Ito and coworkers developed an interface in

which th

transpor

source t

the cap

interfac

F

include

(162). A

layer ch

IV. Mec

T

spectro

volume

need fo

analysis

mechan

for the p

attempt

observe

conside

energy

from th

particle

the soft

by mean

which the column effluent is combined with an aqueous glycerol solution and transported to the mass spectrometer source by way of a capillary. Inside the source the sample is sputtered directly from a frit which is attached to the end of the capillary (160, 161). The operation of continuous-flow FAB as an LC/MS interface has been described (120-123).

Finally, FAB experiments carried out subsequent to a separation step include the analysis of bands formed by polyacrylamide gel electrophoresis runs (162). Also, liquid SIMS has been used directly to characterize the spots on thin layer chromatography plates (163).

IV. Mechanistic Considerations

The practice of desorption ionization has become widespread in the mass spectrometry community. This popularity (which is evidenced by the significant volume of research that this chapter attempts to summarize) attests to a great need for the advantages inherent to mass spectrometry with regard to the analysis of nonvolatile species. Unfortunately, a clear understanding of the mechanisms operative in desorption ionization is not so widespread. Especially for the particle impact techniques, much debate and confusion accompanies any attempt to identify and prioritize a few factors of overriding importance to the observed results. A lack of concensus about these matters is not surprising considering the complexity of these experiments, particularly with regard to energy transfer. Indeed, the observation of any molecular weight information from thermally fragile, nonvolatile molecules subjected to conditions of keV particle bombardment is, in itself, remarkable. The phenomenon is tantamount to the soft vertical propulsion of intact, whole eggs from a carefully arranged stack, by means of repeated and vigorous blows with a sledgehammer. Elucidation of

the mech

rigorous u

importanc

address t

a.

A

technique

available

technique

have bee

tendency

desorptio

form abu

(3-10).)

attention,

the vario

number o

upon the

analysis

laser des

preferent

N

discussio

events in

models h

the mechanism is further complicated by introduction of a liquid matrix. A rigorous understanding of the fundamental processes involved, and their relative importance , is critical for continued refinement of FAB. This discussion will address the considerable effort put forth to realize this objective.

a. Unified Models

A general observation regarding many of the desorption ionization techniques pertains to similarities in the appearance of the mass spectral data available from each. Various comparisons in the performance of different techniques for the analysis of a particular compound (or class of compounds) have been documented (164-170). The most striking spectral similarity is in the tendency to produce stable, even-electron ions from the analyte. (Field desorption is not usually included in this group, due to its pronounced capacity to form abundant odd-electron ions. A separate theory has been formulated for FD (3-10).) The tendency to produce even-electron ions has received much attention, although significant differences are also evident in spectra obtained by the various techniques. For example, the degree of fragmentation and the number of fragmentation pathways stimulated for the analyte is highly dependent upon the technique employed. Also, a very interesting study involving the direct analysis of lyophilized membranes and cells by FAB, plasma desorption, and laser desorption reveals the proclivity of the different techniques to desorb/ionize preferentially different classes of compounds from these complex mixtures (168).

Nevertheless, the observed spectral similarities have stimulated much discussion about the applicability of a unified model to describe collectively the events involved in desorption ionization for the various techniques. Several such models have been proposed, usually with emphasis placed on characteristics of

the techn

models w

Th

was large

of four m

at the sa

to the sa

which it

capacity

spike ver

LD. Coll

point of

by the is

impact.

desorptio

only cont

could ha

after des

ion/molec

to a very

layer adj

approxim

be on the

substantia

environme

could eas

spectra.)

the technique with which the author is most intimately acquainted. Two unified models will be considered here.

The first was published by Cooks and Busch in 1983 (171). This model was largely influenced by their extensive experience with SIMS. It is composed of four major points. The first point suggests isomerization of the primary energy at the sample surface. Alternatively stated, this means that the energy imparted to the sample is transmuted to a common form, regardless of the means by which it was imparted. An example of energy isomerization would be the capacity of a collision cascade (triggered by particle impact) to produce a thermal spike very closely related to the thermal activation provided by a laser pulse in LD. Collision cascades will be considered in more detail presently. The second point of the model describes a low energy desorption event which is stimulated by the isomerized energy at some discrete distance from the point of particle impact. Thirdly, Cooks and Busch advocate separate consideration of the desorption and ionization processes. Therefore, everything described thus far only contributes to desorption of the species from the sample surface. Ionization could have been accomplished prior to energy deposition (preformed ions), or after desorption of the neutral. The latter process would probably occur as an ion/molecule reaction in the selvedge region. (The term "selvedge" (172) refers to a very high pressure plasma formed by particle impact, which is localized in a layer adjacent to the sample surface. Pachuta and Cooks have performed approximate calculations which suggest the pressure of the selvedge region to be on the order of 3.5×10^4 torr for molecular SIMS. They suggest it would be substantially higher when sputtering from a liquid surface (26). In such an environment, one would expect a large number of gas phase collisions which could easily dictate the nature of the ions observed in the resulting mass spectra.) The final point in this model attributes the significant fragmentation

apparen
adduct i
importar
M
may hav
Vestal r
supplied
least loc
the forr
These
evapora
constitu
which e
some c
(within t
clusters
charged
cluster
intermed
adduct f
S
thought-
somewh
The rem
mechani
those inv

apparent in the mass spectrum to unimolecular dissociation of the molecular adduct ions in the gas phase. Figure 1.8 provides a compact summary of the important features of this model.

Marvin Vestal also proposed a unified model in 1983 (19). This model may have been significantly influenced by his development of thermospray. The Vestal model also is composed of four major points. First, energy must be supplied rapidly enough to superheat a liquid sample, or melt a solid sample (at least locally) and then superheat the resulting liquid. The second point suggests the formation of bubbles underneath the surface of the superheated liquid. These bubbles might be produced by dissolved gases in the liquid or the evaporation of volatile impurities. Boiling of these bubbles to the surface constitutes the third step. This is described as a rapid, nonequilibrium process which emits a spray of charged and neutral clusters from the liquid. Finally, some charged clusters which contain the nonvolatile analyte rapidly desolvate (within the time scale of the analysis) to form molecular adduct ions. Neutral clusters may participate in ion/molecule reactions at this point to become charged. An important feature of this model is the formation of a highly solvated cluster containing the analyte in the gas phase. The cluster serves as an intermediate vehicle for the analyte between energy deposition and molecular adduct formation.

Speculation about unified theories is very interesting and has led to thought-provoking ideas. The utility of such models, however, is restricted to a somewhat general treatment of the processes attendant to desorption ionization. The remainder of this section will attempt to focus more exclusively on the mechanisitic concerns associated with keV particle impact techniques, especially those involving sputtering from liquid matrices.

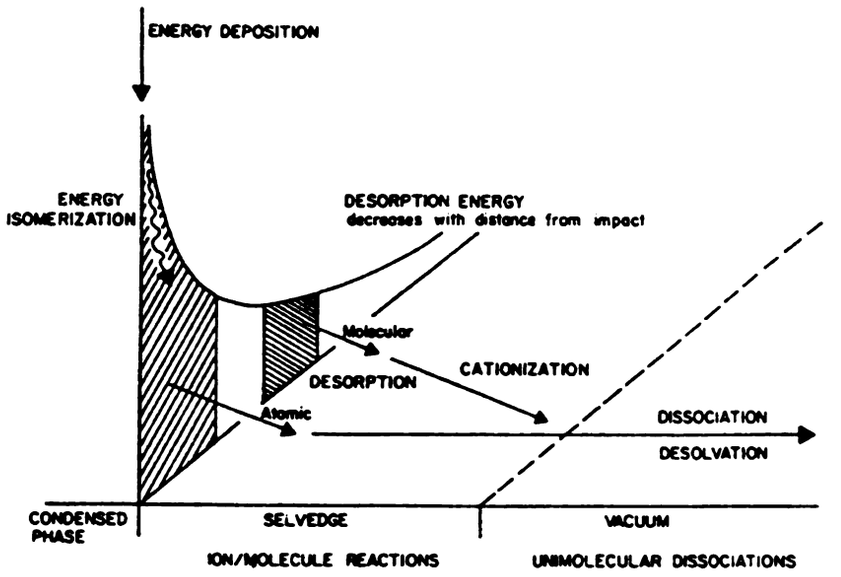

Figure 1.8. Schematic diagram of the unified model for desorption ionization proposed by Cooks and Busch in 1983. Reprinted from reference 171 with permission of Elsevier Science Publishers.

b.

At
collection
constitutes
process is
the contex
area is ch
atoms are
These ato
the prima
which em
affected b
approxima
dissipation

The
upon dista
the immed
transfer in
unstable f
thought to
nuclear e
discussion
ejection o
thermalize
proposed

b. Energy Deposition

At keV energies, an incident particle perceives an organic sample as a collection of individual atoms. Momentum transfer to the sample atoms constitutes the primary means of energy loss for the incident particle. This process is known as a collision cascade and has been studied, especially within the context of atomic and molecular SIMS (25, 173, 174). The immediate impact area is characterized by significant bond breakage and sample damage as many atoms are displaced or recoiled by a direct collision with the primary particle. These atoms, in turn, collide with additional atoms in the sample and propagate the primary energy through a "cascade" of nuclear, collision-like interactions which emanate in all directions from the point of impact. The surface area affected by the collision cascade has been estimated in one instance to be approximately 200 A^2 (175). Figure 1.9 shows an artist's conception of energy dissipation occurring by means of a collision cascade.

The degree of sample excitation along the collision cascade depends upon distance from the impact site. The most highly energized region will be in the immediate vicinity of the primary particle impact. Rapid and intense energy transfer in this area extensively damages the sample, producing prolific and unstable fragmentation. Neutrals, ions, radicals, electrons, and photons are all thought to inhabit this catastrophic environment (176). Significant conversion of nuclear excitation into electronic excitation (a process usually confined to discussions of MeV particle impact) is even postulated by Michl to result in the ejection of free electrons (173). Michl also discusses the possibility of a thermalized electron population in this highly activated region. It has been proposed that the widespread chemical noise (or contribution at every mass)

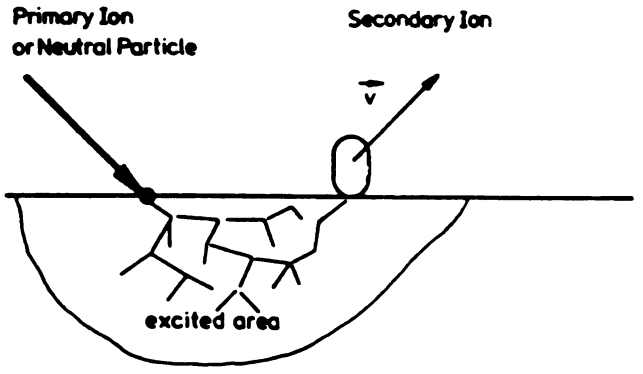

Figure 1.9. Artist's conception of energy transfer through a collision cascade. Adapted from reference 178 with permission of Elsevier Science Publishers.

obse

impa

conti

Activ

mod

addu

repr

from

this

Mar

(nor

ass

fail

sur

key

ion

for

ren

val

fra

wi

re

pr

in

observed in FAB spectra arises from the tumultuous events occurring near the impact site (177).

As the collision cascade propagates away from the impact site and continually transfers energy to the cold surroundings, it begins to quench. Activation of the sample at the far reaches of the cascade becomes much more moderate. It is believed that ejection of large, intact molecules and molecular adducts occurs at a distinct distance from the hot impact site (178), as represented in Figure 1.9. This process may be described as a concerted push from a dense linear cascade which terminates at the surface (25). Alternatively, this lower energy desorption might be characterized as a largely thermal process. Many workers believe that the collision cascade terminates in a transient (nonequilibrium), but intense, thermal spike (173, 179). Maximum temperatures associated with the spike have been estimated to be near 10^4 K (180).

In describing the events associated with a collision cascade, one must not fail to consider the localized transformation of some fraction of the impacted surface into a high pressure, high temperature gas, or selvedge region. This is a key feature of many of the mechanisms advanced to describe desorption ionization by particle impact (171-173, 179, 181). An explosive evaporation to form the selvedge may be a direct result of the thermal spike. It should also be remembered that the previous discussion of a collision cascade is considered as valid for a liquid sample as it is for a solid sample. This is due to the short time frame of a collision cascade (c.a., 10^{-13}-10^{-12} sec) during which a liquid sample will appear essentially indistinguishable from a solid sample (25). Finally, a review concerning the role of the collision cascade in desorption ionization is provided by Pachuta and Cooks, and recommended as a reference for the interested reader (179).

Several parameters associated with primary beam impact are important for optimization of the experiment. One of these is the angle with which the primary beam intersects the sample surface. This incident angle is measured between the primary beam vector and the normal to the surface of the sample pedestal. Systematic studies have shown the optimum incident angle (in terms of maximizing secondary ion abundance) to be within the range of 60°-70° (55, 182, 183). Such large, grazing angles tend to localize energy deposition into the surface region of the sample. Three-dimensional Monte Carlo calculations performed by Magee show a much greater tendency of the collision cascade to intersect with the sample surface, especially at long distances from the impact site, for these larger sputtering angles (25).

Another parameter of interest is the angle between the primary beam and the secondary ion beam. An interesting study involving liquid SIMS (91) varied this angle while maintaining a constant incident angle between the primary beam and the sample. The results showed a significant increase in high mass analyte ion abundance for vitamin B_{12} (molecular weight of 1354 u) and Met-Lys-bradykinin (molecular weight of 1318 u) by employing a nearly linear geometry of primary and secondary ion beams, in comparison to the more conventional 90° geometry, or a 70° angle between the two ion beams. This observation suggests that the nearly "in-line" geometry allows a more efficient collection of those secondary ions desorbed in a direction approximately equal to that of the momentum of the primary particle. It was also noted that the optimal primary ion current for the in-line geometry was substantially lower than that characteristic of the 90° geometry. Unfortunately, the in-line geometry also provided greater abundances for the high mass glycerol cluster ions than did the other configurations.

abund

increa

improv

carrie

xenor

neon

intens

prima

cons

dicta

parti

incr

ene

per

cor

ver

Ab

a 5

lic

a

to

The mass of the incident particle is an important factor in determining the abundance of the secondary ion yield. Several different studies indicate that increasing the mass of the primary particle (at constant kinetic energy) results in improved sensitivity (182, 184, 185). These comparisons have generally been carried out with monatomic noble gases, and show superior performance for xenon in comparison to argon, which in turn provides better sensitivity than a neon primary beam (182). One study directly correlates the secondary ion intensity with the momentum of the primary atom (182). Consideration of the primary particle mass provides insight into the basis for a cesium ion beam constituting a favorable alternative (73, 90).

Consistent with the observation that primary beam momentum appears to dictate sputtering yields are the results of studies in which the energy of a particular incident particle is varied. In general, these studies document an increase in secondary ion yield (especially at high mass) as the primary beam energy is increased (90, 183). This factor also explains the enhanced performance of cesium guns, which commonly operate at higher energies than commercially available FAB guns (which are typically restricted to 0-10 keV). A very interesting investigation into this experimental parameter was conducted by Aberth and Burlingame, who used a cesium beam which could be adjusted within a 5-30 keV range (186).

c. Role of the Matrix

As noted previously, important advantages are associated with the use of liquid matrices in conjunction with keV particle impact techniques. Among these advantages are a substantially decreased tendency for the molecular adduct ion to decompose (or fragment) (31), and a longlived secondary ion current which

usual

expla

samp

a liq

This

sho

Not

sol

ana

the

eit

Th

fo

a

th

a

t

i

t

usually provides reproducible mass spectra. The latter observation is often explained by the capacity of the liquid to constantly replenish the surface of the sample with undamaged analyte. In the following sections, the characteristics of a liquid matrix which may contribute to these advantages will be considered.

An important aspect of the FAB matrix is its proclivity to form clusters. This capacity is exhibited in the background spectra of the various matrices (as shown in the glycerol spectrum displayed in Figure 1.3) almost without exception. Not only does the matrix form clusters with itself, but it also clusters with (or solvates) the analyte. Numerous reports describe adduct formation between the analyte and one or more matrix molecules. Daughter spectra obtained from these ions (both with and without CAD) usually contain strong contributions from either the desolvated parent ion, or the matrix monomer (58, 187-190). Therefore, desolvation of clusters has been suggested as an important pathway for molecular adduct ion formation.

Many proposed mechanisms include a cluster intermediate in which the analyte is solvated by matrix molecules (19, 26, 31, 60, 177, 179). In general, these mechanisms discuss the liberation of large clusters (containing solvated analyte) by the sputtering process. Some of the internal energy associated with the cluster complex can then be released by breaking relatively weak intermolecular bonds (as opposed to relatively strong intramolecular bonds). As the intermolecular bonds are broken, the solvent (matrix) molecules are consecutively (or in collective groups) "shed" from the cluster, ultimately producing a relatively low energy analyte monomer. Should a net charge be associated with the cluster, the release of neutral matrix molecules may bestow the charge upon the analyte molecule. The final stages of this process have actually been documented by MS/MS for cationized saccharides (190). Gas

phas

intera

the b

surfa

wou

depe

also

con

liqu

sar

(17

ne

as

sig

co

tra

A

p

phase acidities and basicities would be expected to dictate these ion/molecule interactions.

Macfarlane suggests an important role for the matrix solvent is to reduce the binding interactions between analyte molecules with each other, and with the surface (60). This shielding, solvation sphere is intuitively satisfying in that it would be expected to absorb much of the punishment attendent to energy deposition, while protecting the analyte monomer. Such an explanation would also partially explain why at least some solubility of the analyte in the matrix is considered essential for successful analyses (191).

Observation of cluster formation by keV particle impact is not limited to liquid samples. SIMS has been used to study clusters produced from solid samples of salts (172) and low temperature solids (room temperature gases) (173). Certain salts show extensive clustering behavior when impacted by a neutral beam in the absence of a liquid matrix, and have been used to advantage as calibration compounds. Other salts, which do not provide stable cluster signals when sampled neat, do provide such signals when sputtered from a concentrated matrix solution. This effect is attributed to a lowering of the energy transferred to the salt cluster when it is solvated by liquid matrix molecules (192). A review focusing on the study of clustering phenomena by mass spectrometry is provided by Campana (193).

A series of articles by Katz and coworkers describes the sputtering characterisics of several pure liquids (including glycerol) as a function of temperature (194-196). Their results indicate a gradual decline in the capacity of these compounds to produce clusters as the temperature of the liquid is decreased significantly below its freezing point. At the lower temperature extremes (indicative of the solid state), these mass spectra become generally featureless, with nearly equal contributions at each mass. This behavior may

indicate the importance of relatively weak intermolecular bonding (in liquids as opposed to solids) for the liberation of intact molecular species and large clusters. Particle bombardment spectra of tetramethyltetraphenyltrisiloxane (diffusion pump oil) at low temperatures show an increasing contribution from radiation-damaged products as a function of time. This behavior is reversible, however, since an increase in temperature of the same sample no longer is accompanied by an accumulation of radiation-damaged products. Again, these observations may point to the importance of relatively weak intermolecular interactions for the ejection of large aggregates, which might assist in removing radiation-damaged products.

A study by Field involving prolonged bombardment of glycerol at room temperature documents a more subtle collection of radiation-induced products at long sputtering times (197). Some of these products are rationalized in terms of recombinations of carbon-centered radical species. Field suggests that these radicals may be formed through momentum transferring collisions in the collision cascade. An interesting extension of this study was carried out by Keough and coworkers, who performed gamma irradiation (which does not involve momentum transfer) of glycerol, and suggested that the major products observed resulted from recombination of oxygen-centered radicals with carbon-centered radicals (198).

d. Surface Effects

A vital aspect in understanding keV sputtering from liquids is that the ions represented in the resultant mass spectra are somehow associated with the surface composition of the sample (in this discussion the term "surface" is not meant to strictly apply to the uppermost molecular layer, but more generally

refers to the sample volume in the vicinity of the gas-liquid interface). The evidence to support this contention is overwhelming. To begin with, the penetration depth of the incident particle into the liquid is believed to lie within 50 to 100 A of the gas-liquid interface (177, 199). Therefore, all the processes associated with energy deposition and the collision cascade are concentrated in the vicinity of the sample surface. Ligon and Dorn have very carefully documented the suppression in desorption ionization of less surface-active components by more surface-active components in equimolar mixtures of surfactants which are characterized by differing hydrophobic chain lengths (200, 201). Other work with surfactant mixtures reflects the same effect (137). The importance of surface concentration in the analysis of peptides has been studied (202, 203). In one such study, peptide hydrophobicity was correlated to the extent of surface population in glycerol (the extent of surface population was evaluated by surface tension measurements of the glycerol solutions) (203). Suppression effects observed for mixtures of peptides have received much attention (113, 114, 204). Suppression has been documented in mixtures of glycopeptides for those components which contain a high number of (the inherently hydrophilic) sugar units (205). These hydrophilic portions of the molecule would be expected to display minimal surface activity in hydrophilic matrices such as glycerol. A discussion regarding the importance of surface concentration in FAB is included in several reviews of the technique (70, 192, 206). One report denies the need for any solubility of the analyte in the matrix at all (207).

The nonlinearities in calibration curves for larger amounts of analyte which were alluded to in the discussion of quantitation by FAB (63, 70, 131, 133, 134) have been explained in terms of surface effects. Examples of such curves are shown in Figure 1.10. The levelling of these curves is rationalized by the

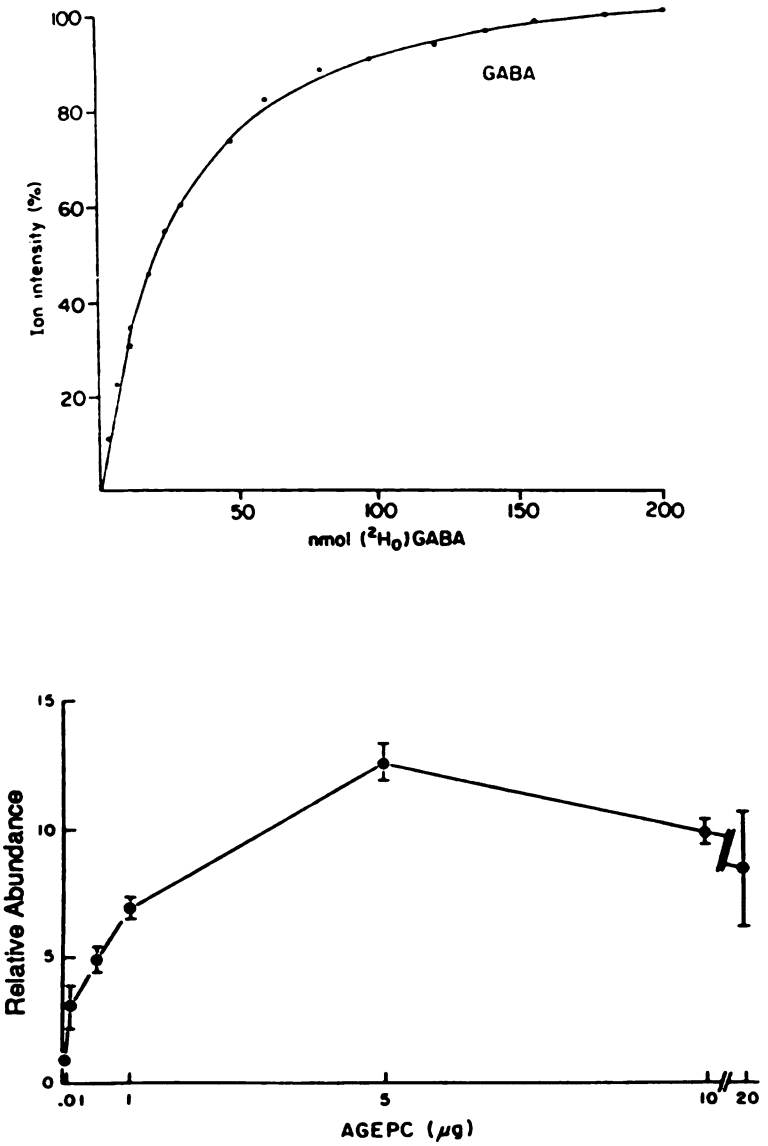

Figure 1.10. Nonlinear calibration curves obtained from FAB experiments. The upper plot corresponds to the analysis of 4-aminobutyric acid (GABA) in acidified glycerol, and the lower plot corresponds to the analysis of acetyl glyceryl ether phosphocholine (AGEPC) in glycerol. Adapted from references 131 and 134 with permission of John Wiley and Sons Ltd.

establishment of an optimal surface concentration of the analyte in the matrix. Increased amounts of analyte beyond this optimal surface concentration do not increase the mass spectrometric reponse, and may even decrease it. Such curves will be presented in Chapter 2 as evidence to suggest pronounced surface population of the matrix by the analyte in certain optimized sample compositions.

Attempts have been made to characterize bulk solution properties (such as equilibrium constants) by FAB mass spectra. These studies have met with mixed success. As mentioned previously, Caprioli and coworkers found the distribution of ions in the gas phase to adequately reflect those present in solution while monitoring the kinetics of enzyme catalyzed reactions (116-119). Caprioli reports the determination of dissociation constants for weak acids by FAB-MS analyses (208). The latter measurements required dielectric constant corrections in order to compare aqueous dissociation constants with equilibria occurring in mixed glycerol/water solutions. A study by Connolly and Orth expressed doubt regarding the validity of these corrections, and revealed no correlation between glycerol solution equilibria and the abundances of secondary ions formed in the FAB experiment (209).

Various sample preparations have been developed to benefit from the surface-sensitive nature of the FAB technique. Ligon and Dorn have used surfactants, bearing the opposite charge of the ion measurement mode, to selectively bind preformed ions near the surface of the sample in a manner analogous to the operation of an ion exchange resin (201). Care is taken to select an oppositely charged surfactant which shows little tendency to fragment. This sample modifier exhibits minimal spectral interference since it predominantly desorbs with the wrong polarity. Not only does this strategy provide increased sensitivity for the analyte, but it also suppresses the interfering matrix spectrum

by occupying the sample surface. This methodology has been used successfully for the analysis of small inorganic ions which have little tendency by themselves to reside at the surface of the matrix (210, 211). Ligon and Dorn have also used this approach quantitatively (136).

Derivatization reactions have been employed to increase the surface activity of the analyte in the matrix (212-214). Simple reactions should be chosen, which provide a high yield of the desired product. The most useful derivatives for FAB-MS analysis not only confer a high degree of surface activity in the matrix, but also impart a charge on the analyte. The importance of preformed analyte ions in the matrix will be considered shortly.

The thermodynamic treatment for the tendency of a surface active species (in a dilute solution) to accumulate at the interface between two phases was derived by Gibbs (215).

$$\frac{d\gamma}{d(\ln c_S)} = -\Gamma_S RT$$

In this relationship, $d\gamma$ corresponds to the change in surface tension of the dilute solution, c_S is the bulk concentration of the solute, and Γ_S is defined as the surface concentration (or surface excess concentration). Γ_S becomes constant upon solute monolayer formation (assuming isothermal conditions), and one consequently observes a linear relationship (with negative slope) in a plot of γ versus $\ln c_S$. Changes in surface tension have been correlated to changes in secondary ion abundance of analyte with respect to matrix as a logarithmic function of bulk concentration for several surfactants. These curves show a linear region where monolayer formation is thought to occur (191, 216). Prior to solute monolayer formation, Γ_S increases as a function of bulk concentration. Surface excess concentrations have been calculated and also correlated to

secon
functi
and e
to be

seco
requi
ever
deba
bulk
som
mat
(25)
me
(21
su
wh
As
pr
of
by
g!
sp
ra
e
r
r

secondary ion abundances for solutions of individual peptides in glycerol as a function of bulk concentration (203). Therefore, the agreement between theory and experiment with regard to the importance of surface concentration appears to be satisfying to the extent to which it has been tested.

A remarkable feature of the FAB experiment is the reproducibility of secondary ion abundances over long periods of time. This spectral longevity requires some mechanism for surface renewal after an individual sputtering event. The process which accounts for the surface renewal has been a point of debate. Barber and coworkers point to diffusion of undamaged analyte from the bulk as the probable means of surface renewal. This explanation would require some solubility of the analyte in the matrix to provide a reservoir of undamaged material to present to the FAB beam (191). Calculations performed by Magee (25) and Bursey and coworkers (217) support the role of diffusion in the FAB mechanism. Experiments conducted by Ligon (218) and Wong and coworkers (219) have been interpreted by the authors to negate the role of diffusion in the surface renewal mechanism. The latter group has also contributed calculations which have been interpreted as evidence against the process of diffusion (177). As an alternative to diffusive surface renewal, Wong and coworkers have presented a surface self-cleaning sputtering mechanism (219). The basic tenet of this mechanism is that layers of molecules are transported into the gas phase by each primary particle impact. An estimate is made that approximately 1000 glycerol molecules are sputtered per keV impact by a xenon atom. This sputtering yield is proposed to be sufficient for the nearly complete removal of radiation-damaged products. The authors argue that such a mechanism eliminates the need for diffusive transport, since a new surface is created by removal of large portions of the sample. Other potential contributors to surface renewal may be convection (212), and side-filling processes which are driven by

variations in surface tension produced by particle impact (200). The latter process may be important in explaining the enhanced results observed when a primary beam focused to dimensions smaller than those of the sample surface is employed (92).

e. Fragmentation

An interlaboratory study has shown that the analyte fragmentation patterns observed in FAB mass spectra are as reproducible as those associated with electron impact ionization (220). The analytically useful fragmentation discussed in this section should be distinguished from the low level ion abundances at every mass which have been postulated to arise from analyte and matrix fragmentation in the highly energized area very near to the site of particle impact. Moon and Winograd have measured the polar angle distributions of sputtered ions and interpreted this data as strong evidence for significant fragmentation occurring on the surface of the sample (221). Due to the very strong similarity in the fragments observed in conventional FAB spectra with those obtained from CAD (26, 222) (a known gas phase process) and the observation of metastable decomposition (155, 223), however, the most generally accepted view of fragmentation is as a result of unimolecular dissociation in the gas phase (179).

Other interesting results concerning fragmentation have been reported. Winger and coworkers present evidence of decreasing analyte fragmentation as the primary beam energy is increased in a static SIMS study (224). They believe this trend may also be applicable to sputtering from liquid matrices. Very interesting results were reported for the FAB-MS/MS analysis of some phosphorylated peptides from glycerol (225). In the positive ion mode, fragmentation was associated with gas phase decomposition, while in the

negativ

matrix

matrix

obser

identit

very i

type

advan

been

facilita

and c

differe

and t

fragm

and c

chain

cation

daugh

partic

determ

though

ions in

negative ion mode, decomposition was attributed to reactions with the glycerol matrix in the condensed phase. The occurrence of reactions involving the FAB matrix will be addressed in a subsequent section.

Work with MS/MS has shown that the extent and type of fragmentation observed from molecular adduct ions of peptides is strongly dependent upon the identity of the cation (e.g., H^+, Na^+, K^+, Ag^+, etc.) (226). This result raises the very interesting possibility of directing fragmentation by favoring formation of one type of adduct ion over another. Such a capability would be especially advantageous in the analysis of peptides, since a great deal of attention has been devoted to increasing the structural information available from peptides to facilitate their primary sequence determination. A series of papers by Russell and coworkers (227-229) attributes these changes in fragmentation behavior to differences in both the binding site and the binding energy between the molecule and the various cations. Some correlations are drawn regarding the types of fragmentation favored by molecular adducts involving particular cations. Gross and coworkers have shown fragmentation remote from the charge site for long chain alcohols and fatty acids in MS/MS experiments involving CAD of the cationized molecules (230, 231). Analogous behavior was not observed in the daughter ion spectra of the protonated molecules.

f. Preformed Ions

In all the literature devoted to clarifying the mechanisms operative in keV particle impact techniques, the most hotly contested question probably involves determining the precise location of the ionization step. Two separate schools of thought have evolved to explain this issue. The first advocates the existence of ions in the matrix prior to particle bombardment. Once these ions are formed in

the con

mass a

neutral

in the g

repres

by his

and p

depro

four s

(to c

fragm

disso

prefc

(233

of pu

solu

anal

(ma

A s

and

Mic

a

spe

FAI

of

the condensed phase, they are desorbed with charge retention and subsequently mass analysed. The second school of thought advocates the desorption of neutral species which become charged through ion/molecule reactions occurring in the gas phase. Each idea will be considered in turn.

The "precursor" model advanced by Benninghoven (178, 232) strongly represents the importance of preformed ions. This model was largely influenced by his experience with SIMS, but he extends the concept to the FAB experiment and points out the facility with which glycerol can form ions by protonation and deprotonation in the condensed phase. Benninghoven describes the model in four steps. These include precursor formation, the fast transfer of kinetic energy (to desorb the ion), charge sign conservation of the ejected ion, and fragmentation (directly from the rapid kinetic energy transfer or from unimolecular dissociation in the gas phase). Peter Williams considers the ejection of preformed molecular adducts from polar solvents to be a very plausible process (233).

Compelling experimental evidence has accrued to support the significance of preformed ions in contributing to the resultant mass spectra. The effect of solution pH on $[M+H]^+$ peak intensities was investigated for several basic analytes (57). These experiments involved evaporation of sample solutions (maintained at various pH values) on a surface prior to molecular SIMS analysis. A straightforward correlation was documented between analyte ion abundance and pH of the original solution. Experiments conducted in our own laboratory at Michigan State University directly relate the protonation of porphyrin molecules in a thioglycerol matrix (established independently by visible absorption spectroscopy) to the presence of significant ion abundance in the corresponding FAB spectrum (234). Ion abundance has been shown to increase as a function of solution conductivity (235). Experiments by Cotter and coworkers which

utilized
differer
combir
all thr
interpr
contrib

proces
certair
expect
and ev
(an ea
reveal
FAB te
to isol
beam.
cluster
matrice
no sig
convinc
separat
on one
matrix o
complex

utilized a probe split into three regions to allow independent desorption of three different salts, showed no evidence of mixed cluster formation involving combinations of the individual salts. Since mixed clusters were observed when all three salts were desorbed from the same surface, these reults were interpreted as evidence for direct emission of the clusters with insignificant contribution from gas phase interactions (236).

g. Gas Phase Ionization

Several investigators have described the ionization step as a gas phase process (73, 237). The high pressures proposed for the selvedge region certainly suggest an environment in which many gas phase collisions would be expected (26). Experimental evidence for this argument has also been gathered and evaluated. Interestingly enough, other experiments involving divided probes (an earlier example was used to argue for the emission of preformed ions) have revealed that a significant degree of gas phase interaction is associated with the FAB technique. In one such experiment, two different FAB matrices were applied to isolated regions of the probe tip and simultaneously bombarded by the FAB beam. The resultant spectra showed pronounced contributions from mixed cluster ions (clusters containing at least one molecule from each of the pure matrices). Subsequent evaluation of the purity of the separated samples showed no signs of cross contamination, and the mixed cluster formation was convincingly interpreted as resulting from gas phase interactions (238). In a separate study involving a divided probe, alkali ions were dispersed in a matrix on one half of the probe tip, while a crown ether was dispersed in the same matrix on the other half. The FAB spectra obtained from this experiment showed complexation of alkali ions by the crown ether (239). Another report discusses

the ga
spectro
even-el
interact
experin
process
model
behavio
compon

with th
analyte
in the
ionizati
explosi
and ul
ion/mo
analyte
is an
basiciti
solution
reduce
sample
are app
phase
solution
misgivi

the gas phase introduction of organophosphorus compounds into a mass spectrometer source during keV bombardment of a FAB matrix. The formation of even-electron ions from the analyte was believed to occur through gas phase interactions with desorbed species from the matrix (240). Although these experiments illustrate the FAB environment as conducive to gas phase processes, some of the results are weakened by the use of volatile analytes as model compounds. Care should be exercised in extrapolating the gas phase behavior of relatively small, volatile compounds to that of large, nonvolatile compounds.

A series of papers by Kebarle and coworkers has been strongly identified with the gas phase argument (241-246). In this work, gas phase basicities for analytes sampled as mixtures are correlated to relative ion abundances observed in the FAB mass spectra. A "gas collision model" is developed to explain the ionization process exclusively in terms of ion/molecule reactions. A "phase explosion model" is subsequently formulated to describe the desorption process, and ultimately combined with the former model in the "phase explosion ion/molecule model". Although justifying relative ion abundances for a mixture of analytes by their relative gas phase basicities is a potentially powerful concept, it is an extremely difficult correlation to demonstrate because the gas phase basicities for a series of analytes will generally tend to follow the order of their solution phase basicities. The importance of these experiments is significantly reduced by the exclusive dependence upon volatile analytes, which are often sampled from solutions of inordinately high concentration. Conclusions which are applied to the analysis of thermally fragile, nonvolatile species (for which gas phase basicity values are not available) that are sampled from dilute matrix solutions are open to question. Fenselau and Cotter express some of these misgivings in a recent review (206).

model
mecha
surfac
phase
phase
be co
deter
divers
Certa
factor
interp
aspec

mecha
An ex
determ
phase
cowork
role fo
differen
since t
differenc
in surfac

The convincing evidence which has been put forth in support of both models makes it difficult to dismiss either. Indeed, a complete picture of the FAB mechanism requires the consideration of several important factors including the surface composition of the sample, the capacity to form ions in the condensed phase, and the stability (or reactivity) of the analyte in the gas and condensed phases. Therefore, the unique characteristics of each individual sample should be considered before deciding which mechanistic forces will be dominant in determining the mass spectral pattern. A strength of the FAB experiment is the diversity of ways in which the system (and results) can be manipulated. Certainly, systems have been contrived to exaggerate the importance of one factor with respect to others. This opportunity should be exploited, but not interpreted to summarily exclude the general importance of the mechanistic aspects which were discriminated against.

Of course, camparisons regarding the relative importance of the various mechanistic features for a particular sytem are helpful (although somewhat rare). An example is the study by Lacey and Keough (247) which attempted to determine the relative importance of surface activity effects in comparison to gas phase basicity effects for some of the compounds studied earlier by Kebarle and coworkers (243). Their results were interpreted to attribute a significantly greater role for surface effects in determining the mass spectral behavior than differences in gas phase basicity. This conclusion was not particularly surprising since the Kebarle group had discussed an instance in their work where differences in gas phase basicity were presumably overshadowed by differences in surface activity (243).

h. Products of FAB

As previously mentioned, the majority of useful ions reflected in FAB mass spectra are of the relatively stable, even-electron variety. Exceptions to this statement will now be discussed (i.e., the observation of significant abundances of odd-electron ions). The somewhat rare detection of multiply charged ions in the FAB experiment will also be considered, along with the topic of neutral desorption.

It has been reported by several laboratories that volatile analytes which are exposed to the FAB beam form abundant, odd-electron ions in ratios which are very analogous to those in their EI mass spectra (248-255). The explanation for this phenomenon involves the likelihood that a fast atom can eject an electron from a molecule in the gas phase, just as an energetic electron can. This information is very interesting in that it reveals yet another process which is possible in the environment created by fast atom bombardment. Its mechanistic significance is limited, however, because this process has not been observed to be dominant in the analysis of nonvolatile species. FAB was not developed to substitute for established (and better understood) gas phase ionization techniques, but to complement them.

Odd-electron ions have also been formed in large abundance from nonvolatile analytes which are less polar in nature (256). This behavior can be facilitated in many cases by the use of nonpolar, aromatic matrices which possess a shortage of labile hydrogens, such as o-nitrophenyl octyl ether (NPOE) (68), and (to a lesser extent) nitrobenzyl alcohol (NBA). De Pauw has elegantly demonstrated the ability to selectively favor formation of a radical cation through a one-electron transfer reaction to an appropriate acceptor additive (257). This reaction occurs in solution because it requires the solvation energy of

a po
dem
a va
(25
suc
dur

the
sta
rec
or
Ha
ga
A
th
si
ch

n
n
ic
a
c

a polar solvent. Cerny and Gross have employed high resolution analyses to demonstrate that the unexpectedly high abundances of $[M+2]^+$ ions observed for a variety of compounds is largely contributed to by the radical $[M+2H]^{+\cdot}$ species (258). They propose a mechanism for the formation of this ion which involves successive protonations of the neutral, followed by a one-electron reduction during desorption.

The observation of intact multiply charged ions is extremely infrequent in the practice of FAB-MS. This has been explained as resulting from the lower stability of these ions, a slower rate for their desorption, and a preponderance of recombination reactions occurring in the desorption ionization process to partially or fully neutralize them. In a molecular SIMS study of zwitterionic compounds, Hand and Cooks suggest that minimization of the total charge transferred to the gas phase may be an important principle governing desorption ionization (259). A report by Schronk and Cotter appears to indicate that these restrictions against the desorption of multiply charged ions are somewhat alleviated with increasing size of the analyte. This result is rationalized to occur because of a decreased charge density for larger multiply charged ions (260).

It is widely believed that the desorption of any charged species from neutral analytes during FAB is a rare event in comparison to the desorption of neutrals (261). Therefore, several studies have utilized an additional means of ionization to enhance the signal strengths obtained from FAB. Increases in ion abundance by orders of magnitude have been reported for experiments which combined EI (262, 263) and CI (261) ionization modes with FAB.

FAB-M
Little e
conde
topic h
involv
previo
anioni
provic
the ur
exper

Glish
reduc
thiam
organ
disulf
latter
activa
matri
altho
Pelze
glyce
mech
signif

i. Reactions Involving Matrix

This final portion of the literature review devoted to mechanistic aspects of FAB-MS will consider reactions which occur in the presence of the FAB matrix. Little effort will be made to distinguish whether these reactions take place in the condensed phase or the gas phase, since such judgements are difficult and this topic has already been addressed. Most of these reactions (but not all) directly involve the participation of the matrix compound as a reactant. Reactions previously mentioned (e.g., protonation, deprotonation, cationization, and anionization) will not be the focus of this discussion. Some of these reactions provide desired information in the resulting mass spectrum, while many reflect the undesired consequence of using a reactive matrix in the desorption ionization experiment.

Reduction of the analyte constitutes a noteworthy process in FAB-MS. Glish and coworkers have demonstrated (with MS/MS) the ability of glycerol to reduce the thiamine cation and provide misleading information in the analysis of thiamine hydrochloride (143). Successive reductions of cations from various organic dyes have been documented in the glycerol matrix (264). Reduction of disulfide bonds in peptides has been observed under FAB conditions (265). The latter study demonstrated the importance of the primary beam energy in activating the reaction. The reduction was also shown to occur in three different matrices (including glycerol, thioglycerol, and dithiothreitol/dithioerythritol), although the reaction rate was dependent upon the matrix chosen. Results from Pelzer and coworkers demonstrate reduction for various compound classes in glycerol, and postulate a hydrogen radical addition mechanism (266). This mechanism fits well with the suggestion by Field (197) and Ligon (267) that a significant population of carbon-centered radicals are formed from glycerol under

conditions of fast atom bombardment. A complementary population of hydrogen radicals could participate in the reduction process. A report of dehalogenation of nucleosides during FAB proposes a radical intermediate for the reaction (268). Glycerol deuterated at the carbon positions was used in this work. Mass shifts indicated that the majority of hydrogen substitution (after dehalogenation) originated from the glycerol carbon atoms. In studying the reduction of aromatic oximes during FAB, Gross and coworkers propose initial protonation followed by reduction (269). This mechanism is analogous to that earlier suggested by Cerny and Gross for the formation of $[M+2H]^{+\cdot}$ and $[M+3H]^{+}$ ions (258). A publication by Williams and coworkers postulates the existence of a significant thermal electron population resulting from energy deposition. Capture of these low energy electrons is then suggested as an intermediate step in the course of several reduction reactions which have been observed during FAB (270).

Oxidation of the analyte has also occurred in the FAB matrix. Hydride abstraction from long-chain ethers was shown to occur in the hydrocarbon chain remote from the oxygen, resulting in $[M-H]^{+}$ formation. This behavior was predominant in the NBA matrix, whereas it was comparable to $[M+H]^{+}$ formation in a glycerol/thioglycerol matrix (271). Direct hydride abstraction was proposed to account for the favored detection of the oxidized pyridinium cation over the dihydropyridine form in the FAB analysis of some dihydropyridines (272). The extent of this behavior was found to be dependent on the particular matrix used.

Reactions involving the transfer of larger groups have been reported. Duffin and Busch discuss the transfer of methyl and ethyl groups from sulfonium salts to the triethanolamine matrix (273). Hand and coworkers attribute the formation of $[M-CH_3]^{-}$ from carnitine to methyl abstraction by the glycerol matrix (274). An analogous observation resulted from the analysis of some zwitterionic compounds in triethanolamine (259). Debenzylation was documented for a

dibenzyl
formulat
observe
larger a
covalent
Q
species
(from th
examine
the mas
probe ti
inorganic
magnesi
substitut
bis-cate
between
at least
reactivity
as the m
glycerol
catalyze
Ti
matrix c
determin
exchang
shift obs

dibenzylphosphoserine sampled from glycerol (275). Dass and Desiderrio have formulated a mechanism to account for the abundant $[M+H+12]^+$ ion commonly observed for peptides sputtered from hydroxylated matrices. This addition and larger additions to the protonated peptide molecule were rationalized as covalently bound reaction products between the peptide and matrix (276).

Quite dramatic transformations have occurred in the analysis of inorganic species by FAB. Among these is the essentially complete exchange of copper (from the probe tip) for mercury in trisubstituted phosphine metal halides examined from both NBA and PEG 200. This reaction was confirmed not only by the mass spectrum, but also from the grey deposit of mercury visible on the probe tip subsequent to the analysis (277). Substitution of glycerol to an inorganic metal center was shown for species containing tin, antimony, magnesium, and iron (189). The analysis of some alkali silicates revealed substitution of catechol by glycerol (278). Identical behavior was observed for bis-catechol spiroborates sampled from glycerol (279). The extreme reactivity between boron-containing compounds and typical FAB matrices was exploited in at least one instance to study the reaction chemistry of such compounds. This reactivity was curbed (when desired) by using tetraethylene glycol diethyl ether as the matrix (280). Chan and Cook discuss an esterification reaction between glycerol and EDTA (in an electrohydrodynamic ionization experiment) which was catalyzed by iron (281).

This topic will be closed with another example of how reactions in the matrix can be used to advantage. Deuterated glycerol has been employed to determine the number of active hydrogens in different analytes. Minimal back exchange allows the determination of this property by the magnitude in mass shift observed during bombardment (282, 283). An excellent review of interfacial

reactions

coworkers

It is

dynamic e

can be sig

these vari

and in the

explain s

factor wh

can acco

receive c

V. Appli

T

techniqu

here to

compou

inclusio

more e

structu

acids

twenty

reactions accompanying desorption ionization is provided by Detter and coworkers (284).

It is hoped that this discussion of the FAB mechanism has illustrated a dynamic environment in which many types of interactions are possible, and which can be significantly influenced by several different factors. The balance between these various stimuli should be considered in the design of FAB experiments, and in the interpretation of the corresponding results. Mechanisms put forth to explain such results should emphasize flexibility, and not hinge upon a single factor whose importance some experiments exaggerated. Mechanisms which can accomodate a diversity of stimuli (19, 171) will, in the opinion of this author, receive continued attention as the entire process is more carefully defined.

V. Applications

The explosion of activity involving FAB since the introduction of this technique is extensively represented in the literature. No attempt will be made here to exhaustively catalog this work. Instead, some major classes of compounds which have been addressed by FAB will be touched upon, with the inclusion of some appropriate references. Whenever possible, references to more extensive reviews will be provided.

a. Peptides

Proteins perform vital functions in living systems. These large and very structurally complex molecules are actually composed of much simpler amino acids which are linked together by peptide bonds. There are approximately twenty common amino acids which are arranged in a specific order to provide a

particular pu
characterize
bonded to
nitrogen of
different fo
glutamine/
acids to co
spectrome
biopolyme
desorptio
readily io
characte
compou
like thes
FAB-MS
existing
peptide
reactio
be de
inform
whic
FAB
tha
Alt
FA

particular protein with its unique functional capabilities. All the amino acids are characterized by a common backbone, but they differ in the identity of a group bonded to the carbon atom situated between the carbonyl carbon and amine nitrogen of the backbone. The nominal mass of this distinguishing group is different for all the common amino acids except for the leucine/isoleucine and glutamine/lysine pairs. This fact, along with the predictable tendency of amino acids to combine in linear chains by way of peptide linkages suggest that mass spectrometry would be a powerful tool in the structure elucidation of these biopolymers. The nonvolatility of these compounds implicates the need for a desorption ionization technique. FAB is a natural choice due to an abundance of readily ionizable groups in peptides (both acidic and basic), and a hydrophobic character (imparted by the distinguishing group) relative to highly hydroxylated compounds, which allows significant surface activity in such matrices. Reasons like these go far to explain the successful marriage between peptide analysis and FAB-MS.

Because proteins and many peptides are too large for direct analysis in existing mass spectrometers, digestion with a proteolytic enzyme (which cleaves peptide linkages involving specific amino acids) is usually required. These reactions produce mixtures of peptides, whose individual molecular weights can be determined (in the absence of suppression effects) in a FAB analysis. Such information can be sufficient in itself to confirm or reject a peptide sequence which has been predicted by other means. This process has become known as FAB-mapping (285).

The primary sequences of the individual peptides (if they are not larger than 2,000-3,000 u) can be determined solely by FAB-MS in many cases. Although sequence information from a pure peptide can often be obtained by FAB in a conventional mass analysis, this process is facilitated by the use of

tandem ma
spectrometr
mixtures (w
imparted by
deduction o

Biem
convention
Edman app
terminus,
retention t
peptides)
Cyclic pep
the Edma
requires
techniqu

A
widely a
nomenc
modifica
(101).
been r
leucine

Peptid
in res
have
surfa

tandem mass spectrometry incorporating CAD (286-288). Tandem mass spectrometry allows structure elucidation for individual components of the digest mixtures (which contain other peptides and the interfering matrix). The energy imparted by CAD increases the formation of fragment ions which are vital for the deduction of the primary sequence.

Biemann views the FAB technique as complementary to the more conventional Edman degradation for the sequencing of peptides (101). The Edman approach involves cleavage of one amino acid after another from the N-terminus, followed by identification of the cleaved amino acids from HPLC retention times. This process can be rather time intensive (especially for long peptides) and it is stymied when the N-terminus is blocked (e.g., acylated). Cyclic peptides (which do not have a free N-terminus) cannot be addressed by the Edman procedure. FAB is often able to surmount these obstacles, but requires significantly more material (usually nanomoles) than the Edman technique (which typically requires less than 100 picomoles).

A nomenclature proposed by Roepstorff and Fohlman (289) has been widely adopted to describe the fragmentation observed for peptides. This nomenclature is represented in Figure 1.11. Biemann has suggested modification of this nomenclature to add specificity in the description of ion types (101). A novel fragmentation process involving the formation of "w ions" has also been reported (290). Interpretation of the w ions can be used to differentiate leucine and isoleucine (291).

A hydrophobicity index has been used to predict the relative tendencies of peptides to occupy the surface of hydrophilic matrices. This index was adopted in response to the observation of suppression effects between peptides, which have been described (113, 114, 204). The index was based on the relative surface activities of the individual amino acids in water as determined by Bull and

Figure 1

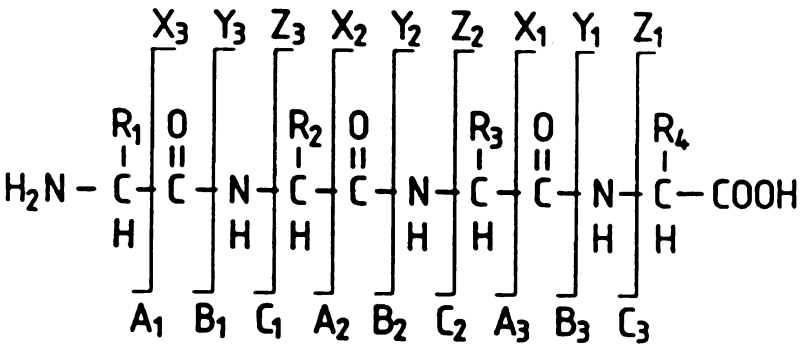

Figure 1.11. Representation of the nomenclature for peptide ions proposed by Roepstorff and Fohlman. Adapted from reference 289 with permission of John Wiley and Sons Ltd.

Breese (
to consi
terminal
(203) w
octapept

M
associat
has exp
Some im
will now

b.

W
themselv
challeng
techniqu
phase) a
are not t
by dehyd
not near
problema
hydroxyla
similarity
surface a
sugar un
desorptio

Breese (292). Some criticism of this index has been directed toward its inability to consider the secondary structure of the peptide, or the influence of free N-terminal and C-terminal groups. At least one alternative index has been utilized (203) which is based on the liquid chromatographic behavior of model octapeptides.

Much of the excitement surrounding FAB-MS in the last decade has been associated with its capacity to characterize peptides. This class of compounds has experienced the most prolific application of the FAB technique to date. Some important work related to this topic, along with several extensive reviews, will now be referenced for the interested reader (101, 293-298).

b. Saccharides

Whereas peptides possess properties which predominantly lend themselves toward favorable FAB analysis, the properties of saccharides tend to challenge successful and routine application of this desorption ionization technique. To begin with, saccharides do not form ions (in solution or the gas phase) as readily as peptides. Strongly basic groups which faciltate protonation are not typically present (when protonation does occur, it is often followed rapidly by dehydration). The hydroxyl groups of saccharides are somewhat acidic, but not nearly as acidic as the carboxylic acid groups of peptides. Another problematic feature of saccharides is their close stuctural similarity to the highly hydroxylated compounds which are commonly used as matrices. This stuctural similarity implies great solubility of the saccharide in the matrix, and hence, little surface activity. It has already been mentioned that increasing the number of sugar units in glycopeptides was shown to exacerbate suppression of their desorption ionization by more surface-active sample components (205). Not only

does the
profoundl
of much
Sacchari
number o
as mono
situation
oligosacc
linear cha
structures
of the s
oligosacc
isomers,
the disco
ion signa
other cla

Fa
FAB-MS
peptides
some sa
facilitate
sodium
concentr
(190). I
easily io
Fragmer
which bi

does the FAB analysis of saccharides suffer from these inherent traits (which profoundly decrease the sensitivity of their detection), but also from the demand of much more stringent structural information from the mass spectra. Saccharides are most often encountered in the hexose form, which includes a number of closely related isomers. Differentiation between these isomers (even as monosaccharides) is not a trivial exercise for mass spectrometry. The situation is further complicated when the hexose units combine to form oligosaccharides. These biopolymers do not form exclusively in predictable linear chains (as do peptides), but can exist as highly branched and complex structures, due to the ability of the hexose units to substitute at various positions of the saccharide ring. Therefore, the complete stucture elucidation of oligosaccharides requires not only the distinction between various hexose isomers, but also the determination of the substitution pattern, which may involve the discovery of branching points. Extraction of all this intricate information from ion signals which are significantly less intense than those available from many other classes of compounds often represents a formidable task.

Factors such as those mentioned above have restricted the application of FAB-MS to saccharides, at least relative to the explosive application noted for peptides. Negative ion detection has been employed to exploit the tendency of some saccharides to donate protons (299). Positive ion detection has been facilitated in many cases by the formation of adduct ions with cations such as sodium or potassium. It has been determined that both the type and concentration of cations in the sample is critical for optimization of this strategy (190). Effort has been directed toward the synthesis of derivatives which are easily ionized and impart significant surface activity to the saccharide (300, 301). Fragmentation has been observed to generally occur at the glycosidic linkages which bind the sugar rings. Reinhold and Carr have contributed an important

review reg
saccharide

c.

Olig
characteri
analyzed
stabilize a
molecular
their FAB
much les
304). As
increased
allowed
nucleosid
FAB-MS
cyclic nu
concernin

d.

As
analyzed
represen
As a star

review regarding the use of mass spectrometry in the structure elucidation of saccharides (302).

c. Nucleotides

Oligonucleotides represent another class of biopolymers whose characterization has greatly benefited from the advent of FAB. They are usually analyzed in the negative ion mode due to the ability of the phosphate group to stabilize a negative charge. Not only do these compounds provide abundant molecular weight information, but they are also subject to ready sequencing from their FAB mass spectra. Indeed, their sequence determination by FAB-MS is much less time consuming than when accomplished by classical methods (303, 304). As was observed for peptides, the sequence specific information can be increased by employing MS/MS with CAD (305). MS/MS with CAD has also allowed the differentiation of isomeric cyclic nucleotides (146). Derivatized nucleosides and nucleotides have demonstrated enhanced fragmentation by FAB-MS (306). FAB has been used to follow the hydrolysis reaction catalyzed by cyclic nucleotide phosphodiesterase (307). Schram provides a recent review concerning the role of FAB-MS in the analysis of nucleotides (308).

d. Miscellaneous

As previously mentioned, a detailed coverage of all those compounds analyzed by FAB is beyond the scope of this dissertation. References representative of some particular compound classes will be provided, however. As a starting point, a few very important reviews will be cited which incorporate a

more extens

312).

Additi

crown ethe

organometa

glycosides

(332), poly

(337), and

more extensive treatment to the many applications reported of FAB-MS (309-312).

Additional problems to which FAB has been applied include the analysis of crown ether complexes (239, 313, 314), metal isotope ratios (315-317), organometallics (318-320), porphyrins (234, 321), glycoconjugates (322, 323), glycosides (324-326), steroids (327), bile acids (146), lipids (328-331), antibiotics (332), polyaromatic hydrocarbons (333, 334), polymers (335, 336), plasticizers (337), and dyes (264, 338, 339).

VI. Refer

1. Bec
2. Sch
3. Gor
4. Swa
5. Hol
   3, 3
6. Bec
7. Hol
8. Bec
9. Cot
10. Lig
11. Eva
12. Ch
13. Bal
14. Co
15. Sc
    10
16. Cc
17. M
    R
18. M
    2(
19. V
20. Al
    1;

VI. References

1. Beckey, H.D. *J. Mass Spectrom. Ion Phys.* **1969**, *2*, 500.
2. Schulten, H.R. *Int. J. Mass Spectrom. Ion Phys.* **1979**, *32*, 97.
3. Gomer, R. *J. Chem. Phys.* **1959**, *31*, 341.
4. Swanson, L.W.; Gomer, R. *J. Chem. Phys.* **1963**, *39*, 2813.
5. Holland, J.F.; Soltmann, B.; Sweeley, C.C. *Biomed. Mass Spectrom.* **1976**, *3*, 340.
6. Beckey, H.D.; Rollgen, F.W. *Org. Mass Spectrom.* **1979**, *14*, 188.
7. Holland, J.F. *Org. Mass Spectrom.* **1979**, *14*, 291.
8. Beckey, H.D. *Org. Mass Spectrom.* **1979**, *14*, 292.
9. Cotter, R.J.; Yergey, A.L. *Anal. Chem.* **1981**, *53*, 1306.
10. Ligon, W.V. *Anal. Chem.* **1982**, *54*, 588.
11. Evans, C.A., Jr.; Hendricks, C.D. *Rev. Sci. Instrum.* **1972**, *43*, 1527.
12. Chan, K.W.S.; Cook, K.D. *Anal. Chem.* **1983**, *55*, 1306.
13. Baldwin, M.A.; McLafferty, F.W. *Org. Mass Spectrom.* **1973**, *7*, 1353.
14. Cotter, R.J. *Anal. Chem.* **1980**, *52*, 1589A.
15. Schroder, E.; Budzikiewicz, H. *Int. J. Mass Spectrom. Ion Proc.* **1985**, *66*, 101.
16. Cotter, R.J.; Fenselau, C. *Biomed. Mass Spectrom.* **1979**, *6*, 287.
17. Macfarlane, R.D.; Skowronski, R.P.; Torgerson, D.F. *Biochem. Biophys. Res. Commun.* **1974**, *60*, 616.
18. McNeal, C.J.; Macfarlane, R.D.; Thurston, E.L. *Anal. Chem.* **1979**, *51*, 2036.
19. Vestal, M.L. *Mass Spectrom. Rev.* **1983**, *2*, 447.
20. Alai, M.; Demirev, P.; Fenselau, C.; Cotter, R.J. *Anal. Chem.* **1986**, *58*, 1303.

21. Jordan, E.A.; Macfarlane, R.D.; Martin, C.R.; McNeal, C.J. *Int. J. Mass Spectrom. Ion Phys.* **1983**, *53*, 345.

22. Cotter, R.J. *Anal. Chem.* **1988**, *60*, 781A.

23. Yefchak, G.E.; Enke, C.G.; Holland, J.F. *Int. J. Mass Spectrom. Ion Proc.* **1989**, *87*, 313.

24. Benninghoven, A.; Jaspers, D.; Sichtermann, W. *Appl. Phys.* **1976**, *11*, 35.

25. Magee, C.W. *Int. J. Mass Spectrom. Ion Phys.* **1983**, *49*, 211.

26. Pachuta, S.J.; Cooks, R.G. In *Desorption Ionization Mass Spectrometry: Are SIMS and FAB the Same?*; Lyon, P.A., Ed.; ACS Symposium Series 291; American Chemical Society, Washington, DC, **1985**.

27. Grade, H.; Cooks, R.G. *J. Am. Chem. Soc.* **1978**, *100*, 5615.

28. Kambara, H.; Hishida, S.; Naganawa, H. *Org. Mass Spectrom.* **1982**, *17*, 67.

29. Surman, D.J.; Vickerman, J.C. *J. Chem. Soc., Chem. Commun.* **1981**, 324.

30. Amster, I.J.; Loo, J.A.; Furlong, J.J.P.; McLafferty, F.W. *Anal. Chem.* **1987**, *59*, 313.

31. Busch, K.L.; Hsu, B-H.; Xie, Y-X.; Cooks, R.G. *Anal. Chem.* **1983**, *55*, 1157.

32. Posthumus, M.A.; Kistemaker, P.G.; Meuzelaar, H.L.C.; Ten Noever de Brauw, M.C. *Anal. Chem.* **1978**, *50*, 985.

33. Van der Peyl, G.J.Q.; Haverkamp, J.; Kistemaker, P.G. *Int. J. Mass Spectrom. Ion Phys.* **1982**, *42*, 125.

34. Van Breemen, R.B.; Snow, M.; Cotter, R.J. *Int. J. Mass Spectrom. Ion Phys.* **1983**, *49*, 35.

35. Denoyer, E.; Van Grieken, R.; Adams, F.; Natusch, D.F.S. *Anal. Chem.* **1982**, *54*, 26A.

36. Blakley, C.R.; Carmody, J.J.; Vestal, M.L. *J. Am. Chem. Soc.* **1980**, *102*, 5931.

37. Vestal, M.L. *Int. J. Mass Spectrom. Ion. Phys.* **1983**, *46*, 193.

38. Covey, T.R.; Lee, E.D.; Bruins, A.P.; Henion, J.D. *Anal. Chem.* **1986**, *58*, 1451A.

39. Barber, M.; Bordoli, R.S.; Sedgwick, R.D.; Tyler, A.N. *J. Chem. Soc., Chem. Commun.* **1981**, 325.

40. Iribarne, J.V.; Thomson, B.A. *J. Chem. Phys.* **1976**, *64*, 2287.

41. Thomson, B.A.; Iribarne, J.V. *J. Chem. Phys.* **1979**, *71*, 4451.

42. Thomson, B.A.; Iribarne, J.V.; Dziedzic, P.J. *Anal. Chem.* **1982**, *54*, 2219.

43. Whitehouse, C.M.; Dreyer, R.N.; Yamashita, M.; Fenn, J.B. *Anal. Chem.* **1985**, *57*, 675.

44. Wong, S.F.; Meng, C.K.; Fenn, J.B. *J. Phys. Chem.* **1988**, *92*, 546.

45. Covey, T.R.; Bonner, R.F.; Shushan, B.I.; Henion, J. *Rapid Commun. Mass Spectrom.* **1988**, *2*, 249.

46. Mann, M.; Meng, C.K.; Wong, S.F.; Fenn, J.B. Presented at the 37th ASMS Conference on Mass Spectrometry and Allied Topics, Miami Beach, Florida, May 21-26, **1989**.

47. Chakel, J.; Covey, T.; Shushan, B.; Scott, G. Presented at the 37th ASMS Conference on Mass Spectrometry and Allied Topics, Miami Beach, Florida, May 21-26, **1989**.

48. Covey, T.R.; Sushan, B.I.; Bonner, R.F.; Henion, J. Presented at the 37th ASMS Conference on Mass Spectrometry and Allied Topics, Miami Beach, Florida, May 21-26, **1989**.

49. Mann, M.; Meng, C.K.; Fenn, J.B. *Anal. Chem.* **1989**, *61*, 1702.

50. Beuhler, R.J.; Flanigan, E.; Greene, L.J.; Friedman, L. *J. Am. Chem. Soc.* **1974**, *96*, 3990.

51. Yergey, A.L.; Cotter, R.J. *Biomed. Mass Spectrom.* **1982**, *9*, 286.

52. Daves, G.D., Jr. *Acc. Chem. Res.* **1979**, *12*, 359.

53. Bombick, D.D.; Allison, J. *Anal. Chem.* **1987**, *59*, 458.

54. Devienne, F.M.; Roustan, J.C. *Org. Mass Spectrom.* **1982**, *17*, 173.

55. Barber, M.; Bordoli, R.S.; Sedgwick, R.D.; Tetler, L.W. *Org. Mass Spectrom.* **1981**, *16*, 256.

56. Barber, M.; Bordoli, R.S.; Sedgwick, R.D.; Tyler, A.N. *Nature* **1981**, *293*, 270.

57. Inchaouh, J.; Blais, J.C.; Bolbach, G.; Brunot, A. *Int. J. Mass Spectrom. Ion Proc.* **1984**, *61*, 153.

58. Keough, T. *Anal. Chem.* **1985**, *57*, 2027.

59. McLafferty, F.W. *Org. Mass Spectrom.* **1980**, *15*, 114.

60. Macfarlane, R.D. *Acc. Chem. Res.* **1982**, *15*, 268.

61. Ackermann, B.L., Ph.D. Dissertation, Chemistry Department, Michigan State University, **1986**.

62. Gower, J.L. *Biomed. Mass Spectrom.* **1985**, *12*, 191.

63. Lehmann, W.D.; Kessler, M.; Konig, W.A. *Biomed. Mass Spectrom.* **1984**, *11*, 217.

64. Buko, A.M.; Phillips, L.R.; Fraser, B.A. *Biomed. Mass Spectrom.* **1983**, *10*, 324.

65. Ackermann, B.L.; Coutant, J.E. Presented at the 35th ASMS Conference on Mass Spectrometry and Allied Topics, Denver, Colorado, May 24-29, **1987**.

66. Witten, J.L.; Schaffer, M.H.; O'Shea, M.; Cook, J.C.; Hemling, M.E.; Rinehart, K.L., Jr. *Biochem. Biophys. Res. Commun.* **1984**, *124*, 350.

67. Lattimer, R.P. *Int. J. Mass Spectrom. Ion Proc.* **1983**, *55*, 221.

68. Meili, J.; Seibl, J. *Org. Mass Spectrom.* **1984**, *19*, 581.

69. Busch, K.L.; Hsu, B-H.; Wood, K.V.; Cooks, R.G.; Schwartz, C.G.; Katritzky, A.R. *J. Org. Chem.* **1984**, *49*, 764.

70. De Pauw, E. *Mass Spectrom. Rev.* **1986**, *5*, 191.

71. Williams, D.H.; Bradley, C.; Bojesen, G.; Santikarn, S.; Taylor, L.C.E. *J. Am. Chem. Soc.* **1981**, *103*, 5700.

72. Sharp, T.R.; White, M.R.; Davis, J.F.; Stang, P.J. *Org. Mass Spectrom.* **1984**, *19*, 107.

73. Rudat, M.A.; McEwen, C.N. *Int. J. Mass Spectrom. Ion Phys.* **1983**, *46*, 351.

74. Caldwell, K.A.; Gross, M.L. *Anal. Chem.* **1989**, *61*, 494.

75. Dell, A.; Morris, H.R. *Biochem. Biophys. Res Commun.* **1982**, *106*, 1456.

76. Haskins, N.J.; New, A.P. *Rapid Commun. Mass Spectrom.* **1989**, *3*, 335.

77. Appelhans, A.D. *Int. J. Mass Spectrom. Ion Proc.* **1989**, *88*, 161.

78. Ross, M.M.; Wyatt, J.R.; Colton, R.J.; Campana, J.E. *Int. J. Mass Spectrom. Ion. Proc.* **1983**, *54*, 237.

79. McDowell, R.A.; Morris, H.R. *Int. J. Mass Spectrom. Ion Phys.* **1983**, *46*, 443.

80. Aberth, W.; Straub, K.M.; Burlingame, A.L. *Anal. Chem.* **1982**, *54*, 2029.

81. Franks, J. *Int. J. Mass Spectrom. Ion Phys.* **1983**, *46*, 343.

82. McIlraith, A.H. *J. Vac. Sci. Technol.* **1972**, *9*, 209.

83. Ligon, W.V., Jr. *Int. J. Mass Spectrom. Ion Phys.* **1982**, *41*, 205.

84. Mahoney, J.F.; Goebel, D.M.; Perel, J.; Forrester, A.T. *Biomed. Mass Spectrom.* **1983**, *10*, 61.

85. Perel, J.; Faull, K.; Mahoney, J.F.; Tyler, A.N.; Barchas, J.D. *Am. Lab.* **1984**, *16*, 94.

86. Appelhans, A.D.; Delmore, J.E.; Dahl, D.A. *Anal. Chem.* **1987**, *59*, 1685.

87. Hunt, D.F.; Shabanowitz, J.; Yates, J.R., III; Zhu, N.Z.; Russell, D.H.; Castro, M.E. *Proc. Natl. Acad. Sci. U.S.A.* **1987**, *84*, 620.

88. Olthoff, J.K.; Cotter, R.J. *Nucl. Instrum. Methods Phys. Res., Sect. B* **1987**, *B26*, 566.

89. Tecklenburg, R.E., Jr.; Castro, M.E.; Russell, D.H. *Anal. Chem.* **1989**, *61*, 153.

90. Aberth, W. *Anal. Chem.* **1986**, *58*, 1221.

91. Aberth, W.; Burlingame, A.L. *Anal. Chem.* **1984**, *56*, 2915.

92. Stoll, R.G.; Harvan, D.J.; Hass, J.R. *Int. J. Mass Spectrom. Ion Proc.* **1984**, *61*, 71.

93. Stoll, R.; Schade, U.; Rollgen, F.W.; Giessmann, U.; Barofsky, D.F. *Int. J. Mass Spectrom. Ion Phys.* **1982**, *43*, 227.

94. Barofsky, D.F.; Giessmann, U.; Bell, A.E.; Swanson, L.W. *Anal. Chem.* **1983**, *55*, 1318.

95. McEwen, C.N.; Hass, J.R. *Anal. Chem.* **1985**, *57*, 890.

96. Cole, R.B.; Guenat, C.; Hass, J.R.; Linton, R.W. *Anal. Chem.* **1987**, *59*, 1930.

97. Cotter, R.J. *Anal. Chem.* **1984**, *56*, 2594.

98. Olthoff, J.K.; Honovich, J.P.; Cotter, R.J. *Anal. Chem.* **1987**, *59*, 999.

99. Watson, J.T. *Introduction to Mass Spectrometry*, 2nd edition, Raven Press, New York, New York, **1985**.

100. Barber, M.; Bordoli, R.S.; Elliott, G.J.; Horoch, N.J.; Green, B.N. *Biochem. Biophys. Res. Commun.* **1983**, *110*, 753.

101. Biemann, K. *Biomed. Environ. Mass Spectrom.* **1988**, *16*, 99.

102. Dell, A.; Taylor, G.W. *Mass Spectrom. Rev.* **1984**, *3*, 357.

103. Matsuo, T. *Mass Spectrom. Rev.* **1989**, *8*, 203.

104. Yergey, J.; Heller, D.; Hansen, G.; Cotter, R.J.; Fenselau, C. *Anal. Chem.* **1983**, *55*, 353.

105. Yergey, J.A.; Cotter, R.J.; Heller, D.; Fenselau, C. *Anal. Chem.* **1984**, *56*, 2262.

106. Bartmess, J.E.; Phillips, L. Presented at the 33rd Annual Conference on Mass Spectrometry and Allied Topics, San Diego, California, May 26-31, **1985**.

107. Bartmess, J.E.; Phillips, L.R. Presented at the 34th Annual Conference on Mass Spectrometry and Allied Topics, Cincinnati, Ohio, June 8-13, **1986**.

108. Bartmess, J.E.; Phillips, L.R. *Anal. Chem.* **1987**, *59*, 2012.

109. Bard, A.J.; Faulkner, L.R. *Electrochemical Methods, Fundamentals and Applications*, J. Wiley and Sons, New York, New York, **1980**, 298.

110. Caprioli, R.M.; Fan, T. *Anal. Chem.* **1986**, *58*, 2949.

111. Caprioli, R.M.; Fan, T. *Biochem. Biophys. Res. Commun.* **1986**, *141*, 1058.

112. Caprioli, R.M.; Moore, W.T.; Fan, T. *Rapid Commun. Mass Spectrom.* **1987**, *1*, 15.

113. Clench, M.R.; Garner, G.V.; Gordon, D.B.; Barber, M. *Biomed. Mass Spectrom.* **1985**, *12*, 355.

114. Naylor, S.; Findeis, A.F.; Gibson, B.W.; Williams, D.H. *J. Am. Chem. Soc.* **1986**, *108*, 6359.

115. Caprioli, R.M. *Trends Anal. Chem.* **1988**, *7*, 328.

116. Caprioli, R.M.; Smith, L.A.; Beckner, C.F. *Int. J. Mass Spectrom. Ion Phys.* **1983**, *46*, 419.

117. Smith, L.A.; Caprioli, R.M. *Biomed. Mass Spectrom.* **1983**, *10*, 98.

118. Smith, L.A.; Caprioli, R.M. *Biomed. Mass Spectrom.* **1984**, *11*, 392.

119. Caprioli, R.M.; Smith, L. *Anal. Chem.* **1986**, *58*, 1080.

120. Caprioli, R.M.; DaGue, B.; Fan, T.; Moore, W.T. *Biochem. Biophys. Res. Commun.* **1987**, *146*, 291.

121. Mock, K.; Firth, J.; Cottrell, J.S.; *Org. Mass Spectrom.* **1989**, *24*, 591.

122. Lisek, C.A.; Bailey, J.E.; Benson, L.M.; Yaksh, T.L.; Jardine, I. *Rapid Commun. Mass Spectrom.* **1989**, *3*, 43.

123. Moseley, M.A.; Deterding, L.J.; deWitt, J.S.M.; Tomer, K.B.; Kennedy, R.T.; Bragg, N.; Jorgenson, J.W. *Anal. Chem.* **1989**, *61*, 1577.

124. Moseley, M.A.; Deterding, L.J.; Tomer, K.B.; Jorgenson, J.W. *Rapid Commun. Mass Spectrom.* **1989**, *3*, 87.

125. Reinhoud, N.J.; Niessen, W.M.A.; Tjaden, U.R.; Gramberg, L.G.; Verheij, E.R.; van der Greef, J. *Rapid Commun. Mass Spectrom.* **1989**, *3*, 348.

126. Wang, T-C.L.; Shih, M-c.; Markey, S.P.; Duncan, M.W. *Anal. Chem.* **1989**, *61*, 1013.

127. Seifert, W.E., Jr.; Ballatore, A.; Caprioli, R.M. *Rapid Commun. Mass Spectrom.* **1989**, *3*, 117.

128. Roboz, J.; Holland, J.F.; McDowall, M.A.; Hillmer, M.J. *Rapid Commun. Mass Spectrom.* **1988**, *2*, 64.

129. Caprioli, R.M. *Biochem.* **1988**, *27*, 513.

130. Gaskell, S.J.; Finlay, E.M.H. *Trends Anal. Chem.* **1988**, *7*, 202.

131. Clay, K.L.; Stene, D.O.; Murphy, R.C. *Biomed. Mass Spectrom.* **1984**, *11*, 47.

132. Ackermann, B.L.; Watson, J.T.; Newton, J.F., Jr.; Hook, J.B.; Braselton, W.E., Jr. *Biomed. Mass Spectrom.* **1984**, *11*, 502.

133. Beckner, C.F.; Caprioli, R.M. *Anal. Biochem.* **1983**, *130*, 328.

134. Beckner, C.F.; Caprioli, R.M. *Biomed. Mass Spectrom.* **1984**, *11*, 60.

135. Millington, D.S.; Roe, C.R.; Maltby, D.A. *Biomed. Mass Spectrom.* **1984**, *11*, 236.

136. Ligon, W.V., Jr.; Dorn, S.B. *Anal. Chem.* **1985**, *57*, 1993.

137. Simms, J.R.; Keough, T.; Ward, S.R.; Moore, B.L.; Bandurraga, M.M. *Anal. Chem.* **1988**, *60*, 2613.

138. Clay, K.L.; Murphy, R.C. *Int. J. Mass Spectrom. Ion Phys.* **1983**, *53*, 327.

139. Gilliam, J.M.; Landis, P.W.; Occolowitz, J.L. *Anal. Chem.* **1983**, *55*, 1531.

140. Rapp, U.; Kaufmann, H.; Hohn, M.; Pesch, R. *Int. J. Mass Spectrom. Ion Phys.* **1983**, *46*, 371.

141. Gilliam, J.M.; Landis, P.W.; Occolowitz, J.L. *Anal. Chem.* **1984**, *56*, 2285.

142. Amster, I.J.; Baldwin, M.A.; Cheng, M.T.; Proctor, C.J.; McLafferty, F.W. *J. Am. Chem. Soc.* **1983**, *105*, 1654.

143. Glish, G.L.; Todd, P.J.; Busch, K.L.; Cooks, R.G. *Int. J. Mass Spectrom. Ion Proc.* **1984**, *56*, 177.

144. Amster, I.J.; McLafferty, F.W. *Anal. Chem.* **1985**, *57*, 1208.

145. Lyon, P.A.; Crow, F.W.; Tomer, K.B.; Gross, M.L. *Anal. Chem.* **1984**, *56*, 2278.

146. Kingston, E.E.; Beynon, J.H.; Newton, R.P.; Liehr, J.G. *Biomed. Mass Spectrom.* **1985**, *12*, 525.

147. Kiplinger, J.P.; Bursey, M.M. *Org. Mass Spectrom.* **1988**, *23*, 342.

148. Russell, D.H.; Bricker, D.L. *Anal. Chim. Acta* **1985**, *178*, 117.

149. Bricker, D.L.; Russell, D.H. *J. Am. Chem. Soc.* **1986**, *108*, 6174.

150. Poulter, L.; Taylor, L.C.E. *Int. J. Mass Spectrom. Ion Proc.* **1989**, *91*, 183.

151. Alexander, A.J.; Thibault, P.; Boyd, R.K.; Rinehart, K.L.; Curtis, J.M. Presented at the 37th ASMS Conference on Mass Spectrometry and Allied Topics, Miami Beach, Florida, May 21-26, **1989**.

152. Sato, K.; Asada, T.; Ishihara, M.; Kunihiro, F.; Kammei, Y.; Kubota, E.; Costello, C.E.; Martin, S.A.; Scoble, H.A.; Biemann, K. *Anal. Chem.* **1987**, *59*, 1652.

153. Demirev, P.; Olthoff, J.K.; Fenselau, C.; Cotter, R.J. *Anal. Chem.* **1987**, *59*, 1951.

154. Forst, W. *Theory of Unimolecular Reactions*, Academic Press, New York, New York, **1973**.

155. Robins, R.H.; Crow, F.W. Presented at the 37th ASMS Conference on Mass Spectrometry and Allied Topics, Miami Beach, Florida, May 21-26, **1989**.

156. Tomer, K.B. *Mass Spectrom. Rev.* **1989**, *8*, 445.

157. Tomer, K.B. *Mass Spectrom. Rev.* **1989**, *8*, 483.

158. Dobberstein, P.; Korte, E.; Meyerhoff, G.; Pesch, R. *Int. J. Mass Spectrom. Ion Phys.* **1983**, *46*, 185.

159. Stroh, J.G.; Cook, J.C.; Milberg, R.M.; Brayton, L.; Kihara, T.; Huang, Z.; Rinehart, K.L., Jr.; Lewis, I.A.S. *Anal. Chem.* **1985**, *57*, 985.

160. Ito, Y.; Takeuchi, T.; Ishii, D.; Goto, M. *J. Chromatogr.* **1985**, *346*, 161.

161. Kokkonen, P.; van der Greef, J.; Niessen, W.M.A.; Tjaden, U.R.; ten Hove, G.J.; van der Werken, G. *Rapid Commun. Mass Spectrom.* **1989**, *3*, 102.

162. Camilleri, P.; Haskins, N.J.; Hill, A.J. *Rapid Commun. Mass Spectrom.* **1989**, *3*, 346.

163. Doherty, S.J.; Busch, K.L. Presented at the 36th ASMS Conference on Mass Spectrometry and Allied Topics, San Francisco, California, June 5-10, **1988**.

164. Cerny, R.L.; Sullivan, B.P.; Bursey, M.M.; Meyer, T.J. *Anal. Chem.* **1983**, *55*, 1954.

165. David, L.; Della Negra, S.; Fraisse, D.; Jeminet, G.; Lorthiois, I.; Le Beyec, Y.; Tabet, J.C. *Int. J. Mass Spectrom. Ion Phys.* **1983**, *46*, 391.

166. van der Greef, J.; ten Noever de Brauw, M.C. *Int. J. Mass Spectrom. Ion Phys.* **1983**, *46*, 379.

167. Kloppel, K.D.; von Bunau, G.; Weyer, K. *Int. J. Mass Spectrom. Ion Phys.* **1983**, *46*, 463.

168. Heller, D.N.; Fenselau, C.; Cotter, R.J.; Demirev, P.; Olthoff, J.K.; Honovich, J.; Uy, M.; Tanaka, T.; Kishimoto, Y. *Biochem. Biophys. Res. Commun.* **1987**, *142*, 194.

169. Werner, E.; Main, D.E.; Standing, K.G.; Chait, B.T. *Anal. Chem.* **1988**, *60*, 1494.

170. Lay, J.O., Jr.; Getek, T.A.; Kelly, D.W.; Slikker, W., Jr.; Korfmacher, W.A. *Rapid Commun. Mass Spectrom.* **1989**, *3*, 72.

171. Cooks, R.G.; Busch, K.L. *Int. J. Mass Spectrom. Ion Phys.* **1983**, *53*, 111.

172. Honda, F.; Lancaster, G.M.; Fukuda, Y.; Rabalais, J.W. *J. Chem. Phys.* **1978**, *69*, 4931.

173. Michl, J. *Int. J. Mass Spectrom. Ion Phys.* **1983**, *53*, 255.

174. Whitlow, H.J.; Hautala, M.; Sundqvist, B.U.R. *Int. J Mass Spectrom. Ion Proc.* **1987**, *78*, 329.

175. Harrison, D.E., Jr.; Kelly, P.W.; Garrison, B.J.; Winograd, N. *Surf. Sci.* **1978**, *76*, 311.

176. Kidwell, D.A.; Ross, M.M.; Colton, R.J. *Int. J. Mass Spectrom. Ion Proc.* **1987**, *78*, 315.

177. Wong, S.S.; Rollgen, F.W. *Nucl. Instrum. Methods Phys. Res., Sect. B* **1986**, *14*, 436.

178. Benninghoven, A. *Int. J. Mass Spectrom. Ion Phys.* **1983**, *53*, 85.

179. Pachuta, S.J.; Cooks, R.G. *Chem. Rev.* **1987**, *87*, 647.

180. McNeal, C.J. *Anal. Chem.* **1982**, *54*, 43A.

181. Lancaster, G.M.; Honda, F.; Fukuda, Y.; Rabalais, J.W. *J. Am. Chem. Soc.* **1979**, *101*, 1951.

182. Martin, S.A.; Costello, C.E.; Biemann, K. *Anal. Chem.* **1982**, *54*, 2362.

183. Faull, K.F.; Barchas, J.D.; Kenyon, C.N.; Goodley, P.C. *Int. J. Mass Spectrom. Ion Phys.* **1983**, *46*, 347.

184. Stoll, R.; Schade, U.; Rollgen, F.W.; Giessmann, U.; Barofsky, D.F. *Int. J. Mass Spectrom. Ion Phys.* **1982**, *43*, 227.

185. Morris, H.R.; Panico, M.; Haskins, N.J. *Int. J. Mass Spectrom. Ion Phys.* **1983**, *46*, 363.

186. Aberth, W.H.; Burlingame, A.L. *Anal. Chem.* **1988**, *60*, 1426.

187. Puzo, G.; Prome, J.C. *Org. Mass Spectrom.* **1984**, *19*, 448.

188. Tondeur, Y.; Clifford, A.J.; DeLuca, L.M. *Org. Mass Spectrom.* **1985**, *20*, 157.

189. Emary, W.B.; Cooks, R.G.; Toren, P.C. *Anal. Chem.* **1986**, *58*, 1218.

190. Puzo, G.; Prome, J.C. *Org. Mass Spectrom.* **1985**, *20*, 288.

191. Barber, M.; Bordoli, R.S.; Elliott, G.J.; Sedgwick, R.D.; Tyler, A.N. *Anal. Chem.* **1982**, *54*, 645A.

192. Wong, S.S.; Rollgen, F.W. *Int. J. Mass Spectrom. Ion Proc.* **1986**, *70*, 135.

193. Campana, J.E. *Mass Spectrom. Rev.* **1987**, *6*, 395.

194. Katz, R.N.; Chaudhary, T.; Field, F.H. *J. Am. Chem. Soc.* **1986**, *108*, 3897.

195. Katz, R.N.; Chaudhary, T.; Field, F.H. *Int. J. Mass Spectrom. Ion Proc.* **1987**, *78*, 85.

196. Katz, R.N.; Field, F.H. *Int. J. Mass Spectrom. Ion Proc.* **1989**, *87*, 95.

197. Field, F.H. *J. Phys. Chem.* **1982**, *86*, 5115.

198. Keough, T.; Ezra, F.S.; Russell, A.F.; Pryne, J.D. *Org. Mass Spectrom.* **1987**, *22*, 241.

199. Standing, K.G.; Chait, B.T.; Ens, N.; McIntosh, G.; Beavis, R. *Nucl. Instrum. Methods* **1982**, *198*, 33.

200. Ligon, W.V.; Dorn, S.B. *Int. J. Mass Spectrom. Ion Proc.* **1984**, *57*, 75.

201. Ligon, W.V., Jr.; Dorn, S.B. *Int. J. Mass Spectrom. Ion Proc.* **1984**, *61*, 113.

202. Allmaier, G.M. *Rapid Commun. Mass Spectrom.* **1988**, *2*, 74.

203. Allmaier, G.M. *Anal. Chim. Acta* **1989**, *223*, 349.

204. Naylor, S.; Moneti, G.; Guyan, S. *Biomed. Environ. Mass Spectrom.* **1988**, *17*, 393.

205. Naylor, S.; Skelton, N.J.; Williams, D.H. *J. Chem. Soc., Chem. Commun.* **1986**, 1619.

206. Fenselau, C.; Cotter, R.J. *Chem. Rev.* **1987**, *87*, 501.

207. Zhang, M-Y.; Liang, X-Y.; Chen, Y-Y.; Liang, X-G. *Anal. Chem.* **1984**, *56*, 2288.

208. Caprioli, R.M. *Anal. Chem.* **1983**, *55*, 2387.

209. Connolly, M.J.; Orth, R.G. *Anal. Chem.* **1987**, *59*, 903.

210. Ligon, W.V., Jr.; Dorn, S.B. *Int. J. Mass Spectrom. Ion Proc.* **1985**, *63*, 315.

211. Ligon, W.V., Jr.; Dorn, S.B. *Int. J. Mass Spectrom. Ion Proc.* **1986**, *68*, 337.

212. Ligon, W.V., Jr.; Dorn, S.B. *Int. J. Mass Spectrom. Ion Proc.* **1986**, *78*, 99.

213. Ligon, W.V., Jr. *Anal. Chem.* **1986**, *58*, 485.

214. Ligon, W.V., Jr.; Dorn, S.B. *Anal. Chem.* **1986**, *58*, 1889.

215. Atkins, P.W. *Physical Chemistry*, 3rd edition, Oxford University Press, Oxford, **1986**.

216. Barber, M.; Bordoli, R.S.; Elliott, G.J.; Sedgwick, R.D.; Tyler, A.N. *J. Chem. Soc., Faraday Trans. 1*, **1983**, *79*, 1249.

217. Bursey, M.M.; Marbury, G.D.; Hass, J.R. *Biomed. Mass Spectrom.* **1984**, *11*, 522.

218. Ligon, W.V., Jr. *Int. J. Mass Spectrom. Ion Phys.* **1983**, *52*, 183.

219. Wong, S.S.; Rollgen, F.W.; Manz, I.; Przybylski, M. *Biomed. Mass Spectrom.* **1985**, *12*, 43.

220. Clay, K.L.; Wahlin, L.; Murphy, R.C. *Biomed. Mass Spectrom.* **1983**, *10*, 489.

221. Moon, D.W.; Winograd, N. *Int. J. Mass Spectrom. Ion Phys.* **1983**, *52*, 217.

222. Busch, K.L.; Unger, S.E.; Vincze, A.; Cooks, R.G.; Keough, T. *J. Am. Chem. Soc.* **1982**, *104*, 1507.

223. Evershed, R.P.; Prescott, M.C.; Kabbouh, M.; Rees, H.H. *Rapid Commun. Mass Spectrom.* **1989**, *3*, 352.

224. Winger, B.E.; Hand, O.W.; Cooks, R.G. *Int. J. Mass Spectrom. Ion Proc.* **1988**, *84*, 89.

225. Perich, J.W.; Johns, R.B.; Liepa, I.; Chaffee Csiro, A.L. *Org. Mass Spectrom.* **1988**, *23*, 797.

226. Tang, X.; Ens, W.; Standing, K.G.; Westmore, J.B. *Anal. Chem.* **1988**, *60*, 1791.

227. Mallis, L.M.; Russell, D.H. *Anal. Chem.* **1986**, *58*, 1076.

228. Mallis, L.M.; Russell, D.H. *Int. J. Mass Spectrom. Ion Proc.* **1987**, *78*, 147.

229. Russell, D.H.; McGlohon, E.S.; Mallis, L.M. *Anal. Chem.* **1988**, *60*, 1818.

230. Adams, J.; Gross, M.L. *J. Am. Chem. Soc.* **1986**, *108*, 6915.

231. Adams, J.; Gross, M.L. *Anal. Chem.* **1987**, *59*, 1576.

232. Benninghoven, A. *Int. J. Mass Spectrom. Ion. Phys.* **1983**, *46*, 459.

233. Williams, P. *Int. J. Mass Spectrom. Ion Phys.* **1983**, *53*, 101.

234. Musselman, B.D.; Watson, J.T.; Chang, C.K. *Org. Mass Spectrom.* **1986**, *21*, 215.

235. Huang, Q-W.; Wu, G-L.; Tang, H-T. *Int. J. Mass Spectrom. Ion Proc.* **1986**, *70*, 145.

236. Cotter, R.J.; Van Breemen, R.; Yergey, J.; Heller, D. *Int. J. Mass Spectrom. Ion Phys.* **1983**, *46*, 395.

237. Schroder, E.; Munster, H.; Budzikiewicz, H. *Org. Mass Spectrom.* **1986**, *21*, 707.

238. Munster, H.; Theobald, F.; Budzikiewicz, H.; Schroder, E. *Int. J. Mass Spectrom. Ion Proc.* **1987**, *79*, 73.

239. Miller, J.K.; Balasanmugam, K.; Fulcher, A. *Org. Mass Spectrom.* **1989**, *24*, 497.

240. Groenewold, G.S.; Todd, P.J. *Anal. Chem.* **1985**, *57*, 886.

241. Sunner, J.A.; Kulatunga, R.; Kebarle, P. *Anal. Chem.* **1986**, *58*, 1312.

242. Sunner, J.A.; Kulatunga, R.; Kebarle, P. *Anal. Chem.* **1986**, *58*, 2009.

243. Sunner, J.; Morales, A.; Kebarle, P. *Anal. Chem.* **1987**, *59*, 1378.

244. Sunner, J.; Morales, A.; Kebarle, P. *Anal. Chem.* **1988**, *60*, 98.

245. Sunner, J.; Morales, A.; Kebarle, P. *Int. J. Mass Spectrom. Ion Proc.* **1988**, *86*, 169.

246. Sunner, J.; Morales, A.; Kebarle, P. *Int. J. Mass Spectrom. Ion Proc.* **1989**, *87*, 287.

247. Lacey, M.P.; Keough, T. *Rapid Commun. Mass Spectrom.* **1989**, *3*, 46.

248. Kralj, B.; Kramer, V.; Vrscaj, V. *Int. J. Mass Spectrom. Ion Phys.* **1983**, *46*, 399.

249. Dube, G. *Org. Mass Spectrom.* **1984**, *19*, 242.

250. Clayton, E.; Wakefield, A.J.C. *J. Chem. Soc., Chem. Commun.* **1984**, 969.

251. Bojesen, G.; Moller, J. *Int. J. Mass Spectrom. Ion Proc.* **1986**, *68*, 239.

252. Renner, D.; Spiteller, G. *Biomed. Environ. Mass Spectrom.* **1986**, *13*, 401.

253. Balasanmugam, K.; Miller, J.M.; Smith, R.W. *Org. Mass Spectrom.* **1988**, *23*, 685.

254. Takayama, M.; Fukai, T.; Nomura, T.; Nojima, K. *Rapid Commun. Mass Spectrom.* **1989**, *3*, 4.

255. Miller, J.M.; Balasanmugam, K. *Anal. Chem.* **1989**, *61*, 1293.

256. Dass, C.; Seshadri, R.; Israel, M.; Desiderio, D.M. *Biomed. Environ. Mass Spectrom.* **1988**, *17*, 37.

257. De Pauw, E. *Anal. Chem.* **1983**, *55*, 2195.

258. Cerny, R.L.; Gross, M.L. *Anal. Chem.* **1985**, *57*, 1160.

259. Hand, O.W.; Cooks, R.G. *Int. J. Mass Spectrom. Ion Proc.* **1989**, *88*, 113.

260. Schronk, L.R.; Cotter, R.J. *Biomed. Environ. Mass Spectrom.* **1986**, *13*, 395.

261. Freas, R.B.; Ross, M.M.; Campana, J.E. *J. Am. Chem. Soc.* **1985**, *107*, 6195.

262. Metral, C.J.; Day, R.A. *Anal. Lett.* **1986**, *19*, 217.

263. Creaser, C.S.; Crosland, S. *Anal. Chem.* **1989**, *61*, 1310.

264. Gale, P.J.; Bentz, B.L.; Chait, B.T.; Field, F.H.; Cotter, R.J. *Anal. Chem.* **1986**, *58*, 1070.

265. Yazdanparast, R.; Andrews, P.; Smith, D.L.; Dixon, J.E. *Anal. Biochem.* **1986**, *153*, 348.

266. Pelzer, G.; De Pauw, E.; Viet Dung, D.; Marien, J. *J. Phys. Chem.* **1984**, *83*, 5065.

267. Ligon, W.V., Jr. *Int. J. Mass Spectrom. Ion Phys.* **1983**, *52*, 189.

268. Sethi, S.K.; Nelson, C.C.; McCloskey, J.A. *Anal. Chem.* **1984**, *56*, 1975.

269. Santana-Marques, M.G.O.; Ferrer-Correia, A.J.V.; Gross, M.L. *Anal. Chem.* **1989**, *61*, 1442.

270. Williams, D.H.; Findeis, A.F.; Naylor, S.; Gibson, B.W. *J. Am. Chem. Soc.* **1987**, *109*, 1980.

271. Baldwin, M.A.; Welham, K.J.; Toth, I.; Gibbons, W.A. *Org. Mass Spectrom.* **1988**, *23*, 697.

272. Prokai, L.; Hsu, B-H.; Farag, H.; Bodor, N. *Anal. Chem.* **1989**, *61*, 1723.

273. Duffin, K.L.; Busch, K.L. *Int. J. Mass Spectrom. Ion Proc.* **1986**, *74*, 141.

274. Hand, O.W.; Hsu, B-H.; Cooks, R.G. *Org. Mass Spectrom.* **1988**, *23*, 16.

275. Perich, J.W.; Liepa, I.; Chaffee, A.L. *Org. Mass Spectrom.* **1988**, *23*, 680.

276. Dass, C.; Desiderio, D.M. *Anal. Chem.* **1988**, *60*, 2723.

277. Ashton, P.R.; Rose, M.E. *Org. Mass Spectrom.* **1986**, *21*, 388.

278. Cerveau, G.; Chuit, C.; Corriu, R.J.P.; Reye, C.; Aubagnac, J.L. *Int. J. Mass Spectrom. Ion Proc.* **1989**, *91*, 145.

279. Okamoto, Y.; Takei, Y.; Rose, M.E. *Int. J. Mass Spectrom. Ion Proc.* **1989**, *87*, 225.

280. Rose, M.E.; Webster, M.J. *Org. Mass Spectrom.* **1989**, *24*, 567.

281. Chan, K.W.S.; Cook, K.D. *Anal. Chem.* **1983**, *55*, 1422.

282. Verma, S.; Pomerantz, S.C.; Sethi, S.K.; McCloskey, J.A. *Anal. Chem.* **1986**, *58*, 2898.

283. Bentz, B.L.; Gale, P.J. *Int. J. Mass Spectrom. Ion Proc.* **1987**, *78*, 115.

284. Detter, L.D.; Hand, O.W.; Cooks, R.G.; Walton, R.A. *Mass Spectrom. Rev.* **1988**, *7*, 465.

285. Morris, H.R.; Panico, M.; Taylor, G.W. *Biochem. Biophys. Res. Commun.* **1983**, *117*, 299.

286. Desiderio, D.M.; Katakuse, I. *Mass Spectros.* **1985**, *33*, 351.

287. Hunt, D.F.; Yates, J.R., III; Shabanowitz, J.; Winston, S.; Hauer, C.R. *Proc. Natl. Acad. Sci. USA* **1986**, *83*, 6233.

288. Biemann, K.; Scoble, H.A. *Science* **1987**, *237*, 992.

289. Roepstorff, P.; Fohlman, J. *Biomed. Mass Spectrom.* **1984**, *11*, 601.

290. Stults, J.T.; Watson, J.T. *Biomed. Environ. Mass Spectrom.* **1987**, *14*, 583.

291. Johnson, R.S.; Martin, S.A.; Biemann, K.; Stults, J.T.; Watson, J.T. *Anal. Chem.* **1987**, *59*, 2621.

292. Bull, H.B.; Breese, K. *Arch. Biochem. Biophys.* **1974**, *161*, 665.

293. Gibson, B.W.; Biemann, K. *Proc. Natl. Acad. Sci. USA* **1984**, *81*, 1956.

294. Hartman, N.R.; Jardine, I. *Biomed. Environ. Mass Spectrom.* **1986**, *13*, 361.

295. Biemann, K. *Int. J. Mass Spectrom. Ion Phys.* **1982**, *45*, 183.

296. Williams, D.H.; Bradley, C.V.; Santikarn, S.; Bojesen, G. *Biochem. J.* **1982**, *201*, 105.

297. Biemann, K. *Anal. Chem.* **1986**, *58*, 1288A.

298. Biemann, K.; Martin, S.A. *Mass Spectrom. Rev.* **1987**, *6*, 1.

299. Dell, A.; Oates, J.E.; Morris, H.R.; Egge, H. *Int. J. Mass Spectrom. Ion. Phys.* **1983**, *46*, 415.

300. Wang, W.T.; LeDonne, N.C., Jr.; Ackermann, B.; Sweeley, C.C. *Anal. Biochem.* **1984**, *141*, 366.

301. Honda, S.; Kakehi, K.; Ohmura, T.; Morita, M. *Biomed. Environ. Mass Spectrom.* **1988**, *15*, 233.

302. Reinhold, V.N.; Carr, S.A. *Mass Spectrom. Rev.* **1983**, *2*, 153.

303. Grotjahn, L.; Frank, R.; Blocker, H. *Int. J. Mass Spectrom. Ion Phys.* **1983**, *46*, 439.

304. Grotjahn, L.; Blocker, H.; Frank, R. *Biomed. Mass Spectrom.* **1985**, *12*, 514.

305. Sakurai, T.; Matsuo, T.; Kusai, A.; Nojima, K. *Rapid Commun. Mass Spectrom.* **1989**, *3*, 212.

306. Schram, K.H.; Slowikowski, D.L. *Biomed. Environ. Mass Spectrom.* **1986**, *13*, 263.

307. Newton, R.P.; Walton, T.J.; Brenton, A.G.; Kingston, E.E.; Harris, F.M. *Rapid. Commun. Mass Spectrom.* **1989**, *3*, 178.

308. Schram, K.H. *Trends Anal. Chem.* **1988**, *7*, 28.

309. Caprioli, R.M. *Mass Spectrom. Rev.* **1987**, *6*, 237.

310. Burlingame, A.L.; Whitney, J.O.; Russell, D.H. *Anal. Chem.* **1984**, *56*, 417R.

311. Burlingame, A.L.; Baillie, T.A.; Derrick, P.J. *Anal. Chem.* **1986**, *58*, 165R.

312. Burlingame, A.L.; Maltby, D.; Russell, D.H.; Holland, P.T. *Anal. Chem.* **1988**, *60*, 294R.

313. Johnstone, R.A.W.; Lewis, I.A.S. *Int. J. Mass Spectrom. Ion Phys.* **1983**, *46*, 451.

314. Johnstone, R.A.W.; Lewis, I.A.S.; Rose, M.E. *Tetrahedron*, **1983**, *39*, 1597.

315. Smith, D.L. *Anal. Chem.* **1983**, *55*, 2391.

316. Dolnikowski, G.G.; Watson, J.T.; Allison, J. *Anal. Chem.* **1984**, *56*, 197.

317. Eagles, J.; Fairweather-Tait, S.J.; Portwood, D.E.; Self, R.; Gotz, A.; Heumann, K.G. *Anal. Chem.* **1989**, *61*, 1023.

318. Bowen, R.D.; Danks, T.N.; Mitchell, D.; Thomas, S.E. *Org. Mass Spectrom.* **1988**, *23*, 674.

319. van Breemen, R.B.; Martin, L.B.; Schreiner, A.F. *Anal. Chem.* **1988**, *60*, 1314.

320. Cetini, G.; Operti, L.; Vaglio, G.A.; Bandini, A.L.; Banditelli, G.; Minghetti, G. *Org. Mass Spectrom.* **1989**, *24*, 479.

321. Schwarz, H.; Eckart, K.; Taylor, L.C.E. *Org. Mass Spectrom.* **1982**, *17*, 458.

322. Sweeley, C.C.; Nunez, H.A. *Ann. Rev. Biochem.* **1985**, *54*, 765.

323. Egge, H.; Peter-Katalinic, J. *Mass Spectrom. Rev.* **1987**, *6*, 331.

324. Komori, T.; Kawasaki, T.; Schulten, H-R. *Mass Spectrom. Rev.* **1985**, *4*, 255.

325. Isobe, R.; Komori, T.; Abe, F.; Yamauchi, T. *Biomed. Environ. Mass Spectrom.* **1986**, *13*, 585.

326. Pare, J.R.J.; LaFontaine, P.; Belanger, J.; Sy, W-W.; Jordan, N.; Loo, J.C.K. *J. Pharm. Biomed. Anal.* **1987**, *5*, 131.

327. Gaskell, S.J.; Brownsey, B.G.; Brooks, P.W.; Green, B.N. *Int. J. Mass Spectrom. Ion Phys.* **1983**, *46*, 435.

328. Catlow, D.A. *Int. J. Mass Spectrom. Ion Phys.* **1983**, *46*, 387.

329. Tomer, K.B.; Crow, F.W.; Knoche, H.W.; Gross, M.L. *Anal. Chem.* **1983**, *55*, 1033.

330. Ross, M.M.; Neihof, R.A.; Campana, J.E. *Anal. Chim. Acta* **1986**, *181*, 149.

331. Heller, D.N.; Murphy, C.M.; Cotter, R.J.; Fenselau, C.; Uy, O.M. *Anal. Chem.* **1988**, *60*, 2787.

332. Gower, J.L. *Int. J. Mass Spectrom. Ion Phys.* **1983**, *46*, 431.

333. Self, R.; Eagles, J.; Galletti, G.C.; Mueller-Harvey, I.; Hartley, R.D.; Lea, A.G.H.; Magnolato, D.; Richli, U.; Gujer, R.; Haslam, E. *Biomed. Environ. Mass Spectrom.* **1986**, *13*, 449.

334. Karchesy, J.J.; Hemingway, R.W.; Foo, Y.L.; Barofsky, E.; Barofsky, D.F. *Anal. Chem.* **1986**, *58*, 2563.

335. Bletsos, I.V.; Hercules, D.M.; Greifendorf, D.; Benninghoven, A. *Anal. Chem.* **1985**, *85*, 2384.

336. Ballistreri, A.; Garozzo, D.; Giuffrida, M.; Montaudo, G. *Anal. Chem.* **1987**, *59*, 2024.

337. Lay, J.O., Jr.; Miller, B.J. *Anal. Chem.* **1987**, *59*, 1323A.

338. Monaghan, J.J.; Barber, M.; Bordoli, R.S.; Sedgwick, R.D.; Tyler, A.N. *Int. J. Mass Spectrom. Ion Phys.* **1983**, *46*, 447.

339. Ventura, F.; Figueras, A.; Caixach, J.; Rivera, J.; Fraisse, D. *Org. Mass Spectrom.* **1988**, *23*, 558.

Chapter 2. Influence of the Ratio of Glycerol to Analyte on the FAB-MS Response of Peptides

I. Introduction

Sample preparation is a critical factor in determining the quality of FAB-MS results. As described in Chapter 1, the mass spectrometrist would prefer to maximize the signal from the analyte and minimize the interfering matrix spectrum. Various strategies in sample preparation have evolved to accomplish these goals. Many workers add acidic or cationic modifiers to their samples to enhance the analyte ion abundance in the positive ion mode; however, this method also increases the abundance or complexity of the matrix spectrum in many cases (1, 2). Significantly different approaches in application of the matrix compound to the sample pedestal are employed. Some laboratories deposit a 1-2 ul portion of matrix on the probe tip (3). Another report describes application of glycerol in "a layer of 0.2 ul" (4). Other laboratories apply the matrix from a solution of a particular concentration (e.g., 50% aqueous glycerol (5)).

Our work originated with the observation that application of the glycerol matrix in a dilute aqueous solution (rather than neat) allows a significant enhancement in the spectral quality of conventional direct probe FAB analyses. This observation prompted a systematic study regarding the effects of analyte, glycerol, and water quantity upon the FAB-MS results for five different peptides. Analyses of peptide mixtures were then evaluated in the same systematic manner. The experimental findings suggest that the molar ratio of glycerol to analyte is critical in optimizing the desorption ionization behavior of the sample.

The optimum occurs at the point where the formation and detection of analyte ions is differentially favored over that of the matrix ions.

II. Experimental

a. Mass Spectrometry

All experiments were performed upon a double-focusing (EB geometry) JEOL HX-110 mass spectrometer. This instrument is equipped with a FAB gun which produces a 6-keV xenon atom beam that was used for this work. The source pressure with the xenon beam operating was approximately $3x10^{-6}$ torr. A resolving power of 3000 was employed at an acceleration potential of 8 or 10 kV. For the comparisons strictly involving bradykinin, scans were collected over a mass interval from 30 to 1200 u, in a period of 10.1 sec, allowing 2.8 sec between consecutive scans. For those runs utilized in the comparison of results from the five individual peptides and the peptide mixtures, a mass range of 0 to 1300 u was scanned in 11.1 sec, allowing 2.1 sec between scans. All data were acquired, stored, and processed with the JEOL DA5000 data system.

b. Materials

The six peptides ([Val^4]-angiotensin III, proenkephalin, bradykinin, substance P (residues 1-9), fibronectin related peptide, and NPNANPNANPNA) used were purchased from Sigma Chemical Co. and glycerol was obtained from Mallinckrodt, Inc. Aqueous matrix solutions were prepared in terms of weight percentage glycerol. The glycerol was used as received without further purification.

c. Sample Preparation and Analysis

All aqueous solutions of matrix and analyte were applied with Hamilton syringes. Sample application began by depositing the glycerol matrix upon the probe tip. The analyte portion was then added and the sample stirred with the syringe needle for approximately 15 sec. Results from samples stirred in this manner were shown to be more precise than results from unstirred samples. All sample compositions reported below describe the sample prior to exposure to the vacuum. The probe was introduced into the source of the mass spectrometer immediately after evacuating the vacuum lock. At this point, the FAB beam, acceleration potential, repeller potential, and lens potentials were adjusted to optimize the peak shape and intensity at a selected m/z value (e.g., m/z 185). Only minor adjustments were needed for each parameter because of prior focusing, and the entire process, from probe insertion to initiation of the scan, was accomplished in approximately 1 min. Due to the transient desorptive behavior of some samples, on occasions when extensive focusing (requiring longer than one minute) was necessary, the probe was removed from the source without the acquisition of data and a new sample was applied. For this reason, also, the first scan of each run was utilized for data comparison.

For the analyses of the individual peptides, ion abundances represented in the figures were divided by the fullscale value of the output device; hence, they are intended to be interpreted in an absolute sense. Appropriate peaks in the bradykinin spectrum have been labeled according to the nomenclature suggested by Roepstorff and Fohlman (6) and modified by Biemann (7). Figures illustrating bradykinin ion response under various conditions are based on a representative cross section of the mass spectrum: one ion of low mass (e.g., m/z 70), another

of intermediate mass (e.g., m/z 527), and the $[M+H]^+$ ion (m/z 1060); other significant bradykinin ions (m/z 120, 491, 572, 805, and 903) in each spectral region usually behaved in an analogous manner. Comparison of results (absolute peak intensity values) was limited to those data collected from an individual session on the mass spectrometer. Results from different days were not compared because of differences in instrumental conditions (e.g., source cleanliness and settings of detection electronics).

For the analyses of the peptide mixtures, fractional total ionization (FTI) values (8) were employed as a measure of peptide response. The formulation of these values will be carefully described in the appropriate section.

III. Results and Discussion

a. 4 nmol of Bradykinin Sampled from 1 ul of 56% Aqueous Glycerol vs. 1 ul of 5% Aqueous Glycerol

Figure 2.1a shows a spectrum of 4 nmol of bradykinin dispersed in 56% (w/w) glycerol in water (prior to exposure to the vacuum). This sample was prepared by adding 1.0 ul of an aqueous bradykinin solution (4 nmol/ul) to 1 ul of glycerol. Those peaks denoted by a "G" correspond to glycerol matrix ions. Figure 2.1b shows a spectrum of 4 nmol of bradykinin dispersed in an environment of 5% (w/w) glycerol in water. This sample was obtained by adding 1.0 ul of the aqueous bradykinin solution to 1.0 ul of 10% glycerol in water. Interestingly, the spectra display significant differences. The spectrum taken from the sample containing less glycerol and more water (Figure 2.1b) shows a much better visibility of analyte peaks over matrix peaks, although both samples contained the same amount of bradykinin. This improvement occurs from the

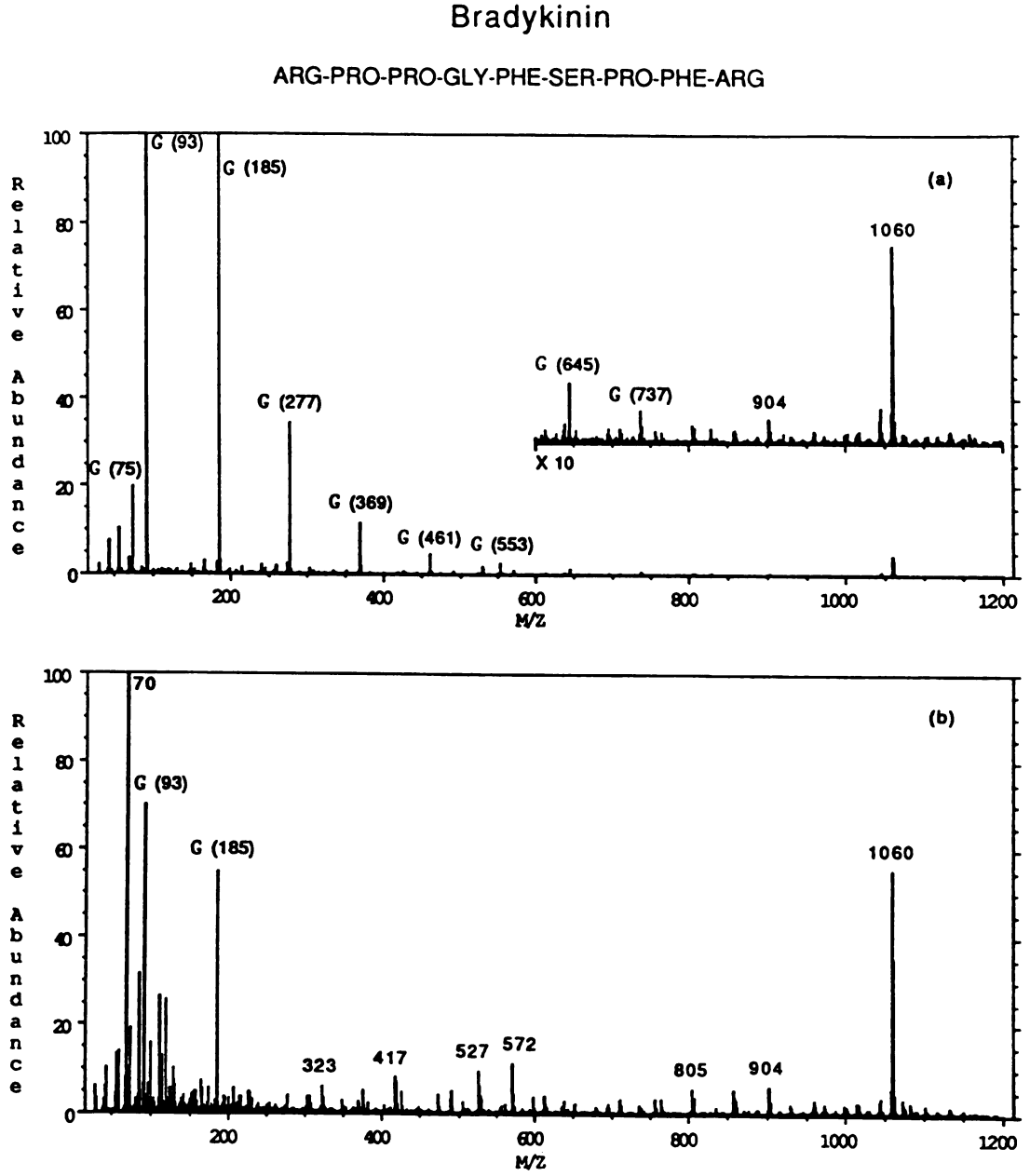

Figure 2.1. (a) FAB mass spectrum of 1.0 ul of aqueous bradykinin solution (4 nmol/ul) added to 1 ul of glycerol. Major peaks derived from the glycerol matrix are labeled with a "G". (b) FAB mass spectrum of 1.0 ul of bradykinin solution added to 1.0 ul of 10% aqueous glycerol.

$[M+H]^+$ signal at m/z 1060, through peaks corresponding to structurally significant fragment ions, to lower mass immonium ions.

b. Response Profiles for Bradykinin and Glycerol Ions as a Function of Glycerol/Water Composition

To more carefully characterize this effect, mass spectral results from samples composed of 1%, 2%, 5%, 21%, and 56% glycerol in water were compared. Each sample contained 4 nmol of bradykinin and the total sample volume in each case was initially 2 ul. Figure 2.2 shows peak intensities for selected analyte ions (divided by the fullscale signal of the output device) plotted against weight percent of glycerol. Each point represents the mean of three separate runs (the first scan was evaluated from each run) and the error bars correspond to one standard deviation of these data. For all analyte ions there is a significant increase in abundance as the sample consists of more water and less glycerol. This enhancement reaches a maximum followed by a decline in abundance as the glycerol becomes scarce. Interestingly, the optimum matrix composition does not appear to be identical for all analyte ions. While the higher mass analyte ion abundances maximize at 5% glycerol (as viewed in Figure 2.2), the ion abundances for m/z 70 maximize at 2% glycerol. The peak at m/z 70 corresponds to an immonium ion which is indicative of the proline amino acid residue. For bradykinin and the other peptides investigated in this work, peak intensities for the immonium ions and other especially low mass fragment ions maximized at slightly lower proportions of glycerol in water than the peak intensities for other analyte ions. This trend, which may appear subtle given the precision of results obtained from the two sample compositions shown in Figure 2.2, is nonetheless reproducible in the repeated formulation of these curves.

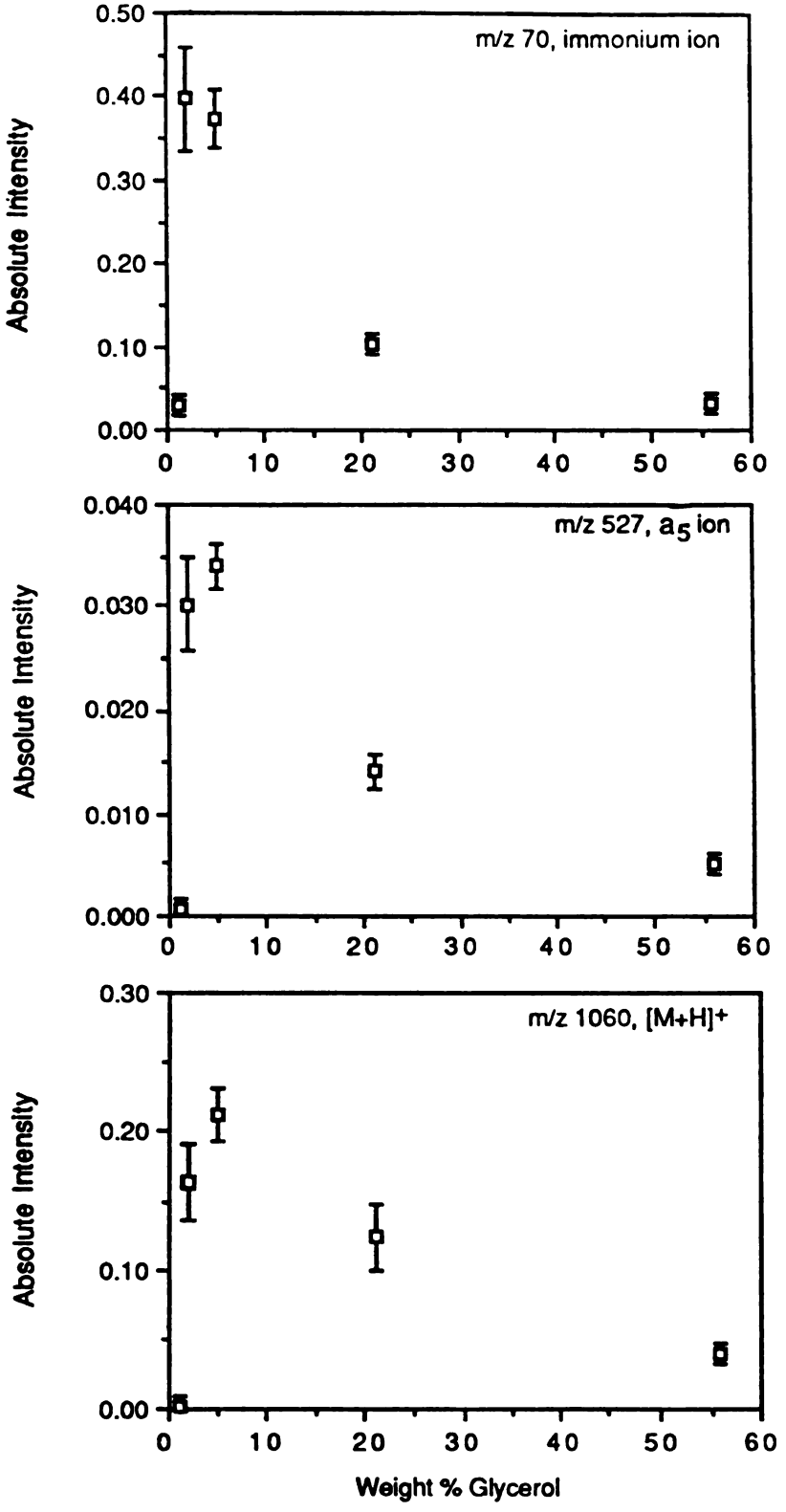

Figure 2.2. Plots of peak intensity for selected bradykinin ions (m/z 70 (top), m/z 527 (middle), and m/z 1060) versus weight percentage glycerol. Each sample contained 4 nmol of bradykinin and the total sample volume in each case was 2 ul.

This effect is also evident in the mass spectra for these sample compositions, which display a significant increase in the fragmentation processes resulting in the formation of the relatively stable, low mass ions. A possible explanation for this increased fragmentation will be considered shortly.

Figure 2.3 shows the corresponding data for selected matrix ions. Quite clearly, the glycerol peak intensities decrease substantially as the amount of glycerol in the sample declines. Accordingly, the net effect observed in Figure 2.1 is due to two complementary factors. Increasing the amount of water and decreasing the amount of glycerol in the sample appears to bolster analyte ion abundances and diminish matrix ion abundances significantly. This result is analogous to the observations of Caprioli while using the continuous-flow FAB probe (9).

c. Ionization Efficiency for Bradykinin Sampled from 1 ul of 56% Aqueous Glycerol vs. 1 ul of 5% Aqueous Glycerol

Another difference in results obtained from the two sample compositions represented in Figure 2.1 involves the time dependence of the experiment. While the sample containing more glycerol maintains a signal over a relatively long period of time, the signal from the sample containing less glycerol is more transient. The ion abundances produced from the latter environment tend to diminish comparatively rapidly; consequently, the first spectrum obtained under these circumstances is often the most useful. This observation prompted a comparison of ionization efficiency of the analyte as a function of matrix composition. An assessment of ionization efficiency was accomplished by integrating the ion current for several analyte ions while analyzing samples containing the same amount of bradykinin, but different concentrations of matrix,

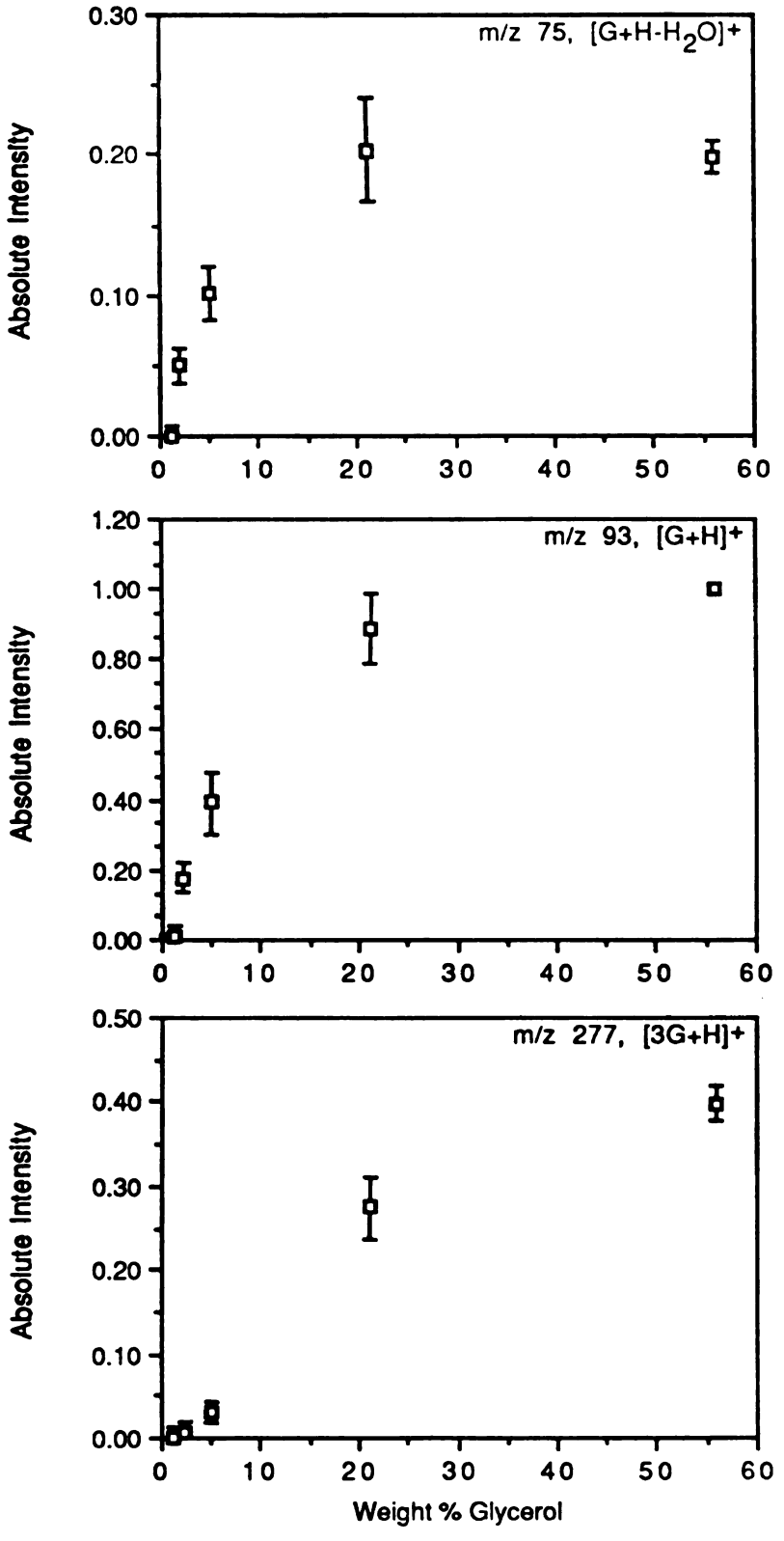

Figure 2.3. Plots of peak intensity for selected glycerol ions (m/z 75 (top), m/z 93 (middle), and m/z 277) versus weight percentage glycerol. Each sample contained 4 nmol of bradykinin and the total sample volume in each case was 2 ul.

namely, 2 ul portions of 56% and 5% glycerol in water (the same two sample compositions represented in Figure 2.1). Accordingly, spectra from both these sample compositions were collected continuously until the $[M+H]^+$ signal (m/z 1060) could no longer be distinguished from detector noise (this required approximately 30-40 minutes for the samples containing more glycerol and approximately 10-15 minutes for the samples containing less glycerol). The signal areas under the mass chronograms for analyte ions at m/z 70, 120, 417, 527, 572, 805, and 1060 were then integrated. This comparison was carried out 3 times (on three separate days). The data indicate that analyte in the 5% aqueous glycerol sample experiences enhanced desorption ionization (more ions detected) in comparison to that in the 56% aqueous glycerol sample. The ionization efficiency is increased by a factor of 2. This trend was observed for all analyte ions examined.

d. Role of Water in Spectral Enhancement

The phenomenon described in Figures 2.1, 2.2, and 2.3 raises interesting questions. For instance, does the increased water or the decreased glycerol content account for the greater analyte signal observed when analyzing samples of lower weight percentage glycerol as shown in Figure 2.2? Is water a reagent responsible for the spectral enhancement or merely a passive carrier which supplies variable quantities of matrix for the analyte? A series of experiments was designed and conducted to definitively answer these questions. Part 1 of Table 2.1 breaks down the samples represented in Figures 2.2 and 2.3 into their individual components. The molar ratios of glycerol and water, respectively, to the analyte are listed also. The amount of bradykinin present in each case was constant (4 nmol). From inspection of Figures 2.2 and 2.3, the composition of

Table 2.1. Sample compositions represented in Figures 2.2-2.5.

Part 1 (4 nmol Bradykinin(B) in each)

Sample	% Glycerol	Amt Glycerol(G) mg(mmol)	Molar G/B	Amt Water(W) mg(mmol)	Molar W/B
1	56	1.3(0.014)	4,000	1.00(0.056)	10,000
2	21	0.44(0.0048)	1,000	1.65(0.092)	20,000
3	5	0.10(0.0011)	300	1.92(0.11)	30,000
4	2	0.05(0.0005)	100	1.96(0.11)	30,000
5	1	0.02(0.0002)	50	1.98(0.11)	30,000

Part 2 (4 nmol Bradykinin(B) in each)

Sample	% Glycerol	Amt Glycerol(G) mg(mmol)	Molar G/B	Amt Water(W) mg(mmol)	Molar W/B
A	8	0.11(0.0012)	300	1.16(0.064)	20,000
B	7	0.10(0.0011)	300	1.42(0.079)	20,000
C	3	0.10(0.0011)	300	2.92(0.16)	40,000
D	8	0.41(0.0044)	1,000	4.68(0.26)	60,000

sample 3 was chosen as that providing the optimum results for this quantity of analyte. Sample 3 initially contained 0.10 mg of glycerol and 1.92 mg of water, along with the 4 nmol of bradykinin. Experiments were performed to determine whether this particular level of glycerol or this particular level of water was responsible for the observed effect.

Sample compositions A, B, and C listed in part 2 of Table 2.1 were prepared from the optimal amount of glycerol used in sample 3, but widely varying amounts of water. The range of water quantities incorporated into samples A-C is quite large with respect to the range of water quantities used in samples 1-5 (part 1 of Table 2.1), within which the relatively sharp optimization was observed in Figure 2.2. Samples A-C also contained 4 nmol of bradykinin and each sample was analyzed in triplicate. These results are compared to those obtained from the optimal sample composition (sample 3) in Figure 2.4 for selected analyte ions and in Figure 2.5 for selected matrix ions. These data indicate a correlation of the FAB response to the glycerol/analyte relationship and not the water/analyte relationship. Note the good agreement between the data (Figures 2.4 and 2.5) collected from samples A, B, and C and that obtained from the designated optimum sample (sample 3).

Finally, sample D is included to demonstrate that the effect cannot be attributed to the weight percentage of glycerol in water present in the original sample. Both samples A and D initially contain 8% glycerol in water, but sample D shows significantly inferior results in Figures 2.4 and 2.5 because it contains more than the optimum ratio of glycerol to bradykinin. Indeed, the results from sample D much more closely resemble those from sample 2 (part 1 of Table 2.1) which is composed of a similar ratio of glycerol to bradykinin.

These data indicate that macroscopic amounts of water play no role in the enhancement mechanism within the range of water quantities employed in this

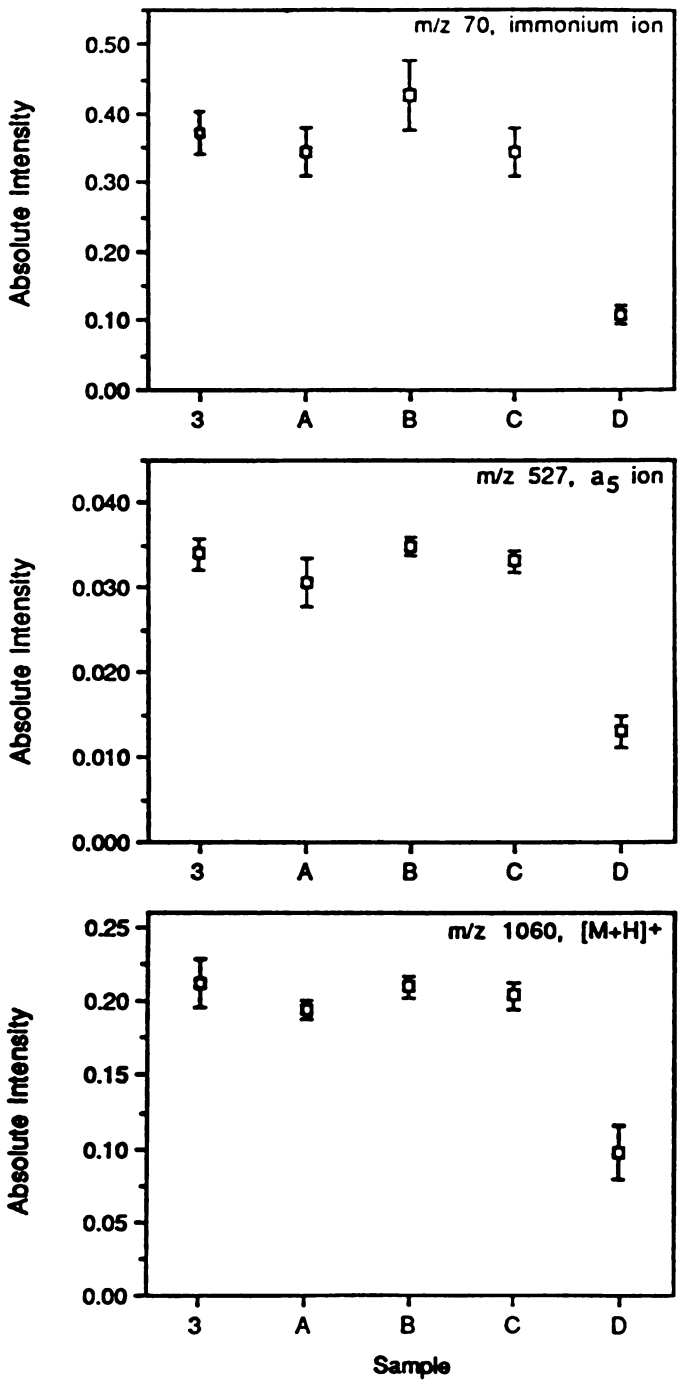

Figure 2.4. Peak intensity for selected bradykinin ions (m/z 70 (top), m/z 527 (middle), and m/z 1060) plotted against sample composition (described in Table 2.1). Samples A, B, and C contain the same amount of glycerol, but significantly different amounts of water than the optimum composition (sample 3, Table 2.1). Sample D contains more than the optimum amount of glycerol and water, but the same weight percentage of glycerol in water as sample A.

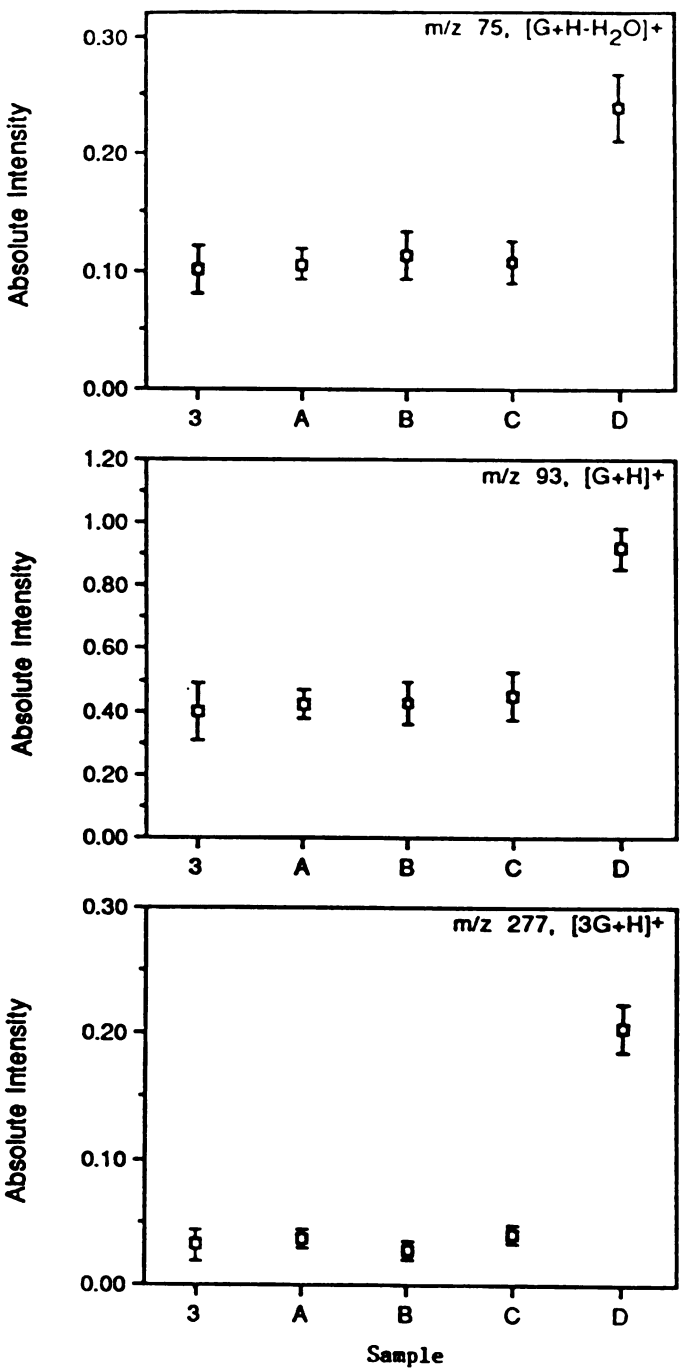

Figure 2.5. Peak intensity for selected glycerol ions (m/z 75 (top), m/z 93 (middle), and m/z 277) plotted against sample composition (described in Table 2.1). Samples A, B, and C contain the same amount of glycerol, but significantly different amounts of water than the optimum composition (sample 3, Table 2.1). Sample D contains more than the optimum amount of glycerol and water, but the same weight percentage of glycerol in water as sample A.

study. This conclusion prompted a series of simplistic measurements to ascertain how much water the optimal portion of the hygroscopic glycerol might hold under the influence of the vacuum. Therefore, gravimetric measurements were made of the optimal sample composition both before and after exposure to the reduced pressure conditions in the vacuum lock. Assuming that the vacuum removes water, but not glycerol, from the sample, it was determined that nearly 100% of the water is gone by the time the probe is inserted into the source. It is important to note that these results do not preclude the participation of trace levels of water in determining the spectral data. Greater than trace levels of water, however, are definitely not involved in the mass spectral enhancement. Therefore, a system which was tertiary in sample preparation became viewed as a binary one (simply a mixture of analyte in glycerol) by the inception of the FAB-MS analysis.

e. Evidence of Surface Enrichment Contributing to Spectral Enhancement

Up to this point, a constant amount of bradykinin had been used in all the experiments; thus, the actual ratio of glycerol to bradykinin had varied according to the quantity of glycerol used. Once attention focused on the glycerol/analyte relationship in the sample, it was decided to manipulate the glycerol to bradykinin molar ratio by varying the amount of bradykinin in a constant amount of glycerol. Therefore, calibration curves were constructed for bradykinin sampled from the larger, 1.3 mg portion of glycerol and also the optimal, 0.10 mg portion.

Results obtained with the larger amount of glycerol (1.3 mg) are plotted in Figure 2.6 for various bradykinin ions as a function of bradykinin quantity. Data points correspond to 1, 4, 8, and 12 nmol of bradykinin dispersed in approximately 1.3 mg of glycerol. Ion current at each m/z value shows a roughly

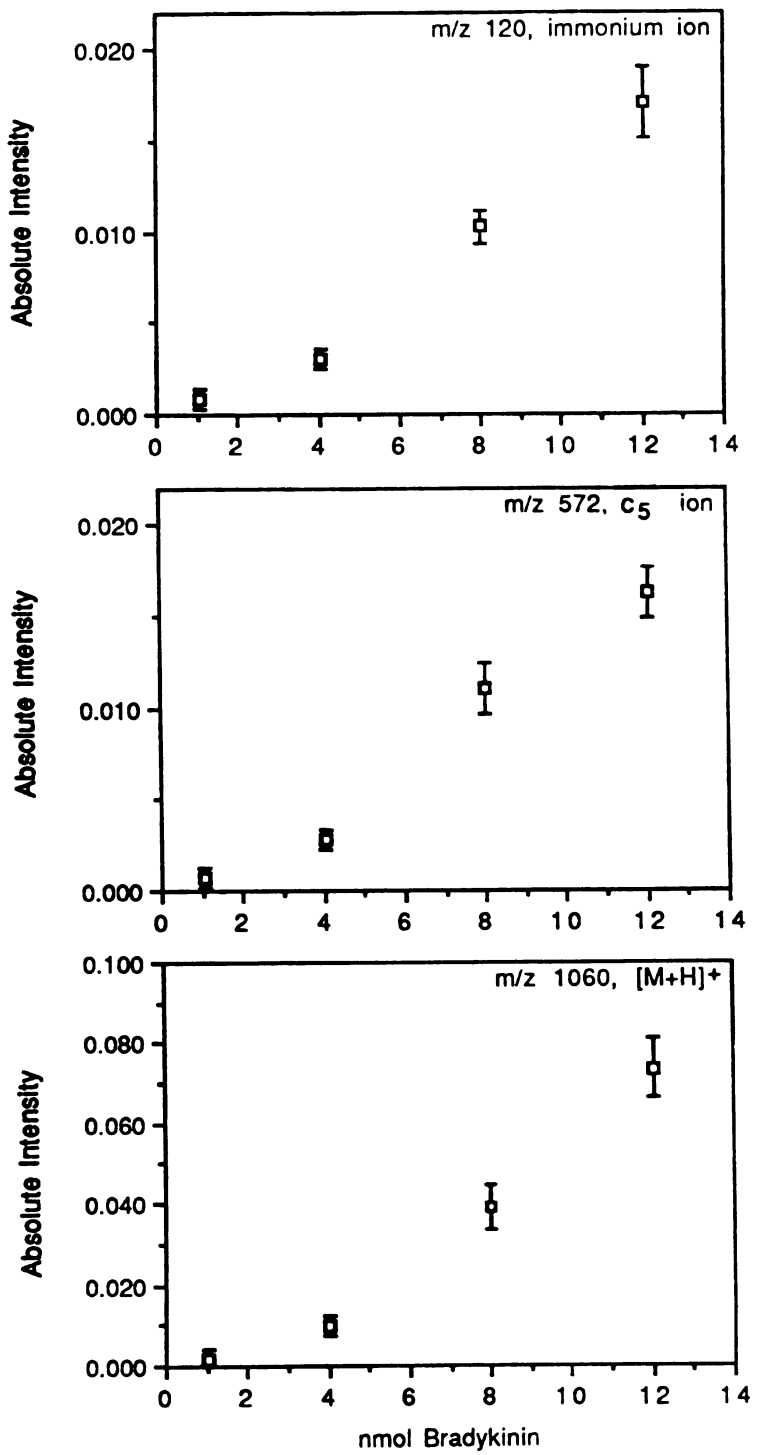

Figure 2.6. Response for selected bradykinin ions (m/z 120 (top), m/z 572 (middle), and m/z 1060) produced from samples composed of the indicated amount of bradykinin in 1.3 mg of glycerol.

linear response within the range of bradykinin quantities employed. Figure 2.7 shows the response for various glycerol ions as a function of bradykinin amount. In general, these plots show little change in glycerol ion response as 1 to 12 nmol of bradykinin are mixed into the constant amount (1.3 mg) of glycerol, with the exception of some higher mass cluster ions (e.g., m/z 369) which seem to fall off in abundance with increasing bradykinin concentration. A possible explanation for this latter observation is discussed below.

Results obtained with the smaller amount of glycerol (0.10 mg) are presented in Figures 2.8 and 2.9. These figures correspond to experiments analogous to those represented in Figures 2.6 and 2.7, respectively. The analyte ion current in Figure 2.8 shows little linearity and a tendency to "plateau", or even decrease, with increasing bradykinin concentration. Analyte response curves of this shape have been observed by others using FAB-MS (1, 10-13). As discussed in Chapter 1 (p. 52), this behavior is believed to result from optimizing the concentration of the analyte at the matrix surface; once this optimal surface concentration is achieved, further increases in analyte sample quantity yield no improvement in analyte ion response.

Figure 2.9 shows the matrix ion response for the 0.10 mg glycerol samples. These data provide an even more striking contrast with the curves in Figure 2.7 (from the 1.3 mg glycerol samples). Small additional increments of bradykinin substantially reduce matrix ion abundances detected from the 0.10 mg glycerol samples (Figure 2.9), where they had very little effect during analyses of samples containing 1.3 mg of glycerol (Figure 2.7). This behavior also can be interpreted as a surface effect, in which small additional increments of analyte begin to dominate the surface of the matrix and strongly suppress desorption ionization of the more abundant glycerol molecules.

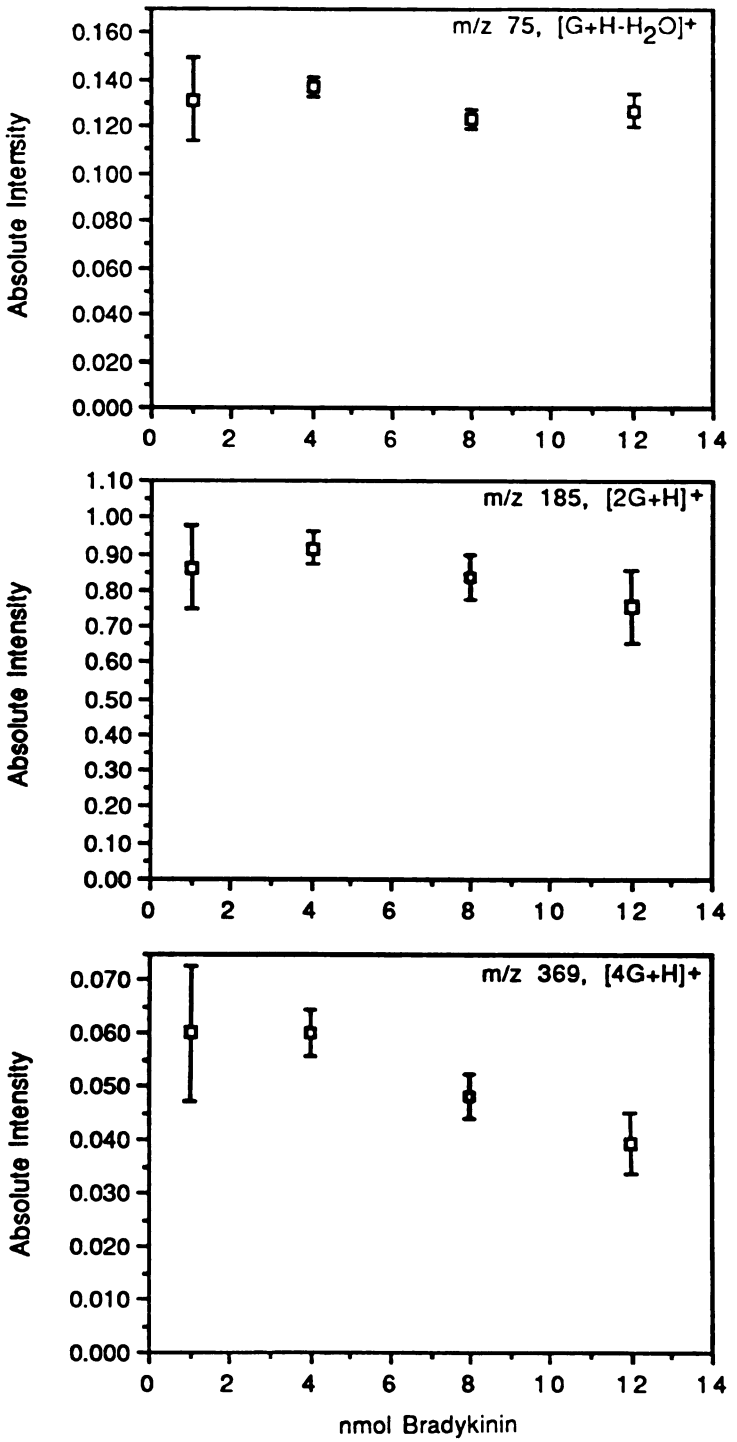

Figure 2.7. Response for selected glycerol ions (m/z 75 (top), m/z 185 (middle), and m/z 369) produced from samples composed of the indicated amount of bradykinin in 1.3 mg of glycerol.

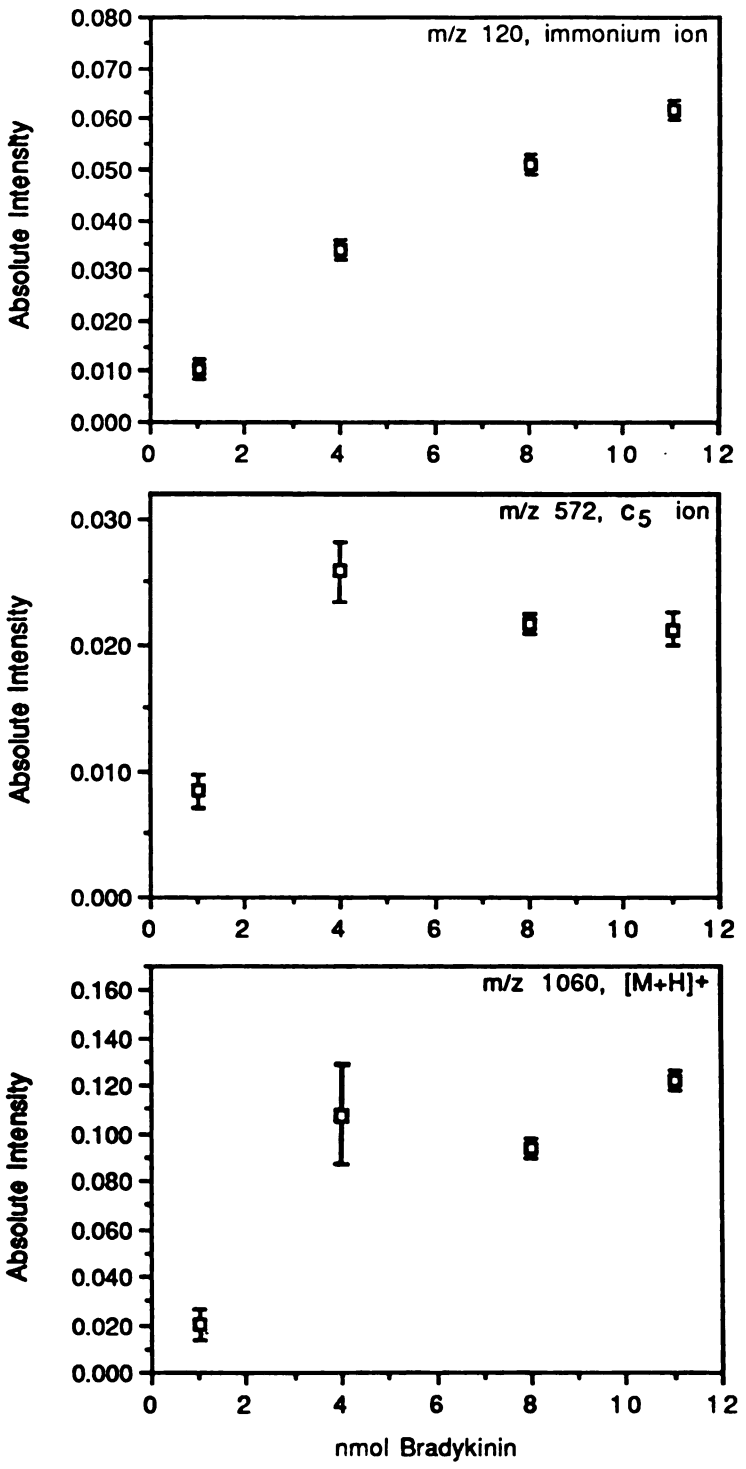

Figure 2.8. Response for selected bradykinin ions (m/z 120 (top), m/z 572 (middle), and m/z 1060) produced from samples composed of the indicated amount of bradykinin in 0.10 mg of glycerol.

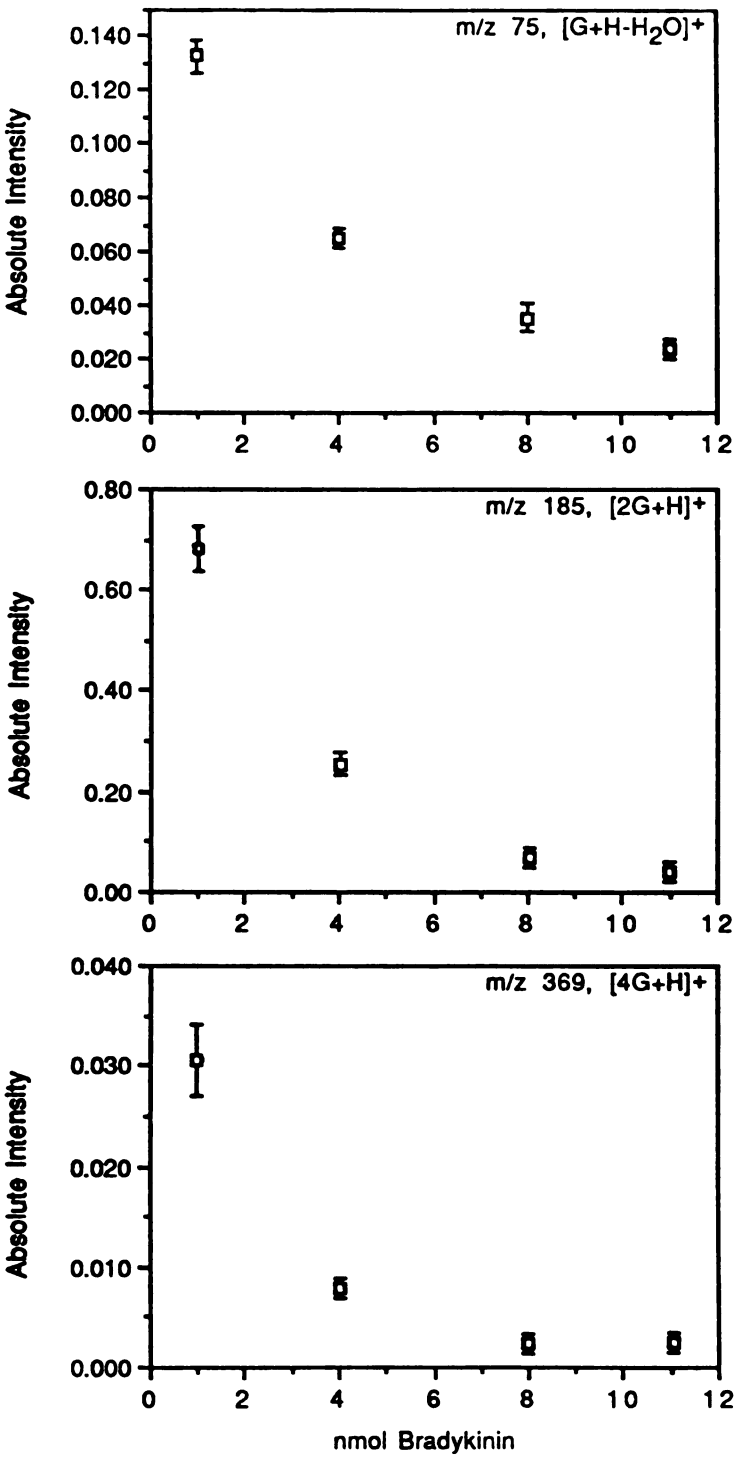

Figure 2.9. Response for selected glycerol ions (m/z 75 (top), m/z 185 (middle), and m/z 369) produced from samples composed of the indicated amount of bradykinin in 0.10 mg of glycerol.

The onset of this surface coverage effect is also apparent in Figure 2.7 (1.3 mg glycerol samples) in the response profile of the largest glycerol cluster shown (m/z 369); for higher concentrations of bradykinin, fewer glycerol cluster ions are produced. The diminished response at m/z 369 may indicate sufficient analyte surface population to interfere with the creation of these larger cluster ions. This interpretation is consistent with that from a previous discussion regarding the effect of surface coverage on glycerol cluster ion detection (14).

f. Proposed Model to Explain Mass Spectral Enhancement

These results stimulated consideration of the following model to explain the mass spectral enhancement. Chapter 1 (p. 51) described the importance of surface effects in FAB, and the tendency of FAB mass spectra to reflect the surface composition of the sample. We postulate that concentrating a certain amount of analyte into a smaller portion of glycerol facilitates surface population of the glycerol by the analyte. This expectation is supported by the theory developed by Gibbs (discussed in Chapter 1, p. 55), which predicts an increase in surface excess concentration as a function of bulk concentration. When 4 nmol of bradykinin are mixed with 1.3 mg of glycerol, the ratio of glycerol to bradykinin molecules is approximately 4,000 to 1. Samples of this composition did not show pronounced evidence of surface effects. In the samples containing the 0.10 mg portions of glycerol, however, the ratio of glycerol to bradykinin molecules is approximately 300 to 1. Pronounced evidence of surface effects did result from analysis of samples containing this smaller portion of matrix. The smaller glycerol volume will decrease dispersion of the analyte, and provide an increased surface area to volume ratio. The increased surface concentration will

be driven by a higher bulk concentration, resulting in significant analytical advantages.

In this process, water is considered primarily as a convenient vehicle for depositing minute portions of glycerol on the sample probe tip. Microscopic examination of the optimal sample composition (0.10 mg of glycerol and 1.92 mg of water) after exposure to reduced pressure in the vacuum lock revealed a very thin layer of viscous material uniformly distributed over the sample stage. In view of the high precision of results obtained from these samples, evaporation of the water seems to be involved in providing a relatively specialized sample preparation.

A plausible explanation for the increased formation of low mass fragments for the samples containing the smallest portions of glycerol (in Figure 2.2) may be provided by the clustering mechanism discussed in Chapter 1 (p. 49), which allowed for excess energy dissipation through desolvation in the gas phase. Once the ratio of matrix to analyte drops to the point where the glycerol presence at the sample surface is significantly reduced, clusters in the gas phase may consist of substantially fewer glycerol molecules. These smaller clusters would have less capacity to release energy through desolvation, and the analyte would be left with more energy for fragmentation. This explanation also has been advanced by Dass and Desiderio (4), who, likewise, observed increased fragmentation while concentrating the analyte in the matrix.

g. Effect of Peptide Hydrophobicity Upon Spectral Enhancement

In considering a model which emphasizes surface effects, one might expect differences in the enhancement behavior for analytes which possess different surface activities in glycerol. To address this question, a comparison

study was undertaken with five peptides (including bradykinin) of comparable size, but widely differing values of the Bull and Breese Hydrophobicity Index (15). These peptides are listed in Table 2.2 along with their amino acid sequences, the mass of each protonated molecule, and the calculated Bull and Breese index. It should be noted that the most negative values of the Bull and Breese index correspond to the most hydrophobic peptides.

Figure 2.10 displays the mass spectral response for the $[M+H]^+$ ion of three of the peptides listed in Table 2.2 as a function of sample composition. The peptides represented include the most hydrophobic ([Val^4]-angiotensin III), the peptide of intermediate hydrophobicity (bradykinin), and the least hydrophobic (NPNANPNANPNA). These curves are analogous to those shown in Figure 2.2 (as evidenced by the similar shape of the bradykinin curve), but contain two important differences. The first pertains to the sample composition axis, which was changed from weight percent glycerol to absolute amount of glycerol. The second change regards the addition of a sample composition (2.3 umol of glycerol) to provide greater resolution of these curves and facilitate the identification of a trend among them. All samples represented in Figure 2.10 contained 4 nmol of analyte. A trend is indeed apparent as the $[M+H]^+$ peak intensities for the most hydrophobic peptide ([Val^4]-angiotensin III) are maximized in larger portions of glycerol than are the $[M+H]^+$ peak intensities for bradykinin. Likewise, the ion abundances of the least hydrophobic peptide (NPNANPNANPNA) are maximized in smaller portions of glycerol than are those of bradykinin. Curves generated for other important peaks throughout the mass spectrum of each of the three peptides showed close agreement with those displayed in Figure 2.10 (with the exception of those corresponding to immonium ions). These results are consistent with a model emphasizing surface effects because the most hydrophobic peptide, which has the greatest tendency to

Table 2.2. Peptides used for experiments represented in Figures 2.10 and 2.11.

Peptide	Sequence	$[M+H]^+$	Bull and Breese Hydrophobicity Index
[Val^4]-Angiotensin III	Arg-Val-Tyr-Val-His-Pro-Phe	917	-463
Proenkephalin	Tyr-Gly-Gly-Phe-Met-Arg-Gly-Leu	900	-268
Bradykinin	Arg-Pro-Pro-Gly-Phe-Ser-Pro-Phe-Arg	1060	-104
Fibronectin Related Peptide	Cys-Gln-Asp-Ser-Glu-Thr-Arg-Thr-Phe-Tyr	1249	+119
NPNANPNANPNA	Asn-Pro-Asn-Ala-Asn-Pro-Asn-Ala-Asn-Pro-Asn-Ala	1207	+555

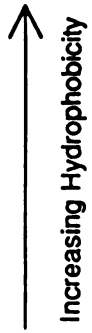

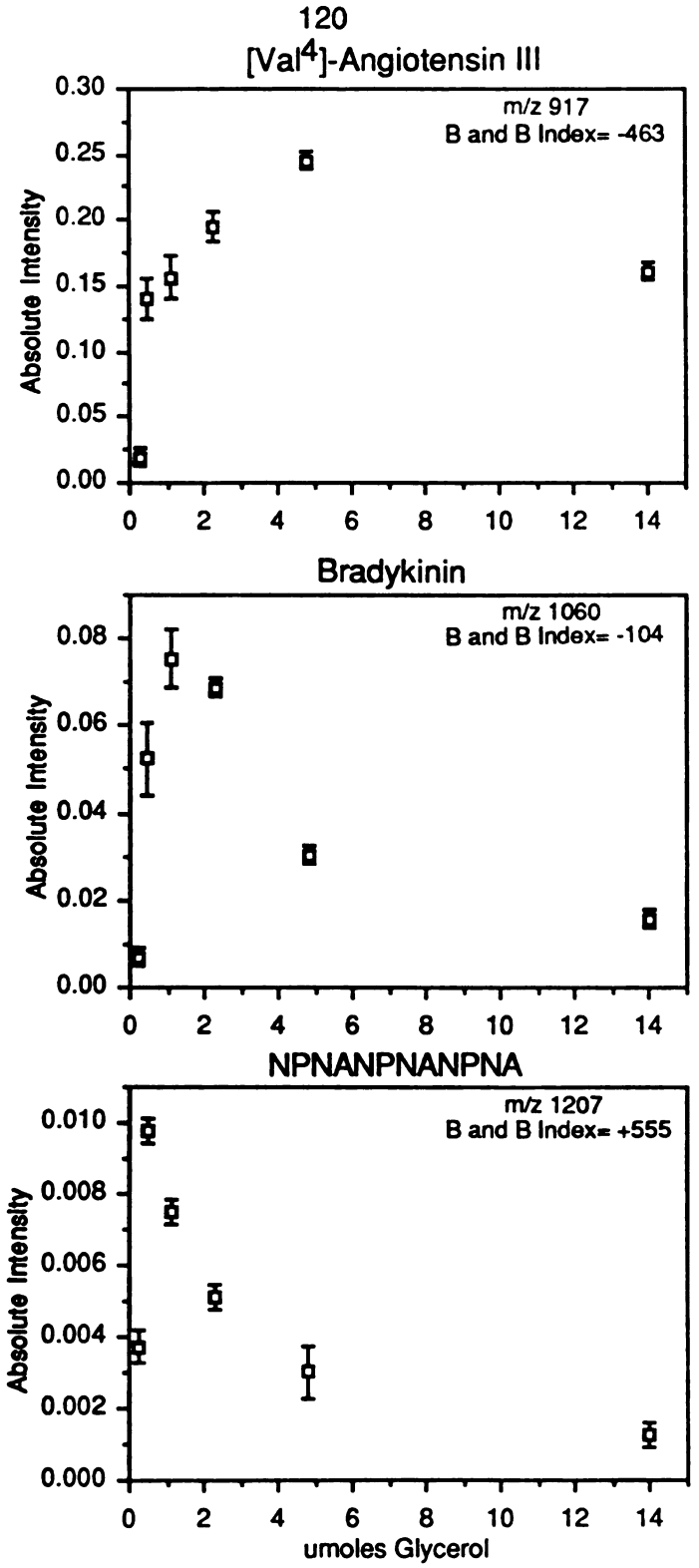

Figure 2.10. Plots of $[M+H]^+$ peak intensity for three peptides versus the absolute amount of glycerol in sample. All samples contain 4 nmol of analyte.

reside at the glycerol surface, would be expected to tolerate larger portions of glycerol in establishing its optimal surface concentration. In contrast, the least hydrophobic peptide would require the smallest portions of glycerol before it is forced toward the surface and the enhancement is observed. Data from samples containing the other two peptides in Table 2.2 (proenkephalin and fibronectin related peptide) also fit into this trend in optimization as a function of hydrophobicity.

A related trend is also apparent for the glycerol ion response in this set of experiments. Figure 2.11 shows peak intensities for m/z 93 ($[glycerol+H]^+$) plotted in a manner similar to that in Figure 2.10. Samples containing the most hydrophobic peptide show significant suppression of the glycerol peak in relatively large portions of glycerol, whereas samples containing the least hydrophobic peptide show no substantial diminution of glycerol peak intensity until the smallest portions of glycerol are used. It is interesting to note that the segments of these curves where the glycerol peaks are strongly suppressed correspond to the segments in which the accompanying analyte signals are strongly enhanced (in Figure 2.10). This fact implies the existence of a competition between analyte and matrix, which is also consistent with a model emphasizing surface effects.

In another facet of the study, the dependence of the glycerol peak intensity as a function of glycerol sample size was investigated. Samples containing only the appropriate portion of glycerol (without any peptide) were evaluated for comparison with the data represented in Figure 2.11. Figure 2.12 shows the response at m/z 93 for one such series of experiments. The contrast between Figure 2.12 and the two upper curves in Figure 2.11 verifies the tendency of the more hydrophobic peptides to suppress desorption ionization of the matrix. The similarity between Figure 2.12 and the lower curve in Figure 2.11 reveals the

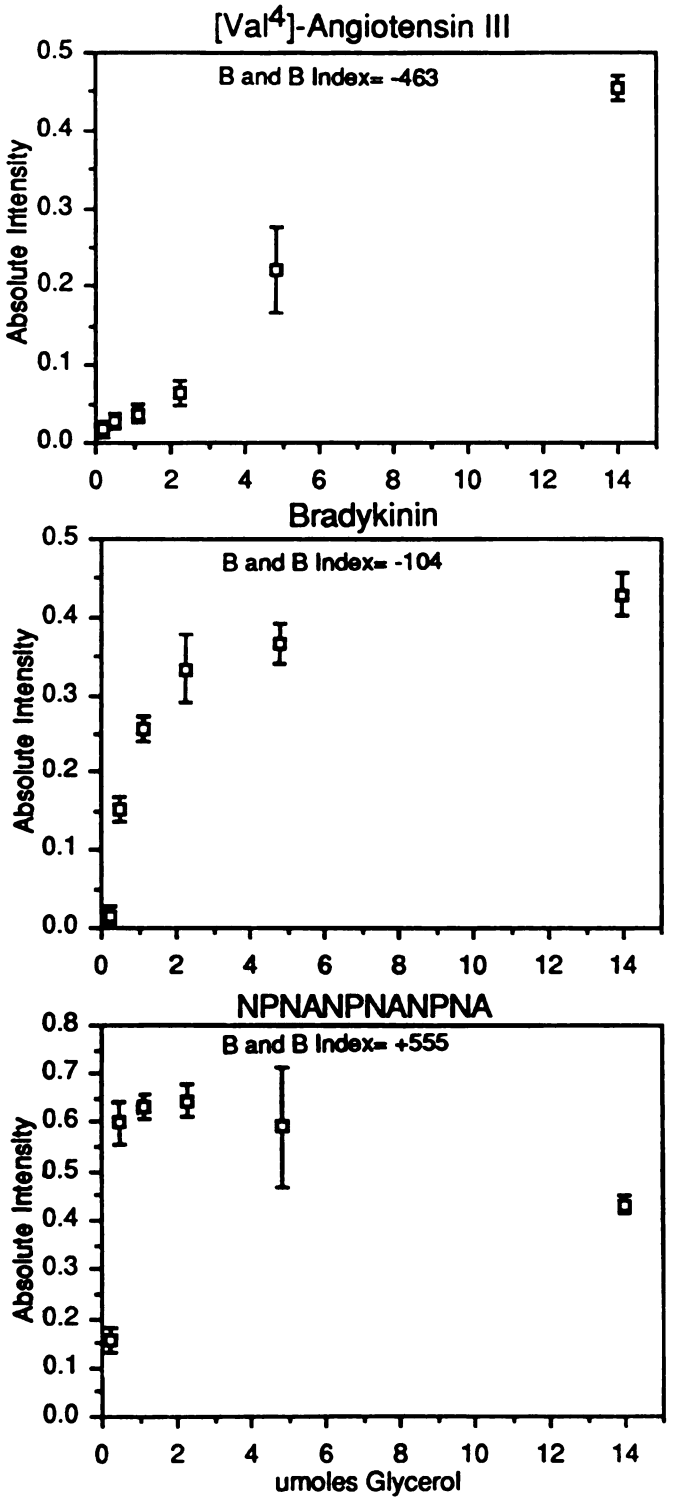

Figure 2.11. Plots of $[glycerol+H]^+$ peak intensity (at m/z 93) versus absolute amount of glycerol present in samples containing 4 nmol of the indicated peptide.

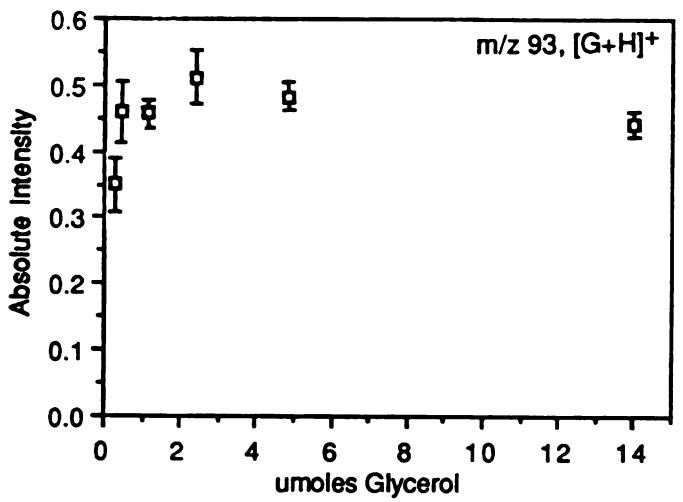

Figure 2.12. Plot of $[glycerol+H]^+$ peak intensity (at m/z 93) versus absolute amount of glycerol present in samples containing no peptide.

inferior capacity of the hydrophilic peptide (NPNANPNANPNA) to suppress the matrix signals.

h. Effect of Constant Ratio of Glycerol to Bradykinin

In pursuing the importance of the ratio of glycerol to analyte in the FAB experiment, a study was designed to analyze a series of samples in which the glycerol to bradykinin ratio was maintained at a constant value while adjusting the absolute quantities of each component. The ratio chosen was approximately 300 glycerol molecules for each bradykinin molecule (a ratio similar to that in the designated optimum sample 3 of Table 2.1), and the experiments encompassed a range from 2 to 12 nmol of bradykinin. The compositions of these samples are listed in Table 2.3. Figure 2.13 shows the abundance of selected analyte ions plotted against the amount of bradykinin present in the sample. One observes little effect of increased analyte sample quantity upon analyte ion response. Likewise, little change in results is observed when glycerol ion response is plotted against glycerol sample quantity (Figure 2.14). Despite an increase in the levels of all sample components by some 600%, the greatest variation observed in the abundance of any ion was 38%; in addition to those plotted in Figures 2.13 and 2.14, peak intensities at m/z 120, 527, 572, 805, 903, 277, and 369 were examined. Spectra from all samples described in Table 2.3 are qualitatively similar. This consistency of spectral results after significant manipulation of sample composition suggests that the ratio of glycerol to bradykinin molecules can be a useful factor in approximating the optimal mass spectral response.

Table 2.3. Sample compositions represented in Figures 2.13 and 2.14.

molar ratio of glycerol to bradykinin = 300:1

umol Glycerol	nmol Bradykinin
0.55	2
1.1	4
2.2	8
3.4	12

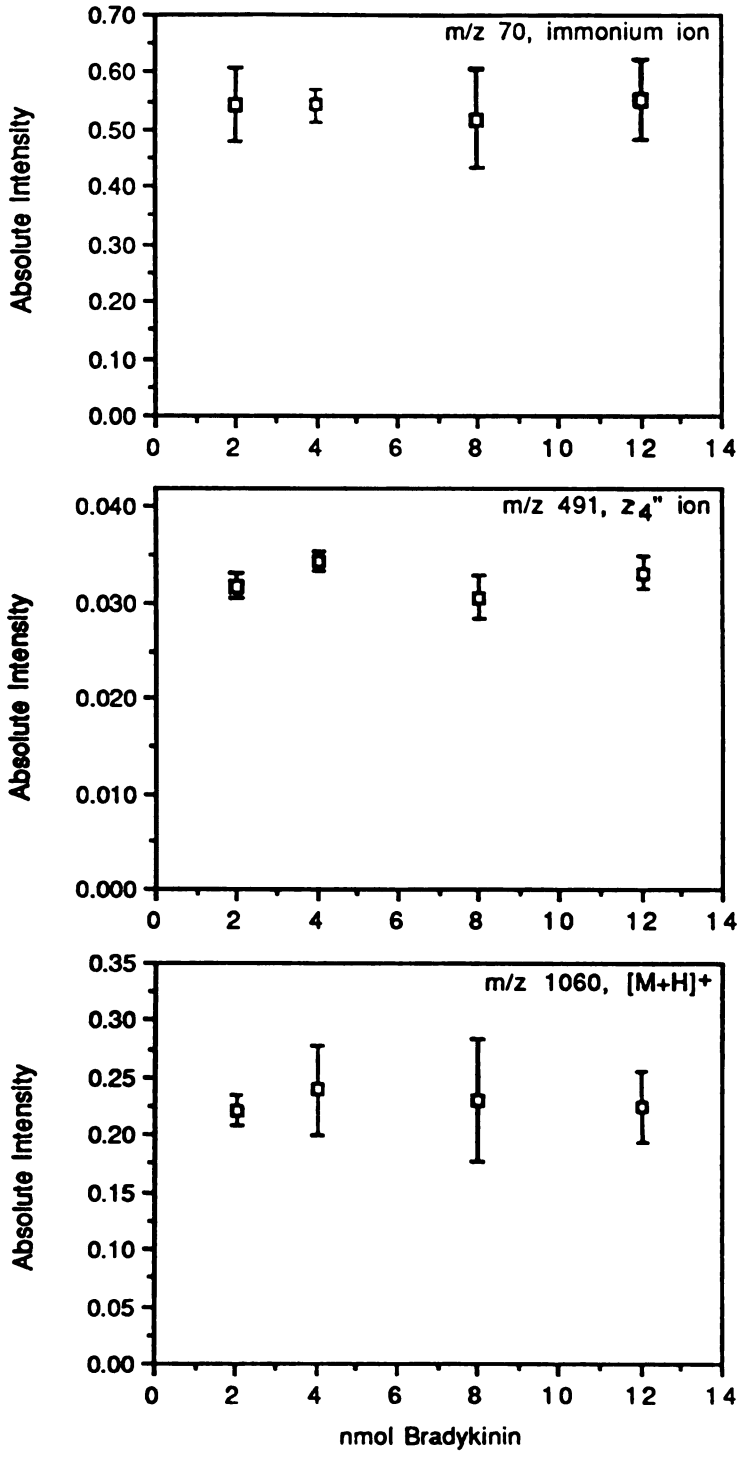

Figure 2.13. Plots of abundance of selected bradykinin ions (m/z 70 (top), m/z 491 (middle), and m/z 1060) versus nmol of bradykinin in sample. All samples possess a constant ratio (300:1) of glycerol molecules to bradykinin molecules, although the absolute quantities of each vary.

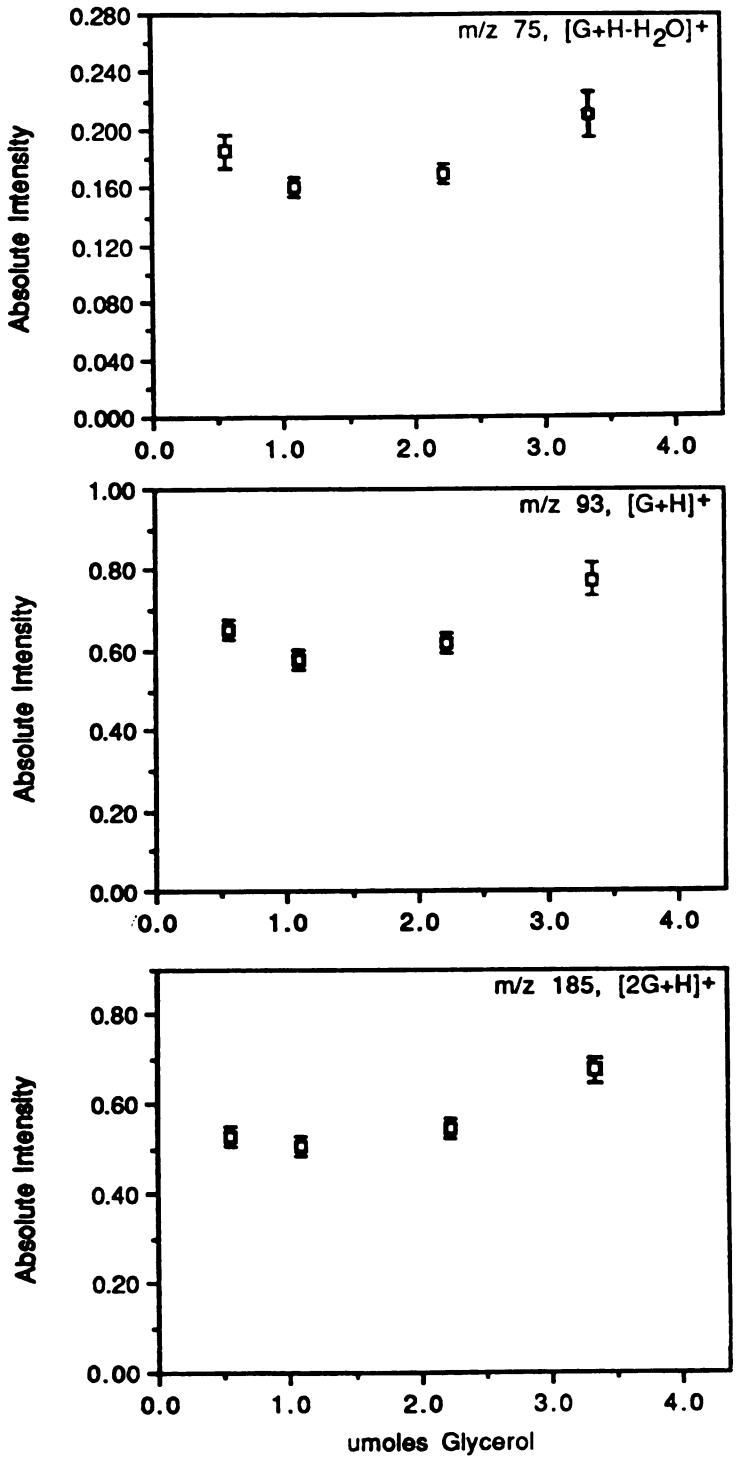

Figure 2.14. Plots of abundance of selected glycerol ions (m/z 75 (top), m/z 93 (middle), and m/z 185) versus umol of glycerol in sample. All samples possess a constant ratio (300:1) of glycerol molecules to bradykinin molecules although the absolute quantities of each vary.

i. Effect of Acidic Modifiers on Optimal and Nonoptimal Sample Compositions

As previously mentioned, acidic modifiers have commonly been included in FAB-MS sample preparations to increase analyte ion abundances in the positive ion mode. A limited comparison of the spectral enhancement resulting from addition of acidic modifiers with that due to manipulation of the ratio of glycerol to analyte was conducted. Samples composed of 1.3 mg of glycerol and 4 nmol of bradykinin (sample 1 in part 1 of Table 2.1) were analyzed by FAB-MS and the results compared to those from similar samples which also contained 100 nmol of HCl. Addition of the acid increased the abundances of the six bradykinin ions which were evaluated (m/z 70, 120, 417, 572, 903, and 1060) by an average of 34%. These acidified samples also displayed increased glycerol ion abundances; the five glycerol ions evaluated (m/z 75, 93, 185, 277, and 369) showed an average increase in abundance of 6%. The optimal sample composition (sample 3 in part 1 of Table 2.1: 4 nmol of bradykinin and 0.10 mg of glycerol) also was analyzed with and without the addition of 100 nmol of HCl. The added acid increased the abundances of the six specified bradykinin ions by an average of 7%. At the same time, the five designated glycerol ions were increased in abundance by an average of 9%. Mass spectra obtained from the optimal sample composition with and without the HCl were indistinguishable in a qualitative sense. For the sake of reference, the abundances of the six bradykinin ions were enhanced by 690% on average by optimizing the ratio of glycerol to bradykinin (nonacidified samples), while the abundances of the five glycerol ions were decreased by an average of 64%. A separate study undertaken with bradykinin, glycerol, and tartaric acid also showed that any

spectral enhancement gained by adding the acidic modifier was insignificant to that gained through optimization of the glycerol to analyte ratio.

j. Influence of Ratio of Glycerol to Analyte on Peptide Mixtures

Based on the model proposed earlier, it was predicted that peptides of varying hydrophobicity might display differences in their enhancement behavior as the ratio of matrix to analyte was optimized. Such differences were indeed noted (in Figures 2.10 and 2.11) and explained in terms of the analytes' relative capacities to occupy the surface of the matrix. One also might expect that suppression effects observed in the analysis of peptide mixtures may be alleviated by optimizing the ratio of matrix to analyte. The reasoning to support this expectation suggests that concentrating a particular mixture of several analytes into smaller portions of matrix would force the less surface-active components near the sample surface. Spectra obtained from the concentrated solutions may then provide a more equitable representation of the sample composition than spectra obtained from dilute matrix solutions, where the component of greatest surface activity would be expected to more fully dominate the surface. This prediction was tested by evaluating three different peptide mixtures, each of which was equimolar in three peptides characterized by substantially different values of the Bull and Breese index. The peptide mixtures are described in Table 2.4.

Suppression effects were monitored by comparing the relative intensities of the $[M+H]^+$ peaks for the peptides. This approach has been used in several previous studies of peptide suppression (16-19). A more satisfactory method would involve summation of all the signals associated with a particular peptide, but this option was not practical due to decomposition of the different peptides

Table 2.4. Peptides used for mixture analyses.

Part 1

Peptide	Sequence	$[M+H]^+$	Bull and Breese Hydrophobicity Index*
$[Val^4]$-Angiotensin III	Arg-Val-Tyr-Val-His-Pro-Phe	917	-463
Proenkephalin	Tyr-Gly-Gly-Phe-Met-Arg-Gly-Leu	900	-268
Bradykinin	Arg-Pro-Pro-Gly-Phe-Ser-Pro-Phe-Arg	1060	-104
Substance P (1-9)	Arg-Pro-Lys-Pro-Gln-Gln-Phe-Phe-Gly	1104	58

Increasing Hydrophobicity

Part 2

Mixture	Peptides	Quantity
1	$[Val^4]$-Angiotensin III Proenkephalin Bradykinin	4 nmol of each
2	$[Val^4]$-Angiotensin III Proenkephalin Bradykinin	500 pmol of each
3	$[Val^4]$-Angiotensin III Proenkephalin Substance P (1-9)	2 nmol of each

into several common fragments. Comparison of the $[M+H]^+$ signals is a valid means to investigate suppression effects as long as the fragmentation for each peptide remains reproducible as a function of sample composition. The tendencies of the peptides to favor formation of low mass fragments at especially low values of the matrix to analyte ratio has been noted, however. Although the increased fragmentation is undesirable for the purposes of this study, it has been exhibited by all the peptides evaluated thus far. Therefore, no pronounced bias for one peptide with respect to the others was anticipated while monitoring suppression effects in such a manner. Also, care was taken to examine three different peptide mixtures (see Table 2.4), each of which was subjected to significantly different ranges of the matrix to analyte ratio, in an effort to identify general trends among the different systems. Those particularly concentrated sample compositions which exhibited extreme fragmentation were not utilized for the purposes of comparison.

Ligon has published a study (8) analogous to the present one, in which equimolar mixtures of four acylcarnitine chlorides (each characterized by a different chain length, and hence, a different surface activity in the matrix) were concentrated into an approximately constant amount of glycerol. The objective of that investigation was to determine how the surface composition of the sample varied as a function of bulk concentration for these equimolar mixtures of the surfactants. The parameter used to represent the relative intensities of the individual components of the mixtures was referred to as the fractional total ionization (FTI) value (8). To obtain the FTI values, Ligon divided the signal from the molecular cation of a single component by the sum of the signals (of the molecular cations) for all four components. This convention was adopted for the present study of suppression effects among peptides. In the ideal case for a three component mixture (assuming equivalent desorption efficiencies,

equivalent ionization efficiencies, and equivalent tendencies to fragment), FTI values of 0.33 for each component would accompany an absence of suppression effects. In the real case (i.e., for the purposes of this study), changes in the FTI values as a function of sample composition can be correlated to increased or decreased suppression among the components of the mixture.

The results of the Ligon study (8) deserve some comment before proceeding. Figure 2.15 shows the FTI plot for the surfactant mixtures. The chain lengths of the individual components are identified in the upper left portion of the figure. It should be noted that the complex interactions involved in multicomponent mixtures of such surfactants are not well understood in a quantitative sense. However, some important characteristics of these mixtures are evident from the data. Throughout the concentration range explored, the relative abundances of the analytes follow their order of chain lengths. Ligon interprets this as an indication that the relative extents of surface population by the analytes follow their order of chain lengths at all concentrations. A second important observation from Figure 2.15 involves a trend in suppression among the surfactants. Maximum suppression is indicated from such a plot for the sample composition exhibiting the greatest difference between the FTI values of the most surface-active component and the least surface-active component. In Figure 2.15, the data representing maximum suppression are indicated with an arrow. Alleviation of suppression is characterized by a gradual converging of the individual FTI values in both the low and high concentration extremes of Figure 2.15. An interesting aspect of Figure 2.15 is that the suppression is not alleviated in a unidirectional manner, but actually displays a local maximum as a function of concentration.

The FTI plot for mixture 1 (see Table 2.4) is shown in Figure 2.16. This figure presents data obtained from mixtures of [Val^4]-angiotensin III,

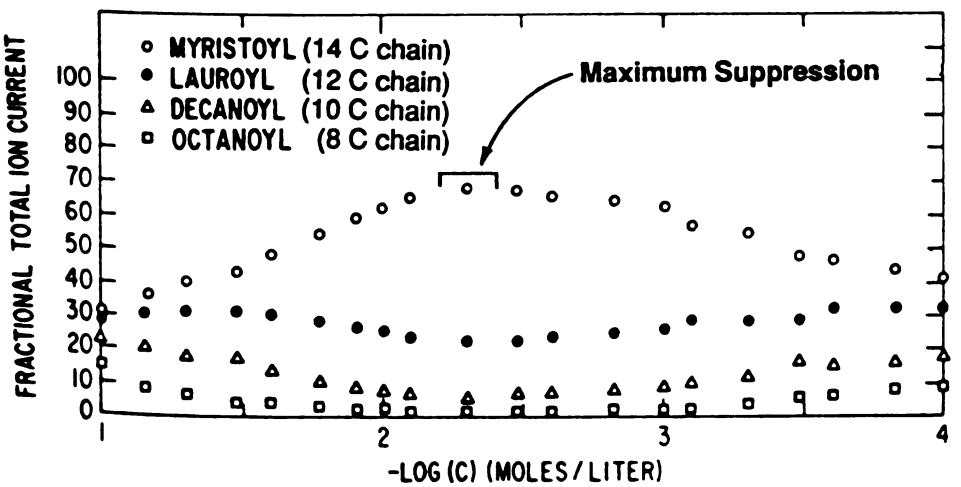

Figure 2.15. Plot of fractional total ion current (FTI) versus total bulk concentration for equimolar solutions of four acylcarnitine chlorides in glycerol. Adapted from reference 8 with permission of Elsevier Science Publishers.

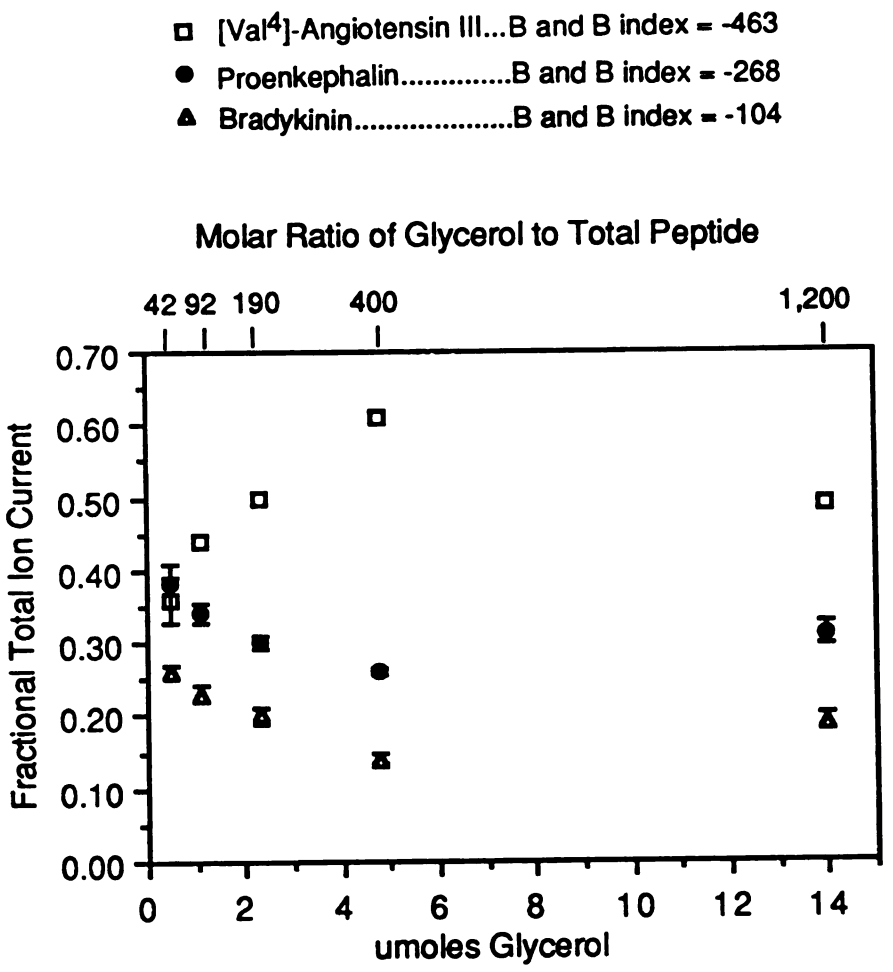

Figure 2.16. FTI plots (comparing $[M+H]^+$ ion abundances) for mixtures containing 4 nmol of each peptide dispersed in the indicated portion of glycerol.

proenkephalin, and bradykinin (4 nmol of each), which were sampled from the indicated portions of glycerol. The ratios of glycerol to total peptide present in the samples are denoted on the upper horizontal axis. Each sample composition was evaluated in three separate mass spectrometric runs, and FTI values were calculated for each run. Figure 2.16 displays the average FTI values along with the appropriate standard deviations (represented as error bars). Inspection of these data reveals important similarities with the data obtained by Ligon (shown in Figure 2.15). To begin with, the relative intensities of the $[M+H]^+$ peaks follow the order of peptide hydrophobicity for all except the most concentrated sample composition. Therefore, the most hydrophobic peptides, which would be expected to dominate the analyte signal, indeed do so. Secondly, a local maximum in suppression (indicated for the sample composition which provides the greatest difference between the FTI values of the most surface-active component ($[Val^4]$-angiotensin III) and the least surface-active component (bradykinin)) occurs as a function of concentration. This pronounced suppression establishes itself when the ratio of glycerol to total peptide is approximately 400. Finally, one observes a significant alleviation in suppression from the mixtures containing 4.8 umol of glycerol to those containing 0.5 umol of glycerol.

Results for mixtures of the same three peptides which are subjected to a significantly different range of the matrix to analyte ratio, are shown in Figure 2.17. These mixtures contained 500 pmol of each peptide. Here again, it is observed that the order of relative $[M+H]^+$ intensities follows the order of peptide hydrophobicity. A local maximum in suppression again is noticed, this time for the samples containing 0.5 umol of glycerol. The ratio of glycerol to total peptide for this sample composition is approximately 330. The close proximity of this value with that obtained from Figure 2.16 (glycerol to total peptide ratio of 400)

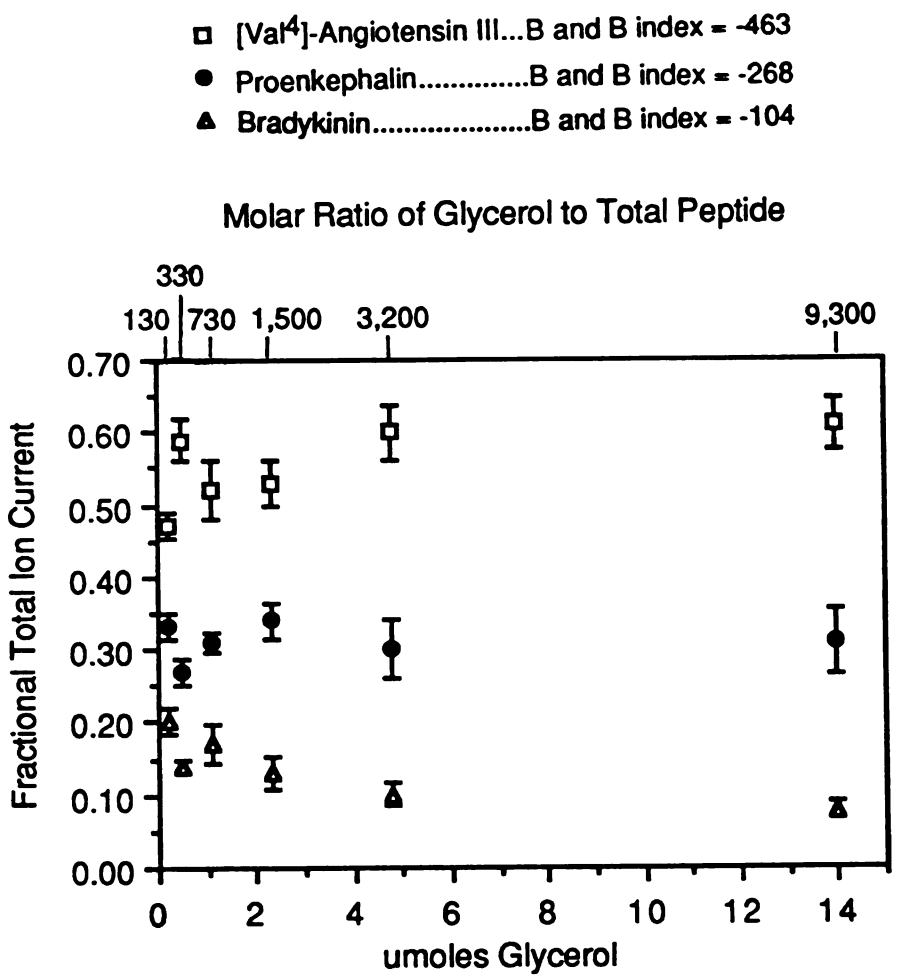

Figure 2.17. FTI plots (comparing $[M+H]^+$ ion abundances) for mixtures containing 0.5 nmol of each peptide dispersed in the indicated portion of glycerol.

again verifies the suitability of the matrix to analyte ratio in characterizing these systems. Finally, significant alleviation of suppression is also observed in Figure 2.17, from the samples containing 14 umol of glycerol to those containing 0.2 umol of glycerol.

A different peptide mixture was utilized for the analyses represented in Figure 2.18. Mixture 3 (see Table 2.4) consists of 2 nmol of [Val^4]-angiotensin III, proenkephalin, and substance P (residues 1-9). Again, one observes the relative abundances of the $[M+H]^+$ ions to be dictated by their relative hydrophobicities. The substitution of an even more hydrophilic compound (substance P (residues 1-9)) for the relatively hydrophilic bradykinin results in even more severe suppression of this component. This effect is evidenced in Figure 2.18 by fractional total ion current values for substance P (residues 1-9) which never exceed 0.10. In the previous two figures, bradykinin was able to capture substantially larger fractions of the analyte ion current in the smaller portions of glycerol. Trends in suppression are more subtle in Figure 2.18 than they were in Figures 2.16 and 2.17, but one nevertheless observes significant alleviation of suppression in comparing the relative response from samples containing 14 umol of glycerol with that from samples containing 0.5 umol of glycerol. The expected local maximum in suppression is also apparent in Figure 2.18, and appears to occur somewhere between the samples containing 2.3 and 1.1 umol of glycerol. The ratios of glycerol to total peptide encompassed by this range are similar to the values corresponding to the suppression maxima in Figures 2.16 and 2.17.

The data shown in Figures 2.16-2.18 are significant for the purposes of this study, because in each case they demonstrate the potential to significantly alleviate suppression effects by reducing the ratio of matrix to analyte. These data are also satisfying in that they suggest the capability to predict the relative

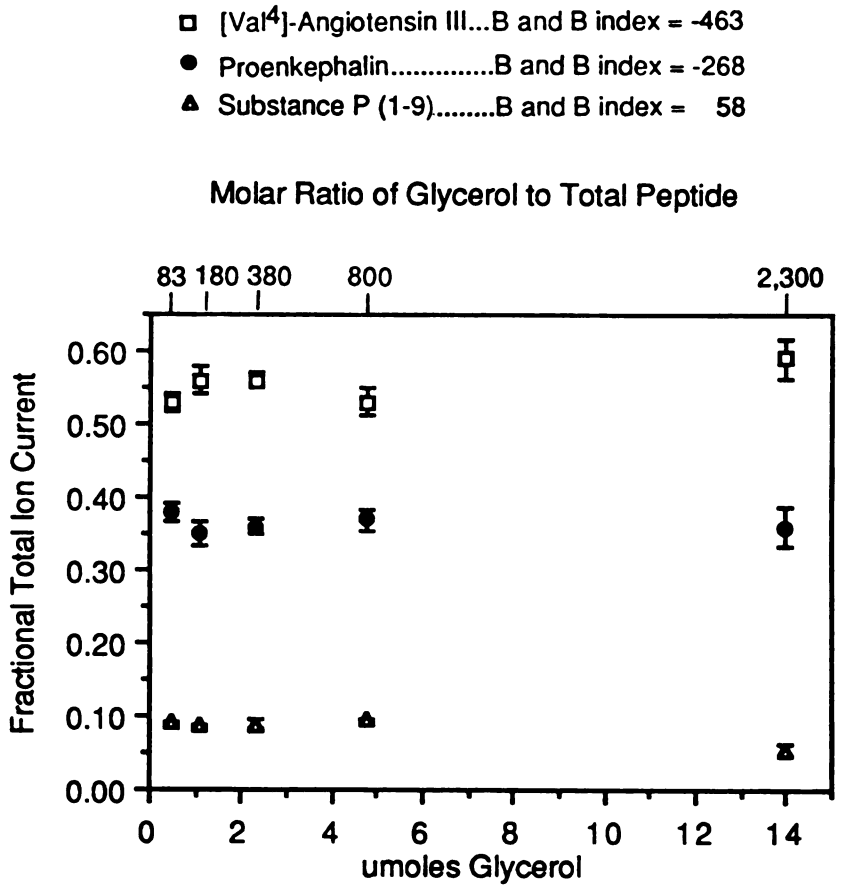

Figure 2.18. FTI plots (comparing $[M+H]^+$ ion abundances) for mixtures containing 2 nmol of each peptide dispersed in the indicated portion of glycerol.

behavior of these mixtures in terms of surface effects as a function of the matrix to analyte ratio.

k. Implications for CF-FAB Mechanism

In Chapter 1, substantial advantages were attributed to the use of dilute aqueous glycerol solutions in the continuous-flow FAB experiment. These advantages included a significant increase in analyte ion abundances, a significant decrease in matrix ion abundances, and the alleviation of suppression effects in comparison to conventional direct probe analyses which incorporated larger portions of glycerol. The increase in analyte ion abundances and the reduction of suppression phenomena have been postulated to arise from the dynamic nature of the continuous-flow experiment, and the higher water content of the samples incorporating the aqueous matrix solutions (9, 18). The decrease in matrix ion abundances was attributed to the smaller portions of matrix deposited on the probe tip (9).

No definitive comments regarding the CF-FAB mechanism can be based on the present work, because no experiments were conducted with a flow probe. However, several observations reported by workers involved with the continuous-flow technique also have been noted in work regarding optimization of the matrix to analyte ratio. Therefore, this research may contain implications which would prove useful in attempting to understand the CF-FAB mechanism.

As has been demonstrated in this chapter, optimization of the matrix to analyte ratio also results in increased analyte ion abundances, decreased matrix ion abundances, and alleviation of suppression effects. Dilute aqueous glycerol solutions were likewise employed to achieve the mass spectral enhancement in this work, although they were not introduced to the probe tip in a continuous

manner. These experiments did not indicate that water played a significant role in the enhancement mechanism, other than by depositing the glycerol on the sample pedestal in a thin and apparently uniform layer. The improved results were alternatively explained in terms of optimizing the matrix to analyte ratio, which allowed for more efficient concentration of the analyte at the surface of the matrix. It is possible that stable operation of the continuous-flow probe provides the same mass spectrometric advantages for the same reasons.

In Chapter 1 (p. 32), it was noted that stable operation of the continuous-flow probe requires careful consideration of parameters which affect the rate of glycerol depletion from the probe tip (including the flow rate of the matrix solution to the probe tip, and the temperature of the probe tip). Reproducible results which display the spectral enhancement are associated with a wet appearance of the sample stage on which no definable droplet is evident (20). It seems feasible that balancing the rate of glycerol depletion from the probe tip with the rate of glycerol deposition could result in maintaining the optimized sample preparation described in this chapter for long periods of time. Figure 2.19 shows representations of the CF-FAB probe tip during stable operation and unstable operation. The thin sample layer depicted for the stable surface is very suggestive of the appearance of the optimal sample composition (sample 3 in Table 2.1) when observed under a microscope after exposure to reduced pressure in the rough vacuum lock.

I. Alternative Mechanistic Explanations

Any complete model advanced to explain desorption ionization behavior requires consideration of both the desorption and the ionization stages of the process. This chapter has focused attention on the surface composition of the

a: beveled sample pedestal

b: capillary

c: liquid sample

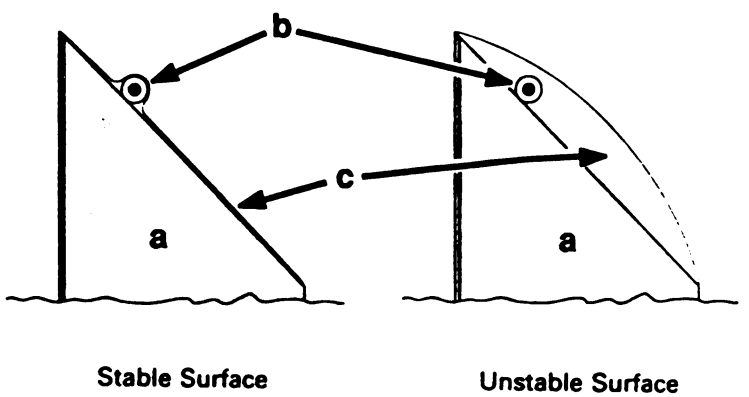

Figure 2.19. Schematic diagram showing the difference in appearance of a stable surface and an unstable surface on the CF-FAB probe tip. Adapted from reference 20 with permission of Heydon and Son Ltd.

sample, because trends in surface composition correlate with the experimental results. Such a focus, however, confines a mechanistic discussion to the processes attendant to desorption, and excludes discussion of processes attendant to ionization. This shortcoming could be addressed within the context of each mechanistic school of thought regarding ionization in FAB analyses: the detection of preformed ions and/or the detection of gas phase ion/molecule reaction products.

The use of a hydrophobicity index to predict the relative tendencies of peptides to occupy the surface of glycerol has been described in this chapter. The suitability of a hydrophobicity index to characterize the relative surface concentrations of peptides in glycerol solutions has been verified experimentally (see Chapter 1, p. 52). Other intrinsic characteristics exist which also would be helpful in correlating ionization effects to the enhancement behavior. Ionization constants (e.g., K_a's) enable the calculation of concentrations of charged species present in solution. Such calculations would be helpful in clarifying the importance of preformed ions in contributing to the mass spectral enhancement. Gas phase basicity values quantify the Gibbs free energy change associated with protonation of a species in the gas phase. This parameter would be helpful in clarifying the importance of gas phase ionization processes (i.e., the gaseous protonation of a neutral analyte) in contributing to the mass spectral enhancement.

It is possible to approximate the influence of preionization (in the condensed phase) upon the enhancement of the FAB response for an analyte. The tendency of bradykinin (B) to form protonated molecules in aqueous solution is addressed by the following equilibrium.

$$B + H_2O \overset{K_b}{\rightleftharpoons} BH^+ + OH^-$$

This equilibrium is governed by the basicity constant K_b.

$$K_b = \frac{[BH^+][OH^-]}{[B]}$$

The most appropriate basicity constant for characterizing the behavior of bradykinin should be that corresponding to the most basic group in the peptide. Arginine contains this highly basic group and the corresponding K_b value is 1.1×10^{-5}. The contribution of glycerol to the population of charged species in solution should be minimal, due to the very low dissociation constant of glycerol ($K_a = 7 \times 10^{-15}$). The basicity constant expression was used to determine the concentration of BH^+ in samples containing 4 nmol of bradykinin dispersed in the volume associated with a nonoptimal portion of glycerol (1 ul), and the volume associated with the optimal portion of glycerol (0.077 ul). These calculations reveal that although the concentration of protonated bradykinin is increased in the smaller portion of solvent, the number of protonated bradykinin molecules is not increased. Therefore, these calculations suggest that preferential ionization in the condensed phase does not contribute to the mass spectral enhancement. Unfortunately, the aqueous ionization constants used for these calculations are not strictly valid for glycerol solutions, due to the difference between the dielectric constants of glycerol and water. Caprioli incorporated experimentally determined corrections for this discrepancy in a FAB-MS study of glycerol solution equilibria (5). The validity of these corrections was later questioned in a related study by Connolly and Orth (21).

It is also interesting to consider the possible influence of gas phase ion/molecule reactions upon the mass spectral enhancement. Assuming a gas

phase ionization model is operative, one might expect an ion/molecule reaction such as the following to be responsible for ionization of the analyte.

$$A + GH^+ \rightarrow AH^+ + G$$

In this expression, A represents the analyte species and G represents glycerol. As the amount of glycerol in the sample declines, the amount of glycerol available for reaction in the gas phase should also decline (although not necessarily by a proportional relationship). This trend is not intuitively compatible with an increased reaction rate (which is indicated by the observed increase in protonated analyte ion abundances). It is possible, however, that the conditions for chemical ionization could reach a local optimum as a function of glycerol content in the sample. It is also possible that as the amount of glycerol present in the sample declines below that optimal value, an analyte characterized by a relatively high gas phase basicity could compete more effectively for the available reagent than an analyte characterized by a lower gas phase basicity. This behavior could allow the capacity to distinguish the enhancement profiles for analytes with different gas phase basicities. It should be noted, however, (as mentioned in Chapter 1, p. 62) that a study by Sunner, Kulatunga, and Kebarle suggests that gas phase basicity effects can be superseded by surface concentration effects (22). A separate study by Lacey and Keough (23) also indicates that surface effects tend to dominate gas phase basicity effects in determining FAB-MS results.

It is not an objective of the model proposed in Section f of this chapter to advocate whether a preformed ion mechanism or a gas phase ionization mechanism is appropriate for understanding FAB-MS. As discussed in Chapter 1 (p. 62), convincing evidence has been put forth in support of both models. It is

the belief of the author that both mechanisms may be operative, and that the relative contribution from each depends upon the characteristics of the particular analyte/matrix combination involved in the analysis. Documenting the enhancement behavior attendant to optimization of the matrix to analyte ratio for all possible combinations of analyte and matrix is beyond the scope of this dissertation. Furthermore, it is logical to expect that preferential concentration of the analyte at the surface of the matrix will result in a mass spectral enhancement regardless of which ionization mechanism is favored. Concentration of preformed ions at the surface of the matrix will increase their sputtering yield as measured in the mass spectrum. Likewise, gas phase ionization of the analyte should be promoted by its concentration at the surface of the matrix, as articulated by Sunner, Morales, and Kebarle (24): "...the present FAB spectra are determined by the "gas"-phase reactions...governed by the gas-phase basicities, but that the concentrations of the participating analytes are not proportional to the ligand bulk concentration but are modified by surface enrichment."

The objective of the proposed model is to provide a rationale for the enhancement behavior. It is believed that an increased surface concentration of the analyte in the smaller portions of glycerol is the primary cause of the mass spectral enhancement. Experiments described in Sections g and j of this chapter were conducted to test the predictive capacity of the proposed model. In Section g, a trend in the enhancement behavior of five analytes characterized by different surface activities in glycerol was predicted and observed. In Section j, the relative behavior of mixtures of analytes was predicted in terms of surface effects. Once again, the experimental data were consistent with predictions based upon the proposed model. Therefore, it is apparent that any variations in ionization phenomena which occur as the sample composition is manipulated are

insignificant in comparison to the importance of the analyte surface concentration in glycerol. Peptides were employed as the model compounds in these confirmative studies for compelling reasons. First of all, studying the behavior of peptides serves an immediate need in the user community, due to the widespread interest in the analysis of this class of compounds. Secondly (and more importantly), the structural characteristics of peptides uniquely lend themselves to investigations of this nature. As described in Chapter 1 (Section **a**) of this dissertation, peptides are related by a common structural backbone. The linear peptides utilized in these studies were all characterized by free N and C termini. Therefore, identical ionizable functionalities were present for all of the model compounds. The structural difference between these compounds relates to the identity of an R group which is associated with each amino acid. The relative hydrophobicities of these distinguishing groups had been ranked by Bull and Breese (15). Thus, due to their close structural similarities and the existence of a scale which relates their relative hydrophobicities, peptides constitute an excellent class of compounds for the study of surface-related phenomena.

IV. Conclusion

It has been shown that the matrix to analyte ratio profoundly affects the quality of FAB-MS results. Although the qualitative information regarding the analyte is maximized when using the smaller portions of glycerol, it is interesting to note that a wider linear response for the analyte results from the use of larger amounts of glycerol. This would indicate that the larger glycerol portions are better suited for quantitative purposes where dynamic range is important.

Mass spectral enhancement can be realized simply by mixing the analyte with a 1 ul portion of 10% (w/w) aqueous glycerol. By introducing less glycerol

into the mass spectrometer source, one also can reasonably expect less rapid contamination of the ion lenses. The only disadvantage encountered by this approach regards ion signals of decreased temporal duration in comparison to those measured from samples introduced in larger amounts of the glycerol matrix. However, for the many applications of FAB-MS which do not require extremely longlived ion currents, this method provides substantial analytical advantages.

V. References

1. DePauw, E. *Mass Spectrom. Rev.* **1986**, *5*, 191.
2. Fenselau, C.; Cotter, R.J. *Chem. Rev.* **1987**, *87*, 501.
3. Clay, K.L.; Wahlin, L.; Murphy, R.C. *Biomed. Mass Spectrom.* **1983**, *10*, 489.
4. Dass, C.; Desiderio, D.M. *Anal. Biochem.* **1987**, *163*, 52.
5. Caprioli, R.M. *Anal. Chem.* **1983**, *55*, 2387.
6. Roepstorff, P.; Fohlman, J. *Biomed. Mass Spectrom.* **1984**, *11*, 601.
7. Biemann, K. *Biomed. Environ. Mass Spectrom.* **1988**, *16*, 99.
8. Ligon, W.V.; Dorn, S.B. *Int. J. Mass Spectrom. Ion Proc.* **1984**, *57*, 75.
9. Caprioli, R.M.; Fan, T. *Biochem. Biophys. Res. Commun.* **1986**, *141*, 1058.
10. Beckner, C.F.; Caprioli, R.M. *Biomed. Mass Spectrom.* **1984**, *11*, 60.
11. Clay, K.L.; Stene, D.O.; Murphy, R.C. *Biomed. Mass Spectrom.* **1984**, *11*, 47.
12. Beckner, C.F.; Caprioli, R.M. *Anal. Biochem.* **1983**, *130*, 328.
13. Lehmann, W.D.; Kessler, M.; Konig, W.A. *Biomed. Mass Spectrom.* **1984**, *11*, 217.
14. Barber, M.; Bordoli, R.S.; Elliott, G.J.; Sedgwick, R.D.; Tyler, A.N. *J. Chem. Soc., Faraday Trans. 1* **1983**, *79*, 1249.
15. Bull, H.B.; Breese, K. *Arch. Biochem. Biophys.* **1974**, *161*, 665.
16. Clench, M.R.; Garner, G.V.; Gordon, D.B.; Barber, M. *Biomed. Mass Spectrom.* **1985**, *12*, 355.
17. Naylor, S.; Findeis, A.F.; Gibson, B.W.; Williams, D.H. *J. Am. Chem. Soc.* **1986**, *108*, 6359.
18. Caprioli, R.M.; Moore, W.T.; Fan, T. *Rapid Commun. Mass Spectrom.* **1987**, *1*, 15.

19. Naylor, S.; Moneti, G.; Guyan, S. *Biomed. Environ. Mass Spectrom.* **1988**, *17*, 393.

20. Seifert, W.E., Jr.; Ballatore, A.; Caprioli, R.M. *Rapid Commun. Mass Spectrom.* **1989**, *3*, 117.

21. Connolly, M.J.; Orth, R.G. *Anal. Chem.* **1987**, *59*, 903.

22. Sunner, J.A.; Kulatunga, R.; Kebarle, P. *Anal. Chem.* **1986**, *58*, 1312.

23. Lacey, M.P.; Keough, T. *Rapid Commun. Mass Spectrom.* **1989**, *3*, 46.

24. Sunner, J.; Morales, A.; Kebarle, P. *Anal. Chem.* **1987**, *59*, 1378.

Chapter 3. Continued Development and Optimization of Thermally Assisted Fast Atom Bombardment Mass Spectrometry

I. Introduction

In 1985, a novel desorption ionization technique known as thermally assisted fast atom bombardment (TA-FAB) mass spectrometry was introduced (1). The pioneering work for this experiment was accomplished at Michigan State University by Ackermann, Watson, and Holland. The original intent of these investigators was to employ solid compounds as FAB matrices, which could be heated to a degree of fluidity conducive to desorption ionization. Besides increasing the range of compounds available as FAB matrices, it was thought that solids might produce less background interference than the conventionally used viscous liquids. Due to their structural similarity with glycerol, saccharides (deposited from aqueous solutions) were evaluated as potential TA-FAB matrices. In the course of this work it became apparent that TA-FAB offered the potential to stimulate differential desorption ionization of analyte versus matrix as a function of temperature. An exciting implication of this result was the capability (in favorable cases) to perform valid background subtractions.

The following chapter describes the author's participation in further developing, understanding, and optimizing the TA-FAB experiment. It begins with a background discussion regarding the fundamentals of TA-FAB. Work intended to clarify the operative mechanism responsible for the TA-FAB phenomenon will then be considered. Attention will be given to implementation of the technique on a new, high performance, high mass instrument, and the

corresponding efforts to apply TA-FAB to the analysis of higher mass compounds. Various aspects of the experiment will be considered throughout this progression, with respect to their influence upon optimization of the technique.

II. TA-FAB Fundamentals

Saccharides which had proven successful as TA-FAB matrices included glucose, fructose, sucrose, thioglucose, and tartaric acid (1). It is important to note that these solids were reproducibly deposited on the TA-FAB emitter in aqueous solutions. One of the objectives of this research was to determine whether these novel matrices provided less matrix interference than the viscous liquids normally used in FAB. Figure 3.1 shows an averaged background spectrum of a 0.5 ul portion of an aqueous fructose solution which was analyzed by TA-FAB. The peak at m/z 203 corresponds to the [fructose+Na]$^+$ ion. This spectrum reveals a pronounced tendency for the fructose monomer to fragment, especially by successive water losses from the protonated molecule (these fragments are observed at m/z 163, 145, and 127). One observes little evidence of fructose cluster formation, however, which would contribute to matrix interference in the higher mass portions of the spectrum. Indeed, besides somewhat minor signals at m/z 325 ([2fructose+H-2H_2O]$^+$) and m/z 365 ([2fructose+Na-H_2O]$^+$), a very clear high mass window is available for the unobstructed viewing of analyte signals. The relatively minor matrix signals at m/z 325 and 365 were not always apparent in analyses involving the analyte (1). This decreased clustering behavior also was noted for the other saccharides utilized as TA-FAB matrices.

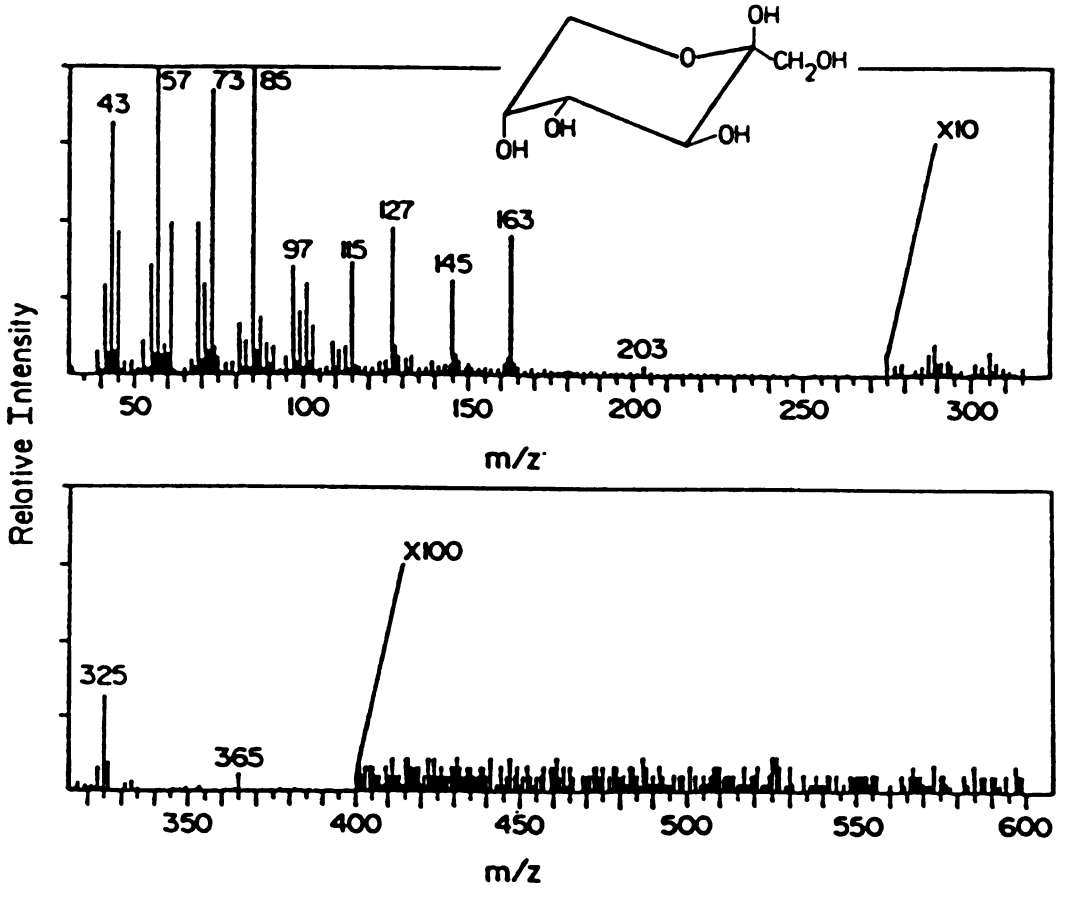

Figure 3.1. Averaged mass spectrum produced from 0.5 ul of an aqueous fructose solution under the conditions of TA-FAB. Adapted from reference 1 with permission of the American Chemical Society.

The TA-FAB experiment contains three distinct stages with respect to desorption ionization of the sample. In the first stage, no heat is applied to the sample (other than the transient heating imparted by the FAB beam), and the resulting spectra are characteristic of the saccharide matrix. During the second stage, the sample is resistively heated and the corresponding mass spectra contain significant contributions from both the analyte and the matrix. Finally, all ion current is strongly diminished in the third stage of the experiment.

An example of this experimental sequence is displayed in Figure 3.2. This figure contains several plots of ion abundance as a function of scan number, and also temperature. This sort of data presentation is called a mass thermogram, to emphasize the changing temperature of the sample during the course of the analysis. The lower set of thermograms correspond to ions derived from the matrix compound, which was fructose in this particular experiment. The fructose thermograms are arranged in order of decreasing mass, from top to bottom. In the first stage of the experiment (before the temperature is raised), significant desorption ionization of the matrix occurs. This desorption ionization continues as a function of temperature until the fructose ion abundances finally decline essentially to zero. The upper set of mass thermograms correspond to ions derived from the tripeptide alanyl-leucyl-glycine (ALG). This analyte, which was present in microgram quantities, experiences negligible desorption ionization before the sample is resistively heated. Once the temperature of the sample is raised, however, strong desorption ionization of the analyte occurs. The temperature corresponding to maximum desorption ionization of the analyte is referred to as the "best matrix temperature" (BMT), in analogy to the "best anode temperature" (BAT) terminology used to describe maximum desorption ionization in the FD experiment. After the BMT, the analyte ion abundances become diminished as the temperature is further increased.

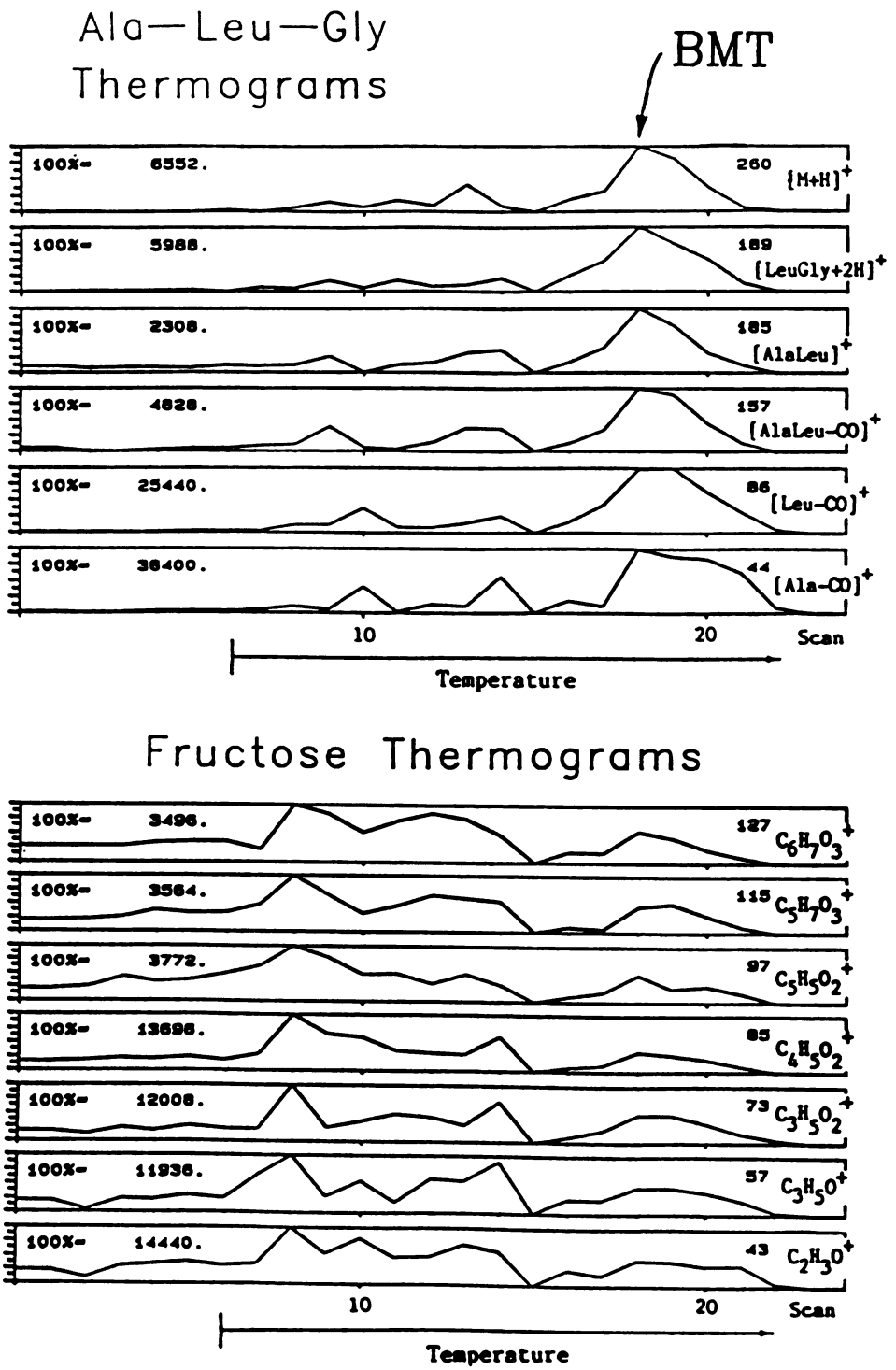

Figure 3.2. Mass thermograms obtained from a TA-FAB analysis of 2 ug of alanyl-leucyl-glycine (upper thermograms) sampled from an aqueous fructose matrix (lower thermograms).

An important feature of the data represented in Figure 3.2 is the similarity in shape of the individual fructose thermograms. Another way of stating this phenomenon is that the fructose thermograms tend to track one another as a function of temperature. Interestingly enough, the analyte thermograms shown in Figure 3.2 also tend to track one another; however, the analyte thermograms do not track the matrix thermograms. Therefore, analyte and matrix experience differential desorption ionization as a function of temperature.

Significant analytical benefits are associated with this differential behavior. For instance, a spectrum obtained prior to heating (which contains information regarding the matrix) may be subtracted from the BMT spectrum (which contains information from both the analyte and the matrix) to obtain a remarkably clean background subtracted spectrum. Another benefit of the differential desorption ionization is the capability to determine whether a signal of unknown origin is derived from the analyte or the matrix by comparison of its mass thermogram with those from known signals.

Mass spectral data from a TA-FAB analysis are compared to data from a conventional FAB analysis in Figure 3.3. In spectrum 3.3a, 1 ug of ALG is sampled by FAB from 0.5 ul of glycerol. The base peak in this spectrum corresponds to the protonated glycerol molecule at m/z 93. A signal of particular interest is at m/z 185, since it not only represents a prominent glycerol background ion ($[2glycerol+H]^+$), but also an important analyte fragment ($[M+H-glycine]^+$). Because this signal is isobaric with a known matrix ion, it would not normally be interpreted as useful for analyte structure elucidation. Figures 3.3b and 3.3c show data from a TA-FAB analysis of the same amount of ALG sampled from 0.5 ul of an aqueous fructose solution. The spectrum in Figure 3.3b is averaged over the BMT region (the period of strong analyte desorption ionization). The base peak in this spectrum corresponds to an analyte fragment

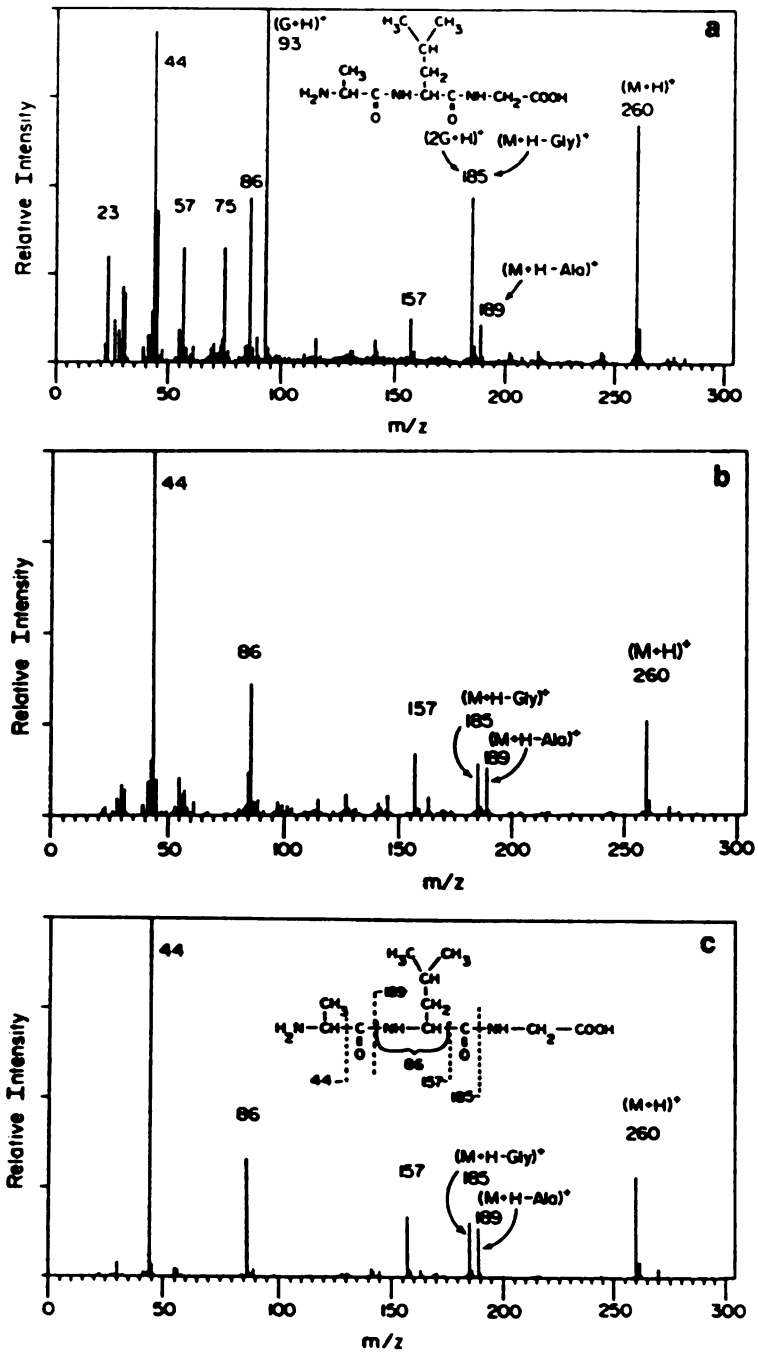

Figure 3.3. (a) Conventional FAB mass spectrum of 1 ug of alanyl-leucyl-glycine in 0.5 ul of glycerol. The letter "G" represents the glycerol monomer. (b) TA-FAB mass spectrum of 1 ug of alanyl-leucyl-glycine in aqueous fructose solution averaged over the BMT region. (c) TA-FAB spectrum after background subtraction. Adapted from reference 1 with permission of the American Chemical Society.

ion (at m/z 44), and the entire mass range is characterized by a substantially greater signal to chemical background ratio than observed in Figure 3.3a. Interference from the matrix is almost completely removed by the background subtraction shown in Figure 3.3c. The TA-FAB results displayed in Figures 3.3b and 3.3c display significantly enhanced visibility of analyte signals with respect to matrix signals in comparison to the FAB results (Figure 3.3a).

Another advantage of TA-FAB was documented in a study involving three cyclic tetrapeptide mycotoxins (2). For these compounds, TA-FAB was demonstrated to provide increased fragmentation (and hence, greater utility for structure elucidation) than was provided by FAB analyses utilizing the glycerol matrix. This discovery was particularly significant since it was made in conjunction with the analysis of peptides. As mentioned in Chapter 1 (p. 68), any method resulting in the increased fragmentation of peptides is considered especially important due to the widespread activity in the sequencing of these biopolymers by mass spectrometry.

III. Experimental

a. Materials

Analyte and matrix compounds were provided from one of several commercial sources unless otherwise noted. Matrix solutions were prepared in terms of weight percent.

b. TA-FAB on Varian MAT CH5

Initial TA-FAB data were obtained on a double-focusing (BE geometry) Varian MAT CH5 mass spectrometer. The CH5 was operated at an acceleration potential of 3 kV. A Model B11NF saddle-field gun with a B50 current regulated power supply (Ion Tech, Ltd., Teddington, U.K.) produced a xenon FAB beam of 6-8 keV for this work. With the FAB gun operating, the source pressure was approximately $1x10^{-5}$ torr. Data were collected, stored, and processed with a dual PDP-8/e data system.

TA-FAB was accomplished on the CH5 by resistively heating the sample on a 97% tungsten, 3% rhenium emitter (5.97 mm x 0.46 mm x 0.02 mm). Current was supplied to the TA-FAB emitter by an emitter current programming unit (ECP) (1), which had previously been designed for the precise regulation of current through FD emitters (3). The ECP provided more than 3 A of current while floating at the 3-kV acceleration potential. A typical current program for a TA-FAB run on the CH5 involved the acquisition of a few scans without the application of heat (0.00 A), followed by a relatively rapid surge of current (e.g., 0.90 A) which was established within one mass spectrometric scan, and finally, a slow current ramp of approximately 100 mA/min.

c. TA-FAB on JEOL HX-110

The JEOL HX-110 was described in Chapter 2 (p. 97). The TA-FAB data from this instrument were acquired at an acceleration potential of either 8 or 10 kV, with a variety of individual scanning parameters. Typical source pressures during TA-FAB were $1-8x10^{-6}$ torr. Modification of the HX-110 for TA-FAB will be discussed in a following section.

d. Sample Preparation

Aliquots of analyte and matrix solutions were applied to the TA-FAB probe tip with Hamilton syringes. After application, mixing of the sample was facilitated either by stirring with the syringe needle, or by gently blowing the sample with a heat gun (which also partially desolvated the sample). A comparison of different sample preparations demonstrated that the order of analyte and matrix application did not affect the results.

e. Viscosity Measurements

Viscosity data were obtained with a Haake RV12 viscometer. This instrument was equipped with an M150 head, an MV1 sensor, and an MV cap. The viscometer was supported by a Hewlett Packard 3497A Data Acquisition/Control Unit and a Hewlett Packard 85 computer. Temperature control was accomplished with a Haake C water bath and a Haake F3 Temperature Controller.

IV. Results and Discussion

a. Mechanistic Investigations

This section discusses work undertaken to clarify the mechanism operative in the TA-FAB experiment already described (i.e., using aqueous saccharide matrices). The intent of this work was not to enter into the debate regarding the FAB mechanism, but to understand the experimental observations

unique to TA-FAB (e.g., the differential desorption ionization of analyte versus matrix). The results presented are predominantly qualitative in nature, and not conclusive. A model which appears to be consistent with these data is hypothesized at the end of the section. B. L. Ackermann (a pioneer of the technique) was an important participant in the acquisition of these data and their interpretation. Because this topic has been the subject of a previous presentation (4) and a portion of B. L. Ackermann's doctoral dissertation (5), the present treatment is intended as a compact summary of the experimental results and proposed mechanism.

Figure 3.4 presents the important temporal characteristics of the TA-FAB experiment. The data in Figure 3.4 were obtained from an actual TA-FAB run, but will be discussed in the general sense as typical of the behavior expected from any sample subjected to TA-FAB. Analyte ion response is represented in the upper mass thermogram in Figure 3.4, and the matrix ion response is represented in the lower thermogram. This figure divides the experiment into three distinct stages as a function of sample temperature. During the first stage, no heating of the sample occurs and the data reveal little desorption ionization of the analyte and significant desorption ionization of the saccharide matrix. Therefore, in analogy to the conventional FAB experiment, the matrix behavior is unlike that of glycerol. During the second stage, significant desorption ionization of analyte and matrix occurs as the sample is resistively heated. To continue the analogy, the matrix does function like glycerol during this temperature interval. Finally, a dramatic diminution in ion abundance accompanies further heating of the sample as is evidenced in stage 3 of the experiment. Again, the matrix does not function in a manner similar to glycerol during conventional FAB. As previously mentioned, all analyte mass thermograms tend to track one another as a function of temperature. The matrix mass thermograms are not quite as

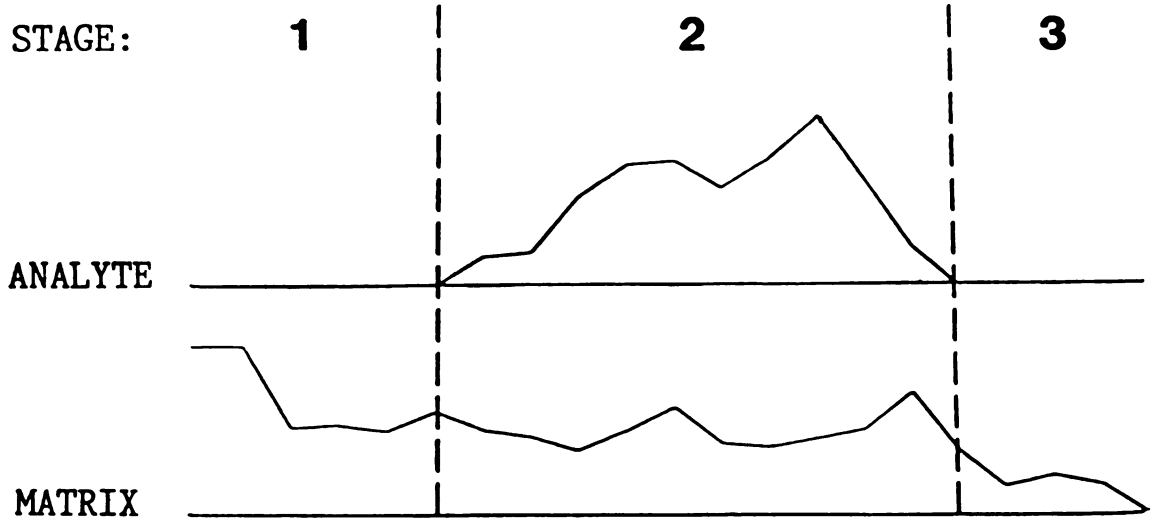

Stage	Heat	Desorption of Analyte	Matrix Behavior
1	No	Little or None	Unlike Glycerol
2	Yes	Strong	Like Glycerol
3	Yes	None	Unlike Glycerol

Figure 3.4. Typical behavior of a sample subjected to TA-FAB represented in the abundance profiles of an analyte ion (upper thermogram) and a matrix ion (lower thermogram).

reproducible or predictable as the analyte thermograms, but they, too, can generally be described as tracking one another during the course of the temperature scan.

Visual observations of the sample on the probe tip have been correlated to the different stages of the experiment. Although these observations are qualitative in nature, they can provide some insight into the changes occurring in the sample as the temperature is manipulated. The observations involved interrupting typical TA-FAB analyses to visually inspect the sample (1.0 ul of analyte solution added to 1.0 ul of fructose solution) during each stage of the experiment. The observations discussed were persistently noted in several different inspection sequences. Those corresponding to stage 1 of the experiment were made after insertion of the probe into the source vacuum and the acquisition of a few mass spectra (which were obtained with no current applied to the emitter). Withdrawal of the probe revealed that the sample had maintained its droplet form upon the emitter band. A very important observation at this point was that the saccharide (which was deposited from an aqueous solution) had retained a significant portion of the water solvent even in the vacuum of the source region ($1x10^{-5}$ torr). This conclusion was obvious from the clear appearance of the sample, and its consistency (tested with a syringe needle), which resembled that of an extremely viscous liquid. The capacity to retain water in the mass spectrometer vacuum had been noted for all the saccharides which had performed successfully as TA-FAB matrices. The viscosity of this highly concentrated saccharide solution warrants further mention, because it appeared substantially greater than that of glycerol (this assertion will be validated presently by viscosity measurements which were carried out on larger scale samples). Withdrawal of the probe during stage 2 (the BMT region) revealed that the sample had lost its original droplet shape and had spread out

more evenly across the tungsten/rhenium band. Such an observation strongly implies an interval of increased fluidity subsequent to stage 1 of the experiment. Determination of the consistency was difficult due to the sample having spread out, but it appeared relatively nonfluid. Finally, inspection of the sample during stage 3 of the experiment revealed an immobile, thin, glassy film spread over the emitter. At this point, the needle of the syringe appeared to make no impression upon the surface of the sample.

The visual observations indicate that at the beginning of the TA-FAB experiment, the sample actually exists as a ternary mixture of analyte, saccharide, and water. The correlation between the capacity of the matrix to retain water under vacuum and successful performance in TA-FAB, suggests that the water component plays a critical role in the TA-FAB phenomenon. Transformation of the sample from an extemely viscous liquid (stage 1) to a dry, glassy state (stage 3) indicates that the water is removed during the application of heat in stage 2. Therefore, it seems possible that removal of the water during the BMT region is associated with desorption ionization of the analyte.

Experimental evidence has been obtained which supports this contention. Should removal of the water from the sample be critical for desorption ionization of the analyte, one would expect an increase in the temporal period of desorption ionization of the analyte to accompany a decrease in the rate of water transport from the sample. This correlation is, in fact, demonstrated in Figure 3.5. The figure displays the mass thermogram for the $[M+H]^+$ ion of alanyl-leucyl-glycine (m/z 260), which was obtained from a sample containing 1.0 ul of the aqueous tripeptide solution (2 ug/ul) added to 1.0 ul of an aqueous fructose solution. The current program for this TA-FAB analysis was altered from the typical one which was described in the experimental section of this chapter. Scans 1-10 were acquired with no heat. During scan 11 the current was quickly increased to 0.80

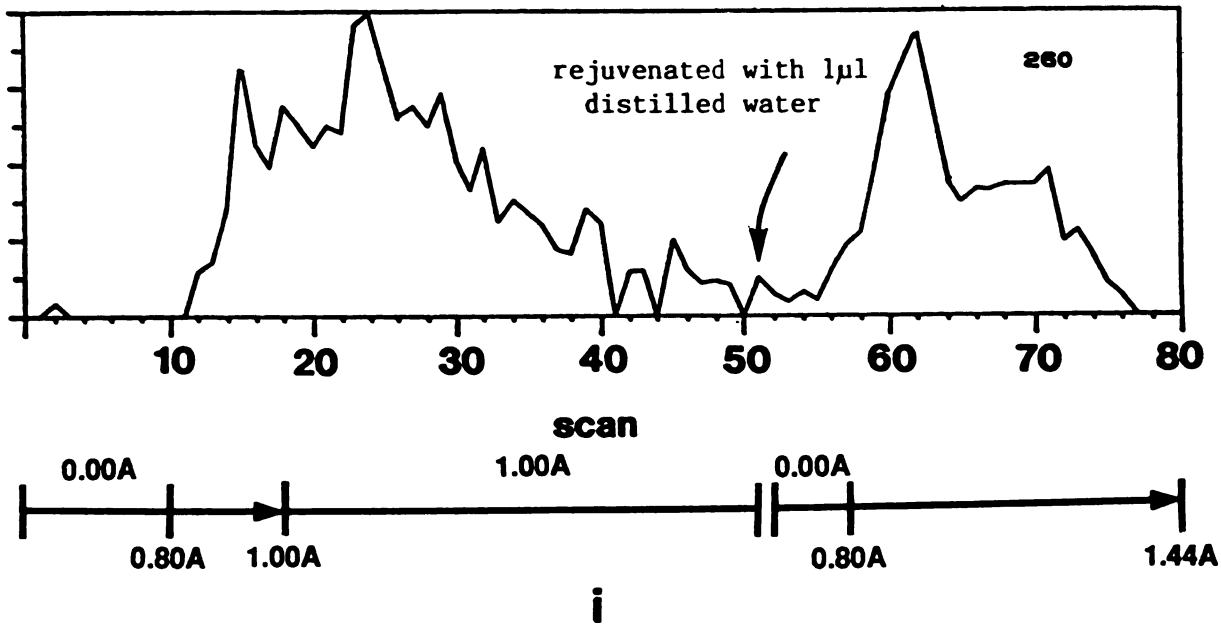

Figure 3.5. Mass thermogram of $[M+H]^+$ ion of alanyl-leucyl-glycine for an atypical TA-FAB experiment: scans 19-51 were obtained while maintaining a constant current (representative of the BMT) through the emitter. This was followed by a typical TA-FAB run which was recorded after rejuvenation of the sample with 1.0 ul of distilled water.

A. Scans 11-18 accompanied a linear current ramp from 0.80 to 1.00 A. The current was then maintained at 1.00 A (a level shown to be representative of the BMT by previous runs) until scan 51 (when the signal at m/z 260 became difficult to distinguish from the background signal). The period of analyte desorption ionization was significantly increased by maintaining the BMT current rather than conducting a continuous ramp through the BMT region. The magnitude of this increase (established by comparison with results obtained from the more common current program) was by a factor of 2 to 3.

Figure 3.5 contains further evidence regarding the importance of water in the TA-FAB experiment. Once the signal at m/z 260 had substantially diminished (scan 51), the probe was removed and the sample was rejuvenated with 1.0 ul of distilled water. After mixing, a typical TA-FAB run was executed (which included a linear current ramp from 0.80 A (scan 57) to 1.44 A (final scan)). The restored intensity of the signal at m/z 260 points to the importance of the water component in the ternary sample for stimulating desorption ionization of the analyte during TA-FAB.

The most reasonable means of water removal from the sample in response to a thermal impetus (during stage 2) was thought to involve some sort of boiling phenomenon. Therefore, it became important to establish whether the temperature range of the TA-FAB experiment approximately corresponded to the boiling point of water. To answer this question, a temperature calibration was required for the TA-FAB emitter. The calibration was accomplished by attaching a copper/constantan thermocouple to the emitter with a thermally conducting, electrically insulating, epoxy adhesive (Omegabond 200, Omega Engineering, Inc., Stamford, Connecticut). Measurements with the thermocouple were actually performed inside the source of the mass spectrometer at operating pressure. The calibration curve is shown in Figure 3.6. Due to a relatively long response

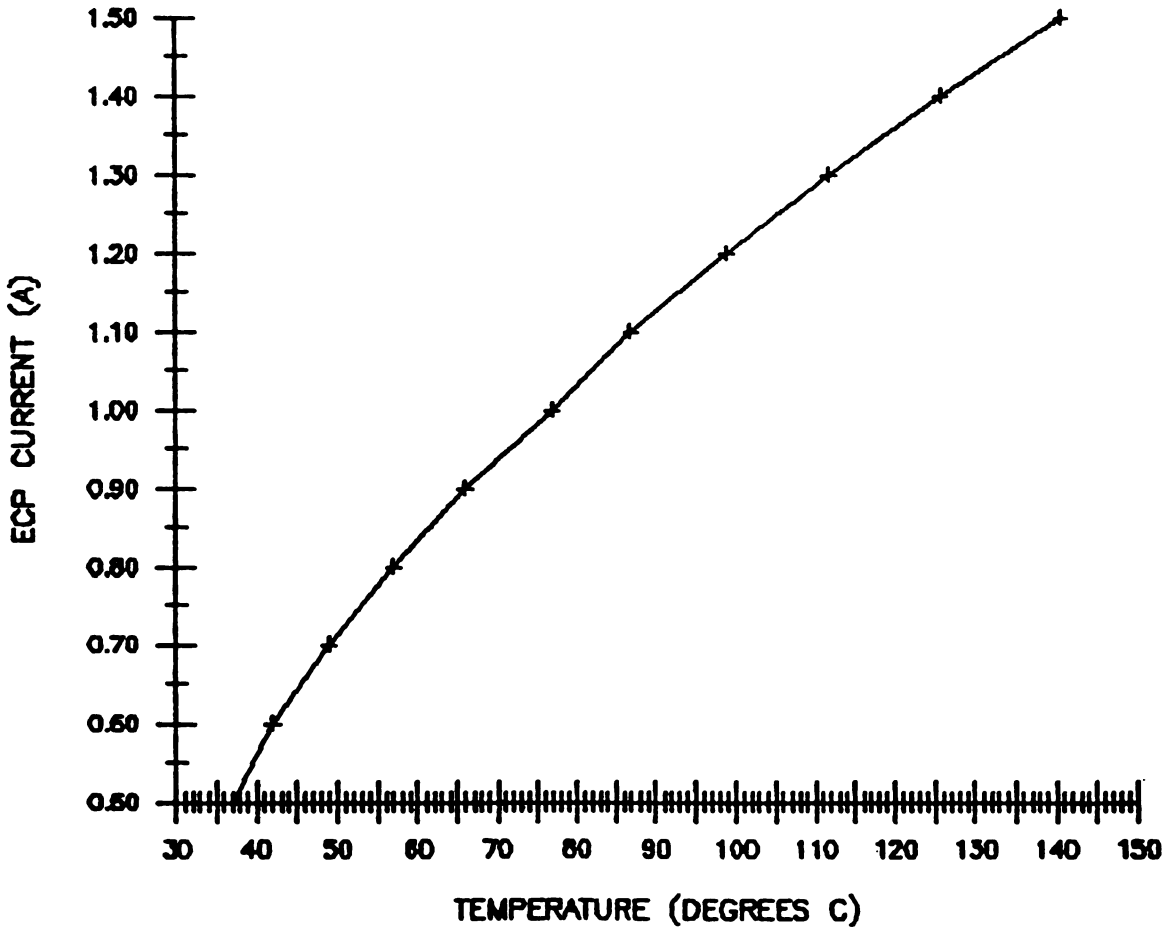

Figure 3.6. Current/temperature relationship obtained for the ECP. The uncertainty of this curve is estimated to be $\pm 10^{o}$C.

time for the thermocouple (probably caused by heating of the epoxy) leading to considerable uncertainty in the current/temperature relationship, verification of this curve was desired. This was accomplished by a series of melting point experiments involving six different solids (myristyl alcohol, stearyl alcohol, stearic acid, arichidic acid, benzil, and α-ketoglutaric acid). These determinations were made on the TA-FAB emitter inside the mass spectrometer source, and were possible because the melting process changed the appearance of the solids. The melting point data confirmed the temperature range indicated by the thermocouple measurements. Although the uncertainty of the curve in Figure 3.6 is estimated to be ±10° C, it indicates an approximate temperature range for the experiment of 0 to 150°C. The range of BMT currents observed over the course of many months of experimentation (primarily with the fructose matrix) was approximately 0.80-1.20 A. This interval corresponds to a temperature range (see Figure 3.6) of 60-105°C. The temperature at which water would boil under the conditions of TA-FAB is difficult to estimate with any certainty, because it would depend upon factors including the decreased pressure inside the source of the mass spectrometer, as well as the boiling point elevation characteristic of a very concentrated aqueous solution of saccharide and analyte. However, the temperature range indicated by these data is certainly consistent with the possibility of water being removed from the TA-FAB sample through a boiling phenomenon.

Supplementary experiments designed to monitor the escape of water from aqueous fructose solutions as a function of temperature included thermogravimetric analysis (TGA) and differential scanning calorimetry (DSC). Unfortunately, these results were reduced in significance due to the inability to conduct the experiments at pressures appropriate for mass spectrometry. A discussion of these data is provided by B. L. Ackermann (5).

As mentioned in Chapter 1 (p. 14), the matrices used in conventional FAB are viscous liquids. The fluid nature of these liquids appears to be an essential requirement for prolonged desorption ionization by keV particle bombardment. Katz and coworkers demonstrated that the sputtering behavior of such liquids (including glycerol) changed substantially when the temperature was lowered below the the freezing points of these compounds (6). These experiments have documented the significant accumulation of radiation-damaged products at the lower temperatures as a function of time (7). Although the precise mechanism for surface renewal of the analyte remains a topic of significant debate (Chapter 1, p. 56), it is widely accepted that the fluidity of a liquid is critical for the occurrence of this phenomenon. Therefore, visual observation that the sample appeared to be more viscous than glycerol during stage 1 of the TA-FAB experiment was interpreted to be important. Steps were subsequently taken to quantitatively verify this point.

Understanding the nature of the ternary samples subjected to TA-FAB requires an appreciation for the extreme solubility of the saccharide component of the matrix in water. At 25°C, a saturated aqueous fructose solution contains 80.29% (w/w) fructose (8). Such highly concentrated saccharide solutions tend to be very viscous. Viscosity measurements of these solutions were obtained on a Haake RV12 viscometer, which required 200-300 ml of sample. This volume of a concentrated aqueous fructose solution was acquired by warming a nearly saturated solution at reduced pressure (to facilitate further concentration). The reduced pressure (10^{-1}-10^{-3} torr) for this procedure was established with a mechanical pump, and was significantly higher than that present in the mass spectrometer source ($1x10^{-5}$ torr). This concentration process was not expected to be as efficient as that experienced by microliter quantities of sample exposed to the higher mass spectrometer vacuum. Indeed, the resulting (apparently

homogenous) solution did not appear as viscous as the TA-FAB sample observed during stage 1 of the experiment. At 26°C, the viscosity of this concentrated fructose solution was found to be more than 10 times greater than that measured for glycerol. Warming the fructose solution to 50°C, however, caused a drop in its viscosity to a value less than that of glycerol (measured at 26°C). Although these measurements were carried out at atmospheric pressure, they are considered valid for lower pressures as well. Therefore, these data indicate that the temperature range encompassed by the TA-FAB experiment is adequate to increase the fluidity of concentrated aqueous fructose samples to a level characteristic of glycerol.

Viscosity measurements also were conducted on a saturated fructose solution. The beaker containing this solution displayed visible precipitate even after several days of stirring at ambient pressure and temperature. The viscosity of this solution was significantly less than that of the fructose solution which had been exposed to the vacuum. Therefore, it appears that the influence of the vacuum stimulates supersaturation of the aqueous fructose sample.

In an attempt to gain further insight into the TA-FAB phenomenon, data were obtained from samples containing the matrix solution (aqueous fructose) without the addition of analyte. Mass thermograms from one such experiment are shown in Figure 3.7. The upper two thermograms correspond to relatively abundant fructose ions, and the lower thermogram is a total ion current trace. These data reveal a definite tendency for the fructose ion abundances to increase as a function of temperature in the absence of analyte. Such an increase has been documented in several similar experiments. The temperature interval of this increase also represents that of the BMT region for runs when the analyte is present. Comparison of the mass thermograms in Figure 3.7 with the typical matrix thermogram represented in Figure 3.4 (obtained from a sample

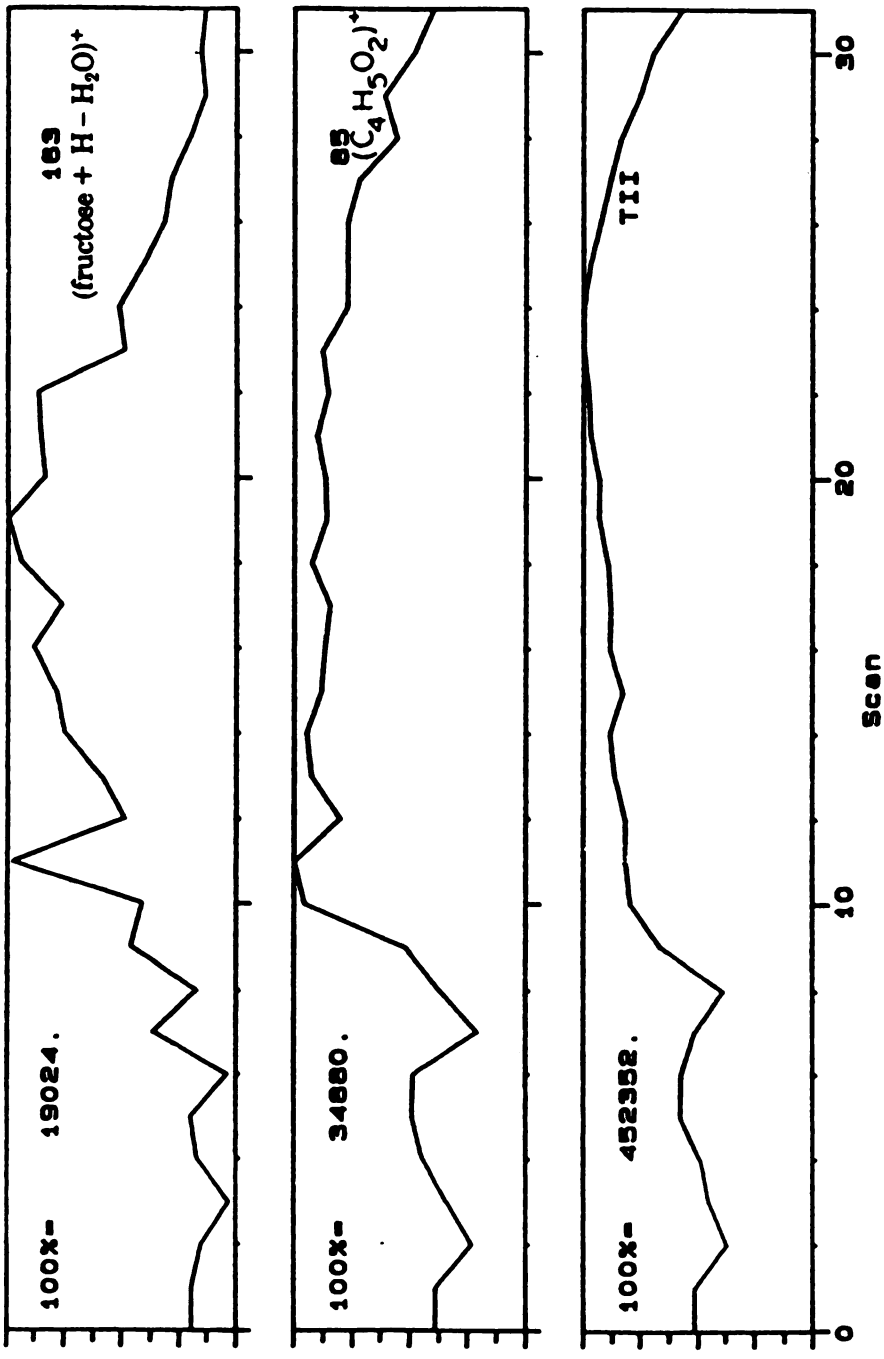

Figure 3.7. Mass thermograms for two fructose ions (upper two panels) obtained when 0.5 ul of an aqueous fructose solution was analyzed by TA-FAB. A total ion current trace is shown in the bottom panel.

containing analyte) or the fructose thermograms in Figure 3.2 (also obtained from a TA-FAB analysis containing analyte) demonstrates the capacity of the analyte to suppress the increase in desorption ionization of the matrix during stage 2 of the experiment. Suppression effects have been linked (in Chapter 1 (p. 31) and Chapter 2 (p. 129)) to differences in surface population of the various sample components.

At this point, a discussion of the differential desorption ionization phenomenon which has been associated with TA-FAB is in order. The change in ion abundance of analyte with respect to matrix in the experiment could be accounted for by three different explanations. The first explanation would involve an increased ionization efficiency of the analyte relative to the matrix as the sample is heated (preferential ionization). Increased desorption of the analyte with respect to the matrix species during stage 2 of the experiment is a second explanation (preferential desorption). The third possibility involves some combination of the first two. Preferential ionization is a difficult argument to justify in TA-FAB because analytes which are preformed ions in aqueous solution (salts), analytes which require protonation for detection, and analytes which require some other cationic addition (e.g., by Na^+ or K^+) for ionization all display similar temporal behavior as a function of temperature. It seems unlikely that the distinct processes which result in formation of these different ion types would be favored in a similar fashion as the temperature of the sample is manipulated. Assuming this reasoning to be valid, one is left with the preferential desorption of the analyte to explain the experimental results. A certain vehicle for preferential desorption of one species with respect to others is its preferential concentration at the surface of the sample. Therefore, the suppression effects described in the previous paragraph can be interpreted to support preferential desorption of analyte versus matrix during the BMT region (stage 2) of the TA-FAB experiment.

Interesting work involving aqueous saccharide solutions which is germane to the present discussion was reported by Mathlouthi (9). In this study, X-ray diffraction was utilized to characterize aqueous solutions of fructose, glucose, and sucrose as a function of concentration. Figure 3.8 displays the set of X-ray diffractograms (plots of diffracted intensity versus angle of diffraction) obtained from fructose solutions. The lowermost trace represents the analysis of pure water, and the two uppermost traces document the response of vitreous (molten fructose which was rapidly cooled) and lyophilized forms of the saccharide. The latter two forms correspond to fructose in the solid state. The other data were collected from aqueous solutions of progressively increasing (from bottom to top) concentration. Although X-ray diffraction is not normally applied to the analysis of aqueous solutions (probably due to an inability to localize individual hydrogen atoms), the technique proved useful in comparing the diffractive behavior of the saccharide solutions as a function of concentration. The important point to note in Figure 3.8 is the increasing trend of the more concentrated fructose solutions to simulate the diffractive behavior of solid fructose. Mathlouthi suggests that the intensity maximum observed for these concentrated solutions between a Bragg angle (angle of diffraction) of 6-8^{o} corresponds to diffraction directed by planes of saccharide molecules. He further believes that the abrupt increase in viscosity documented at the 35-40% concentration threshold of these carbohydrates results from an extent of saccharide organization indicative of prenucleation. Such an interpretation contains interesting implications for the present mechanistic investigations, especially in light of the high viscosity values which have earlier been reported for fructose solutions exposed to vacuum. Mathlouthi interprets the diffractograms from the most concentrated solutions as indicative of "the regular repetition of planes containing associated carbohydrate molecules." He argues that "the same, short-range order of sugar molecules" is present in the

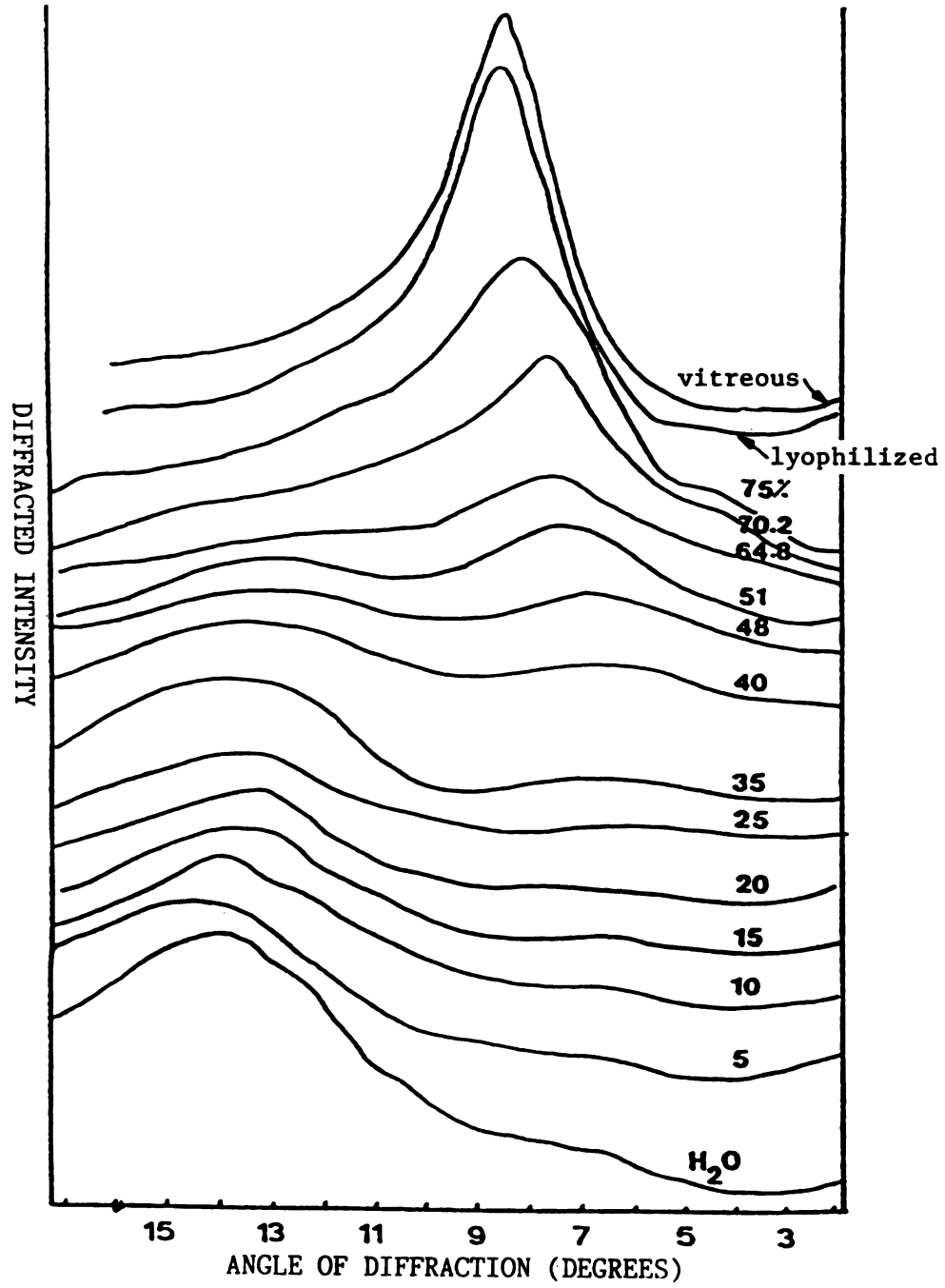

Figure 3.8. X-ray diffractograms obtained for aqueous solutions of fructose at different concentrations (weight %), as well as solid fructose (lyophilized and vitreous). Adapted from reference 9 with permission of Elsevier Science Publishers.

concentrated solutions as is present in the solid forms of the saccharides. Notice in Figure 3.8 the disappearance of the intensity maximum located at a Bragg angle of 13-14° as the concentration of fructose is increased. The disappearance of this signal (which is indicative of the organization of liquid free-water) at the expense of the other intensity maximum indicates a transformation from a preponderance of water-water interactions to a preponderance of fructose-fructose interactions. Such a situation should not be surprising considering that a saturated aqueous fructose solution at 25°C contains only 2.5 molecules of water for each molecule of fructose. Even fewer water molecules would be expected for each fructose molecule during stage 1 of the TA-FAB experiment, because the viscosity measurements actually indicate supersaturation of the sample. It is difficult to conceive of fewer than three water molecules effectively solvating a fructose monomer.

A related, laser-Raman study of solute-solvent interactions in aqueous solutions of the three saccharides (fructose, glucose, and sucrose) also was conducted by Mathlouthi (10) and is relevant to this discussion. These data are interpreted by the authors to suggest that as the saccharides are concentrated in water, sugar-sugar association is promoted, and ultimately, prenucleation occurs. The authors contend that this process is accompanied by water-sugar dissociation. Herein lies the importance of these studies in relation to the TA-FAB phenomenon. Concentrated solutions of simple carbohydrates achieve their greatest stability by maximizing saccharide-saccharide interactions in a very ordered, almost lattice-like network. While concentrating such substances in water, the more stable configuration results from the substitution of saccharide-saccharide interactions for water-saccharide interactions. The same process could result in the exclusion of water (and other impurities such as the analyte) toward the surface of the sample in TA-FAB.

It seems appropriate to draw an analogy between the TA-FAB phenomenon and zone refining, which is a method used to purify metals by successive melting steps, each followed by resolidification (11,12). A gradual purification accompanies this procedure, driven by the formation of an uninterrupted, thermodynamically stable metal lattice by repeatedly breaking and establishing interactions. Although the increased fluidity during stage 2 of the TA-FAB experiment does not result solely from melting (since significant water transport also occurs), it probably provides an environment in which such a partitioning mechanism would be favored.

Examination of the experimental results led to formulation of the ternary perculation (TP) model to explain the unique desorptive behavior associated with TA-FAB. The model will be described within the context of the three distinct stages of the TA-FAB experiment represented in Figure 3.4.

During stage 1 of the experiment, the sample consists of a supersaturated aqueous saccharide solution in which the analyte is dispersed. The sample is dominated by an ordered network of saccharide-saccharide interactions, which is occasionally interrupted by the analyte. Water molecules also are trapped within the saccharide network, but they do not cause the same degree of disruption as do the analyte species. Any analyte trapped near the surface is probably desorbed quickly by the initial dose of fast atoms, but no replenishment of the analyte occurs at the surface due to the high sample viscosity. Therefore, sustained desorption ionization of the analyte does not occur.

Stage 2 of TA-FAB is characterized by substantially decreased sample viscosity (or increased fluidity). The increased fluidity is partially provided by water transport through the sample to the surface. Because the heating is accomplished in a relatively slow, controlled manner, the water removal is thought to proceed through a series of vaporization/condensation equilibria which

progressively migrate away from the lower layers of the sample (near the heating element) to the sample surface. The increased fluidity also is thought to result partially from melting of the saccharide. This contention is supported by the fact that the best matrix temperatures for the different saccharide matrices tend to follow the order of the saccharide melting points (which are all accessible within the temperature range of the experiment). During this period of increased fluidity, preferential population of the surface by the analyte occurs. The analyte transport is supported by the unidirectional flow of water to the surface, as well as the driving force to eventually establish a more ordered, thermodynamically stable saccharide network.

By stage 3 of the experiment, the water has been removed from the sample. The unidirectional flow of solvent to the surface has therefore ceased, resulting in decreased sample fluidity. The remaining mechanism for surface population by the analyte (a process analogous to zone refining) is inhibited by the decreased fluidity. At some point, the heating irreversibly damages the matrix (probably by the onset of polymerization) as has been documented by unsuccessful attempts at this stage to revitalize the matrix with additional water and analyte.

The increased fragmentation observed by TA-FAB in comparison to that in conventional FAB might be explained by the clustering concept developed in Chapter 1 (p. 49) and utilized in Chapter 2. Because TA-FAB matrices display little tendency to form stable clusters (as evidenced by their mass spectra), analyte species may be formed in the gas phase with a reduced capacity for releasing excess internal energy. Fragmentation would be the expected result of this circumstance.

As mentioned at the outset of this section, the ternary perculation model has not been conclusively proven. A few observations relevant to the model will

be noted in the following pages, but, otherwise, the topic will be pursued no further. The original intent of the author was to more rigorously test the points of the model, but for reasons which will become apparent, such experiments were not conducted. Nevertheless, the model represents a plausible explanation for the available information. As a final footnote to this section, it seems appropriate to recall a phrase commonly used by B. L. Ackermann in discussions regarding the TA-FAB phenomenon. He often described the utility of TA-FAB "in making a thermodynamically favorable process kinetically viable." In the more than three years which have elapsed between the original formulation of the model and this writing, the kinetics of the process have had an opportunity to catch up to the timescale of the TA-FAB experiment. In this interval, approximately 250 ml of an apparently homogeneous, supersaturated solution of aqueous fructose (used for viscosity measurements) gradually divided itself into two distinct phases. All surfaces of the beaker which contacted this solution are now heavily laden with fructose crystals which surround the predominantly aqueous portion of the sample. This observation is offered as additional evidence to support the relevance of processes such as zone refining in determining the behavior of concentrated saccharide solutions.

b. Implementation of TA-FAB on the JEOL

Upon receiving a new JEOL HX-110 mass spectrometer at the MSU Mass Spectrometry Facility (by way of the largest DOE grant ever awarded to a university for the purchase of instrumentation), it became desirable to modify this instrument to accomodate TA-FAB. The HX-110 has been described in the Experimental Section of Chapter 2 (p. 97). Figure 3.9 is helpful in understanding the implementation of TA-FAB on this instrument. The upper portion of Figure

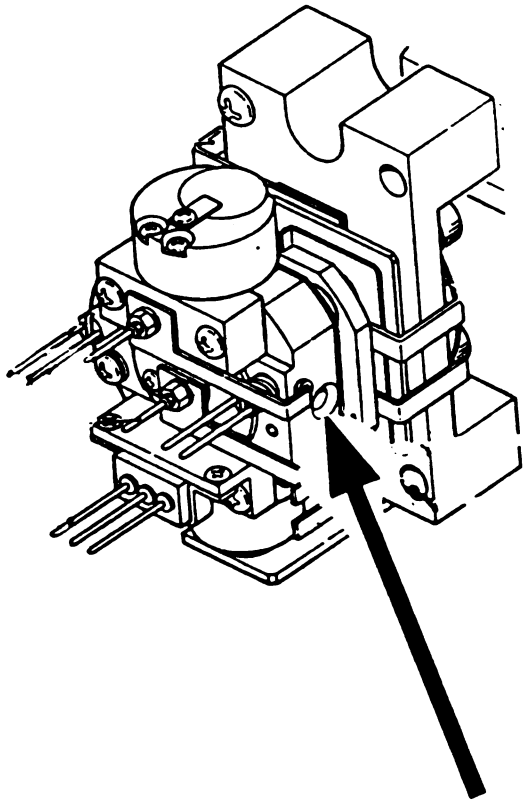

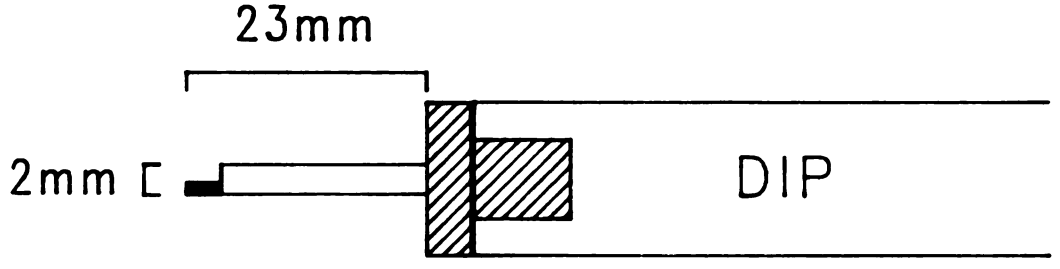

Figure 3.9. Representation of the JEOL HX-110 ion source (upper) and the direct insertion probe as it was modified for TA-FAB (lower). The arrow indicates the opening through which the probe tip is inserted.

3.9 contains a representation of the JEOL source. Because this source accomodates a variety of different ionization modes (including chemical ionization), it is constructed in a relatively tight and contained manner. Due to the closed nature of the source and the small diameter opening through which the direct probe is inserted (indicated by the arrow), design options for the TA-FAB probe were somewhat constrained. A straightforward and effective solution to the design problem is depicted in the lower portion of the figure, however, which shows a representation of the heated direct insertion (solids) probe (DIP) supplied with the HX-110. A special copper piece (indicated by the hatched marks) was machined to fit on the end of the probe. The base of the copper piece is surrounded by the heating coils of the DIP (which are not shown in the figure). A stainless steel rod is inserted into the copper receptor, and held in place with a set screw. The end of the rod was leveled to allow a pedestal for sample deposition (indicated by the darkened area). Application of heat to the sample is therefore accomplished by thermal conduction from the heating coils to the tip of the metal rod. An element of this design not represented in the figure is a teflon sleeve which fits over the stainless steel probe tip to prevent the repeller potential (maintained on the probe tip) from shorting to the acceleration potential (maintained on the source block).

Results obtained with the described apparatus compared favorably with those provided by the CH5. For ease of comparison, the fructose thermograms displayed in Figure 3.2 are reproduced in Figure 3.10, along with fructose thermograms collected from a similar sample subjected to TA-FAB on the JEOL. The larger ion currents produced on the JEOL allowed faster scanning rates than were possible on the CH5. Faster scanning, in turn, provided better resolution of the mass thermograms. The more precise data obtained from the JEOL (lower thermograms in Figure 3.10) validate the claim made earlier, which was based on

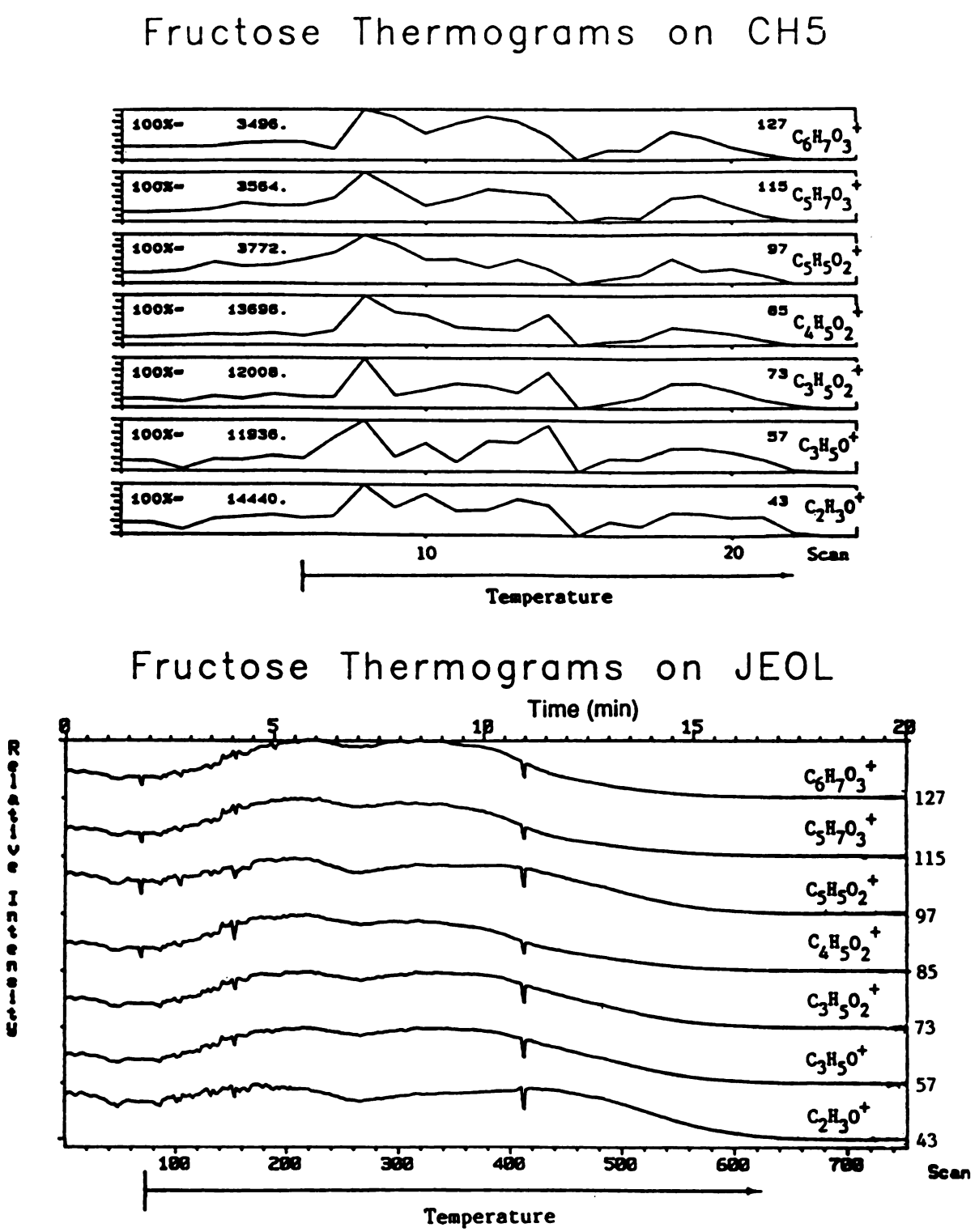

Figure 3.10. TA-FAB data from 2 ug of alanyl-leucyl-glycine mixed with aqueous fructose. The upper fructose thermograms were obtained from the CH5, and the lower fructose thermograms from the JEOL.

data from the CH5 (such as that shown in the upper thermograms of Figure 3.10), that the matrix thermograms tend to track one another as a function of temperature. Each scan represented in the CH5 thermograms was completed in approximately 25 seconds; the individual JEOL scans were acquired in less than 2 seconds. This comparison is also shown for the analyte (alanyl-leucyl-glycine) thermograms in Figure 3.11. The upper thermograms were obtained from the CH5, and the lower data were provided by the JEOL. Again, the JEOL data confirm an observation originally made from CH5 results: that the analyte thermograms tend to track one another as a function of temperature. An expected consequence of the highly resolved desorption profiles obtained from the JEOL would be the opportunity for a valid background subtraction. Figure 3.12 shows the very clean ALG spectrum resulting from such a background subtraction (analyte signals are labeled with an "A"). Data such as those represented in Figures 3.10-3.12 were interpreted as evidence that TA-FAB had successfully been implemented on the JEOL. Attention was then directed toward further optimization and wider application of the experiment on the new, high performance mass spectrometer.

The 2-second scanning period described in this section proved inconvenient for the long term, because the resulting data files occupied an inordinately large amount of computer space. The acquisition of several files of this size in a single session on the mass spectrometer (for a comparative study) was impractical. Therefore, scanning times from 7 to 14 seconds were generally employed for the following experiments. This compromise significantly reduced the size of the data files, while providing more precision in the thermograms than was available from experiments on the CH5 (using 25-second scans).

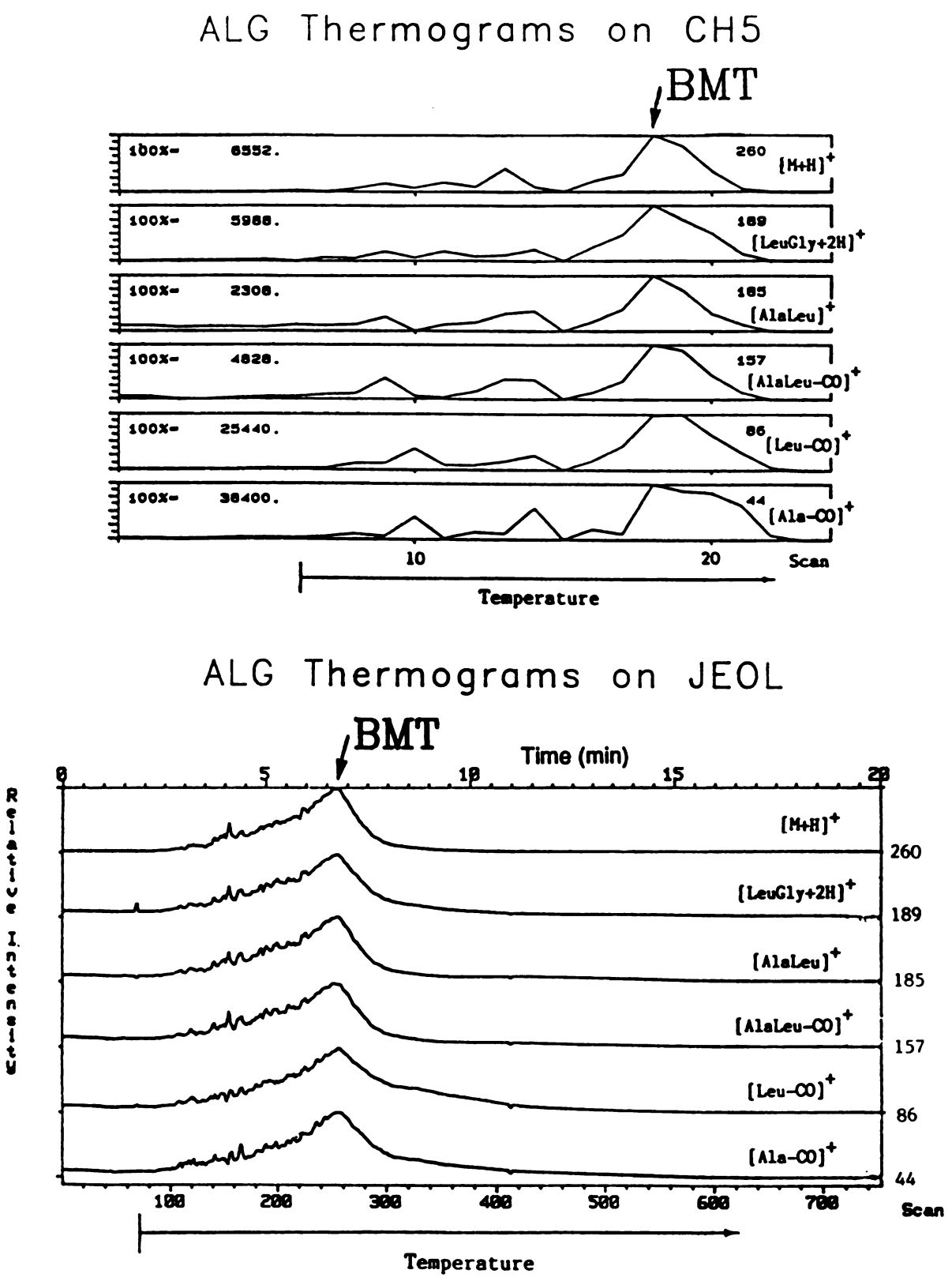

Figure 3.11. TA-FAB data from 2 ug of alanyl-leucyl-glycine mixed with aqueous fructose. The upper ALG thermograms were obtained from the CH5, and the lower ALG thermograms from the JEOL.

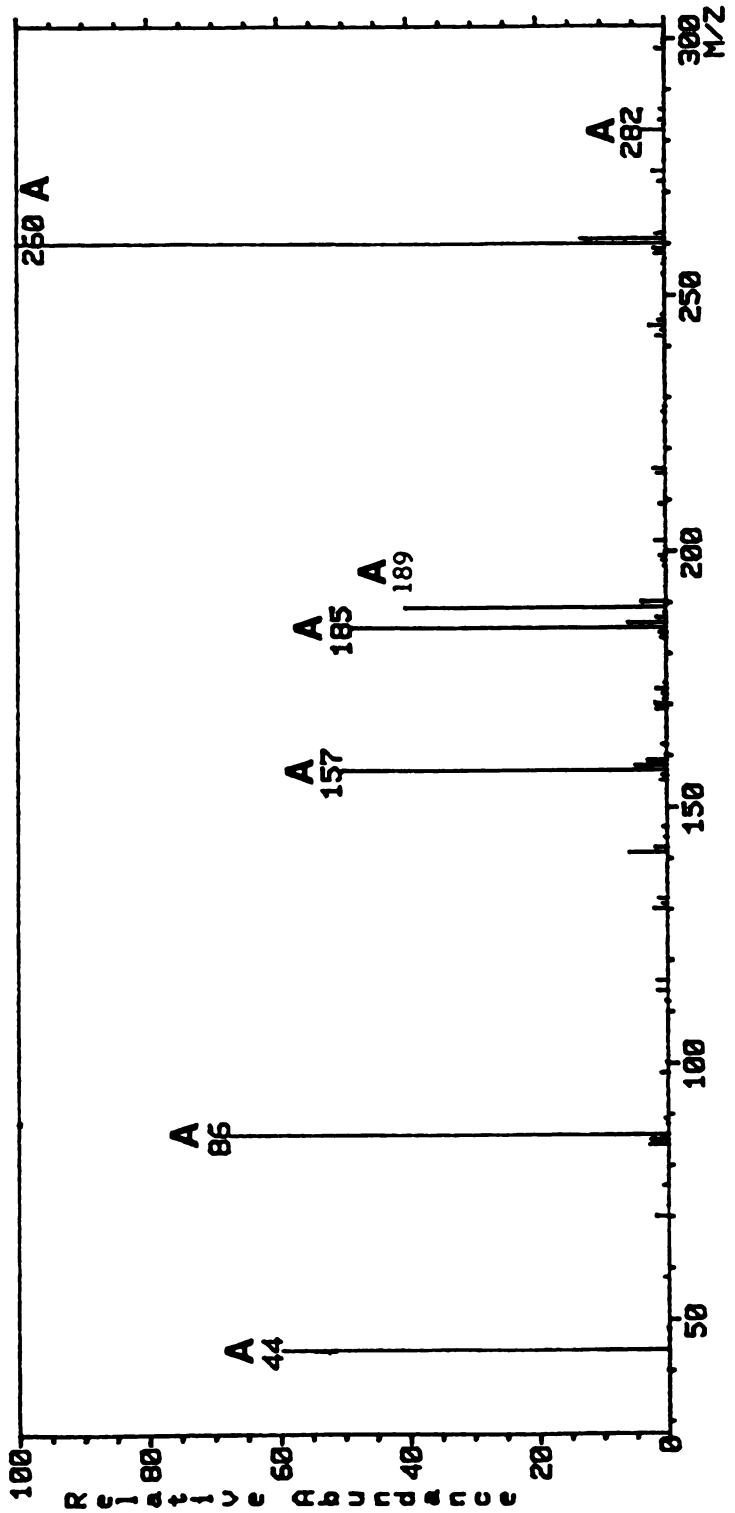

Figure 3.12. Background subtracted spectrum of alanyl-leucyl-glycine (from a sample composed of 2 ug of ALG mixed with aqueous fructose) obtained from a TA-FAB experiment on the JEOL. Analyte signals are labeled with an "A".

c. Optimization of Fructose Composition

An issue which had not been evaluated on the CH5 was the effect of saccharide sample quantity upon the experimental results. To address this question, 1.0 ul aliquots of aqueous solutions containing 1% (w/w), 10%, 20%, 30%, 40%, 50%, 60%, and 70% fructose were mixed with a constant amount of analyte and subjected to analysis by TA-FAB. The amounts of saccharide deposited in these aliquots were 0.01 mg, 0.10 mg, 0.22 mg, 0.34 mg, 0.47 mg, 0.62 mg, 0.77 mg, and 0.94 mg, respectively. The analytes used for these studies were the peptides alanyl-leucyl-glycine and vasotocin (Gly-Arg-Pro-Cys-Asn-Gln-Ile-Tyr-Cys), which were both deposited from aqueous solutions. Figure 3.13 shows the BMT spectrum for an aqueous sample containing 0.62 mg of fructose (deposited as 1.0 ul of a 50% solution) and the BMT spectrum for an aqueous sample containing 0.10 mg of fructose (deposited as 1.0 ul of a 10% solution). Analyte (alanyl-leucyl-glycine) signals are marked with an "A" and fructose signals are marked with a "B". The important point to notice in Figure 3.13 is the enhanced analyte signal with respect to matrix background observed in the BMT spectrum of the sample containing less fructose (lower spectrum). The enhancement was correlated to the absolute amount of fructose present in the sample, and not the concentration of the solution from which the fructose was deposited. This effect (which was observed independently in the studies involving alanyl-leucyl-glycine and the studies involving vasotocin) is believed to result from two complementary factors. As the amount of fructose in the sample declines (from 0.94 mg to 0.10 mg) a pronounced decrease in fructose ion abundance is observed. At the same time, a more subtle increase in analyte ion abundance also appears to manifest itself (the latter effect is less clear; probably due to the inability of the 10-13 second mass spectral scans to capture the true

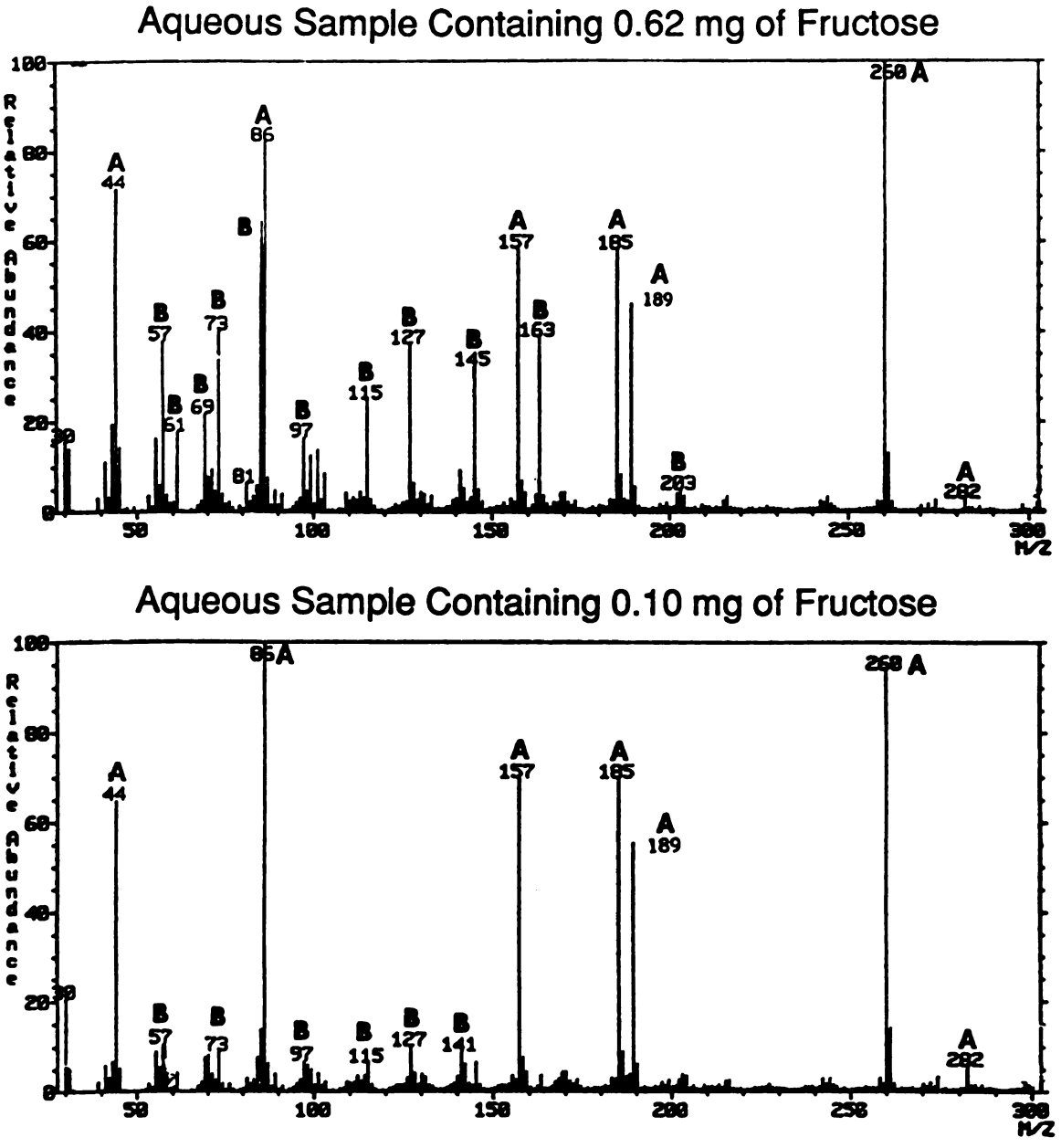

Figure 3.13. BMT spectra in the TA-FAB analyses of 2 ug of alanyl-leucyl-glycine mixed with aqueous solutions containing 0.62 mg (upper spectrum) and 0.10 mg (lower spectrum) of fructose. Analyte signals are marked with an "A" and fructose signals are marked with a "B".

maxima of the analyte desorption profiles). All samples displayed differential desorption as a function of temperature; therefore, background subtraction was possible in each case, resulting in indistinguishable spectra characteristic of the analyte. An implication of the effect displayed in Figure 3.13, in terms of the ternary perculation model, is that the surface concentration of the analyte hypothesized to occur during stage 2 of the experiment is more facile when less fructose is present through which the analyte must migrate.

d. Optimization of Heating Parameters

The different heating configurations utilized on the CH5 and the JEOL provided different advantages and disadvantages for the TA-FAB experiment. The disadvantages associated with resistively heating the sample on the tungsten/rhenium emitter included substantially reduced secondary ion currents for TA-FAB than were observed for conventional FAB analyses (utilizing the standard FAB probe tip) conducted on the same instrument. On the JEOL, secondary ion currents obtained during TA-FAB were much more representative (in terms of magnitude) of those obtained from the conventional FAB experiment. Defocusing of secondary ion signals as the current through the emitter increased also was a relatively common problem experienced on the CH5. Possible warping of the emitter during the course of the current program was speculated to be the source of this defocusing. TA-FAB analyses accomplished on the JEOL did not suffer from this sort of behavior. The particular advantage associated with resistively heating the sample on the tungsten/rhenium emitter was the ability to manipulate the temperature of this surface very precisely. Unfortunately, relying on thermal conduction through 23 mm of metal rod to heat

the sample (as is necessary with the JEOL heating assembly) results in much less precise temperature manipulation of the sample stage.

The less precise temperature control experienced on the JEOL was not regarded as prohibitive, due to the favorable results obtained on this instrument in comparison to those observed from the CH5 (see Figures 3.10-3.12). A distinct lag in temperature, however, was always expected between the reading of the DIP thermocouple (indicative of the temperature adjacent to the heating coils) and the actual temperature at the end of the probe tip. A typical TA-FAB heating program on the JEOL begins with the acquisition of several scans without the introduction of heat, followed by a relatively rapid temperature surge (accomplished by setting the initial temperature value somewhere between 120°C and 180°C on the DIP control panel). Once the thermocouple reading reflected the establishment of this initial temperature near the heating coils, a temperature ramp of 8°C/minute would be initiated. It should be emphasized that the actual temperature at the end of the TA-FAB probe tip would be expected to lag behind that indicated by the thermocouple (which was read on the control panel). As input, this heating program was very similar to that used on the CH5. With both heating configurations, an initial temperature surge was required to stimulate strong desorption ionization of the analyte. Initiating the slow ramp immediately (without the temperature surge) resulted in less distinct differentiation of analyte and matrix desorption profiles. Once the initial temperature surge was established, however, additional manipulation of the temperature program produced little effect on the spectral results. For instance, in one comparative study, temperature ramps of 8, 16, 32, 64, 128, and 256 °C/minute were employed after an initial temperature surge to approximately 180°C. The resulting data showed that the BMT was established progressively earlier in the run in response to the more rapid temperature scans. The profile

shapes and ion abundances, however, were not significantly altered by these variations in temperature program.

e. Evidence of Fructose Polymerization

Monosaccharides are known to undergo polycondensation reactions while in the molten state at temperatures below 220°C (13). Figure 3.14 may be interpreted as evidence of such a process occurring as secondary ion currents diminish during stage 3 of the TA-FAB experiment. The sample analyzed was an aqueous solution containing 0.31 mg of fructose. The two lowermost thermograms in Figure 3.14 correspond to prominent fructose background ions. As the temperature is increased to the point where these ion abundances become strongly reduced (signaling the conclusion of a normal TA-FAB analysis), the detection of a new sequence of ions becomes evident (upper thermograms). The new sequence of signals (at m/z 365, 527, and 689) appear to progressively maximize in order of increasing mass. These signals are not very intense (less than 10% of the base peak), but they are believed to represent the natriated condensation products [2fructose-H_2O+Na]$^+$ (m/z 365), [3fructose-$2H_2O$+Na]$^+$ (m/z 527), and [4fructose-$3H_2O$+Na]$^+$ (m/z 689). The relative intensities of these peaks in scan 179 of the same analysis are shown in Figure 3.15. Such polymerization may explain the irreversible matrix damage which has been described to occur in stage 3 of the experiment.

f. Analysis of Higher Mass Compounds

Once TA-FAB was implemented on the JEOL, it became desirable to characterize the performance of this technique in the analysis of higher mass

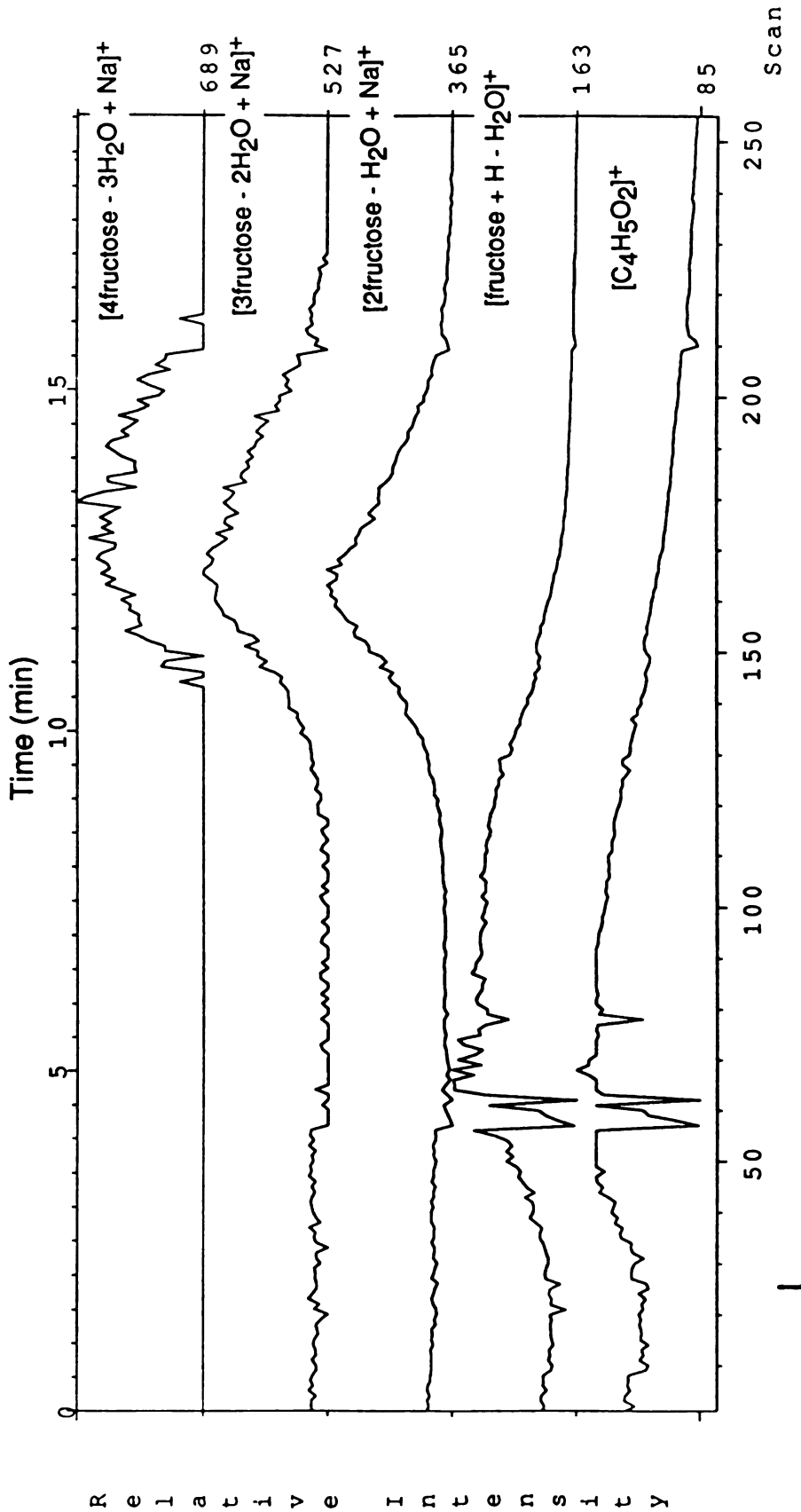

Figure 3.14. Mass thermograms obtained from an aqueous sample containing 0.31 mg of fructose.

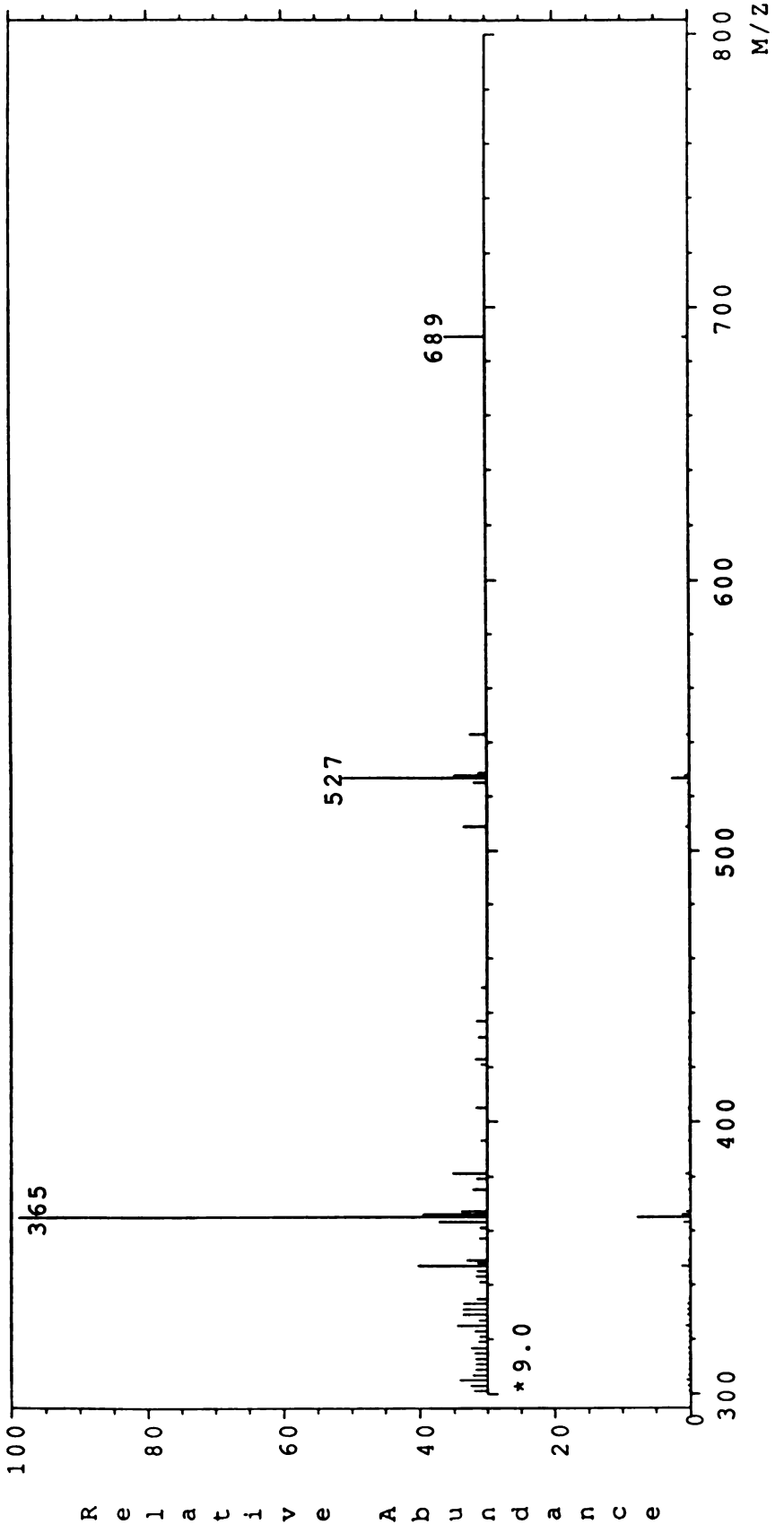

Figure 3.15. Part of scan 179 from the TA-FAB analysis represented in Figure 3.14.

compounds. This is an important issue in the development of any desorption ionization method, where the emphasis naturally lies in the mastery of progressively larger and less volatile compounds than have been addressed previously by mass spectrometry. In the case of TA-FAB, the question of potential advantages for high mass analysis was not a trivial one. As already described, a major advantage inherent to differential desorption of analyte versus matrix is the ability to contend with the undesirable matrix interference. At higher mass (especially above 700 u), the problem of matrix interference becomes less severe (as evidenced in the glycerol mass spectrum shown in Figure 1.3). Therefore, it was hoped that TA-FAB might offer alternative advantages in the analysis of such compounds. The potential to increase fragmentation (as had been documented for smaller, cyclic peptides (2)) with respect to the conventional FAB experiment was one possibility. Increased high mass fragmentation of peptides would be viewed as particularly significant in the mass spectrometry community. The mass range of the CH5 (c.a., 900 u) did not allow a valid investigation of this issue. The JEOL HX-110 (with a mass range of 14,000 u at full acceleration potential), however, was designed to facilitate high mass ion detection. Thus, this instrument was an excellent tool for determining the extent to which TA-FAB could provide advantages for high mass analysis.

Figure 3.16 displays bradykinin mass thermograms obtained during a TA-FAB analysis of 4 nmol of the nonapeptide dispersed in an aqueous solution containing 0.16 mg of fructose. These data are distinctly different from any TA-FAB results discussed thus far, because the analyte desorption profiles do not all track one another as a function of temperature. The mass thermogram corresponding to the $[M+H]^+$ ion (at m/z 1060) is indicative of the desorption behavior expected for the analyte, which has been associated with the removal of water from the sample. Analyte signals which display this behavior include those

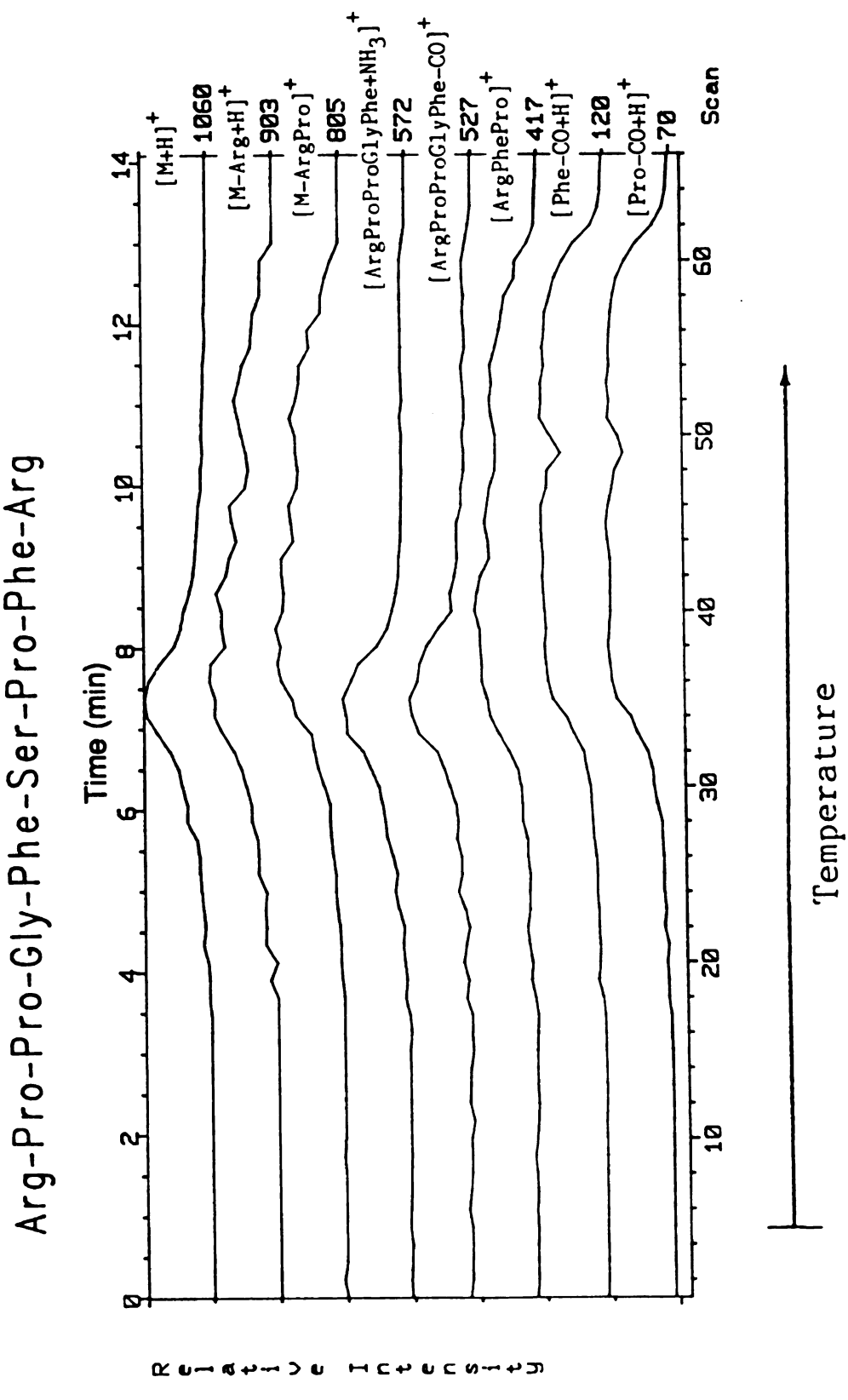

Figure 3.16. Bradykinin thermograms obtained from an aqueous sample containing 4 nmol of the nonapeptide and 0.16 mg of fructose.

at m/z 527 and m/z 572. Other ions, however, (particularly the very stable, low mass immonium ions at m/z 70 and 120) are measured in large abundance well after the time interval associated with desorption ionization involving water removal from the sample. This later period of comparatively harsh desorption ionization (i.e., from scan 45-60) is probably supported solely by fructose which has melted into the liquid state.

The mass spectrum corresponding to maximum abundance of the $[M+H]^+$ ion is shown in Figure 3.17. The important characteristic of this spectrum is the low relative abundance of the $[M+H]^+$ ion (m/z 1060) with respect to the fragment at m/z 70. Such an observation represents extreme fragmentation in comparison to that noticed in a conventional FAB experiment (where the $[M+H]^+$ signal is often the most intense signal associated with bradykinin). As previously suggested, the increased fragmentation, in itself, is not an undesirable result; however, having it channeled predominantly into the formation of extremely low mass ions is undesirable. The mass spectrum measured at a later time during the run is shown in Figure 3.18. The lower spectrum reveals fragmentation that has further increased in comparison to that displayed in Figure 3.17. An expansion of the low mass portion of this spectrum is shown in the upper part of Figure 3.18. The expansion reveals that four peaks dominate the mass spectrum (at m/z 70, 87, 112, and 120). The four ions corresponding to these signals are indicative of individual amino acids which make up the peptide chain, and are therefore associated with relatively catostrophic fragmentation. An important consequence of the extreme fragmentation represented in Figures 3.17 and 3.18 (as has been documented in quantitative comparisons) is the detection of significantly lower high mass ion abundances than those commonly observed in the conventional FAB experiment (using a glycerol matrix). The outlook becomes even less favorable after considering that the FAB/TA-FAB comparison was

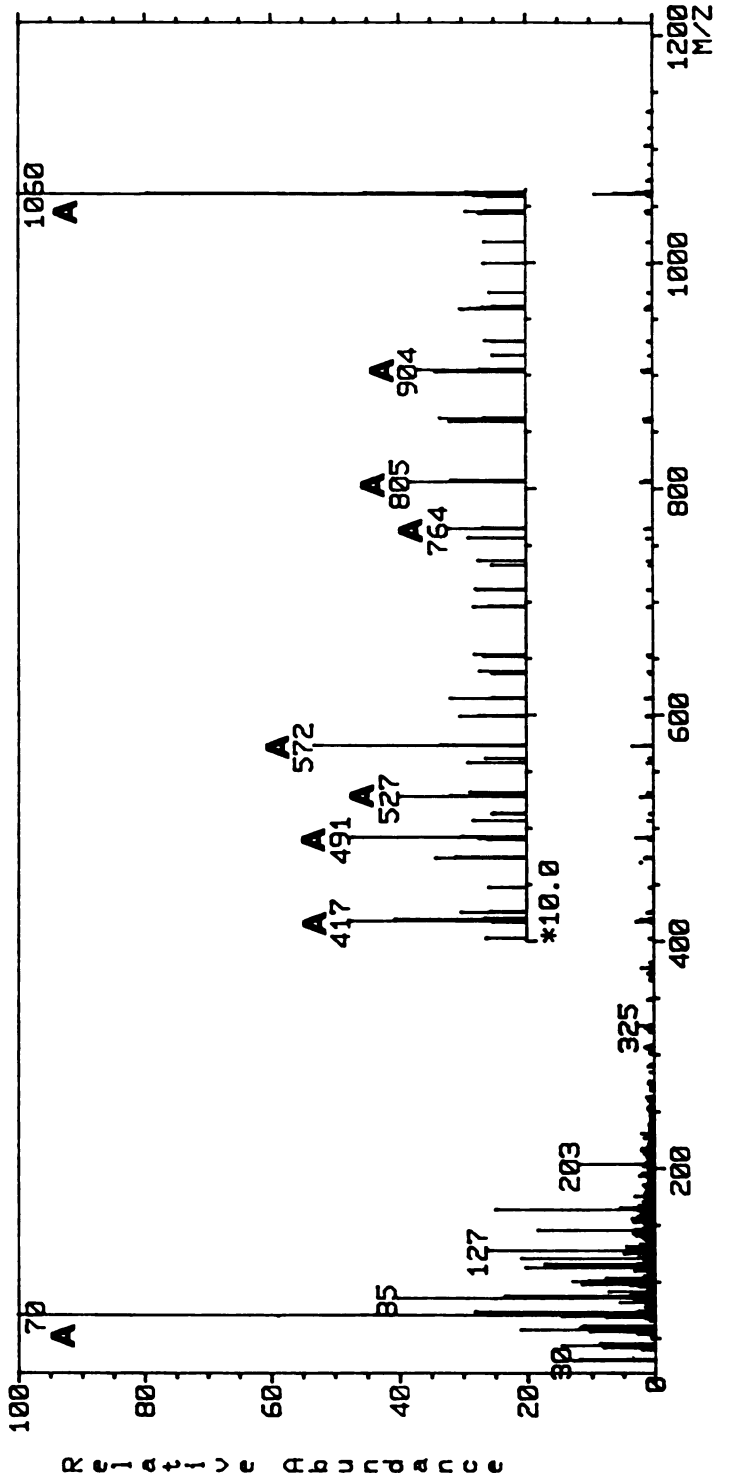

Figure 3.17. Spectrum containing the maximum $[M+H]^+$ signal from the TA-FAB analysis represented in Figure 3.16.

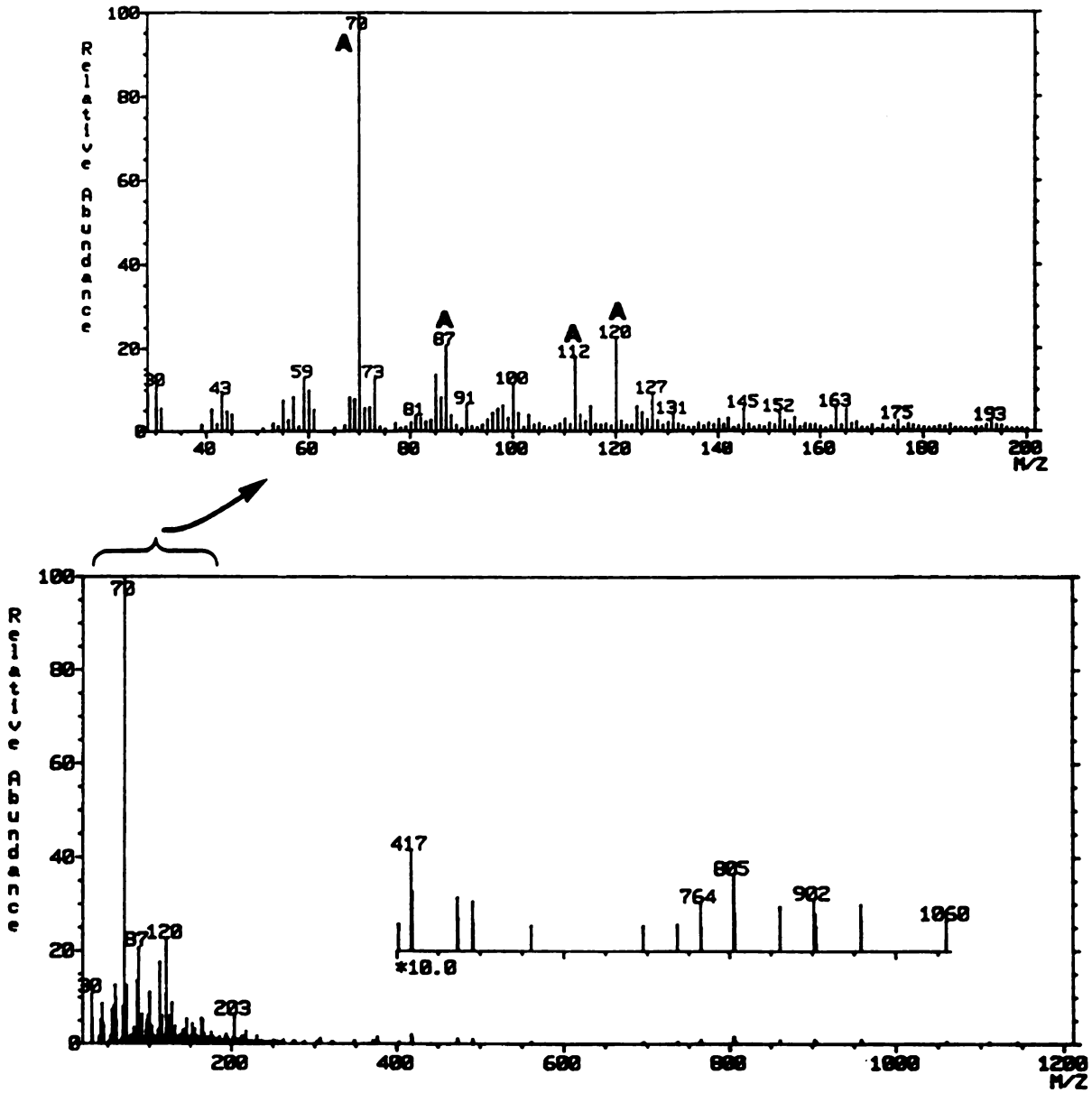

Figure 3.18. (lower) Spectrum obtained during the final stages of the TA-FAB run represented in Figure 3.16. An expansion of the low mass region of this spectrum is shown in the upper portion of the figure.

conducted prior to the work involving optimization of the matrix to analyte ratio in FAB (described in Chapter 2). Therefore, the high mass analyte ion abundances observed during TA-FAB were not comparable to those measured from a nonoptimal (in terms of maximizing analyte signal) FAB sample.

Unfortunately, the observation of extreme fragmentation and reduced high mass analyte ion abundances by TA-FAB (in comparison to conventional FAB analyses) was persistent for a variety of different compounds whose molecular weights exceeded 900 u. These compounds included the peptides [Val^4]-angiotensin III, bradykinin, VHLTPVEK, fibrinogen related peptide, and vasotocin. Three mannosidosis heptasaccharides (provided by Dr. C. C. Sweeley) also were evaluated, along with two oligonucleotides (provided by Dr. J. A. Smith). TA-FAB matrices which were utilized in these comparisons included aqueous solutions of fructose, glucose, sucrose, and tartaric acid. In no instance was the quality of TA-FAB results superior to those obtained by conventional FAB with glycerol. Therefore, rather than offering advantages for high mass analysis, TA-FAB was hampered by a severe limitation.

In retrospect, the favored formation of immonium ions from peptides by TA-FAB should not have been unexpected. This trend was actually apparent in data obtained from the CH5. Figure 3.3 shows TA-FAB results for the tripeptide alanyl-leucyl-glycine (b and c) in comparison to FAB results for the same compound (a). The TA-FAB spectra show significantly reduced relative abundances of the $[M+H]^+$ ion (m/z 260) to immonium ions (m/z 44 and 86) than are evident in the FAB spectrum. Likewise, in the FAB/TA-FAB comparison for the HC-toxins (2), the documented increase in fragmentation is primarily expressed in the formation of immonium ions as opposed to sequence specific ions. A preliminary high mass study was conducted on the CH5 by B. L. Ackermann and J. T. Stults, which involved the TA-FAB analysis of several

peptides within the mass range of 800-900 u (14). The spectra obtained were dominated by signals corresponding to immonium-type ions. Instead of augmenting this deleterious effect, implementation of TA-FAB on the JEOL probably alleviated it to some extent. This statement is supported by the less extensive fragmentation associated with the analysis of alanyl-leucyl-glycine on the JEOL (Figure 3.12) than observed for analyses of the same compound conducted on the CH5 (Figure 3.3, b and c). Reasons for the seemingly less extensive fragmentation on the JEOL probably include improved high mass detection, as well as a lower operating source pressure ($1\text{-}8\times10^{-6}$ torr) in comparison to that characteristic of the CH5 (1×10^{-5} torr).

g. Negative Ion TA-FAB

The performance of TA-FAB in the negative ion mode was evaluated for samples containing the delta sleep inducing peptide (Trp-Ala-Gly-Gly-Asp-Ala-Ser-Gly-Glu, which has a molecular weight of 848 u) and samples containing a mixture of three isomeric mannosidosis heptasaccharides (provided by Dr. C. C. Sweeley, which have a molecular weight of 1193 u) (15). Figure 3.19 shows a fructose background spectrum obtained in the negative ion mode. This spectrum was recorded before the application of heat (and hence, before desorption of the analyte) to an aqueous sample containing 4 ug of the delta sleep inducing peptide and 0.62 mg of fructose. As previously observed in the positive ion mode (Figure 3.1), the fructose fragments extensively under fast atom bombardment and shows a minimal tendency to form clusters. The negative ion spectrum contrasts that obtained in the positive ion mode, however, with respect to a relatively abundant signal which is indicative of the molecular weight of the saccharide ($[M\text{-}H]^-$). No $[M+H]^+$ signal was apparent in the positive ion spectrum

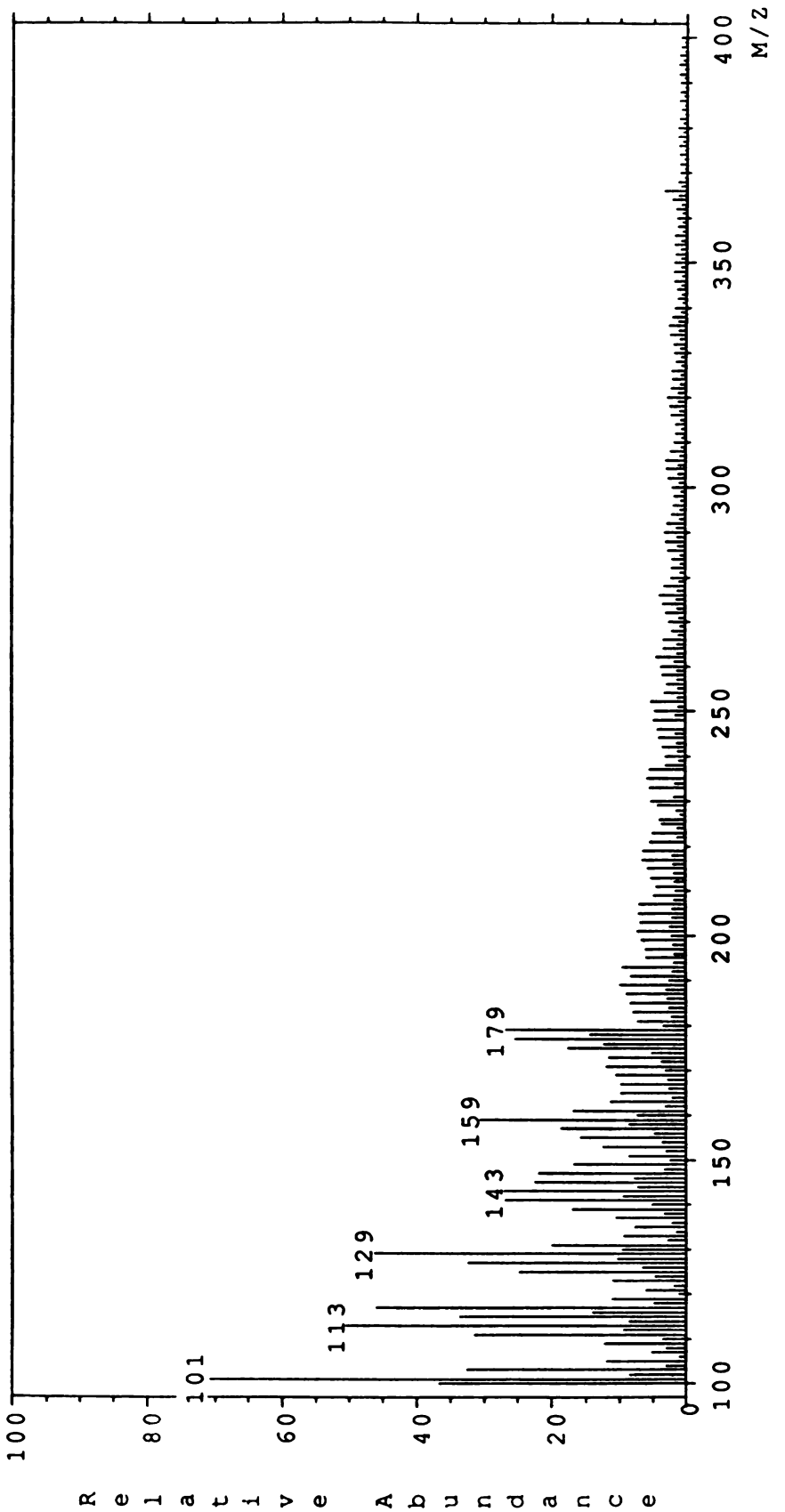

Figure 3.19. TA-FAB background spectrum measured in the negative ion mode. This was the first scan obtained from an aqueous sample containing 4 ug of the delta sleep inducing peptide and 0.62 mg of fructose.

(Figure 3.1); only peaks corresponding to dehydration from the protonated molecule (e.g., m/z 163 and 145), along with the $[M+Na]^+$ ion. Figure 3.20 displays a series of mass thermograms characterizing the TA-FAB analysis from which the spectrum in Figure 3.19 was abstracted. The lower three thermograms correspond to abundant fructose fragment ions which are evident in Figure 3.19. These thermograms, as expected, tend to track one another as a function of temperature. The upper three thermograms in Figure 3.20 correspond to ions derived from the peptide. As expected, these thermograms document a significant response from the analyte to the applied temperature, and also track one another. The noteworthy phenomenon apparent in Figure 3.20 involves the behavior of the signal at m/z 179. This matrix signal (corresponding to $[fructose-H]^-$) clearly tracks the analyte thermograms as a function of temperature. Not only does this matrix signal track the analyte signals, but it constitutes the base peak in the BMT spectrum. These observations (which were reproducible in all negative ion analyses) represent a departure from the characteristics of the TA-FAB experiment in the positive ion mode.

The unique behavior of the m/z 179 ion is not necessarily in conflict with the ternary perculation model. Rather, the correlation of this signal with those derived from the analyte may be interpreted as evidence for the partitioning of analyte to the surface of the sample in stage 2 of the experiment. As described in Chapter 1 (p. 44), the highly energized environment associated with fast atom bombardment is conducive to an abundance of interactions, certainly resulting in the formation of both positive and negative ions from analyte and matrix. The relative tendencies for the formation of these ions will govern their sensitivity in the two operating modes. The most favorable interaction in the present system is the transfer of a proton from the relatively acidic saccharide matrix to the relatively basic analyte (both the peptide, and the heptasaccharides which

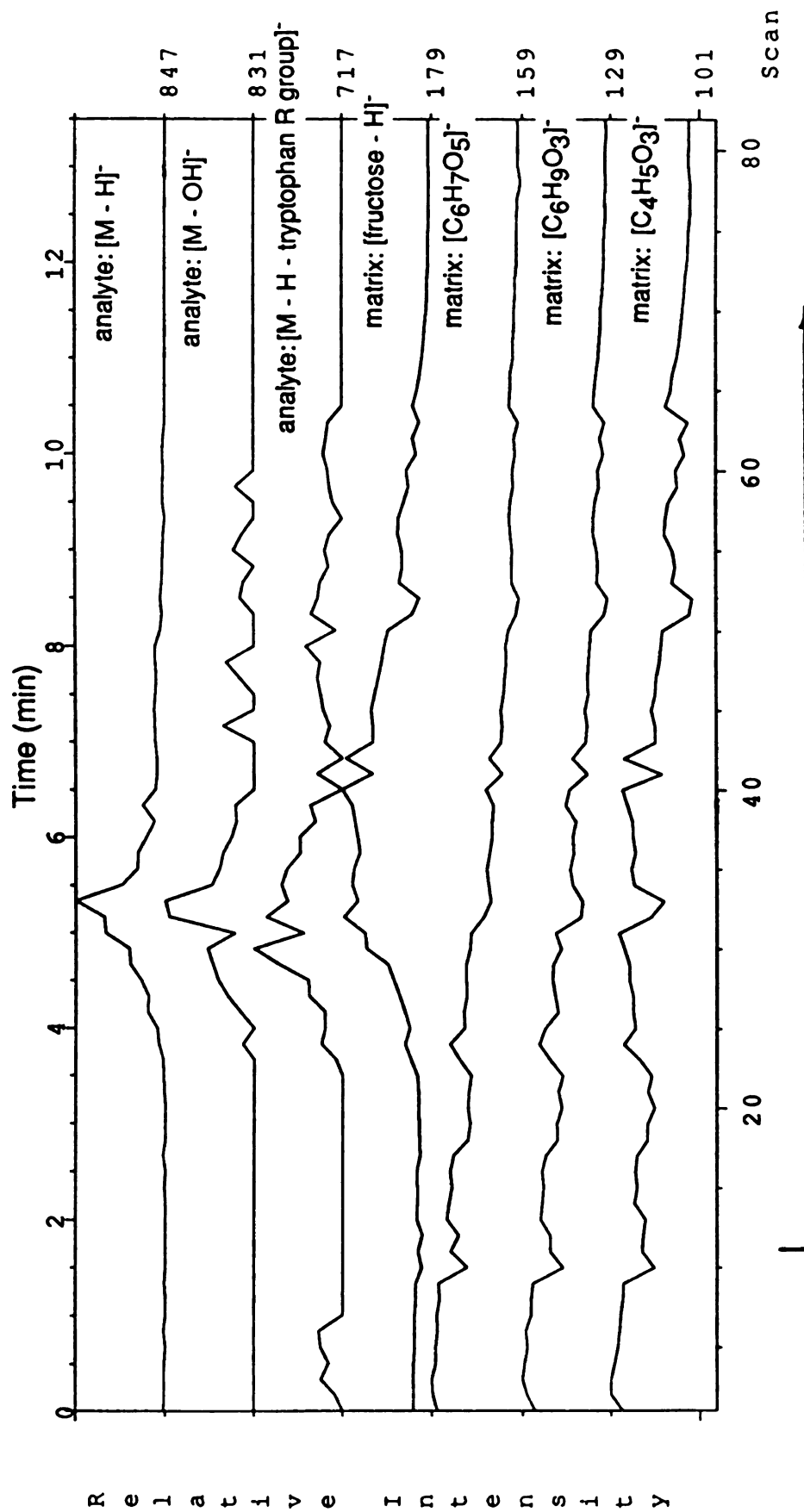

Figure 3.20. Mass thermograms from a negative ion TA-FAB analysis of an aqueous sample containing 4 ug of the delta sleep inducing peptide and 0.62 mg of fructose. The lower 4 thermograms correspond to matrix ions and the upper 3 thermograms correspond to analyte ions.

contain an N-acetyl group). Such an interaction results in the formation of an analyte ion observable in the positive ion mode, and a matrix ion (m/z 179) observable in the negative ion mode. The enhancement of these two signals in stage 2 (the BMT region) of the experiment suggests an increase in the measured rate of this reaction. At this point, it should be remembered that FAB efficiently measures only those interactions involving species present near the surface of the sample. An excellent means for increasing the rate of a reaction occurring near the sample surface would be to concentrate the reactants in the proximity of the surface. Another way of describing this distribution of sample components is in terms of surface population by the analyte (which is suggested in the ternary perculation model). Therefore, an extraction of analyte to the surface of the sample should logically result in an increased yield of the proton transfer reaction products ($[M+H]^+$ from the analyte, and $[fructose-H]^-$ from the matrix) regardless of whether the reaction occurs in the gas or condensed phase. This interpretation is supported by the fact that all analyte ion signals are enhanced within the same time frame; this is an expected consequence of extraction to the surface. Only the abundance of the matrix species which participates in the proton transfer reaction is similarly stimulated, however. Those fructose ions which were not involved in the reaction continue to track one another in a manner distinct from that of the analyte.

Theoretical considerations aside, the negative ion performance of TA-FAB for these analytes was inferior to that of conventional FAB. The behavior of the $[fructose-H]^-$ ion also prevented any possibility of a legitimate background subtraction. For these reasons, TA-FAB in the negative ion mode was not pursued further.

At this juncture, a decision involving the direction of the TA-FAB project became necessary. The original intent of the author was to more rigorously test and refine the ternary perculation model. Evaluation of the higher mass results (which have been described), however, indicated a need to further develop the experiment in an effort to improve its high mass performance. The latter direction was chosen; and therefore, this dissertation will contain no more discussion of the ternary perculation mechanism. Instead, improved high mass performance for the technique will be correlated to development of tertiary glycerol/fructose/water matrices. Before describing the behavior of these unique matrices, however, a simpler system will be considered: TA-FAB conducted with a glycerol matrix.

h. TA-FAB Using Glycerol Matrix

Figure 3.21 presents the results obtained from a TA-FAB analysis of 1.0 ul of an aqueous bradykinin solution (4 nmol/ul) added to 1 ul of glycerol. The lower three thermograms correspond to glycerol ions, and the upper five thermograms correspond to analyte ions. The beginning of this experiment (before heat is applied) represents a conventional FAB analysis in which the ratio of matrix to analyte has not been optimized. Quite interesting changes occur in the desorption ionization behavior of both analyte and matrix with the application of heat. As the sample temperature rises, the glycerol is gradually volatilized, and thus, removed from the probe tip. The volatilization process can be monitored by the substantial decline in glycerol ion abundances which occurs from scans 8-20. During the same 12 scans, all analyte ions experience a significant increase in abundance. Such behavior is not surprising considering the discussion in Chapter 2 of this dissertation. One would expect increased analyte ion

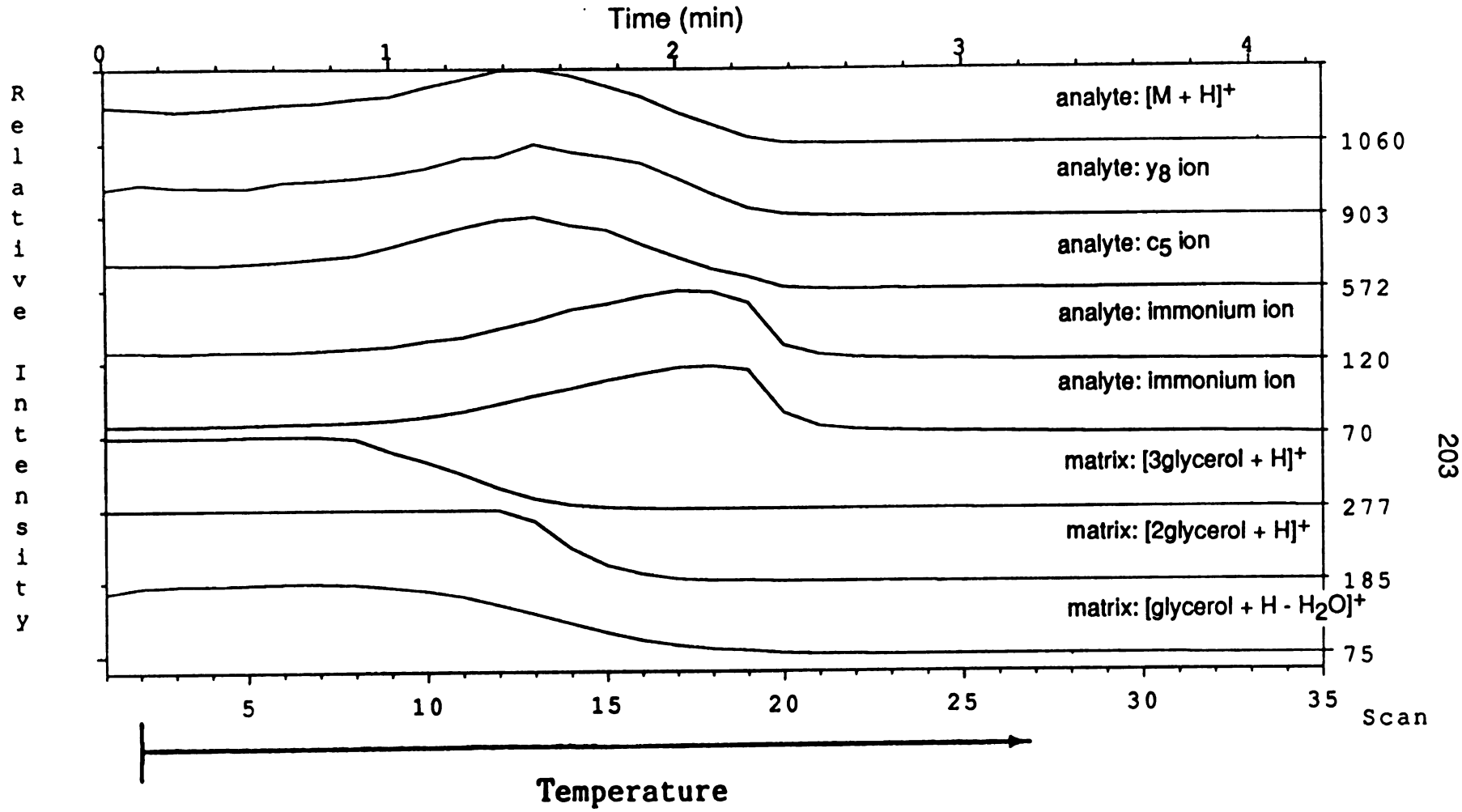

Figure 3.21. TA-FAB analysis of a sample containing 4 nmol of bradykinin mixed with 1 ul of glycerol. The lower three thermograms correspond to glycerol ions, and the upper five thermograms correspond to analyte ions.

abundances and decreased matrix ion abundances as the peptide becomes progressively concentrated into less glycerol. Therefore, this experiment constitutes a within-run optimization of the matrix to analyte ratio. Once the glycerol becomes too scarce to support desorption ionization, the analyte ion abundances rapidly fade. It is interesting to note that the immonium ions (m/z 70 and 120) become maximized in abundance in significantly smaller portions of glycerol than do the higher mass analyte ions (m/z 572, 903, and 1060). The identical observation was pointed out in Chapter 2 (p. 101), in the individual examination of different sample compositions (represented in Figure 2.2). The agreement between these two sets of data, which were collected from substantially different experiments, is very satisfying in terms of verifying the conclusions presented in Chapter 2.

Quite interestingly, analogous spectral enhancement has been reported over much longer time periods in conventional FAB analyses. Figure 3.22 documents matrix and analyte behavior for a sample containing arsenobetaine (see Figure 3.22 for the structure) mixed with glycerol. This study (16) monitored the ion abundance at m/z 185 ($[2glycerol+H]^+$) and m/z 179 ($[M+H]^+$ for the analyte) for a period in excess of 30 minutes. During this time interval, significant concentration of the analyte into the glycerol would be expected as the more volatile matrix is preferentially removed by the influence of the vacuum. This concentration effect is accompanied (as was shown in Chapter 2, and earlier in this section) by a complementary increase in analyte ion abundances and decrease in matrix ion abundances. The application of heat in the TA-FAB experiment (see Figure 3.21) reduces the time necessary for this transformation in sample composition from 30 minutes to approximately 3 minutes.

To further establish the capacity to optimize the matrix to analyte ratio through volatilization of glycerol, quantitative comparisons were conducted

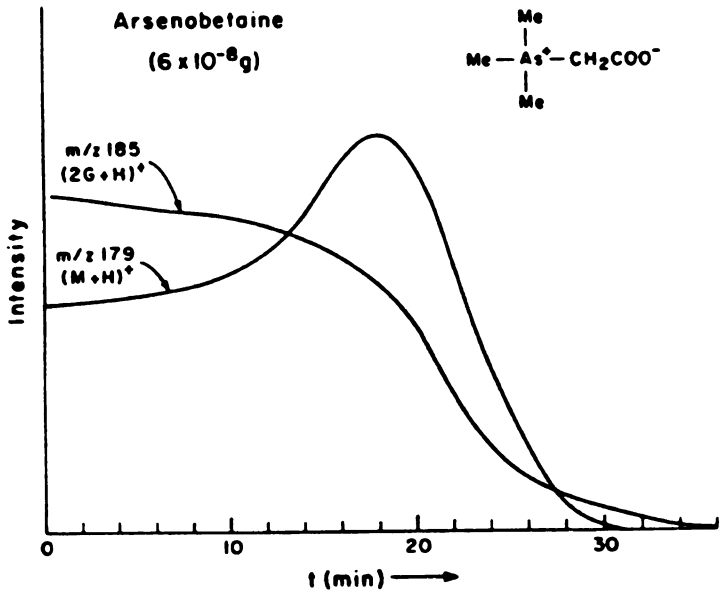

Figure 3.22. Mass chronograms representing a conventional FAB analysis of arsenobetaine dispersed in glycerol. The signal at m/z 185 corresponds to a prominent glycerol ion and that at m/z 179 corresponds to $[M+H]^+$ for the analyte. Reprinted from reference 16 with permission of Elsevier Science Publishers.

between the TA-FAB analysis of 4 nmol of bradykinin in 14 umol of glycerol, and conventional FAB analyses of 4 nmol of bradykinin from both 14 umol of glycerol and the optimal, 1.1 umol portion of glycerol. Figure 3.23 shows the results of this comparison for bradykinin ions of low, intermediate, and high mass. The first two points in each plot document the increase in ion abundance obtained by optimizing the matrix to analyte ratio in conventional FAB analyses. The second pair of points in each plot document the increase in ion abundance observed between the first scan of a TA-FAB experiment (before the application of heat) and a subsequent scan (which was most representative of the optimal FAB results). Each point represents the average of three separate analyses and the error bars correspond to the standard deviation of these data. In each case, the TA-FAB experiment simulates to some degree the increase in ion abundance obtained from optimization of the matrix to analyte ratio. The magnitude of the increase in analyte signal is not always as pronounced as that measured in the conventional FAB case (probably because the mass spectral scan speed (7.5 seconds/scan) was too slow to capture the true maxima of the analyte thermograms). Nevertheless, the trend toward the optimal sample reponse was clear for all analyte ions monitored (besides those included in Figure 3.23, analyte ions at m/z 70, 417, 527, 805, and 903 were evaluated).

The comparison is extended to the glycerol ion abundances in Figure 3.24. Again, the TA-FAB experiment simulates the results from optimization of the matrix to analyte ratio in the conventional FAB experiment: substantially decreased matrix ion abundances. This trend was apparent for all abundant glycerol ions which were monitored (besides those represented in Figure 3.24, this includes signals at m/z 93, 185, 369, and 553).

For the purpose of completeness, it should be noted that mass spectra obtained during the latter stages of TA-FAB runs are qualitatively

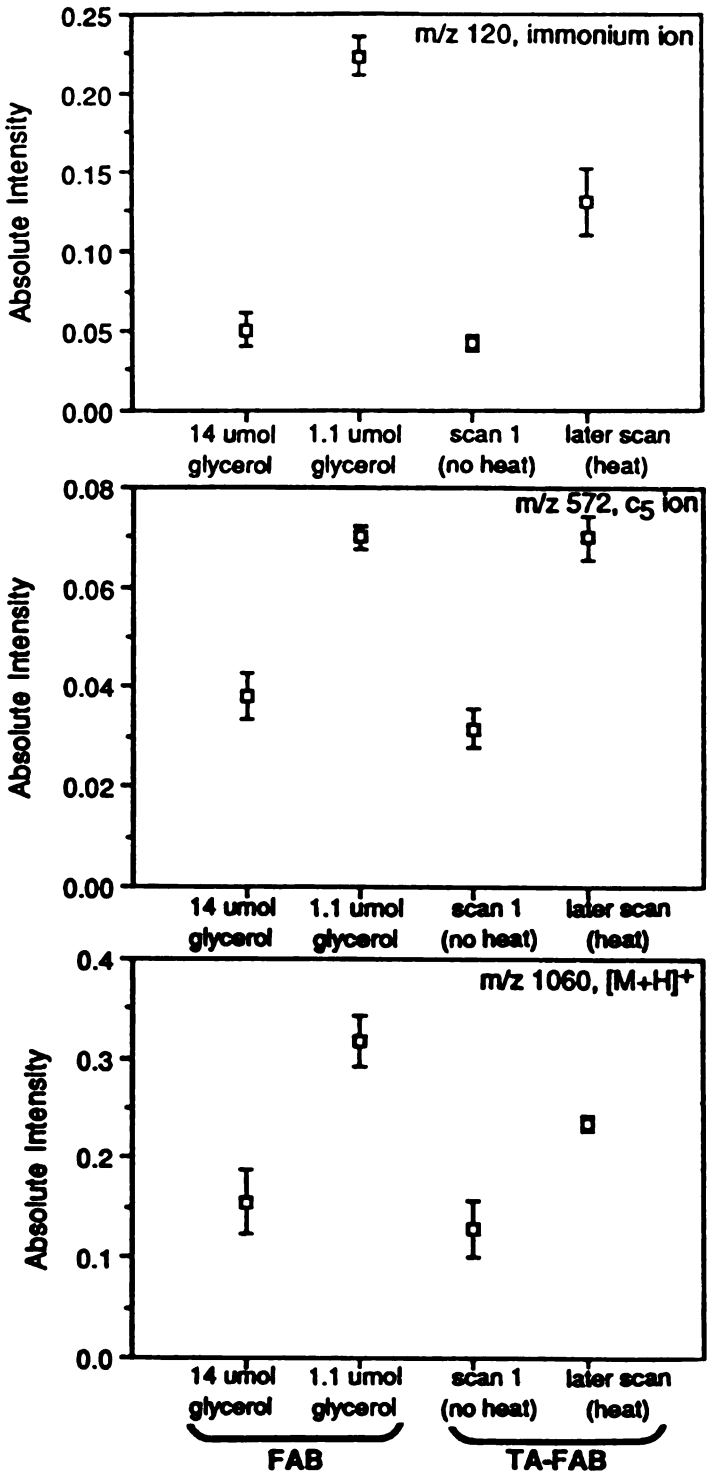

Figure 3.23. Comparison of the mass spectral enhancement obtained by optimizing the matrix to analyte ratio in conventional FAB (first two points) versus that obtained in a TA-FAB analysis using the glycerol matrix (final two points). Each sample contained 4 nmol of bradykinin. The nonoptimal FAB sample and the initial TA-FAB sample contained 14 umol of glycerol. The comparison is made for three bradykinin ions including m/z 120 (upper), m/z 572 (middle), and m/z 1060 (lower).

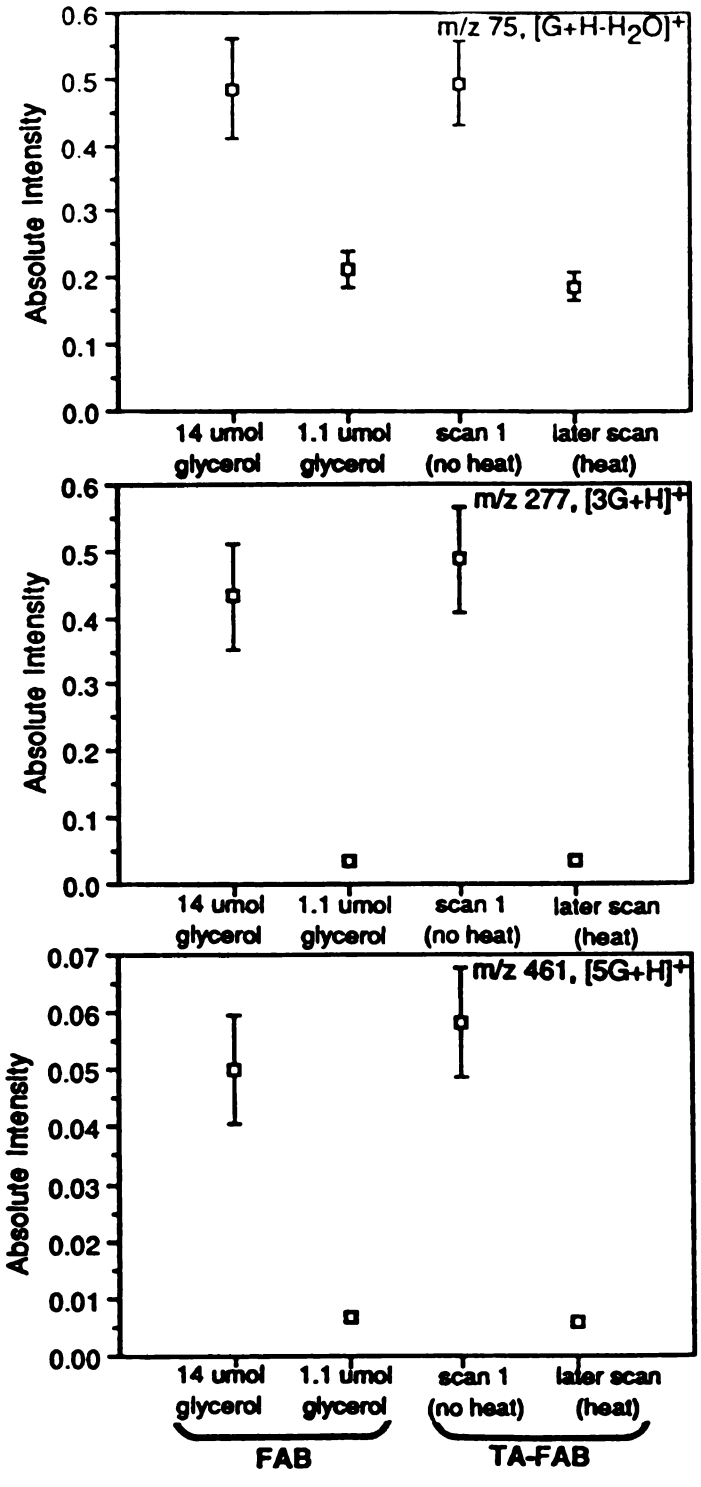

Figure 3.24. Comparison of the mass spectral enhancement obtained by optimizing the matrix to analyte ratio in conventional FAB (first two points) versus that obtained in a TA-FAB analysis using the glycerol matrix (final two points). Each sample contained 4 nmol of bradykinin. The nonoptimal FAB sample and the initial TA-FAB sample contained 14 umol of glycerol. The comparison is made for three glycerol ions including m/z 75 (upper), m/z 277 (middle), and m/z 461 (lower).

indistinguishable from those collected from the optimal sample composition in the conventional experiment. Therefore, all the data indicate the capacity to duplicate results obtained from the optimal matrix to analyte ratio by heating a sample which was initially characterized by a nonoptimal ratio of matrix to analyte.

The data described in the present section are significant in the context of this project. These data support the conclusions drawn in Chapter 2 by demonstrating an alternative and logical means of optimizing the matrix to analyte ratio in FAB-MS. This section also provides an important link between Chapter 2 and the remaining portion of Chapter 3, which will concentrate on understanding the behavior of tertiary TA-FAB matrices.

i. TA-FAB Using Hybrid Matrix

After documenting the disappointing performance of TA-FAB (with the aqueous saccharide matrices) in the analysis of higher mass compounds, a new approach to the problem was attempted. The use of aqueous glycerol solutions in the conventional FAB experiment has been discussed, as has the use of aqueous fructose solutions as TA-FAB matrices. It was eventually suggested to combine these sample preparations (i.e., form tertiary mixtures of glycerol, fructose, and water) and evaluate such solutions as potential TA-FAB matrices. These tertiary mixtures became known as hybrid TA-FAB matrices.

A TA-FAB analysis involving a particular hybrid matrix is represented in Figure 3.25. This figure contains mass thermograms for the several components present in a sample containing 1.0 ul of an aqueous bradykinin solution (4 nmol/ul) added to 1.0 ul of 50% glycerol/20% fructose/30% water. The four lower thermograms correspond to ions derived from the matrix, and the five upper

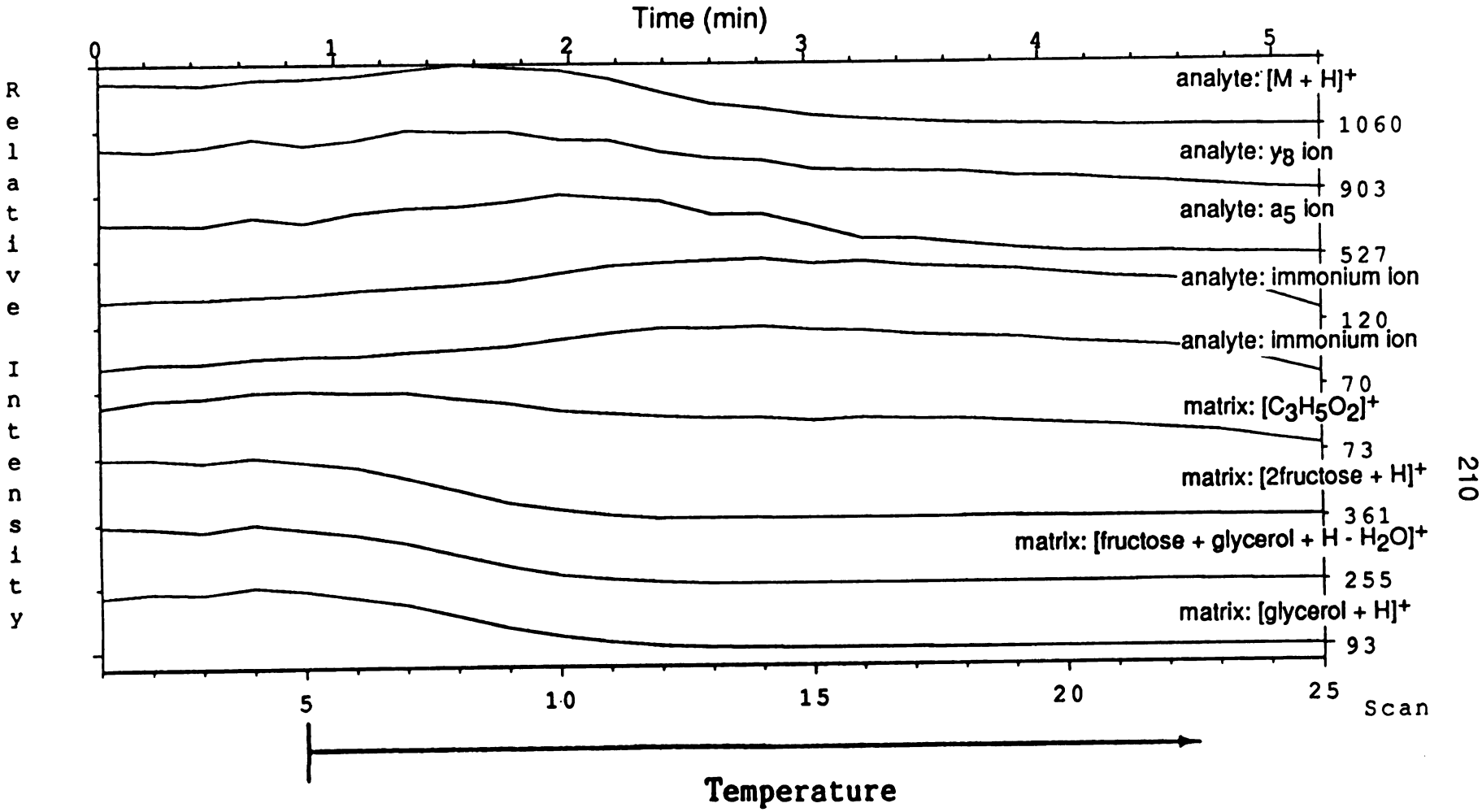

Figure 3.25. TA-FAB analysis of a sample containing 1.0 ul of an aqueous bradykinin solution (4 nmol/ul) added to 1.0 ul of 50% glycerol/20% fructose/30% water. The lower four thermograms correspond to ions derived from the matrix, and the upper five thermograms correspond to analyte ions.

thermograms display the behavior of analyte ions. Two noteworthy ions associated with the hybrid matrix have not been encountered before (either in the TA-FAB analyses involving aqueous fructose, or the FAB analyses involving glycerol). These signals occur at m/z 255 ([fructose+glycerol+H-H_2O]$^+$) and m/z 361 ([2fructose+H]$^+$). At the beginning of the experiment (before the application of heat), one observes substantial desorption ionization from all sample components, including the analyte. Such behavior is not unexpected, considering that the sample at this point is composed predominantly of glycerol. As the sample is heated, however, the glycerol is volatilized (as indicated by the decline in ion abundance at m/z 93). The two relatively intense signals unique to the hybrid matrix (at m/z 255 and 361) diminish along with those corresponding to the glycerol ions. During this period of glycerol removal from the probe tip, the analyte ion abundances are all significantly increased. This behavior appears analogous to that described in the previous section (TA-FAB analyses using glycerol). Once the glycerol is removed from the sample, desorption ionization is supported solely by the remaining fructose matrix component (indicated by the sustained signal at m/z 73, which corresponds to a relatively abundant fructose fragment ion). During this transition, the high mass analyte ion abundances begin to fade. The fructose matrix (as was described earlier in this chapter) provides a relatively harsh environment for desorption ionization, resulting in extreme fragmentation. The latter stages of the thermograms in Figure 3.25 display this tendency, as evidenced by the diminished high mass analyte ion abundances and the flourishing immonium ion signals.

Two mass spectra from this TA-FAB analysis are shown in Figure 3.26. The first spectrum (scan 9) is indicative of the interval in which desorption ionization of the high mass analyte ions is maximized. Those peaks corresponding to matrix interference (denoted by a "B") occupy a wider mass

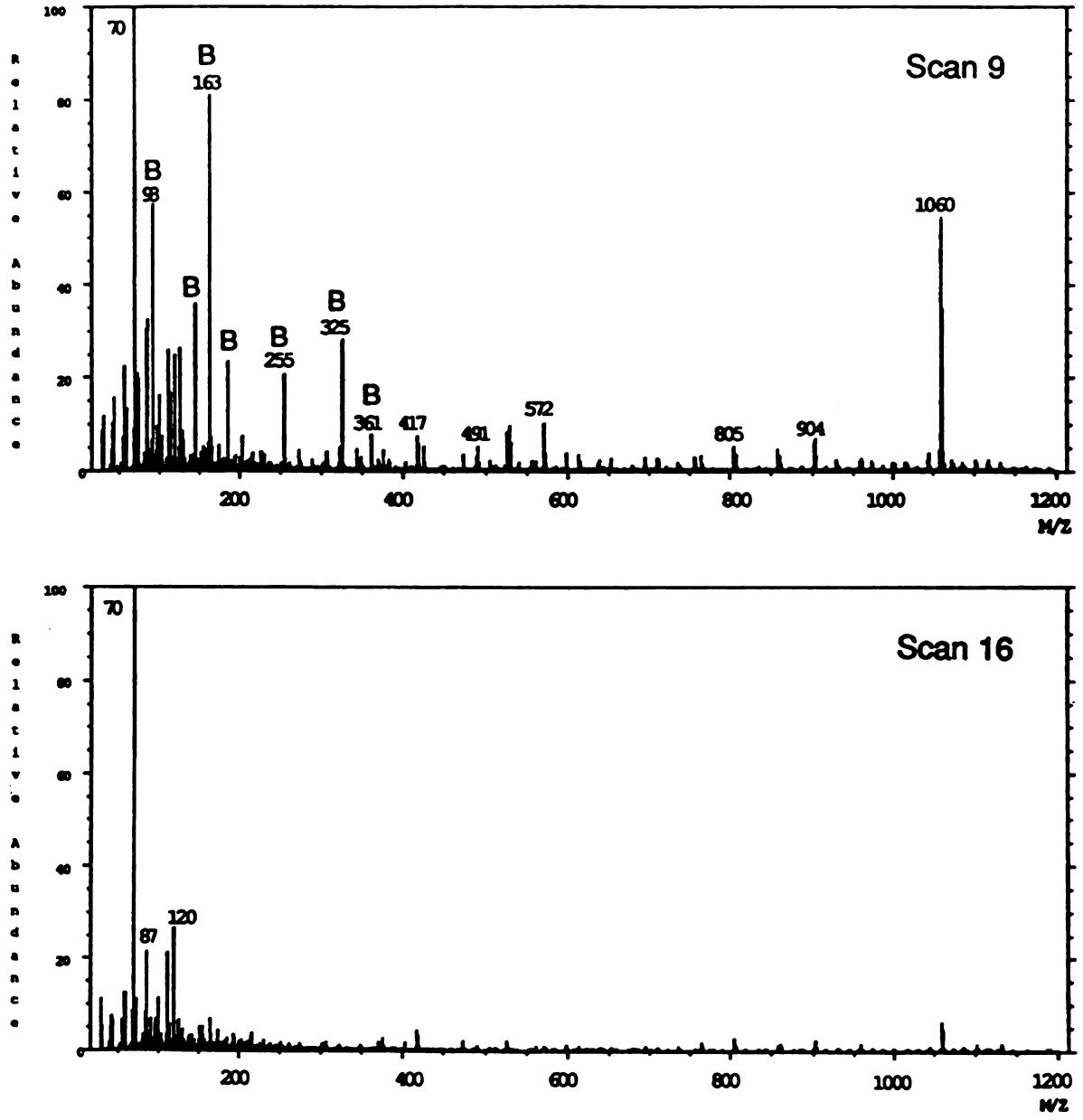

Figure 3.26. Two mass spectra selected from the TA-FAB analysis (using the hybrid matrix) represented in Figure 3.25.

range than did the peaks associated with the aqueous fructose matrix, but a clear mass window for viewing analyte signals exists above m/z 361. Figure 3.26 also displays a later scan (scan 16) in the TA-FAB experiment, which was obtained during sputtering from the harsher fructose environment. This spectrum is dominated by low mass ions (at m/z 70, 87, 112, and 120) indicative of the individual amino acids which form the peptide chain.

Use of hybrid matrices in the TA-FAB experiment has succeeded in substantially increasing high mass analyte ion abundances in comparison to those provided by the aqueous saccharide matrices. The hybrid matrix also adds an interesting feature to TA-FAB analyses: the capacity to alter fragmentation of the analyte by changing the environment for desorption ionization within a single experiment. The upper spectrum in Figure 3.26 was obtained from a sample containing a significant amount of glycerol. In this particular sample composition, desorption ionization of the analyte is relatively soft, allowing maximum sensitivity for high mass ions. Desorption ionization from the fructose-dominated sample (scan 16) imparts more internal energy to the analyte, resulting in much more fragmentation. The informational content of the later spectrum is quite complementary to that present in the earlier spectrum. The benefits of this approach will be evaluated for different classes of compounds in Chapter 4.

j. Optimization of Glycerol/Fructose/Water Matrix Composition

The previous section describes the TA-FAB analysis of a sample containing an aliquot from a particular hybrid matrix. However, due to the great solubility of glycerol and fructose in water, a great range of hybrid matrix compositions is possible. The compositions represented in Figure 3.27 were prepared for comparative studies. The vertical axis in Figure 3.27 corresponds to

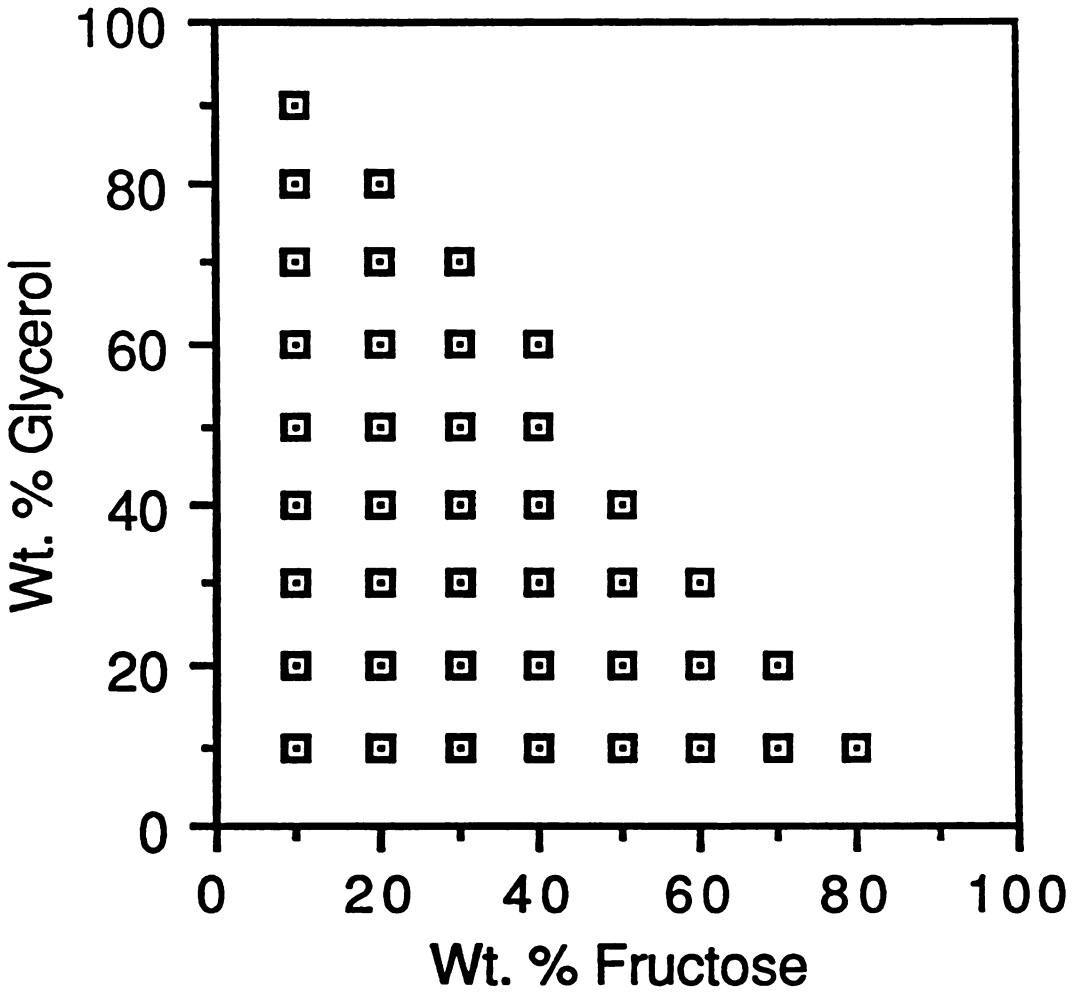

Figure 3.27. Hybrid matrix solutions evaluated for TA-FAB. The understood sample component is weight % water.

weight % glycerol in the sample, the horizontal axis corresponds to weight % fructose, and the understood sample component is weight % water. In the comparative studies, 1.0 ul of an aqueous bradykinin solution (3 or 4 nmol/ul) was mixed with 1.0 ul of the hybrid matrix and subsequently analyzed by TA-FAB. A constant amount of analyte was used for all runs conducted in a particular day. The precision of these analyses was not sufficient to distinguish the results of one sample composition from all the others; however, a few general trends in behavior were established. For instance, the matrix solutions in which the weight % fructose exceeded the weight % glycerol were not conducive to early desorption ionization of the analyte. These solutions required the application of heat before significantly intense analyte signals were observed. Those solutions which contained a higher percentage of glycerol than fructose (by weight) exhibited significant initial desorption ionization of the analyte, which was increased by raising the temperature of the sample. These samples provided the greatest analyte ion abundances. Another trend revealed a decline in the severity of fructose interference observed throughout the run for matrix solutions containing less of the saccharide. The glycerol interference was consistently alleviated by volatilizing that sample component through the application of heat. The most useful hybrid matrices contained significantly more glycerol than fructose. A best estimate of the optimal matrix composition is a 1.0 ul portion of 50% glycerol/20% fructose/30% water.

k. Heating Parameter Optimization for Hybrid Matrix

As described in section **d** of this chapter, the optimization of heating parameters for the JEOL probe is not a particularly precise undertaking. However, it was determined that a significantly different temperature program

than that used for the aqueous fructose matrix (i.e., a temperature surge to 180°C, followed by a ramp of 8°C/minute as read from the DIP thermocouple) improved the results for samples containing the hybrid matrix. The improvement regarded smoothing of the desorption profiles along with shortening the time required for completion of the experiment. A typical heating program for samples containing the hybrid matrix involved an initial temperature surge to approximately 240°C, followed by a ramp of 16°C/minute.

This new temperature program contains implications for the cause of the extreme fragmentation noticed for samples incorporating the aqueous saccharide matrices. The preferential formation of immonium ions from peptides analyzed in these samples might be explained by one of two hypotheses: through thermal degradation of the analyte in response to the elevated temperature, or from an inferior capacity of the saccharides to protect the analyte from the excess energy imparted by the fast atom beam. The hybrid matrix allows less analyte fragmentation at higher temperatures than those employed with the saccharide matrices. This fact argues against the thermal degradation hypothesis. In analyses conducted with the hybrid matrix, the increased fragmentation is closely correlated to the removal of glycerol from the sample. This fact is supportive of the matrix-related hypothesis. Once again, the clustering model (drawn upon to explain increased fragmentation during TA-FAB in the discussion of ternary perculation) appears capable of accounting for the experimental results (Chapter 1, p. 49).

I. Effect of Stainless Steel vs. Copper Probe Tip

In an effort to improve the thermal response of the JEOL TA-FAB probe, experiments were conducted with a copper tip (as opposed to stainless steel).

Copper was chosen because its properties include a substantially greater thermal conductivity than stainless steel. Although the thermal response was improved by use of the copper tip, the experimental results were actually degraded by the observation of significantly greater background interference (relative to the analyte signal) in comparison to that observed from the stainless steel tip. The increased interference was especially notable for the fructose component of the hybrid matrix. The reason for the increased interference may be an improved desorption efficiency for the saccharide from a copper surface relative to a stainless steel surface. Observation of the effect resulted in discontinuation of experiments with the copper probe tip.

m. Alternative Tertiary TA-FAB Matrices

In addition to the glycerol/fructose/water mixtures previously discussed, a variety of other viscous liquid/solid/solvent combinations were tested as potential TA-FAB matrices. The viscous liquid components included glycerol, thioglycerol, nitrobenzyl alcohol, and PEG 200. The solid compounds evaluated were sucrose, glycolic acid, erythritol, threitol, dithioerythritol, dithiothreitol, $CH_3C(CH_2OH)_3$ (provided by Dr. William Reusch), tetradecanoic acid, PEG 600, NH_4Cl, and a variety of hydrated inorganic salts. The solubilizing component for these mixtures was either water or methanol. None of the mixtures performed in a manner superior to the glycerol/fructose/water matrices under conditions of TA-FAB. The criteria of greatest importance in these comparisons were maximizing analyte ion abundances and minimizing matrix interference during the course of the analysis.

n. Proposed Model for TA-FAB Using Hybrid Matrix

At this point, a brief summary will be given of the processes believed to account for the characteristics of the TA-FAB experiment using the hybrid matrix. In the initial phase of the experiment (before the application of heat), desorption ionization of the analyte and matrix occurs from a sample predominantly composed of glycerol. As the sample temperature rises, however, ion abundances characteristic of glycerol progressively diminish (indicating the removal of glycerol from the sample through volatilization). During this important interval of the experiment, the glycerol to analyte ratio becomes optimized, and the mass spectral enhancement associated with this phenomenon is established. It is important to note that although the fructose should also be concentrated in the diminishing glycerol content of the sample, no increase in fructose ion abundance accompanies the increase in analyte ion abundance. This fact may once again indicate the participation of processes analogous to zone refining in the thermally activated behavior of concentrated saccharide samples. In the hybrid system, both glycerol and the analyte would tend to be expelled toward the surface in an attempt to establish a more thermodynamically stable, ordered saccharide network. Any participation of residual water in this critical stage of the experiment is probably not particularly important. The additional fluidity imparted to the sample by the migration of water would be overshadowed by the fluidity imparted by glycerol. In the final stage of the experiment, desorption ionization is supported solely by melted fructose. This relatively harsh environment for desorption ionization results in a significantly greater tendency for fragmentation of the analyte. Once again, this fragmentation may be the consequence of an inferior capacity for the saccharide to cluster with the analyte in the gas phase.

Clusters of reduced size (in comparison to clusters involving glycerol) would allow less opportunity to release energy through desolvation.

V. Conclusion

It has been shown that the application of heat to specially chosen sample compositions provides the capacity to enhance particular aspects of FAB experimental results. Unfortunately, the reduced contamination of ion lenses associated with the optimized sample preparation discussed in Chapter 2 is not characteristic of the TA-FAB matrices described in this chapter. Sputtering from concentrated aqueous saccharide solutions promotes relatively rapid contamination of ion lenses. The problem is further exacerbated by the volatilization of glycerol from the hybrid matrix. This complication, however, is offset by the additional expertise gained from the frequent cleaning of ion sources.

VI. References

1. Ackermann, B.L.; Watson, J.T.; Holland, J.F. *Anal. Chem.* **1985**, *57*, 2656.
2. Ackermann, B.L.; Holland, J.F.; Watson, J.T. *Biomed. Environ. Mass Spectrom.* **1987**, *14*, 501.
3. Maine, J.W.; Soltmann, B.; Holland, J.F.; Young, N.D.; Gerber, J.N.; Sweeley, C.C. *Anal. Chem.* **1976**, *48*, 427.
4. Ackermann, B.L.; Holland, J.F.; Heine, C.E.; Watson, J.T. Presented at the 34th Annual Conference on Mass Spectrometry and Allied Topics, Cincinnati, Ohio, June 8-13, **1986**.
5. Ackermann, B.L., Ph.D. Dissertation, Chemistry Department, Michigan State University, **1986**.
6. Katz, R.N.; Chaudhary, T.; Field, F.H. *Int. J. Mass Spectrom. Ion Proc.* **1987**, *78*, 85.
7. Katz, R.N.; Field, F.H. *Int. J. Mass Spectrom. Ion Proc.* **1989**, *87*, 95.
8. Washburn, E.W., Ed. *International Critical Tables of Numerical Data, Physics, Chemistry and Technology*, volume 2, McGraw-Hill Book Company, New York, New York, **1929**.
9. Mathlouthi, M. *Carbohydr. Res.* **1981**, *91*, 113.
10. Mathlouthi, M.; Luu, C.; Meffroy-Biget, A.M.; Luu, D.V. *Carbohydr. Res.* **1980**, *81*, 213.
11. Cotton, F.A.; Wilkinson, G. *Advanced Inorganic Chemistry*, 4th edition, John Wiley and Sons, New York, New York, **1980**.
12. Brady, J.E.; Holum, J.R. *Fundamentals of Chemistry*, 2nd edition, John Wiley and Sons, New York, New York, **1984**.
13. Guthrie, R.D., Ed. *Carbohydrate Chemistry*, volume 1, The Chemical Society, London, **1968**.

14. Ackermann, B.L.; Stults, J.T. unpublished results.

15. Matsuura, F.; Nunez, H.A.; Grabowski, G.A.; Sweeley, C.C. *Arch. Biochem. Biophys.* **1981**, *207*, 337.

16. Barofsky, D.F.; Giessman, U.; Barofsky, E. *Int. J. Mass Spectrom. Ion Phys.* **1983**, *53*, 319.

Chapter 4. Direct Comparison of FAB and TA-FAB

I. Introduction

The novel research presented in this dissertation has developed along two parallel paths. In Chapter 2, optimization of sample preparation in the conventional FAB experiment was shown to result from manipulation of the matrix to analyte ratio. In Chapter 3, the application of heat to certain sample compositions was shown to enhance particular aspects of the experimental data. The final chapter of this dissertation (Chapter 4) will merge the parallel avenues in a direct comparison, in order to identify the advantages and disadvantages of each approach.

Four unrelated analytes have been chosen for purposes of comparison. These include the linear nonapeptide bradykinin (which was used as a model compound in Chapters 2 and 3), HC-I toxin (a cyclic tetrapeptide), digitonin (a cardiac glycoside), and stachyose (a tetrasaccharide). Each analyte was the focus of a comparative study involving 12 separate mass spectrometric analyses (six by FAB and six by TA-FAB) conducted in an individual experimental session. The six FAB analyses included three which incorporated 14 umol of glycerol, and three which incorporated the more optimal, 1.1 umol portion of glycerol. The six TA-FAB analyses included three which involved an aqueous fructose matrix (containing 0.22 mg of fructose), and three which were obtained with a hybrid matrix (1.0 ul of 50% glycerol/20% fructose/30% water). Quantitative comparisons will be made of the analyte ion abundances measured by each experimental approach, along with the matrix ion abundances (when possible). A comparison of the ease in extracting qualitative information from the mass

spectra also will be emphasized. Finally, general trends in the utility of the different experimental approaches for the analysis of the model compounds will be discussed.

II. Experimental

a. Mass Spectrometry

All experiments were performed upon the JEOL HX-110. A 6-keV xenon atom beam was used, and the source pressure with the beam operating was approximately $3x10^{-6}$ torr. A resolving power of 3000 was employed at an acceleration potential of 10 kV. For bradykinin, scans were collected over a mass interval from 0 to 1300 u, in a period of 11.1 sec, allowing 2.1 sec between consecutive scans. For HC-I toxin, the mass interval was 0-700 u, and the scans were collected in 8.1 sec, with 3.3 sec between consecutive scans. For digitonin, spectra were collected from 0 to 1400 u, in 11.5 sec, with 1.9 sec between scans. For stachyose, the mass interval was 0 to 800 u, and scans were collected in 8.7 sec, with 2.2 sec between consecutive scans. All data were acquired, stored, and processed with the JEOL DA5000 data system.

TA-FAB data were obtained from the stainless steel tip. In each case, the temperature program was initiated after the acquisition of 1 mass spectrum. For the aqueous fructose samples, the temperature program involved a surge to 180°C and a ramp of 8°C/min (as read from the DIP thermocouple). For the samples containing the hybrid matrix, the initial mass scan was followed by a temperature surge to 240°C and a ramp of 16°C/min (as read from the DIP thermocouple). The actual temperature at the probe tip was expected to lag behind that indicated by the thermocouple.

b. Materials

Bradykinin, stachyose, and fructose were purchased from Sigma Chemical Co. Digitonin was obtained from Merck and Co., Inc., and glycerol was purchased from Mallinckrodt, Inc. All these matrials were used as received without further purification.

c. Sample Preparation and Analysis

Sample preparation and analysis were conducted in the manner described in the Experimental Section of Chapter 2 (p. 98).

III. Results and Discussion

a. Bradykinin

Bradykinin is a nonapeptide with a molecular weight of 1059 u. The amino acid sequence of bradykinin is Arg-Pro-Pro-Gly-Phe-Ser-Pro-Phe-Arg. Of the four compounds discussed in this chapter, bradykinin is the only one for which the glycerol to analyte ratio had been optimized by previous work (as detailed in Chapter 2). The optimal glycerol to analyte ratio (c.a., 300) was utilized in this comparison by analyzing 4 nmol of bradykinin from 1.1 umol of glycerol. (The 1.1 umol portion of glycerol also was used in the comparisons for the other compounds, but it should be remembered that this does not necessarily provide the optimal glycerol to analyte ratio for these compounds.) The 4 nmol quantity of bradykinin (deposited as 1.0 ul of an aqueous solution containing 4 nmol/ul)

was also analyzed from 14 umol of glycerol by FAB, from an aqueous solution containing 0.22 mg of fructose by TA-FAB, and from 1.0 ul of 50% glycerol/20% fructose/30% water by TA-FAB.

Figure 4.1 shows a comparison of the absolute ion abundances obtained from the analyte by the four experimental approaches. The displayed signals were measured at m/z 70, 572, and 1060. Each point represents a signal averaged from three separate mass spectrometric analyses. For the FAB analyses (characterized by the first two points in each plot), the signals were obtained from the first scan in each run. For the TA-FAB analyses (the final two points in Figure 4.1), the ion abundances correspond to the maximum signals observed in the course of each experiment. The error bars (as is the convention in this dissertation) represent the standard deviation of these data. The first two points in each plot reflect the ability to increase the analyte ion abundances significantly by optimizing the matrix to analyte ratio in conventional FAB-MS. This result is actually redundant with that from similar experiments represented in Figure 2.2. The final two points in each plot of Figure 4.1 show how the maximum analyte ion abundances observed in TA-FAB compare to those obtained from the nonoptimal and optimal FAB sample compositions. It is interesting to note that the greatest abundances observed for the immonium ion at m/z 70 were observed by TA-FAB. This was also true for the other immonium ion which was evaluated, at m/z 120. For the higher mass analyte ions, however, the TA-FAB results obtained with the aqueous fructose matrix are more indicative of the nonoptimal FAB results, while those obtained with the hybrid matrix are indicative of the optimal FAB results. This trend was generally true for all bradykinin ions above m/z 120 which were evaluated (including m/z 417, 527, 572, 805, 903, and 1060). It seems significant to note that (with the exception of the immonium ions) in no case did the TA-FAB experiment incorporating the

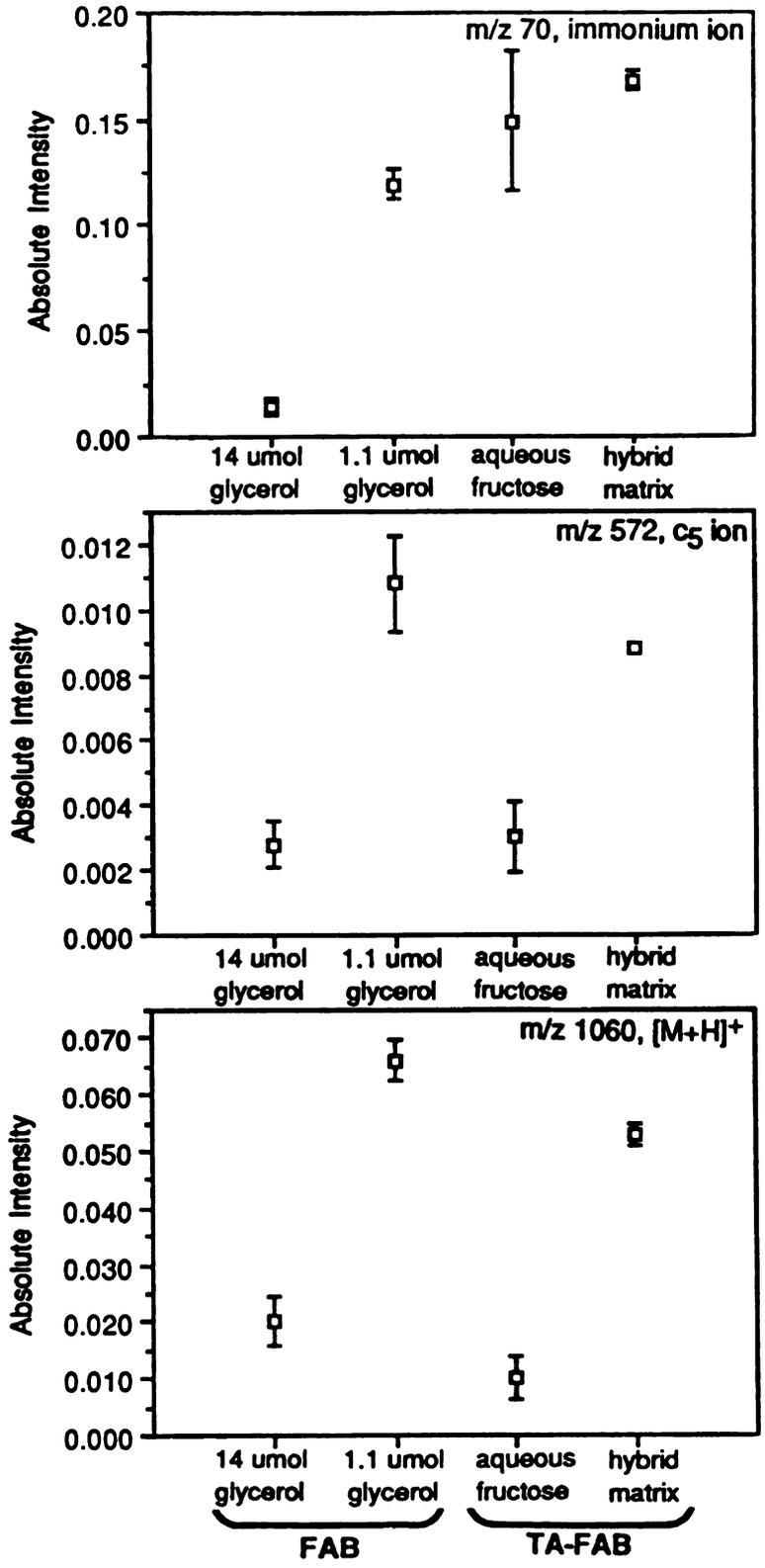

Figure 4.1. Comparison of peak intensities for selected bradykinin ions (m/z 70 (top), m/z 572 (middle), and m/z 1060) which were obtained from the FAB and TA-FAB experiments. Each sample contained 4 nmol of bradykinin.

hybrid matrix provide greater analyte ion abundances than the FAB experiment in which the matrix to analyte ratio had been optimized. This fact supports the contention made in Chapter 3, that the progressive increase in analyte ion abundance observed with the hybrid matrices actually results from optimizing the matrix to analyte ratio on the probe tip as the glycerol is volatilized. Should this be the case, the optimal FAB results represent the maximum signals obtainable by TA-FAB with the hybrid matrix.

A valid comparison of the matrix ion abundances is only possible for the FAB experiments, because the TA-FAB matrices provide their own unique spectral patterns. The decrease in glycerol ion abundance attendant to optimization of the glycerol to bradykinin ratio has already been described, and presented in Figure 2.3.

The qualitative mass spectral improvement which results from optimization of the glycerol to bradykinin ratio in conventional FAB has been demonstrated in Figure 2.1. Likewise, the increased visibility of high mass analyte ion signals obtained by TA-FAB with the hybrid matrix in comparison to TA-FAB with the aqueous fructose matrix is evident from comparison of Figure 3.26 with Figure 3.17. The optimal FAB experiment (1.1 umol of glycerol, Figure 2.1b) offers a slight improvement over TA-FAB (hybrid matrix, upper spectrum in Figure 3.26) for the viewing of high mass analyte signals. This improvement results from less extensive matrix interference for the optimal FAB sample than that associated with the hybrid matrix, especially from m/z 185 to m/z 361. The viewing of low mass bradykinin signals is facilitated by TA-FAB with the hybrid matrix (lower spectrum in Figure 3.26) or the fructose matrix (Figure 3.18) during the latter stages of the experiment when desorption ionization is supported solely by the saccharide. The optimal FAB sample exhibits significant matrix interference in the very low mass portion of the spectrum (Figure 2.1b).

Although the bradykinin thermograms do not all track one another during the experiment (see Figure 3.16), background subtraction is still feasible when using the aqueous fructose matrix. This possibility exists because differential desorption of analyte versus matrix occurs, the matrix thermograms track one another, and the matrix ions are detected in approximately the same abundance during desorption of the analyte as they were before desorption of the analyte. Unfortunately, the background subtracted spectra still suffer from the extreme fragmentation associated with the aqueous fructose matrix, making this approach an inferior alternative.

b. HC-I Toxin

The fungus *Helminthosporium carbonum* produces three toxins which are pathogenic to certain varieties of corn (1). The three toxins (HC-I, HC-II, and HC-III) have already been the focus of a comparison between FAB and TA-FAB (2). In the previous study, TA-FAB (aqueous fructose matrix) was shown to provide superior results to those observed from conventional FAB analyses (in which the matrix to analyte ratio had not been optimized). The mass spectral improvement involved a substantial increase in the analyte signal with respect to the matrix background (which was especially facilitated by background subtraction), and increased fragmentation by TA-FAB. The present investigation will repeat this comparison for the primary toxin (HC-I), and extend it to include the TA-FAB experiment incorporating the hybrid matrix as well as the conventional FAB case with a more optimal matrix to analyte ratio.

Figure 4.2 shows the structure of the HC-I toxin. This peptide contains the unusual amino acid 2-amino-8-oxo-9, 10-epoxydecanoic acid (Aoe, see Figure 4.2), which is associated with the observed toxicity. The molecular weight of this

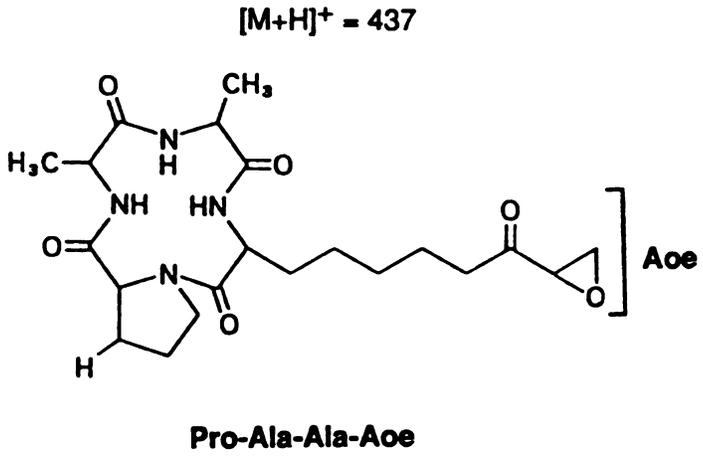

Figure 4.2. Structure of HC-I toxin.

cyclic tetrapeptide is 436 u. The purified HC-I toxin used in this work was provided by Dr. J. D. Walton. A 1.4 ug quantity of the peptide (applied as 1.75 ul of an aqueous solution containing 0.8 ug/ul) was used for each mass spectrometric analysis in the comparative study. Again, the matrices which were combined with this portion of analyte included 14 umol of glycerol (FAB), 1.1 umol of glycerol (FAB), an aqueous solution containing 0.22 mg of fructose (TA-FAB), and a 1.0 ul portion of 50% glycerol/20% fructose/30% water (TA-FAB).

Absolute abundances obtained for HC-I ions from each of the experiments are compared in Figure 4.3. The first point to note from the figure is that a significant increase in abundance results from reducing the glycerol to analyte ratio from 4,000 (14 umol glycerol samples) to 300 (1.1 umol glycerol samples) in the conventional FAB experiment. A second interesting observation is that (with the lone exception of the $[M+H]^+$ ion (m/z 437)) the TA-FAB experiment incorporating the hybrid matrix provides significantly greater analyte ion abundances than the conventional FAB experiment using the smaller (1.1 umol) portion of glycerol. Besides the ions represented in Figure 4.3 (m/z 44 and 240), this trend was observed for analyte signals at m/z 70, 141, 169, 170, 366, and 409. Assuming that the progressive increase in analyte ion abundance associated with the hybrid matrix results from optimization of the matrix to analyte ratio, this observation implies that the 300:1 glycerol to HC-I toxin ratio (in the FAB samples containing 1.1 umol of glycerol) is nonoptimal. It should be remembered that no rigorous optimization of the matrix to analyte ratio for HC-I preceded this investigation. A final trend apparent from the data in Figure 4.3 is the tendency of the ion abundances associated with the original TA-FAB experiment (aqueous fructose) to decrease (in relation to those observed from the other experiments) for the higher mass ions (e.g., m/z 437).

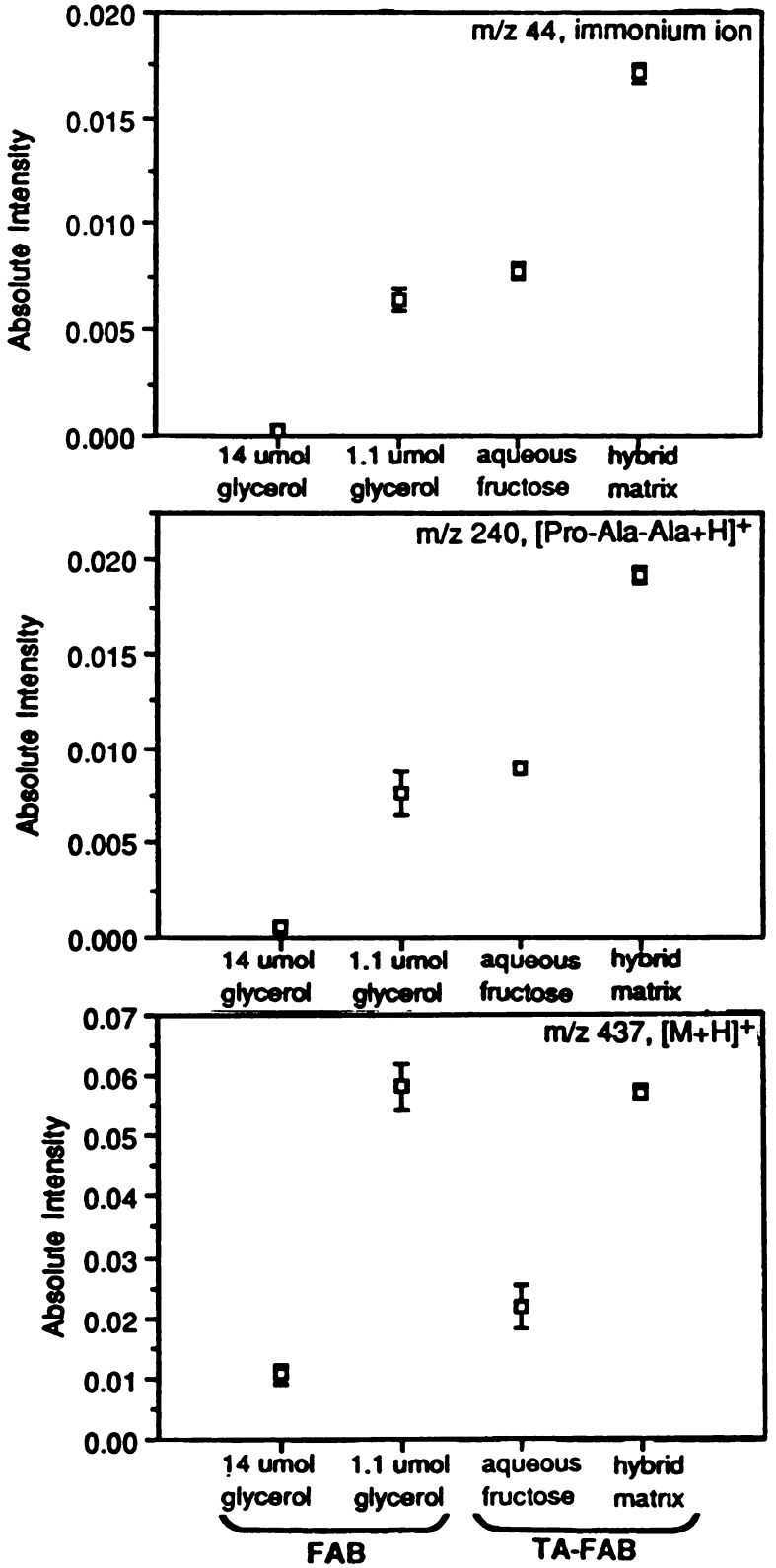

Figure 4.3. Comparison of peak intensities for selected HC-I toxin ions (m/z 44 (top), m/z 240 (middle), and m/z 437) which were obtained from the FAB and TA-FAB experiments. Each sample contained 1.4 ug of the peptide.

Glycerol ion abundances are compared for the FAB experiments in Figure 4.4. For all ions evaluated (including m/z 75, 93, 185, 277, and 369), a significant decrease in glycerol ion intensity accompanied reduction of the glycerol to HC-I ratio from 4,000 (14 umol glycerol samples) to 300 (1.1 umol glycerol samples).

Mass spectra representative of the conventional FAB experiments are shown in Figure 4.5, and spectra from the TA-FAB analyses are displayed in Figure 4.6. The upper spectrum in Figure 4.5 reveals the paucity of information regarding the analyte which is evident from the sample containing 14 umol of glycerol. The informational content concerning the analyte is increased in the lower spectrum of Figure 4.5 (1.1 umol of glycerol), although it is somewhat difficult to distinguish from the matrix interference which exists in the low mass region. Considerable matrix interference also is apparent in the low mass portion of the spectrum obtained from the hybrid matrix (upper spectrum in Figure 4.6). This spectrum was recorded during the period of strong analyte desorption and reduced matrix interference in the TA-FAB analysis. The TA-FAB experiment which incorporated the aqueous fructose matrix also suffered from considerable background interference in the low mass region. This interference could be subtracted, however, resulting in very clean mass spectra, such as that shown in the lower portion of Figure 4.6. Obviously, the TA-FAB experiment with the fructose matrix provides the most favorable results for this particular compound. This conclusion agrees with that formulated in the earlier study by Ackermann, Holland, and Watson (2). Finally, it should be noted that the HC-I thermograms tracked one another in all TA-FAB analyses.

The HC-I data provide an example of the importance of the analyte signal *relative to* the background signal in FAB-MS. Although the TA-FAB experiment using aqueous fructose never produced the greatest abundance for an analyte

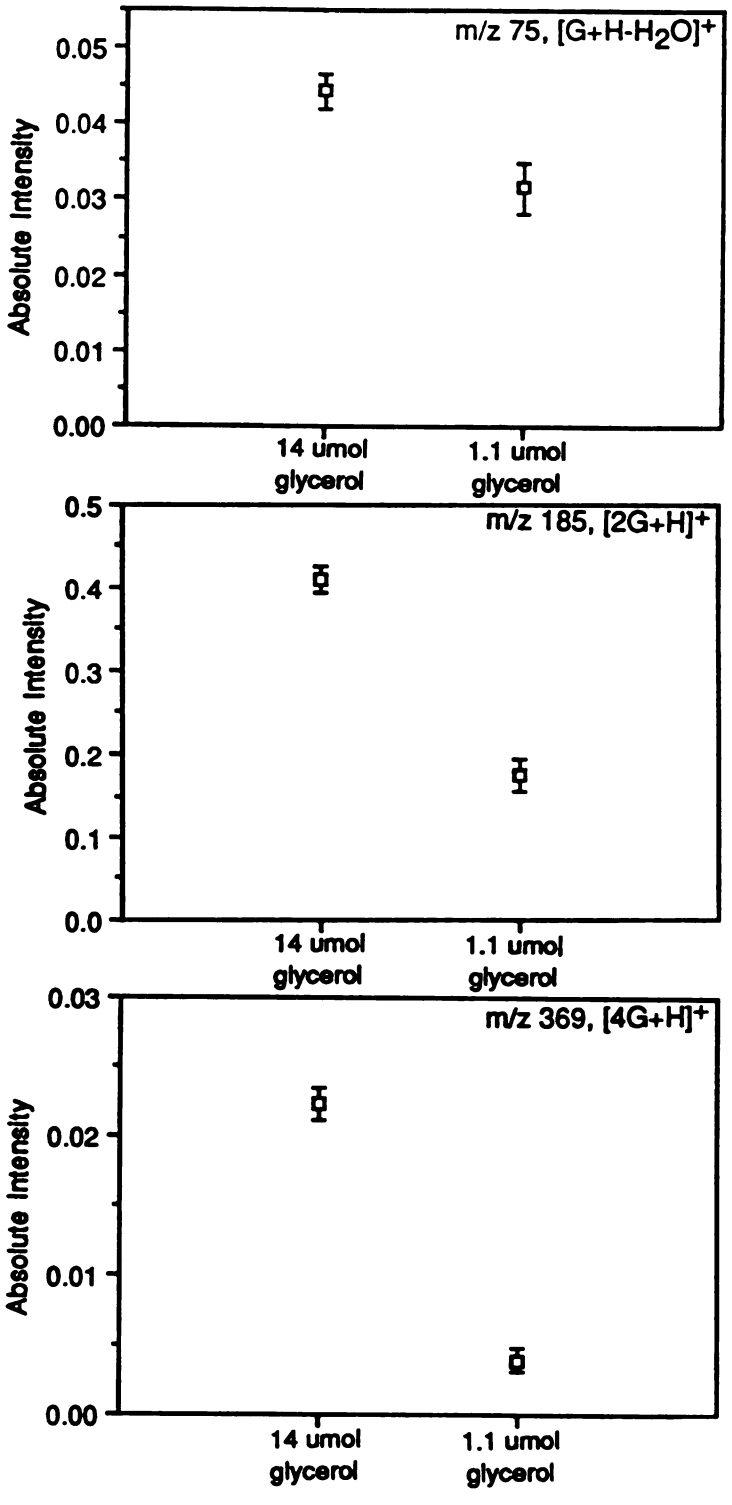

Figure 4.4. Comparison of peak intensities for selected glycerol ions (m/z 75 (top), m/z 185 (middle), and m/z 369) which were obtained from the FAB experiments. Each sample contained 1.4 ug of HC-I toxin.

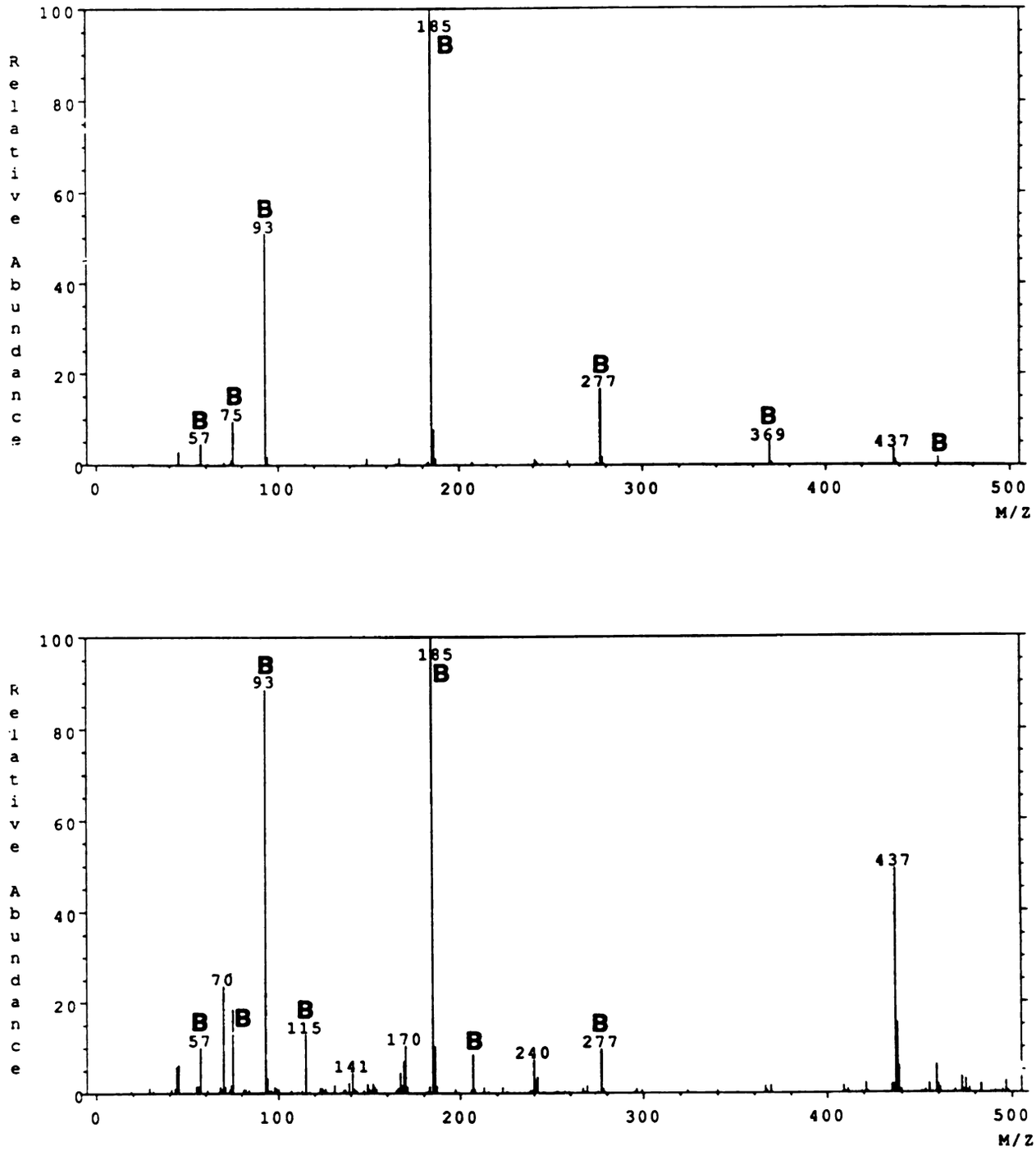

Figure 4.5. (upper) FAB mass spectrum of 1.4 ug of HC-I toxin dispersed in 14 umol of glycerol. Major peaks associated with the matrix background are labeled with a "B". (lower) FAB mass spectrum of 1.4 ug of HC-I toxin dispersed in 1.1 umol of glycerol.

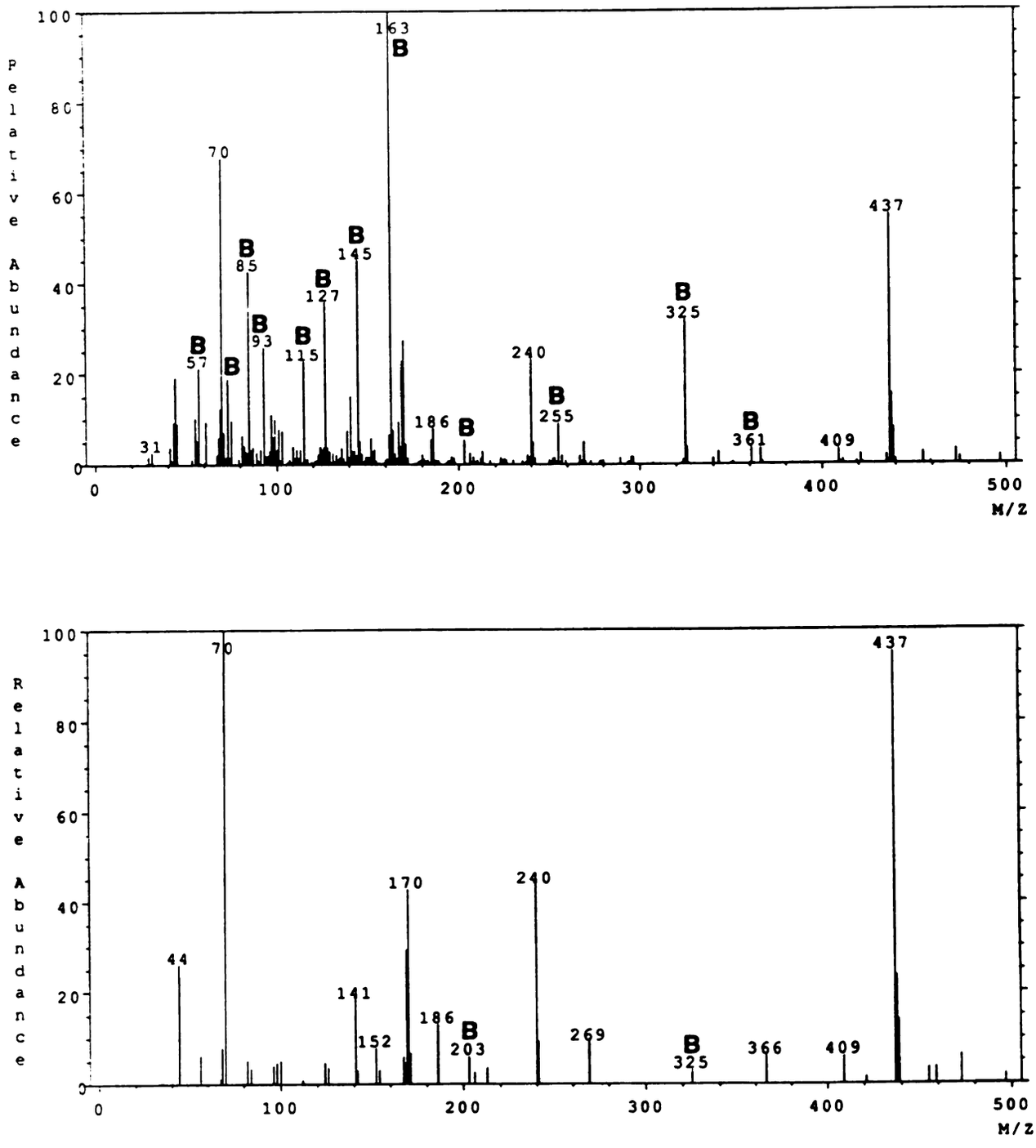

Figure 4.6. (upper) TA-FAB mass spectrum of 1.4 ug of HC-I toxin sampled from hybrid matrix. (lower) Background subtracted TA-FAB mass spectrum of 1.4 ug of HC-I toxin sampled from aqueous fructose matrix.

ion (see Figure 4.3), its ability to remove the matrix interference allowed results which were far superior to those observed from the other experiments.

c. Digitonin

Digitonin is a cardiac glycoside which has previously been analyzed by desorption ionization mass spectrometry (3). The molecular weight of digitonin is 1228 u, and its structure is shown in Figure 4.7. For the comparative studies, 1.0 ul of a solution of digitonin in methanol (2 ug/ul) was added to the FAB and TA-FAB matrix compositions described for the bradykinin and HC-I toxin comparisons.

The conventional FAB mass spectra from samples containing digitonin are shown in Figure 4.8. The upper spectrum in Figure 4.8 was obtained from the sample containing 14 umol of glycerol, and the lower spectrum was obtained from the sample containing 1.1 umol of glycerol. As expected from the results of previous comparisons presented in this dissertation, the spectrum from the sample containing less glycerol exhibits greater visibility of analyte signals throughout the mass range, along with substantially reduced matrix interference than that evident in the spectrum from the sample containing 14 umol of glycerol. An additional difference between the two spectra (which was not present in other comparisons) also is apparent, however. The most prominent peak in the upper spectrum of Figure 4.8 (14 umol of glycerol) which indicates the molecular weight of digitonin corresponds to the $[M+H]^+$ ion (m/z 1229). In the lower spectrum of Figure 4.8 (1.1 umol of glycerol), the most prominent peak which indicates the molecular weight of digitonin corresponds to the $[M+Na]^+$ ion (m/z 1251). Sodium was probably introduced to the sample as an impurity associated with the analyte. Both samples would be expected to contain the same amount of this

$[M+H]^+ = 1229$

$[M+Na]^+ = 1251$

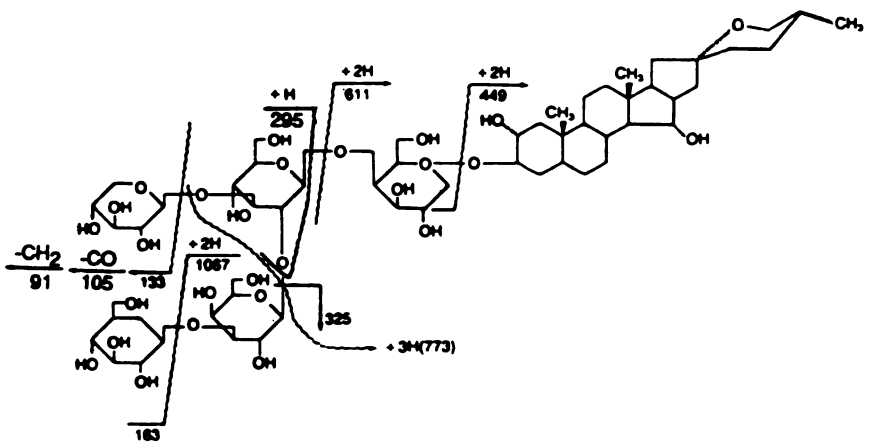

Figure 4.7. Structure of digitonin with a diagram of some important fragmentation pathways.

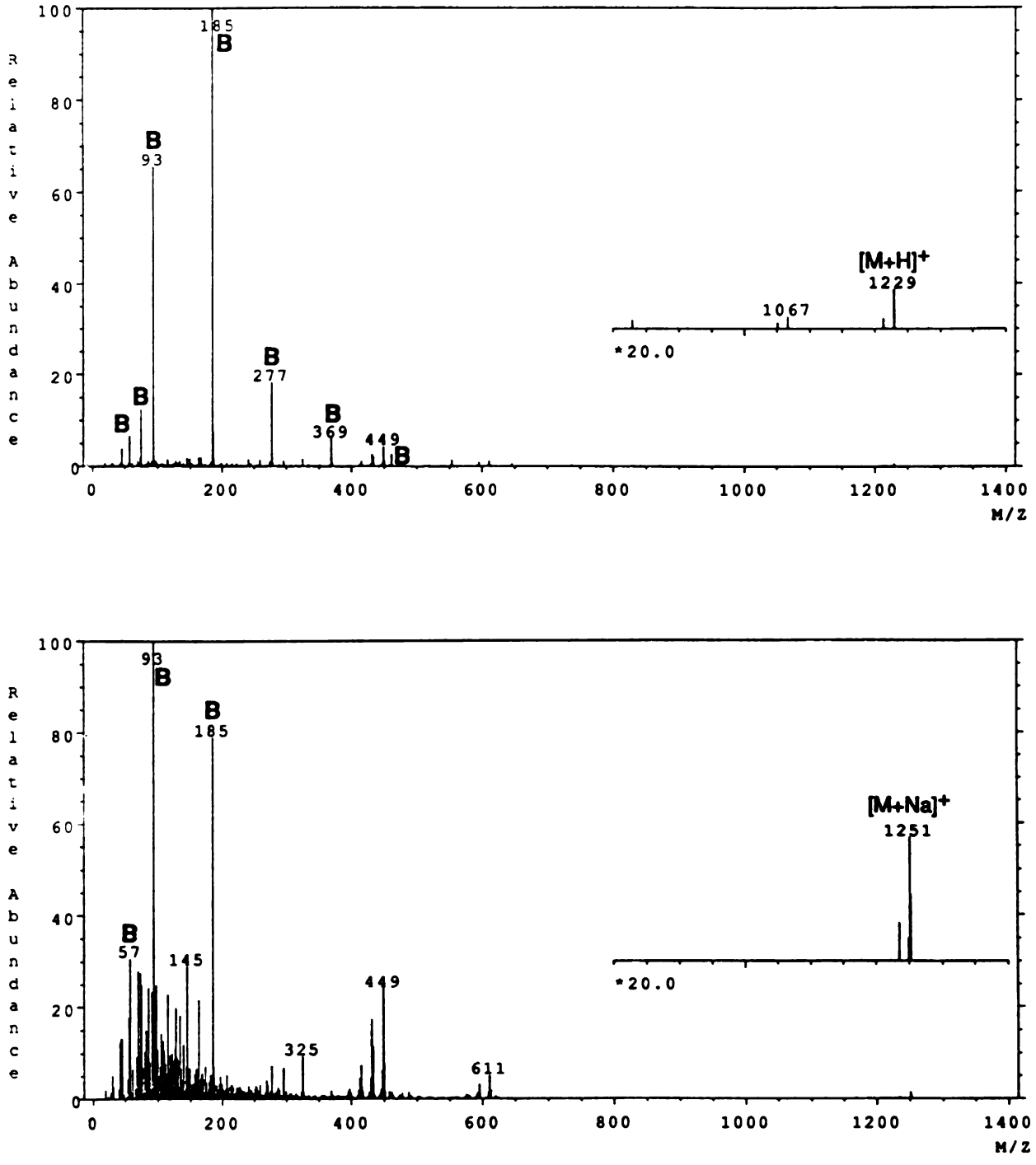

Figure 4.8. (upper) FAB mass spectrum of 2 ug of digitonin dispersed in 14 umol of glycerol. (lower) FAB mass spectrum of 2 ug of digitonin dispersed in 1.1 umol of glycerol.

alkali ion. Therefore, discrimination toward the formation of $[M+Na]^+$ in the sample containing less glycerol may indicate an improved capacity for the analyte to compete for the sodium when less glycerol is present. The idea of a competition between analyte and matrix in the formation of adducts with metal ions has been developed (4, 5). Another explanation (which also may be operative) is that a greater proportion of the sodium ions are positioned near the surface of the 1.1 umol glycerol samples in comparison to the 14 umol glycerol samples. The greater surface concentration of sodium ions in the samples containing less glycerol would result in a greater sampling efficiency of natriated adducts.

Abundances for three digitonin ions are compared in Figure 4.9. Neither the $[M+H]^+$ nor the $[M+Na]^+$ ion abundances are displayed in this figure due to the discriminatory effect mentioned in the previous paragraph. The three ions included (m/z 295, 449, and 611) represent prominent fragments whose signals were readily apparent in all acquired spectra. Once again, Figure 4.9 reflects an increase in analyte ion abundance as the ratio of glycerol to analyte is reduced in the conventional FAB experiment. The increase in analyte ion abundance is not so pronounced as was observed in the previous comparisons. This observation may indicate that the molar ratio of glycerol to digitonin (700) in the samples containing 1.1 umol of glycerol may not be optimal for this particular analyte. Such an explanation is further supported by the observation that the maximum analyte ion abundances obtained from the hybrid matrix (TA-FAB) were significantly greater (for all analyte ions) than those measured from the 1.1 umol glycerol (conventional FAB) samples. Finally, it is once more apparent that as the mass of the analyte ion increases (e.g., m/z 611 in Figure 4.9), the abundances observed from the aqueous fructose matrices (TA-FAB) begin to decline in comparison to those measured from the other experiments.

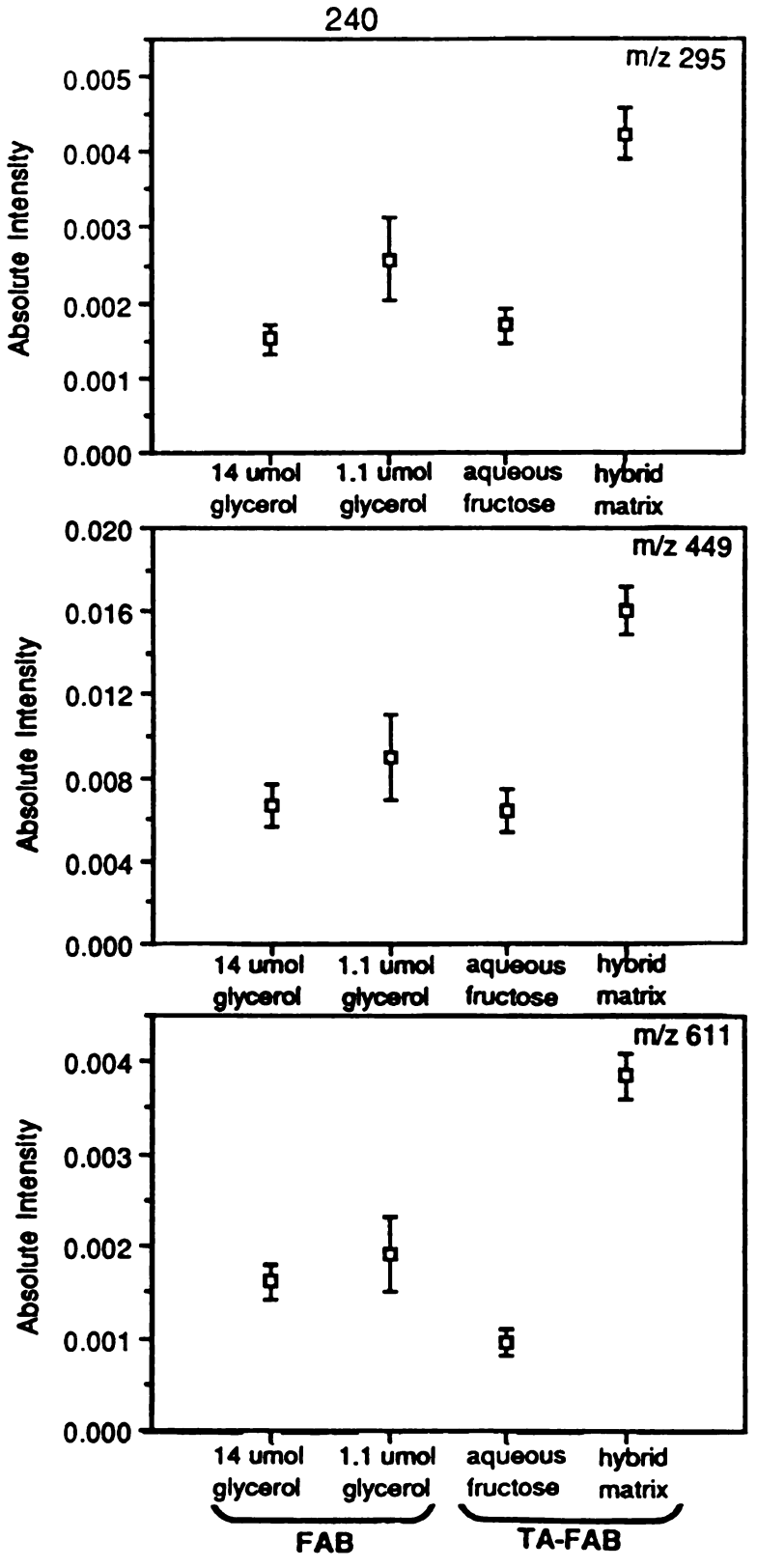

Figure 4.9. Comparison of peak intensities for selected digitonin ions (m/z 295 (top), m/z 449 (middle), and m/z 611) which were obtained from the FAB and TA-FAB experiments. Structures of these fragments are suggested in Figure 4.7. Each sample contained 2 ug of digitonin.

Glycerol ion abundances are compared for the conventional FAB experiments in Figure 4.10. One observes the expected diminution in matrix ion abundance as the glycerol to digitonin ratio is reduced.

In a qualitative sense, the high mass visibility of digitonin signals is approximately the same for the conventional FAB experiment employing 1.1 umol of glycerol (lower spectrum in Figure 4.8), and the TA-FAB experiments (involving both the hybrid matrix and the aqueous fructose matrix). It should be pointed out that the aqueous fructose matrix apparently promotes $[M+Na]^+$ formation, while the hybrid matrix discriminates toward production of the $[M+H]^+$ ion. The mass thermograms of digitonin track one another, and no bias toward the formation of extremely low mass ions at higher temperatures is evident. The viewing of low mass analyte signals is facilitated, however, by background subtraction in TA-FAB analyses involving the aqueous fructose matrix. Figure 4.11 shows a low mass portion of the digitonin spectrum recorded from both the FAB experiment incorporating 14 umol of glycerol (upper spectrum) and the FAB experiment incorporating 1.1 umol of glycerol (lower spectrum). Analyte signals (denoted by the letter "A") are not readily apparent in either of these spectra. In Figure 4.12, the same mass range is displayed from TA-FAB analyses. The upper spectrum in Figure 4.12 was obtained during the period of analyte spectral enhancement in a TA-FAB analysis incorporating the hybrid matrix. Analyte signals in this spectrum also are difficult to distinguish from the extensive matrix interference. The low mass analyte signals are much more visible in the lower (background subtracted) spectrum of Figure 4.12, which corresponds to a TA-FAB analysis using the aqueous fructose matrix. A difficulty in the TA-FAB analysis of digitonin is the similarity in fragmentation arising from the saccharide portion of the analyte and the saccharide component of the TA-FAB matrices.

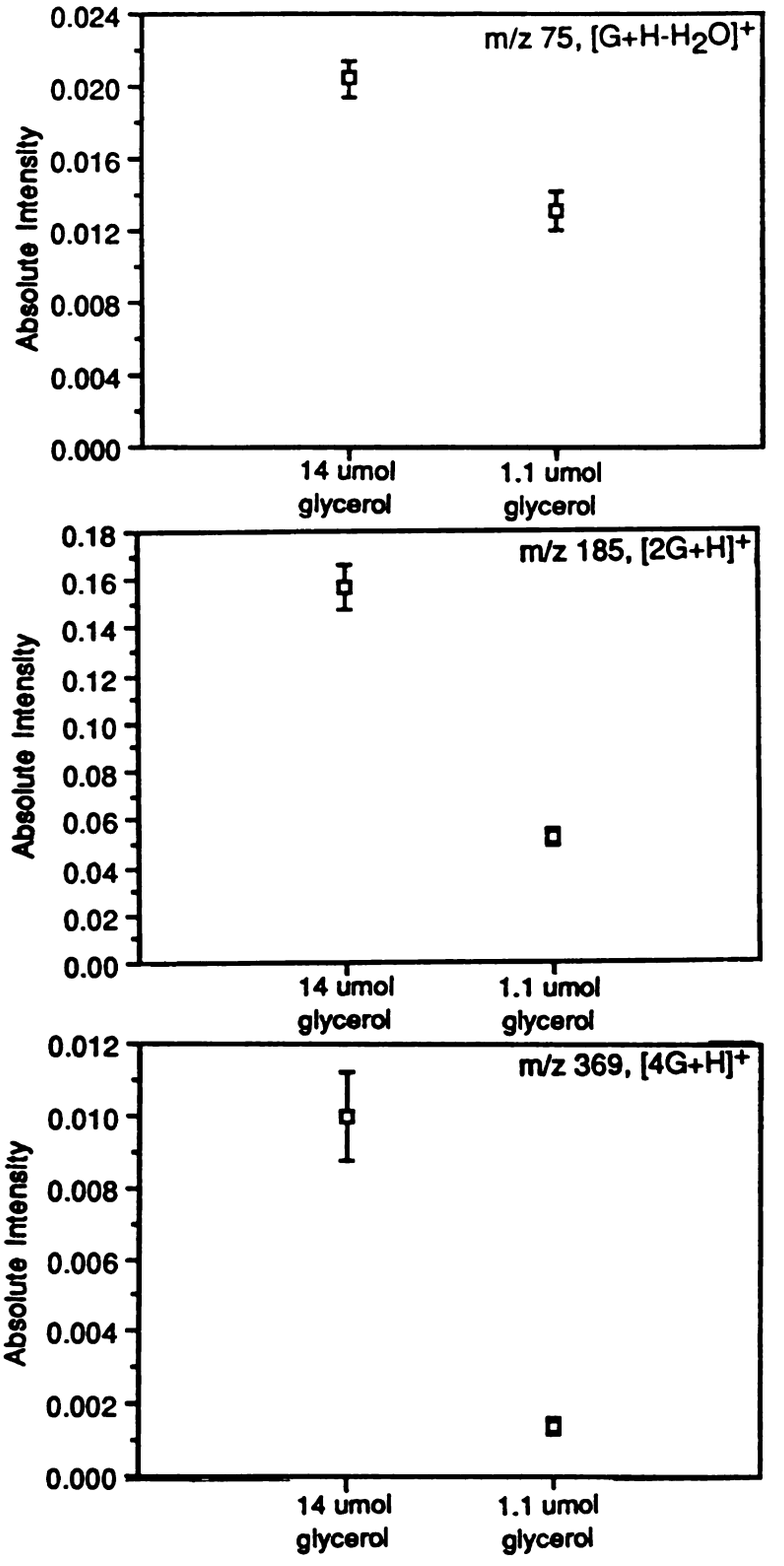

Figure 4.10. Comparison of peak intensities for selected glycerol ions (m/z 75 (top), m/z 185 (middle), and m/z 369) which were obtained from the FAB experiments. Each sample contained 2 ug of digitonin.

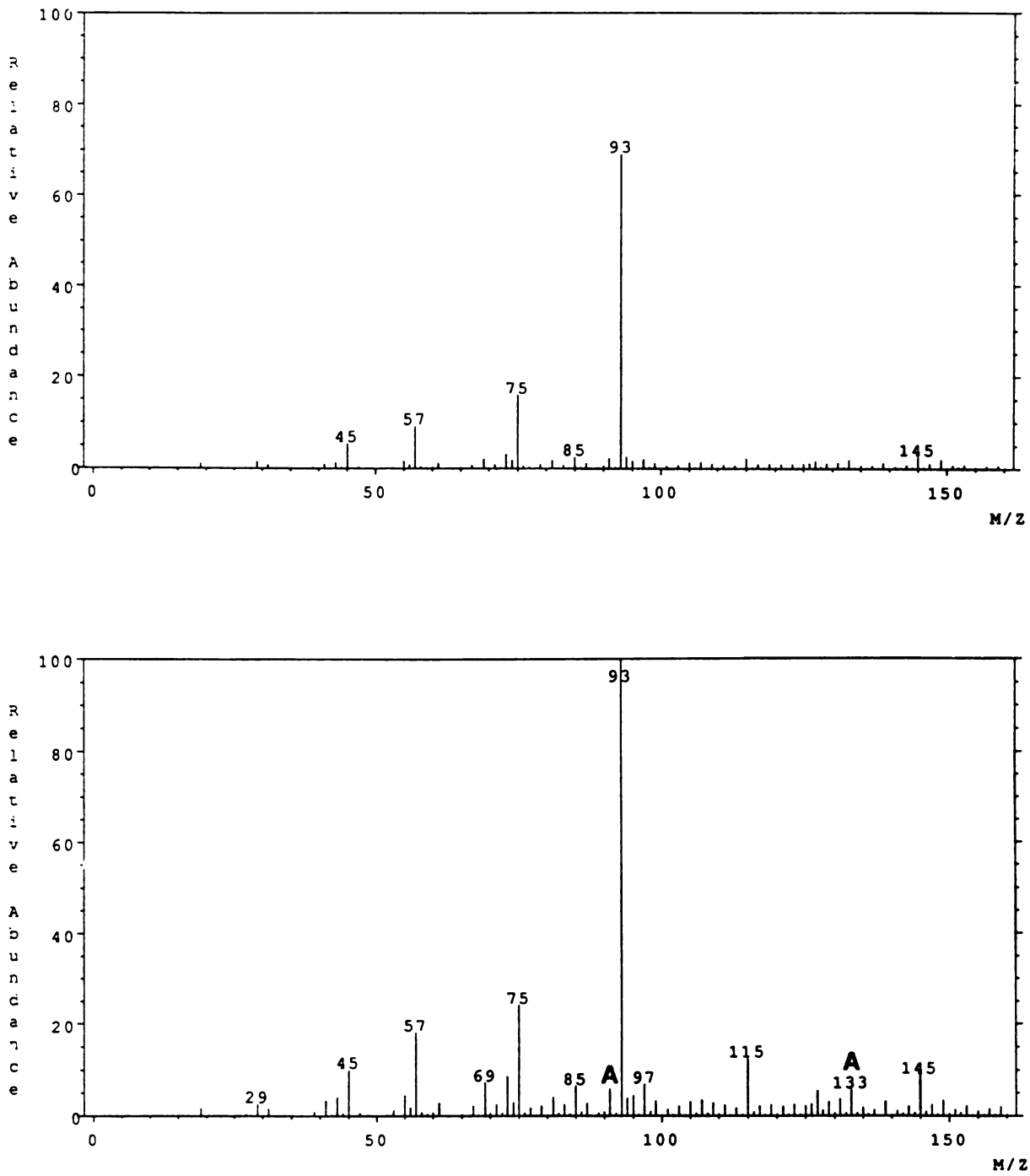

Figure 4.11. (upper) Low mass portion of FAB spectrum from a sample containing 2 ug of digitonin and 14 umol of glycerol. (lower) Low mass portion of FAB spectrum from a sample containing 2 ug of digitonin and 1.1 umol of glycerol. Peaks corresponding to analyte ions are labeled with an "A".

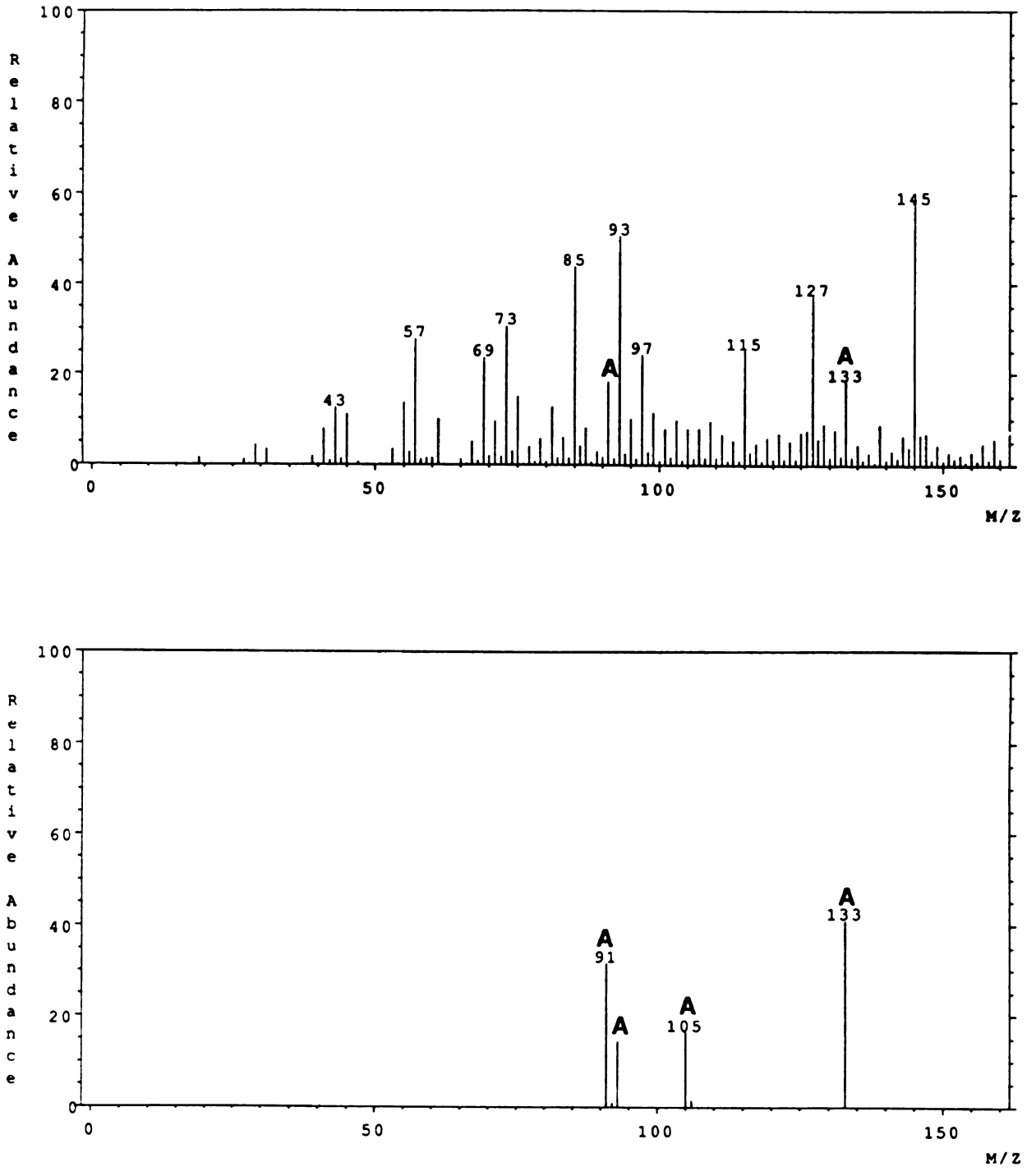

Figure 4.12. (upper) Low mass portion of TA-FAB spectrum from 2 ug of digitonin analyzed from hybrid matrix. (lower) Low mass portion of background subtracted TA-FAB spectrum from 2 ug of digitonin analyzed from aqueous fructose matrix.

d. Stachyose

Stachyose is a tetrasaccharide (its structure is shown in Figure 4.13) with a molecular weight of 666 u. For the mass spectrometric comparison, 19 ug of stachyose (deposited as 1.0 ul of an aqueous solution containing 19 ug/ul) were mixed with each of the matrix compositions described previously in this chapter. Because the FAB-MS performance for saccharides is generally improved in the positive ion mode by promoting the formation of adducts with alkali metal ions, each sample also was spiked with 1 ug of NaCl (deposited as 1.0 ul of an aqueous solution containing 1 ug/ul).

Mass spectra from the conventional FAB analyses are shown in Figure 4.14. The upper spectrum in Figure 4.14 was obtained from a sample containing 14 umol of glycerol. This spectrum reveals relatively little information regarding the analyte. The lower spectrum in Figure 4.14 was obtained from a sample containing 1.1 umol of glycerol. The comparison shown in Figure 4.14 once more indicates the increased visibility of analyte signals which results from a reduction in the glycerol to analyte ratio of the sample. In this case, the ratio was reduced from 500 (14 umol glycerol samples) to 40 (1.1 umol glycerol samples). As was observed in the comparison involving digitonin, the $[M+H]^+$ ion appears to be favored during analyses of the samples containing more glycerol (upper spectrum in Figure 4.14), while $[M+Na]^+$ formation dominates during analyses of the samples containing less glycerol (lower spectrum in Figure 4.14).

The TA-FAB experiments involving stachyose suffered from unforeseen complications. The source of these problems became evident after conducting a background run on an aqueous sample containing 0.22 mg of fructose and 1 ug of NaCl. Mass thermograms from this experiment are shown in Figure 4.15. The two lowermost thermograms in Figure 4.15 correspond to common fructose

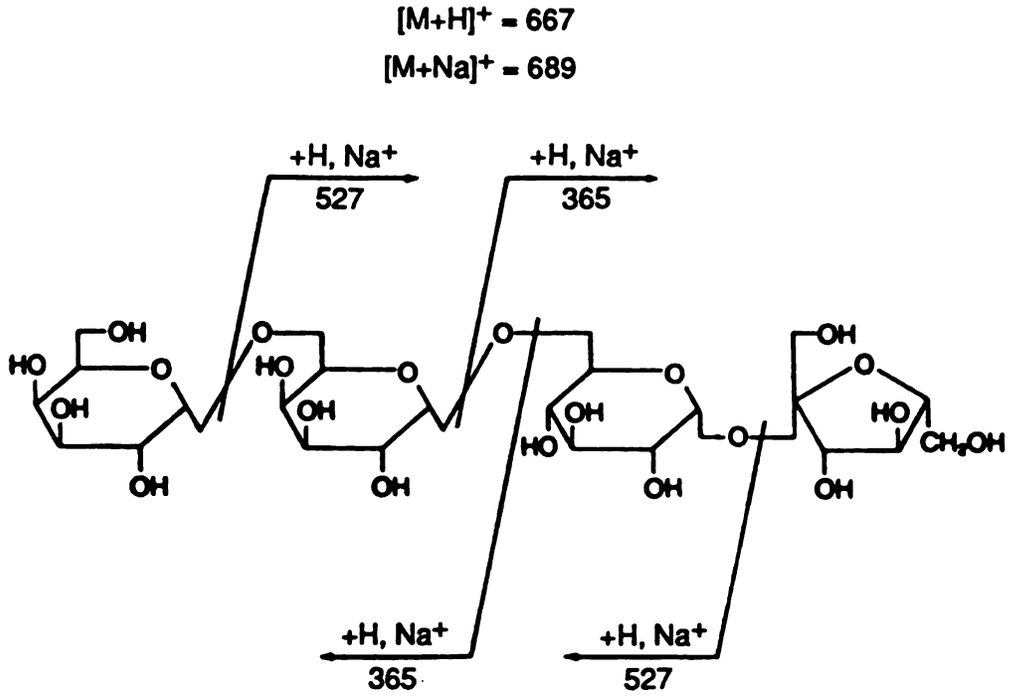

Figure 4.13. Structure of stachyose with a diagram of some important fragmentation pathways.

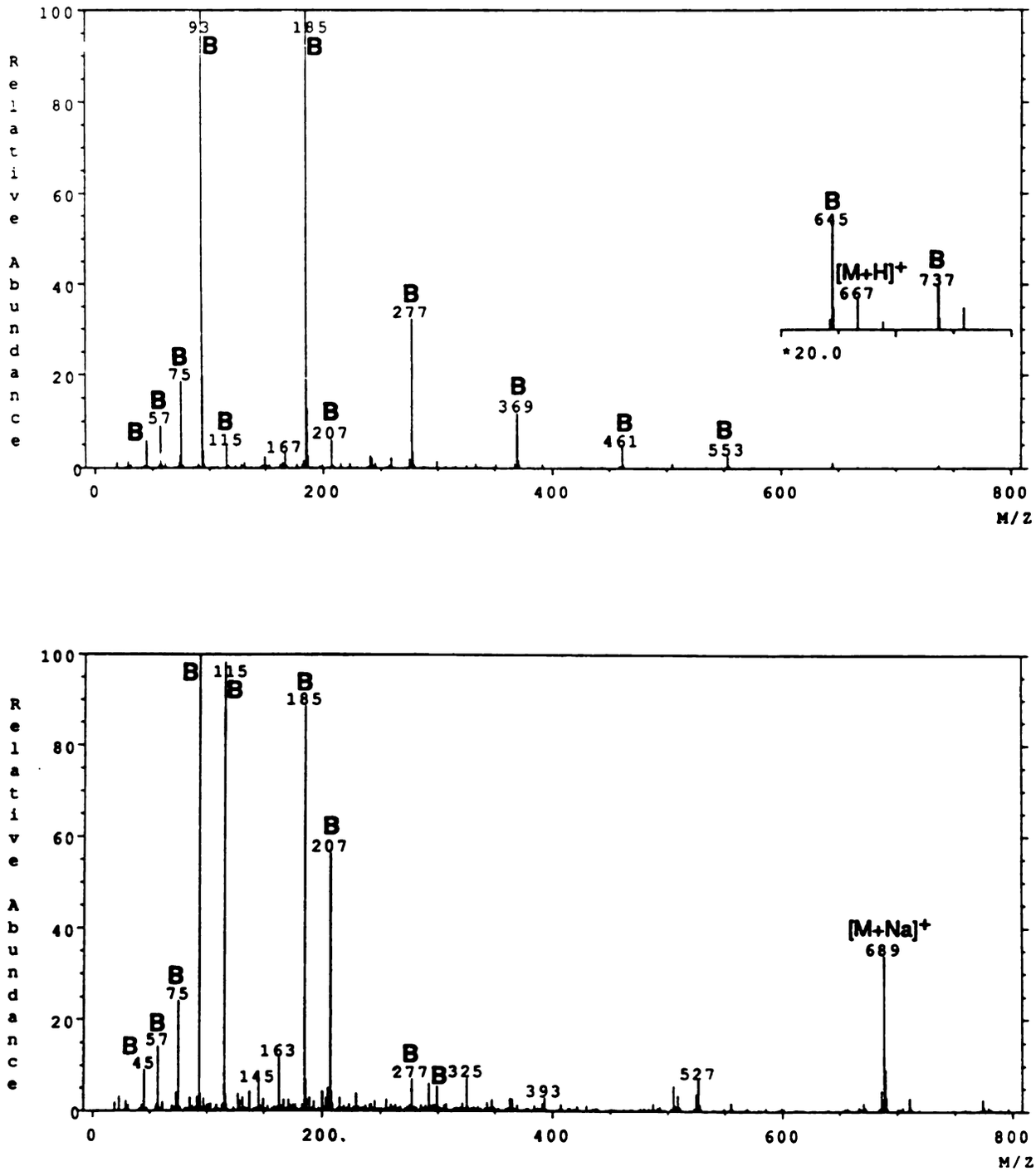

Figure 4.14. (upper) FAB mass spectrum of 19 ug of stachyose and 1 ug of NaCl dispersed in 14 umol of glycerol. (lower) FAB mass spectrum of 19 ug of stachyose and 1 ug of NaCl dispersed in 1.1 umol of glycerol.

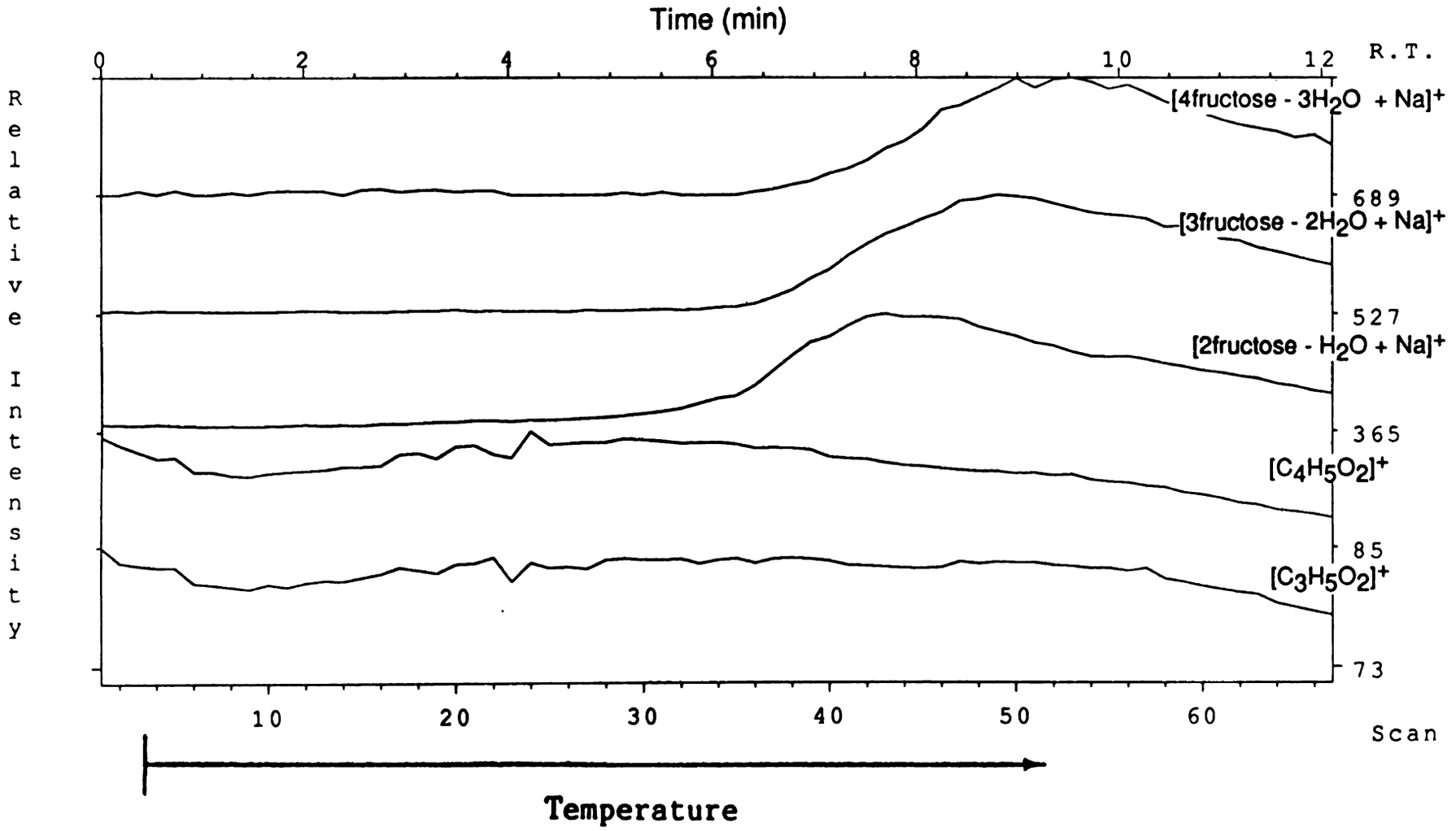

Figure 4.15. Mass thermograms for two common fructose background ions (m/z 73 and 85) and higher mass background ions (m/z 365, 527, and 689). The sample was an aqueous solution containing 0.22 mg of fructose and 1 ug of NaCl.

fragments (m/z 73 and 85). The remaining thermograms represent ion signals at m/z 365, 527, and 689. In Chapter 3, Section **e** of this dissertation, it was proposed that relatively minor signals at these masses correspond to the natriated products of polycondensation reactions involving the saccharide. It appears that the addition of larger amounts of sodium to the sample greatly facilitates the detection of these species. In fact, this new source of matrix interference is shown to dominate the mass spectrum in Figure 4.16 (scan 53 from the run represented in Figure 4.15). Because stachyose also provides important ions at m/z 365, 527, and 689 (see Figure 4.13), these signals were initially misinterpreted from samples containing the analyte. The additional interference is observed from both the aqueous fructose matrix and the hybrid matrix. Its presence severely limits the application of TA-FAB for samples which contain a significant amount of sodium.

Due to the phenomenon discussed in the previous paragraph, the remainder of this comparison will be confined to consideration of the conventional FAB experiments. Figure 4.17 shows analyte ion abundances obtained from the FAB samples. Since the intention of the sample preparation was to promote the formation of sodium adducts, only this type of ion is represented in the figure. The increased analyte ion abundances observed from the samples containing less glycerol, however, was documented for all stachyose ions which were evaluated (m/z 265, 325, 365, 505, 509, 527, 667, and 689), including species which did not contain sodium.

Addition of sodium to the sample complicates the matrix spectrum due to the formation of sodium adducts with glycerol. Figure 4.18 compares the abundances of protonated glycerol species for the FAB experiments. A significant reduction in abundance is observed for these ions when they are measured during the analysis of samples containing 1.1 umol of glycerol.

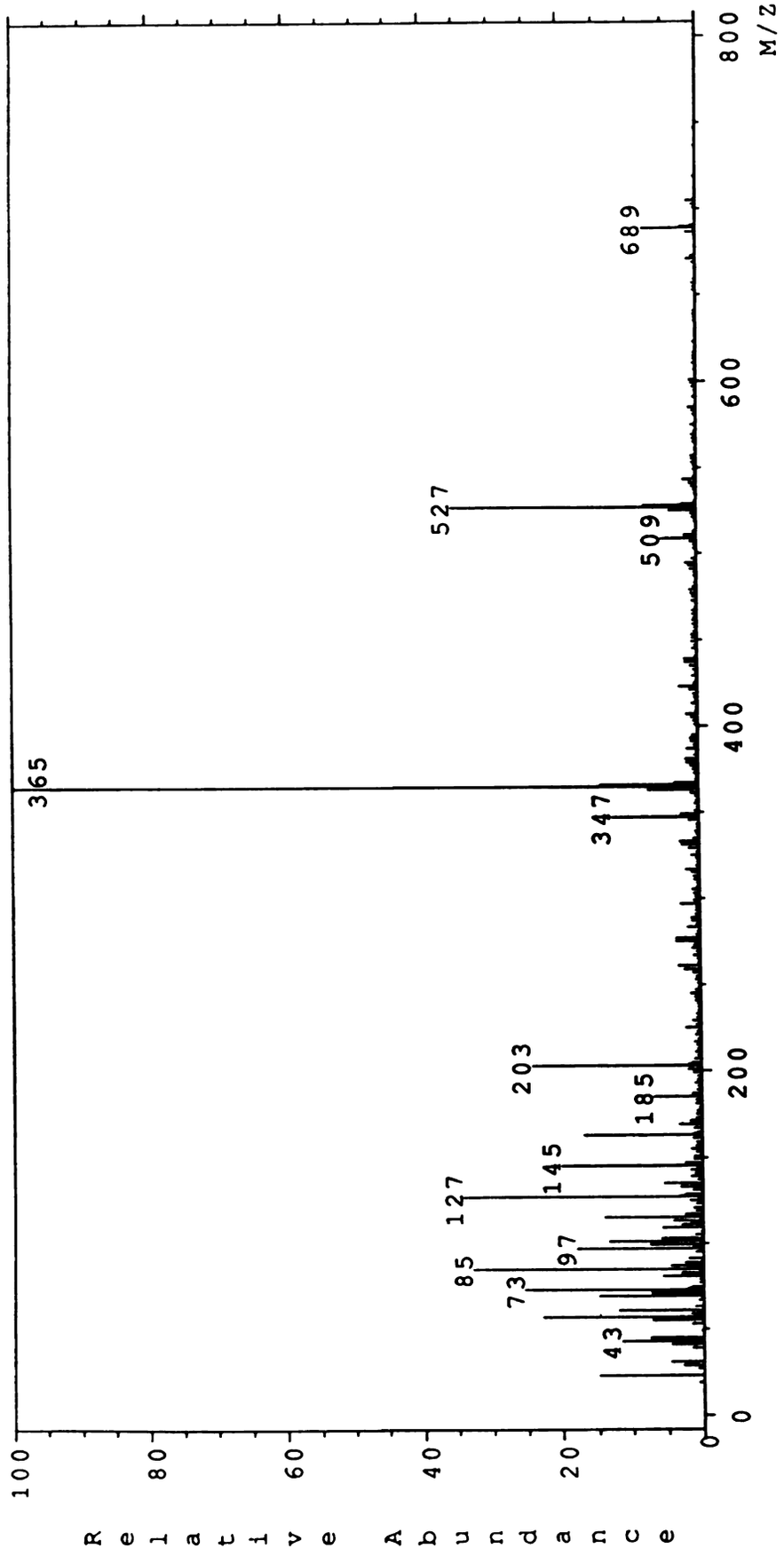

Figure 4.16. Scan 53 from TA-FAB experiment represented in Figure 4.15.

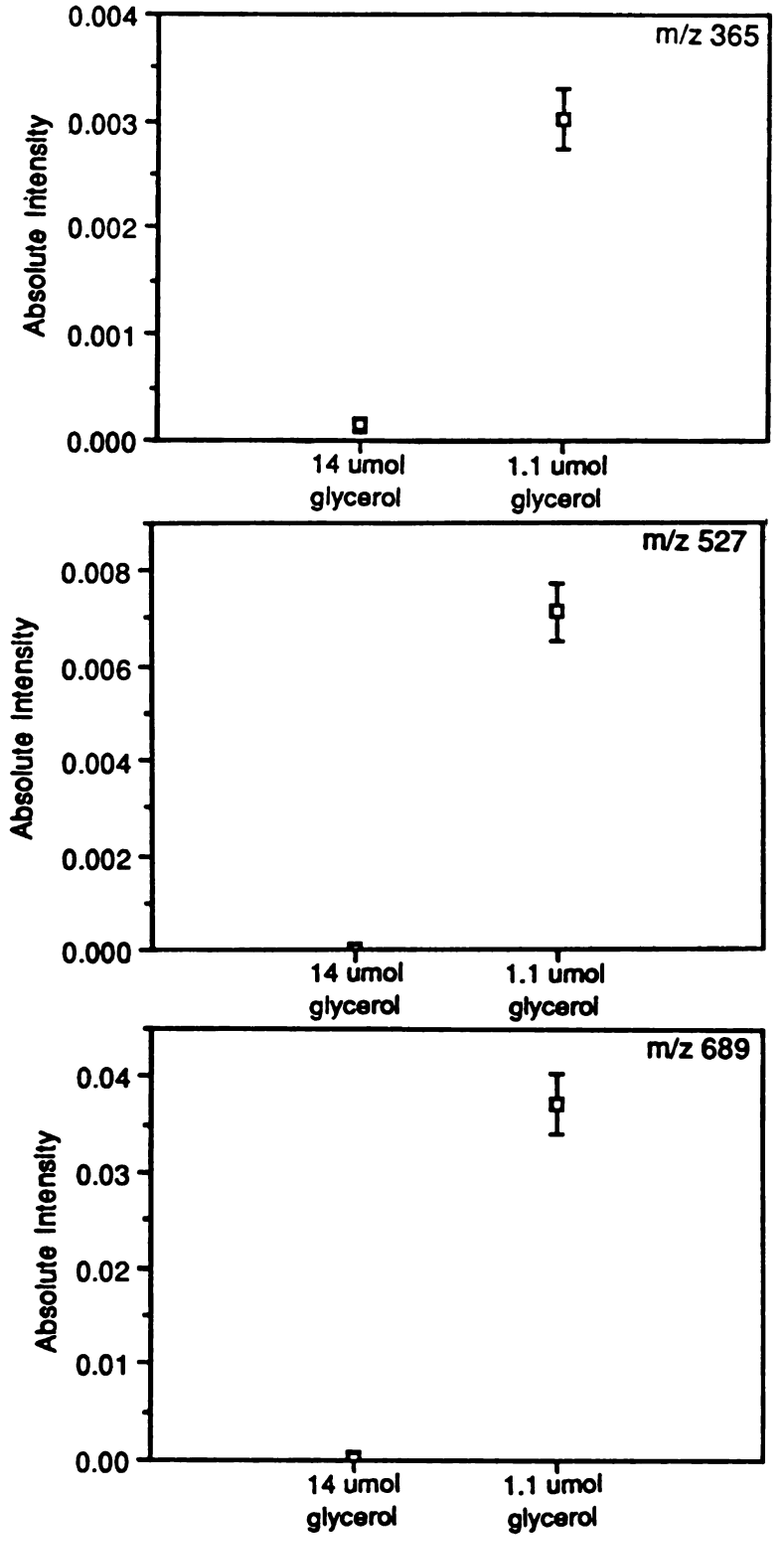

Figure 4.17. Comparison of peak intensities for selected stachyose ions (m/z 365 (top), m/z 527 (middle), and m/z 689) which were obtained from the FAB experiments. Structures of these ions are suggested in Figure 4.13. Each sample contained 19 ug of stachyose and 1 ug of NaCl.

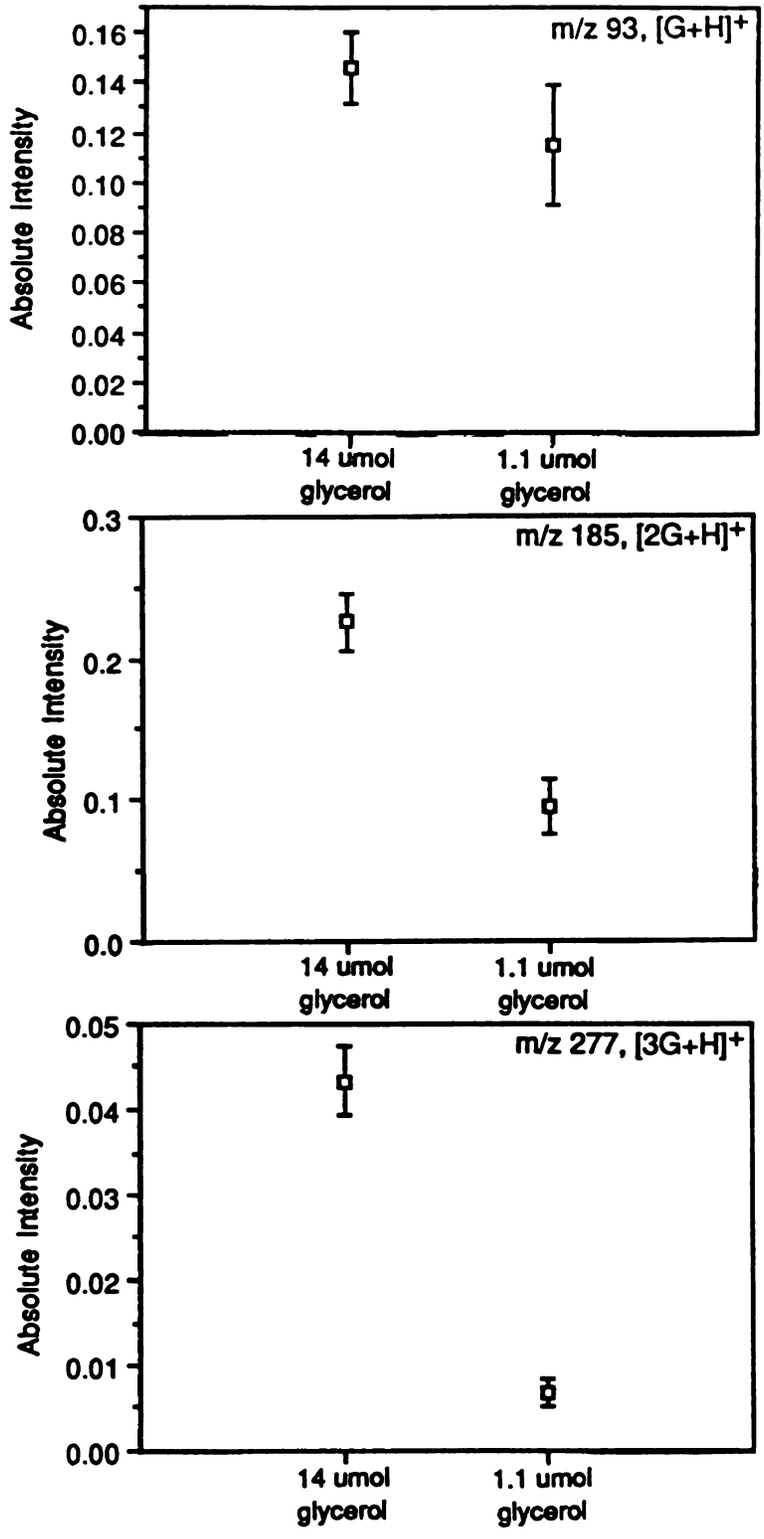

Figure 4.18. Comparison of peak intensities for protonated glycerol ions (m/z 93 (top), m/z 185 (middle), and m/z 277) which were obtained from the FAB experiments. Each sample contained 19 ug of stachyose and 1 ug of NaCl.

Abundances for the natriated counterparts of the ions represented in Figure 4.18 are compared in Figure 4.19. These background ions are present in greater abundance for the samples containing 1.1 umol of glycerol than for the samples containing 14 umol of glycerol. This is a novel observation in terms of the comparisons previously described. It should be pointed out, however, that as the mass of the natriated glycerol ion increases, the difference in abundance between the 1.1 umol glycerol samples and the 14 umol glycerol samples is greatly diminished (see Figure 4.19). Likewise, the decrease in abundance observed for the protonated glycerol ions in the 1.1 umol glycerol samples (see Figure 4.18) becomes more pronounced at higher mass. These factors combine to provide substantially less matrix interference in the high mass window for the samples containing less glycerol, as shown by the spectra in Figure 4.14.

IV. Conclusion

The results presented in this chapter indicate that the mass spectrometric approaches which were compared (conventional FAB experiments incorporating 14 umol of glycerol and 1.1 umol of glycerol, and TA-FAB experiments incorporating the aqueous fructose matrix and the hybrid matrix) provide unique advantages and disadvantages for the analysis of the different analytes. Several general trends in performance were observed, however, and these deserve special comment. For example, the conventional FAB results were significantly improved by reducing the matrix to analyte ratio for each of the analytes investigated. In all cases, the spectral improvement involved an increase in analyte ion abundances coupled with a decrease in matrix ion abundances. This recurring result indicates that manipulation of the matrix to analyte ratio is a powerful tool for optimizing FAB-MS analyses.

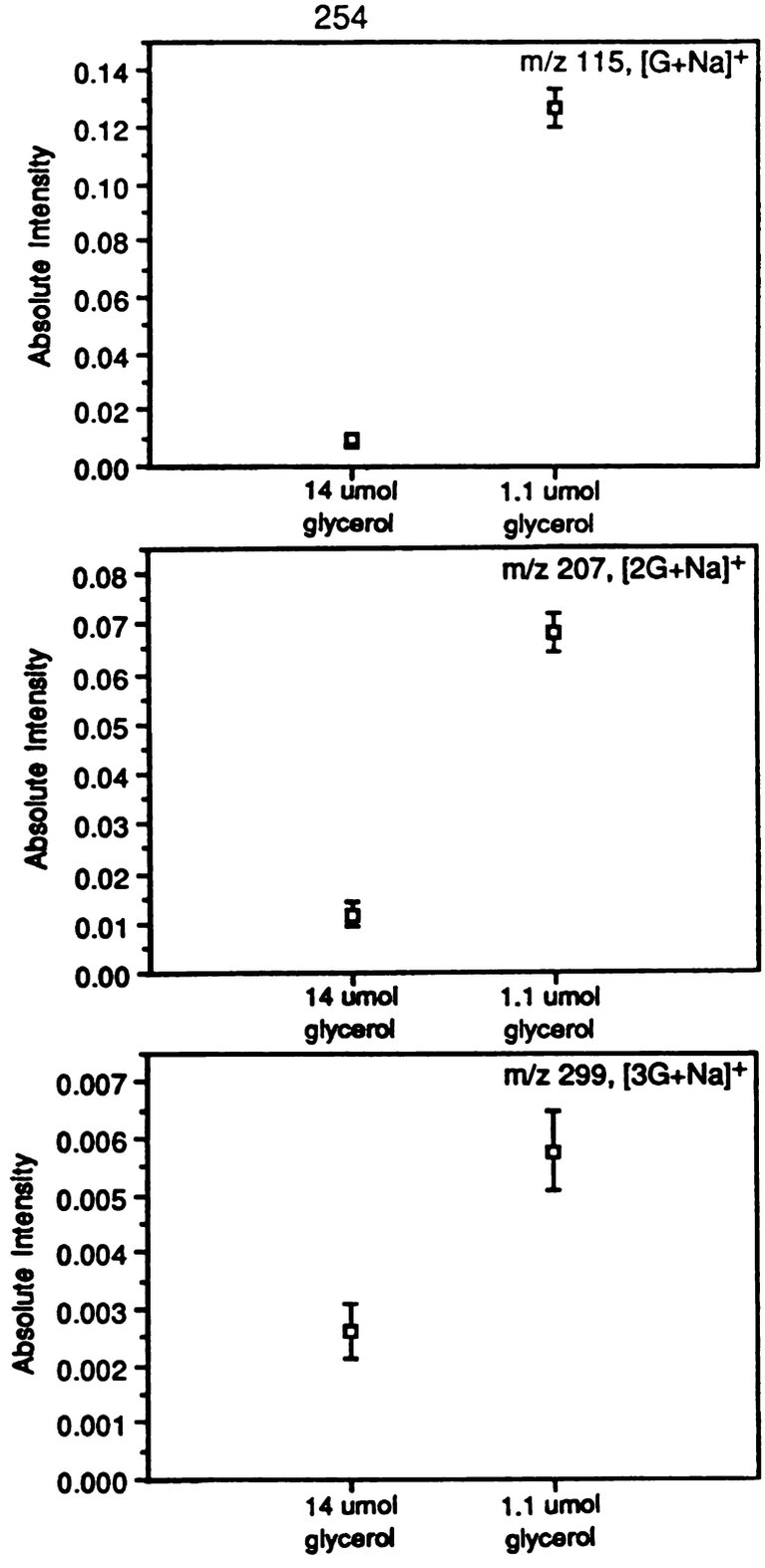

Figure 4.19. Comparison of peak intensities for natriated glycerol ions (m/z 115 (top), m/z 207 (middle), and m/z 299) which were obtained from the FAB experiments. Each sample contained 19 ug of stachyose and 1 ug of NaCl.

It is interesting to note that the TA-FAB experiment involving the hybrid matrix often produced the greatest analyte ion abundances. This observation is probably explained (as previously suggested) by a progressive optimization of the matrix to analyte ratio in the hybrid matrix, whereas the 1.1 umol glycerol samples (for all analytes except bradykinin) were characterized by a nonoptimal ratio. Unfortunately, the increased analyte ion abundances did not necessarily result in an improved visibility of analyte signals, because the interference produced by the hybrid matrix is more extensive than that generally observed from the 1.1 umol glycerol samples. The production of very high abundances of stable, low mass, fragment ions (in the fructose component of the TA-FAB matrices) which was documented for the higher mass linear peptides in Chapter 3 (Section f), was not observed for any other analytes investigated in this chapter. The tendency for the high mass analyte ion abundances obtained from the aqueous fructose matrix to fade (in comparison to those produced by the other experiments) was established in every case. Nevertheless, the aqueous fructose TA-FAB matrix always provided the option of background subtraction, which often allowed the most unobstructed viewing of low mass analyte signals.

V. Future Work

Invariably, it seems that the information gained from an experiment raises new questions, the answers to which can be found only by conducting additional experiments. All the questions associated with this project have not been answered. In regard to optimization of the matrix to analyte ratio in conventional FAB analyses, this approach needs to be implemented with matrices other than glycerol, which are deposited from solvents other than water. Documentation of the spectral enhancement for an increasingly larger number and wider variety of

analytes is also important. An extension of the comparison described in this chapter to more analytes also would be desirable. The original intent of the author was to include more analytes, but this became a difficult goal due to time constraints. A more detailed knowledge of the potential of TA-FAB would certainly result from such an extension. Finally, the TA-FAB experiment involving only a liquid matrix provides an interesting avenue for future work (this approach was explored with glycerol in Chapter 3, Section **h**). There is something inherently attractive in the capability to progressively optimize the matrix to analyte ratio for any compound within a single experiment. It is unfortunate that this process results in such rapid contamination of the ion source.

Whether or not my future will involve conducting any of these experiments (and answering any of these questions) is an uncertain matter. New experiments are waiting, which will be designed to answer different questions. Considering the enjoyment I have experienced with this project, however, I somehow hope it is not completely finished for me.

VI. References

1. Walton, J.D.; Earle, E.D.; Gibson, B.W. *Biochem. Biophys. Res. Commun.* **1982**, *107*, 785.
2. Ackermann, B.L.; Holland, J.F.; Watson, J.T. *Biomed. Environ. Mass Spectrom.* **1987**, *14*, 501.
3. Yang, Y.M.; Lloyd, H.A.; Pannell, L.K.; Fales, H.M.; Macfarlane, R.D.; McNeal, C.J.; Ito, Y. *Biomed. Environ. Mass Spectrom.* **1986**, *13*, 439.
4. Bursey, M.M.; Marbury, G.D.; Hass, J.R. *Biomed. Mass Spectrom.* **1984**, *11*, 522.
5. Keough, T. *Anal. Chem.* **1985**, *57*, 2027.